

Peter James Watts, B.Sc., M.R.Pharm.S.

Department of Pharmaceutical Sciences.

"Microspheres for drug-delivery to the colon."

Submitted to the University of Nottingham for the degree
of Doctor of Philosophy, January 1992.

To my Parents.

Acknowledgments

First and foremost I'd like to thank my three supervisors, Dr. Martyn Davies and Dr. Colin Melia in the Department of Pharmaceutical Sciences and Dr. Clive Wilson of the Department of Physiology & Pharmacology, Queen's Medical Centre for their continual support, advice and encouragement during the past three years.

Thanks are also due to three former members of Clive's lab, Dr. Linda Barrow, Elaine Blackshaw, and Karen Steed for their assistance and advice with gamma-scintigraphic investigations, Dr. Robin Spiller (Department of Therapeutics), Dr. Graham Parr (Reckitt and Colman), Andy Tudor (Pharmaceutical Sciences) for his collaboration on the FT-Raman study, Brian Plummer, Richard Hyde, Pravin Patel and Tony Waite for technical support, Dr. Brian Atkin (Mining Engineering) for the XRF assay, Dr. Dave Barrett (Pharmaceutical Sciences) for advice on HPLC, Dr. Richard Lynn (Pharmaceutical Sciences) and Dr. John Watts (Surrey University) for providing the XPS spectra, Dr. Peter Morgan (School of Agriculture, Sutton Bonington) for polymer molecular weight measurements, and to Dr. John Sargent for providing outstanding electron micrographs.

Finally, the Science and Engineering Research Council and Reckitt & Colman Products are thanked for financial support.

SUMMARY

The work described in this thesis is concerned with the design and evaluation of microsphere-based systems for drug delivery into the colon.

In initial experiments, techniques were devised for the preparation of microspheres from two sustained-release acrylic polymers, Eudragits RL and RS, using emulsification-solvent evaporation techniques. For Eudragit RS microspheres containing the drug 5-aminosalicylic acid, the rate of drug release could be controlled by the type and concentration of surfactant used for preparation. Consequently, formulations could be produced which released encapsulated drug instantaneously or over many hours. The surfactants may have been altering the structure of the microsphere drug-polymer matrix.

Two novel analytical techniques were employed to characterise Eudragit RS microspheres containing sulphasalazine. Fourier transform-Raman spectroscopy was successfully used as a non-destructive method for qualitative and quantitative microsphere characterisation. The technique provided good agreement with a UV-spectrophotometric method in quantifying the amount of drug in microsphere samples. X-ray photoelectron spectroscopy was used to estimate the concentration of sulphasalazine at the microsphere surface for samples produced with or without the use of surfactant. Across a wide range of microsphere drug loadings, the surface drug content remained remarkably constant, but was consistently lower in the samples produced using surfactant.

In a parallel programme of work, using gamma scintigraphy, the transit rate of different sizes of radiolabelled materials through the human colon was investigated to determine whether there was an optimal size to maximise

colon residence. There was no clear evidence of any difference in the colon residence time of 0.2 mm particles, 5 mm tablets, or 8.4 mm tablets, under normal conditions and during accelerated transit. In healthy subjects, 50% of a dose of 0.2 mm particles resided in the ascending colon for an average of 11 hours.

Finally, an in vivo biopharmaceutical evaluation of sulphapyridine-containing Eudragit RS microspheres in the human colon was undertaken. For this study, a neutron activation technique was developed for microsphere radiolabelling. Microspheres could be successfully radiolabelled by incorporation of samarium oxide followed by neutron irradiation. However, it was necessary to minimise the period of irradiation and the amount of incorporated samarium oxide, since high levels of both were found to adversely affect microsphere performance.

The in vivo investigation revealed that the colonic bioavailability of sustained-release microencapsulated sulphapyridine was less than 50% of unencapsulated sulphapyridine powder. This shortfall was possibly due to an interaction of the drug with colonic bacteria or in vitro/in vivo differences in microsphere drug release characteristics.

CONTENTS

	<u>Page</u>
<u>Chapter 1: Introduction.</u>	1
Background.	2
1.1. Microspheres in drug delivery.	
1.1.1. Introduction.	3
1.1.2. Methods of manufacture.	
1.1.2.1. Coacervation/phase separation.	4
1.1.2.2. Suspension cross-linking.	5
1.1.2.3. Emulsion polymerisation.	6
1.1.2.4. Mechanical methods.	6
1.1.2.5. Emulsification-solvent evaporation.	7
1.1.3. Polymers used for microsphere fabrication.	
1.1.3.1. Biodegradable polymers.	17
1.1.3.2. Non-biodegradable polymers.	19
1.1.4. Clinical use of microsphere-based delivery systems.	
1.1.4.1. Parenteral drug-delivery.	26
1.1.4.2. Oral drug-delivery.	30
1.1.4.3. Other routes.	32
1.1.5. Summary.	32
1.2. The colon as a site for drug-delivery.	
1.2.1. Introduction.	34
1.2.2. Structure and function of the colon.	35
1.2.3. Colon environment.	
1.2.3.1. Microorganisms.	38
1.2.3.2. pH in the colon.	38
1.2.3.3. Faecal content.	39
1.2.4. Issues of importance to drug delivery.	
1.2.4.1. Transit of materials through the colon.	39
1.2.4.2. Colonic microflora.	45
1.2.4.3. Absorption of drugs from the colon.	47

1.2.5. Reasons for targeting drugs into the colon.	
1.2.5.1. Local treatment of colonic disease.	49
1.2.5.2. Systemic delivery of drugs.	54
1.2.6. Methods for targeting drugs into the colon.	
1.2.6.1. pH-triggered systems.	56
1.2.6.2. Enzyme-triggered systems.	60
1.2.6.3. Time-dependent systems.	65
1.2.7. Summary.	66
1.3. Aims of the thesis.	68

<u>Chapter 2: Preparation of model Eudragit nanoparticles and microparticles and the effects of changing manufacturing parameters on their properties.</u>	69
--	----

2.1. Introduction.	70
2.2. Experimental.	
2.2.1. Materials.	70
2.2.2. Methods.	
2.2.2.1. Particle preparation.	70
2.2.2.2. Particle size determination.	74
2.2.2.3. Light microscopy.	75
2.2.2.4. Scanning electron microscopy.	75
2.3. Results and Discussion.	
2.3.1. Nanoparticle samples.	
2.3.1.1. Effect of polymer concentration.	76
2.3.1.2. Effect of mixing time.	76
2.3.1.3. Effect of surfactant concentration.	78
2.3.2. Microparticle samples.	
2.3.2.1. Effect of polymer concentration.	82
2.3.2.2. Effect of stirring speed.	82
2.3.2.3. Effect of stirring time.	82
2.3.2.4. Effect of surfactant concentration.	86
2.3.3. Scanning electron microscopy.	86
2.4. Conclusions.	89

Chapter 3: The encapsulation of 5-aminosalicylic acid into Eudragit RS microspheres.	92
3.1. Introduction.	93
3.2. Experimental.	
3.2.1. Materials.	94
3.2.2. Methods.	
3.2.2.1. Microsphere production.	94
3.2.2.2. Assay for drug content.	96
3.2.2.3. Drug release studies.	97
3.2.2.4. Low temperature S.E.M.	97
3.3. Results and Discussion.	
3.3.1. Microsphere production.	98
3.3.2. Microsphere drug release characteristics.	101
3.3.3. Low temperature S.E.M.	105
3.4. Conclusions.	110
Chapter 4: Bulk characterisation of Eudragit RS-sulphasalazine microspheres using Fourier transform-Raman spectroscopy.	113
4.1. Introduction.	114
4.2. Experimental.	
4.2.1. Materials.	118
4.2.2. Methods.	
4.2.2.1. Microsphere production.	118
4.2.2.2. Microsphere assay.	119
4.2.2.3. Microsphere drug release study.	119
4.2.2.4. FTRS analysis.	120
4.3. Results and Discussion.	
4.3.1. Microsphere characterisation.	122
4.3.2. Drug release study.	122
4.3.3. FT-Raman spectra.	
4.3.3.1. Qualitative interpretation.	125
4.3.3.2. Quantitative interpretation.	131
4.4. Conclusions.	137

<u>Chapter 5: Surface characterisation of Eudragit RS-sulphasalazine microspheres using X-ray photoelectron spectroscopy (XPS).</u>	139
5.1. Introduction.	140
5.2. Experimental.	
5.2.1. Materials.	144
5.2.2. Experimental methods.	
5.2.2.1. Microsphere production.	144
5.2.2.2. Microsphere assay.	144
5.2.2.3. XPS analysis.	144
5.3. Results and Discussion.	
5.3.1. Microsphere characterisation.	144
5.3.2. XPS analysis.	
5.3.2.1. Qualitative analysis.	145
5.3.2.2. Quantitative analysis.	145
5.4. Conclusions.	158
<u>Chapter 6: The development of dosage forms for the assessment of transit through the colon.</u>	159
6.1. Introduction.	160
6.2. Experimental.	
6.2.1. Materials.	162
6.2.2. Methods.	
6.2.2.1. Preparation of 0.2 mm particles.	162
6.2.2.2. Tablet preparation.	163
6.2.2.3. Capsule coating.	165
6.2.2.4. Preliminary <u>in vitro</u> experiments.	165
6.2.2.5. <u>In vivo</u> experimentation.	167
6.2.2.6. Further characterisation of "Polymer A" coating.	168
6.3. Results and discussion.	
6.3.1. <u>In vitro</u> capsule evaluation.	
6.3.1.1. Eudragit S alone.	169
6.3.1.2. "Polymer A" alone.	170

6.3.1.3. Dual "Polymer A"/Eudragit S coatings.	170
6.3.2. <u>In vivo</u> evaluation of capsule coatings.	170
6.3.3. Further characterisation of "Polymer A" coating.	171
6.4. Conclusions.	171
<u>Chapter 7: The transit of model dosage forms through the colon, measured using gamma scintigraphy.</u>	173
7.1. Introduction.	174
7.2. Experimental.	
7.2.1. Materials.	177
7.2.2. Methods.	
7.2.2.1. Dosage form production.	177
7.2.2.2. Study design.	177
7.2.2.3. Data analysis.	180
7.3. Results.	
7.3.1. Study 1.	
7.3.1.1. Part A.	184
7.3.1.2. Part B.	186
7.3.2. Study 2.	189
7.3.3. Irritable bowel syndrome.	189
7.4. Conclusions.	192
<u>Chapter 8: Radiolabelling of drug:polymer microspheres using neutron activation techniques.</u>	195
8.1. Introduction.	196
8.2. Incorporation of samarium oxide into Eudragit RS-sulphasalazine microspheres.	
8.2.1. Experimental	
8.2.1.1. Materials.	205
8.2.1.2. Methods.	205
8.2.2. Results and Discussion.	
8.2.2.1. Before irradiation.	210
8.2.2.2. After irradiation.	215

8.3. Incorporation of samarium oxide into Eudragit RS-sulphapyridine microspheres.	
8.3.1. Experimental.	
8.3.1.1. Microsphere production.	230
8.3.1.2. Microsphere size and density.	230
8.3.1.3. Sm ₂ O ₃ content.	230
8.3.1.4. SP content.	230
8.3.1.5. Drug release rate.	231
8.3.1.6. Electron microscopy.	231
8.3.1.7. Effects of irradiation.	231
8.3.2. Results and Discussion.	232
8.3.2.1. Microsphere characterisation.	232
8.3.2.2. Drug release rate.	232
8.3.2.3. Electron microscopy.	236
8.3.2.4. Effects of irradiation.	236
8.4. Conclusions.	241
<u>Chapter 9: A biopharmaceutical evaluation of Eudragit RS-sulphapyridine microspheres in the human colon.</u>	243
9.1. Introduction.	244
9.2. Experimental.	
9.2.1. Materials.	246
9.2.2. Methods.	
9.2.2.1. Microsphere production.	246
9.2.2.2. Microsphere characterisation.	247
9.2.2.3. Microsphere irradiation.	247
9.2.2.4. <u>In vivo</u> investigation.	247
9.3. Results.	
9.3.1. Microsphere characterisation.	252
9.3.2. Transit rate.	257
9.3.3. Pharmacokinetics.	263
9.4. Conclusions.	274
<u>Chapter 10: Concluding remarks.</u>	276
<u>Appendix 1.</u>	282
<u>References.</u>	283

LIST OF FIGURES

- 1.1. Microencapsulation using emulsification-solvent evaporation.
- 1.2. A (water-in-oil)-in-water technique for encapsulation of water-soluble drugs.
- 1.3. Relative permeability of Eudragits RL and RS.
- 1.4. Potential clinical uses of microsphere drug-delivery systems.
- 1.5. Anatomy of the human colon.
- 1.6. Colonic metabolism of sulphasalazine.
- 1.7. Strategies for targeting into the colon: the point of drug release from different delivery systems.
- 1.8. Structure of some 5-ASA prodrugs.
- 2.1. Preparation of Eudragit RL micro- and nanoparticles.
- 2.2. Bimodal distribution of Eudragit RL nanoparticles.
- 2.3. Effect of mixing speed on size of Eudragit RL microparticles.
- 2.4. Effect of mixing time on size of Eudragit RL microparticles.
- 2.5. Effect of SDS concentration on size of Eudragit RL microparticles.
- 2.6. Electron micrographs of Eudragit RL microparticles.
- 3.1. Effect of SDS concentration on rate of release of 5-ASA from microspheres.
- 3.2. Effect of Tween 20 concentration on rate of release of 5-ASA from microspheres.
- 3.3. Electron micrographs of Eudragit RS:5-ASA microspheres prepared without surfactant.
- 3.4. Electron micrographs of Eudragit RS:5-ASA microspheres prepared with 0.25% w/v SDS as surfactant.
- 4.1. Energy changes involved in Rayleigh and Raman scattering.
- 4.2. Schematic of Raman sampling area and collection optics.
- 4.3. FT-Raman spectrum of sulphasalazine.

- 4.4. FT-Raman spectrum of drug-free Eudragit RS microspheres.
- 4.5. FT-Raman spectra of Eudragit RS-sulphasalazine microspheres.
- 4.6. Relationship between peak area ratio and microsphere drug content.
- 4.7. Linear relationship between peak area ratio and microsphere drug content.
- 4.8. Derivation of a linear relationship between drug concentration and peak area ratio.
- 4.9. Microsphere sulphasalazine content determined by FT-RS and UV-spectrophotometry.
- 5.1. Simplified layout of XPS spectrometer.
- 5.2. Wide-scan XPS spectrum of sulphasalazine.
- 5.3. Wide-scan XPS spectrum of surfactant-free, drug-free Eudragit RS microspheres.
- 5.4. Wide-scan XPS spectrum of surfactant-free, Eudragit RS microspheres containing 31.1% w/w sulphasalazine.
- 5.5. Calculation of atomic % composition of microsphere components.
- 5.6. Calculation of atomic % composition of Eudragit RS microspheres containing 18.2% w/w sulphasalazine (SASP).
- 5.7. Experimental vs. theoretical N content: surfactant-containing microspheres.
- 5.8. Experimental vs. theoretical N content: surfactant-free microspheres.
- 6.1. Procedure for dip-coating gelatin capsules.
- 7.1. The gamma-camera.
- 7.2. Divisions of colon used for scintigraphic analysis.
- 7.3. Graph to define ascending colon mean residence time (MRT).
- 7.4. Activity-time profiles of 5 mm tablets for one of subjects without and with lactulose coadministration.
- 8.1. Neutron irradiation of Samarium-152 (Sm).

- 8.2. Effect of samarium oxide incorporation on sulphasalazine release rate.
- 8.3. Radioactivity generated from irradiation of microsphere samples.
- 8.4. Radiation stability of sulphasalazine, measured by HPLC.
- 8.5. Effect of irradiation on sulphasalazine release rate.
- 8.6. Electron micrographs of surface of Eudragit RS:sulphasalazine microspheres.
- 8.7. Electron micrographs of internal structure of Eudragit RS:sulphasalazine microspheres.
- 8.8. Effects of samarium oxide incorporation on microsphere size distribution.
- 8.9. Effect of samarium oxide incorporation on microsphere drug release rate.
- 8.10. Electron micrographs of Eudragit RS:sulphapyridine microspheres containing no samarium oxide.
- 8.11. Electron micrographs of Eudragit RS:sulphapyridine microspheres containing 1.15% w/w samarium oxide.
- 8.12. Electron micrographs of interior of Eudragit RS:sulphapyridine microspheres.
- 8.13. Effect of 15 minute irradiation on sulphapyridine release rate.
- 9.1. Metabolic fate of sulphapyridine.
- 9.2. Release rate of microspheres used for clinical study pre- and post-irradiation.
- 9.3. Electron micrographs of Eudragit RS:sulphapyridine microspheres used for clinical investigation: non-irradiated.
- 9.4. Electron micrographs of Eudragit RS:sulphapyridine microspheres used for clinical investigation: irradiated.
- 9.5. Scintigraphic images of ^{153}Sm -labelled microspheres for subject 4.

- 9.6. HPLC traces of sulphapyridine (SP), acetyl-sulphapyridine (AcSP), and internal standard, sulphadimidine sodium (SDNa).
- 9.7. Mean plasma data from biopharmaceutical study.
- 9.8. Individual sulphapyridine plasma profiles.
- 9.9. Effect of stirring speed on in vitro microsphere drug release rate.

LIST OF TABLES

- 1.1. Criteria for selection of continuous and dispersed phase solvents.
- 1.2. Chemical structure of Eudragit copolymers.
- 2.1. Effect of polymer concentration on the size and polydispersity of Eudragit RL nanoparticles.
- 2.2. Effect of mixing time on the size and polydispersity of Eudragit RL nanoparticles.
- 2.3. Effect of Tween 80 concentration on the size of Eudragit RL nanoparticles.
- 2.4. Effect of polymer concentration on the size of Eudragit RL microparticles.
- 3.1. Eudragit RS:5-ASA microsphere formulation details.
- 3.2. Time for 50% of 5-ASA to be released from microsphere formulations.
- 4.1. Details of Eudragit RS:sulphasalazine microsphere formulations.
- 4.2. In vitro release of sulphasalazine from Eudragit RS microspheres over a 24 hour period.
- 5.1. Details of Eudragit RS:sulphasalazine microsphere formulations.
- 5.2. Experimental and (theoretical) surface atomic composition of Eudragit RS:sulphasalazine microsphere samples.
- 7.1. Colon transit data for study 1A (healthy controls).
- 7.2. Colon transit data for study 1B (coadministration of lactulose).
- 7.3. Colon transit data for 0.2 mm particles vs. 8.4 mm tablets in healthy subjects.
- 7.4. Colon transit data for IBS patients.
- 8.1. Physical properties of some materials suitable for neutron activation and incorporation into dosage forms.
- 8.2. Composition of naturally occurring samarium oxide.
- 8.3. Samarium oxide incorporation efficiency into Eudragit RS:sulphasalazine microspheres.

- 8.4. Drug content and yield of Eudragit RS:sulphasalazine microspheres.
- 8.5. Effect of neutron irradiation on assayed microsphere sulphasalazine content, measured by HPLC.
- 8.6. Time for 50% of sulphasalazine to be released from microspheres (t50%) before and after irradiation.
- 8.7. Eudragit RS:sulphapyridine microsphere formulation details.
- 9.1. Details of microsphere formulation used for clinical investigation.
- 9.2. Ascending colon MRT of radiolabelled ion-exchange resin and Eudragit microspheres.
- 9.3. Radioactivity from microspheres remaining after 24 and 32 hours in the ascending (AC), transverse (TC) and descending (DC) colon.
- 9.4. Bioavailability of sulphapyridine:- Eudragit microspheres (m) vs. unencapsulated drug powder (u).
- 9.5. Mean residence time of sulphapyridine (dMRT) absorbed from powder and microspheres.

ABBREVIATIONS

AcSP	Acetyl-sulphapyridine.
5-ASA	5-aminosalicylic acid.
FTRS	Fourier-transform Raman spectroscopy.
GI	Gastrointestinal.
h	Hour.
IBD	Inflammatory bowel disease.
IBS	Inflammatory bowel syndrome.
In	Indium.
n	Neutron.
NSAID	Non-steroidal antiinflammatory drug.
o/o	Oil-in-oil (emulsion).
o/w	Oil-in-water (emulsion).
PEG	Poly(ethylene glycol).
PLA	Poly(lactic acid).
PLG	Poly(glycolic acid).
PLGA	Lactic/glycolic acid copolymer.
PVA	Poly(vinyl alcohol).
SASP	Sulphasalazine.
SDS	Sodium dodecyl sulphate.
Sm ₂ O ₃	Samarium oxide.
SP	Sulphapyridine.
Tc	Technetium.
w/o/w	(Water-in-oil)-in-water (emulsion).
XPS	X-ray photoelectron spectroscopy.

CHAPTER 1.
INTRODUCTION.

BACKGROUND

The past two decades has seen a rapid growth in the development of novel dosage forms to achieve controlled drug delivery. This has been the result of a number of factors (Langer, 1990):

1. The ability to improve the safety and efficacy of a drug.
2. To allow convenient administration of "difficult" molecules such as peptides and proteins.
3. Potential for providing pulsatile patterns of drug release.
4. The considerable cost of developing new chemical entities means that increasing the lifetime of established drugs by formulation into new delivery systems is an attractive financial option.
5. Scientific advances, especially in polymer science, have made the development of controlled delivery systems feasible.

This introductory chapter discusses two different aspects of controlled drug delivery. The first part describes the production of drug-polymer microspheres, focusing on the solvent evaporation process, and their therapeutic uses. The second part of the introduction discusses the colon as a target for drug delivery.

The experimental work described in this thesis unites these two themes and is concerned with the development of microspheres for colon drug delivery.

1.1. MICROSPHERES IN DRUG-DELIVERY

1.1.1. Introduction

The term "microencapsulation" is used to describe a series of techniques for the production of particulate carriers, in the nm to mm size range, in which a solid or liquid is entrapped within a polymer coat or matrix. Apart from pharmaceuticals, this technology has been used by a number of other industries including food (Reinaccius and Risch, 1988), household products (Bilbrey and Versic, 1990) and agrochemicals (Wilkins, 1990), but perhaps most notably in the manufacture of carbonless carbon paper. To develop this product, the National Cash Register Co. in the 1950s developed the first microencapsulation technique (coacervation/phase separation), for the production of pressure-sensitive dye-containing microcapsules (Green and Schleicher, 1956).

In the literature, "microsphere", "microcapsule" and "microparticle" tend to be used synonymously to describe the products of microencapsulation. Theoretically, "microcapsule" should only apply to systems that are hollow or in which the polymer forms an outer shell, whereas "microsphere" should only apply to systems that are spherical in shape. Sub-micron carriers are generally referred to as nanospheres, nanocapsules or nanoparticles.

The production and use of micro- and nanoparticulates for pharmaceutical applications is a vast topic and has been the subject of many books and reviews (e.g. Arshady, 1989, 1990a,b; Davis et al., 1984b; Davis and Illum, 1989; Deasy, 1984, 1991; Douglas et al., 1987; Guiot and Couvreur, 1986; Juliano, 1985; Kreuter, 1988; Oppenheim, 1981; Tomlinson, 1983). This section aims to provide a general overview of microspheres as drug carriers, but will concentrate in particular on their production using emulsification-solvent evaporation procedures.

1.1.2. Methods of manufacture

There are five principal techniques for producing drug/polymer microspheres of pharmaceutical interest:

- Coacervation/phase separation.
- Suspension cross-linking.
- Emulsion polymerisation.
- Mechanical methods.
- Emulsification-solvent evaporation.

1.1.2.1. Coacervation/phase separation

As mentioned in the introduction, this was the first microencapsulation technique to be developed, and a number of articles describing the method have been published (Arshady, 1990a; Bakan, 1980; Deasy, 1984; Madan, 1978).

Coacervation refers to the aggregation of polymer molecules brought about by their partial desolvation. Partial desolvation is a phase separation process and leaves the polymer existing in a state between full solvation and precipitation.

Coacervation techniques can use aqueous or non-aqueous systems. In an aqueous system, the coating polymers are water-soluble and the material to be encapsulated is water-insoluble or, in the case of liquids, water-immiscible. Aqueous systems can be further subdivided into simple and complex. Simple systems involve one coating polymer, whereas complex involve two, oppositely charged, coating polymers. In non-aqueous systems, the coating polymer is water-insoluble and this technique is suitable for the encapsulation of water-soluble materials.

In practice, the material to be encapsulated, liquid or solid, is dispersed into a solution of the coating polymer by stirring. The coacervating agent is then gradually added. The precise mechanism by which the encapsulation

process takes place is not entirely clear, but the material to be coated may act as nuclei for formation of the coacervates. Alternatively, large coacervates may form which then engulf the material to be encapsulated.

There are numerous examples of the application of phase separation techniques to the preparation of microcapsules of pharmaceutical interest. Although many apply to hydrophilic polymers such as gelatin (e.g. Dixon, 1981; Paradissis and Parrott, 1968; Raymond et al., 1990) and methylcellulose (Salib et al., 1976), the hydrophobic polymer, ethylcellulose, has also been widely used (e.g. Alpar and Walters, 1981; Benita and Donbrow, 1982; Jalsenak et al., 1976). Other polymers used have included the acrylic EudragitsTM (Benita et al., 1985; Chattaraj et al., 1991; El-Sayed et al., 1982) and lactic/glycolic acid copolymer (PLGA) (McGee et al., 1991; Sanders et al., 1984).

1.1.2.2. Suspension cross-linking

In suspension cross-linking, a solution or melt of the polymer of interest is suspended in an immiscible liquid. Hardening of the droplets is then carried out and the microspheres/capsules collected (Arshady, 1989; Deasy, 1984).

The main pharmaceutical application of this technique is for the preparation of albumin microspheres. Here, the drug to be encapsulated is dispersed into an aqueous solution of albumin which is then emulsified into an immiscible liquid e.g. vegetable oil. Cross-linking can be brought about by heating the emulsion or by addition of glutaraldehyde (Arshady, 1989; Deasy, 1984). Pharmaceutical examples include the encapsulation of mitomycin C (Fujimoto et al., 1985), adriamycin (Gupta et al., 1986) and 5-fluorouracil (Sugibayashi et al., 1979).

Suspension cross-linking has also been used to produce microspheres from gelatin (Yoshioka et al., 1981), fibrinogen (Miyuzaki et al., 1986) and haemoglobin (Levy et al., 1982).

1.1.2.3. Emulsion polymerisation

The most noteworthy application of this technique is for the production of biodegradable poly(alkylcyanoacrylate) nanoparticles. Here the alkylcyanoacrylate monomer solution is dispersed into an aqueous phase containing surfactant as stabiliser and drug. The hydroxyl ions present in the aqueous phase act as initiators for polymerisation. To slow down the rate of polymerisation and to enable nanoparticle formation, the aqueous phase has to be made acidic. In such systems, drug is generally considered to be adsorbed to the particle surface (Couvreur et al., 1986).

Examples of drugs incorporated include anticancer agents (Couvreur et al., 1986; Verdun et al., 1986), pilocarpine (Harmia et al., 1986), triamcinolone diacetate (El-Samaligy and Rohdewald, 1983), and insulin (Michel et al., 1991).

1.1.2.4. Mechanical methods

There are a number of techniques especially applicable to the economic large scale manufacture of microencapsulated dosage forms for potential oral administration (Bakan and Anderson, 1976; Deasy, 1991; Li et al., 1988).

These techniques firstly require the production of a drug-containing core. There are two main methods of core production. The first involves spraying a solution of drug and adhesive onto inert sucrose pellets (non-pareils) in a coating pan. Alternatively, extrusion-spheronisation may be used to produce pellets from drug and suitable excipients.

Polymer films are then applied to the drug cores by pan coating or air suspension techniques to generate the

desired properties e.g. enteric protection, sustained release.

1.1.2.5. Emulsification-solvent evaporation

The first report of the application of this technique for the microencapsulation of pharmaceuticals was in 1979 (Beck et al., 1979) in a paper describing the preparation of poly(lactic acid) (PLA) microspheres containing progesterone.

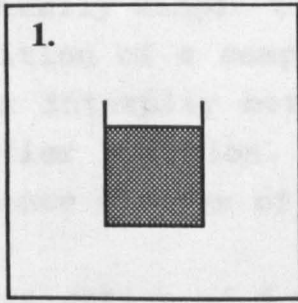
The process is outlined in figure 1.1. In the first step, a solution of polymer containing the drug to be encapsulated (either dissolved or in suspension) is emulsified into a second, immiscible, liquid containing a surfactant. This results in the formation of a dispersion of drug-polymer-solvent droplets.

In the second stage of the process, the solvent is evaporated from the dispersed droplets. In many instances, the volatility of the solvent is sufficient for it to rapidly evaporate at room temperature whilst stirring of the emulsion continues. To hasten evaporation, and for systems where solvent evaporation is less rapid, heat and/or vacuum may be applied. The evaporation of solvent results in precipitation of polymer around the drug and the formation of a suspension of microspheres. The microspheres can then be extracted by filtration or centrifugation and dried.

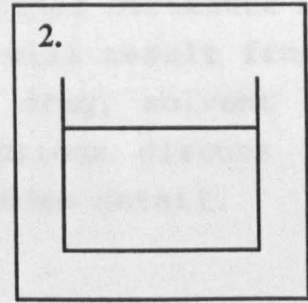
One of the attractions of the solvent evaporation technique is that by selection of suitable solvent systems, hydrophilic and hydrophobic drugs can be encapsulated into a wide range of polymers. In addition, the technique is able to produce microspheres over a wide size range, from nanometre to millimetre.

Although the emulsification-solvent evaporation process is

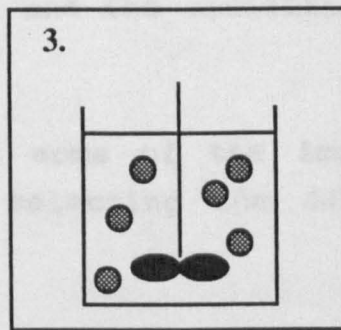
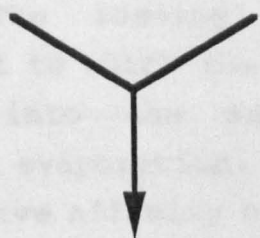
Figure 1.1. Microencapsulation using emulsification-solvent evaporation.



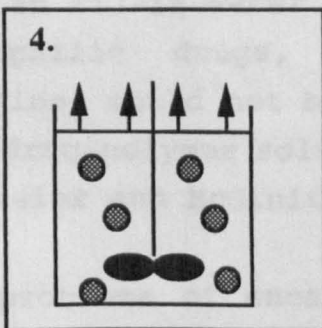
Polymer dissolved in organic solvent. Drug added to form a solution or suspension.



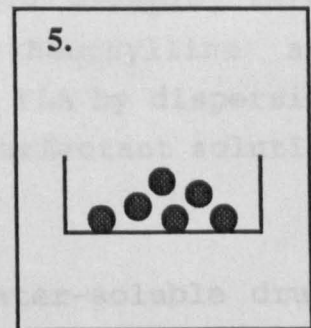
Emulsifier dissolved in second liquid immiscible with drug-polymer solution.



Polymer-drug solution mixed into emulsifier solution to form a dispersion of drug-polymer-solvent droplets.



Solvent removed by:
a) Stirring at room temperature.
b) Application of heat.
c) Application of vacuum.



Completed microspheres recovered by filtration or centrifugation then washed and dried.

conceptually simple to understand, the final structure and composition of a completed microsphere will result from a complex interplay between the polymer, drug, solvent and emulsifier solution. The following sections discuss the importance of some of these factors in more detail.

A. Optimisation of drug loading

Clearly one of the prime objectives in designing a microencapsulation process is to maximise the efficiency of drug encapsulation. The loading efficiency will be determined by the extent to which the drug is lost from the forming microspheres into the surrounding emulsifier solution during solvent evaporation. In turn, this will be determined by the relative affinity of the drug for the two liquid phases i.e. the solvent containing drug and polymer (dispersed phase) and the emulsifier solution (continuous phase).

Table 1.1. lists some of the important criteria to be considered when selecting the dispersed and continuous phase liquids.

In general, poor efficiency of drug encapsulation might be predicted if a polymer solution containing a hydrophilic drug is emulsified into an aqueous surfactant solution to form an oil-in-water dispersion (o/w). For example, three hydrophilic drugs, salicylic acid, theophylline and caffeine, could not be encapsulated into PLA by dispersion of a drug-polymer solution into aqueous surfactant solution (Bodmeier and McGinity, 1987a).

The problems of encapsulating highly water-soluble drugs can be overcome by the use of oil-in-oil (o/o) type emulsion systems where the polymer and drug, contained in a hydrophilic organic solvent are emulsified into an immiscible hydrophobic liquid (e.g. mineral oil). Water-soluble drugs encapsulated in this way have included

Table 1.1. Criteria for selection of continuous and dispersed phase solvents.

Dispersed phase solvent

- 1. Able to dissolve encapsulating polymer.**
- 2. Ideally, able to dissolve drug to be encapsulated.**
- 3. Immiscibility with continuous phase solvent.**
- 4. Lower boiling point than continuous phase solvent.**
- 5. Low toxicity.**

Continuous phase solvent

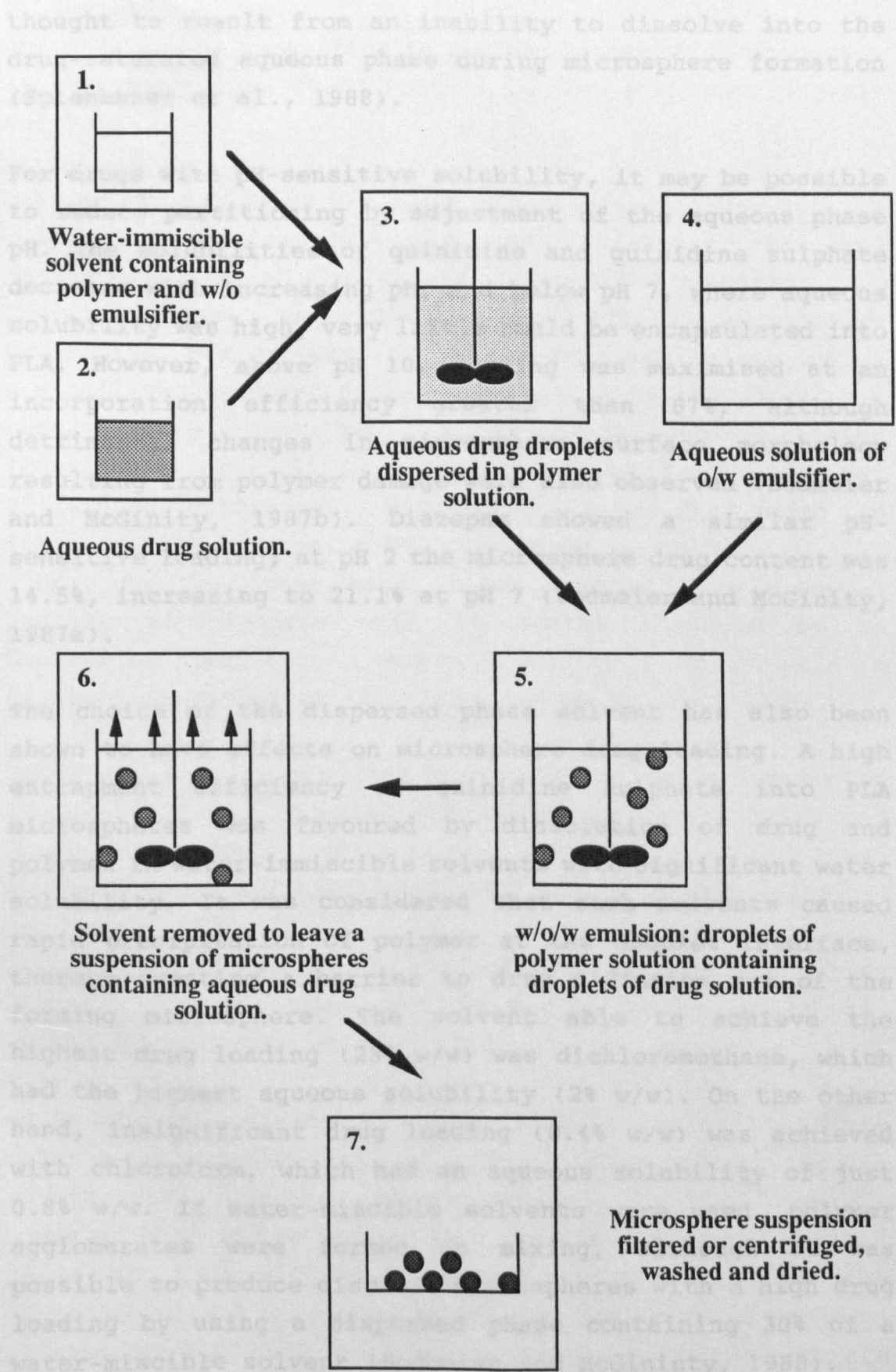
- 1. Immiscibility with dispersed phase solvent.**
- 2. Low solubility toward encapsulating polymer.**
- 3. Low solubility toward drug.**
- 4. Higher boiling point than dispersed phase solvent.**
- 5. Low toxicity.**
- 6. Allows easy recovery and clean-up of microspheres.**

diphenhydramine hydrochloride (Huang and Ghebre-Sellasie, 1989), cephadrine and cefadroxil (Uchida and Goto, 1988), mitomycin C (Tsai et al., 1986) and adriamycin (Wada et al., 1988). However, one of the drawbacks of this technique is clean-up of the completed microspheres. Removal of the oil phase from the microspheres may involve washing with solvents such as hexane, residues of which would be undesirable in the final product.

The problem of microsphere clean-up when using o/o techniques can be avoided by the use of a (water-in-oil)-in-water technique (w/o/w), outlined in figure 1.2. This method has been used to encapsulate the highly water-soluble LHRH agonist, leuprolide acetate (Ogawa et al., 1988). The encapsulating polymer, PLA or PLGA, dissolved in dichloromethane was emulsified into an aqueous drug solution to form a w/o emulsion. This emulsion was then emulsified into 0.5% aqueous poly(vinyl alcohol) (PVA) solution to produce a w/o/w dispersion. Subsequent evaporation of the dichloromethane left an aqueous suspension of microspheres. This technique has also been used for other systems including the entrapment of proteins into PLGA microspheres (Cohen et al., 1991; O'Hagan et al., 1991) and a somatostatin analogue into branched PLGA d-glucose polymers (Bodmer and Kissel, 1991).

Enhancement in drug loading has also been attempted by including drug in the continuous phase as well as the polymer solution. For example, increased loading of quinidine sulphate in PLA microspheres was achieved by using an aqueous surfactant solution saturated with drug (Bodmeier and McGinity, 1987b). In the case of cisplatin-containing polyester microspheres, preloading the external aqueous phase with drug also changed their morphology. In the absence of extra cisplatin the microsphere surface was smooth, but when drug was present in the external phase crystals were seen on the surface. Their presence was

Figure 1.2. A (water-in-oil)-in water technique for encapsulation of water-soluble drugs.



thought to result from an inability to dissolve into the drug-saturated aqueous phase during microsphere formation (Splenhauer et al., 1988).

For drugs with pH-sensitive solubility, it may be possible to reduce partitioning by adjustment of the aqueous phase pH. The solubilities of quinidine and quinidine sulphate decrease with increasing pH, and below pH 7, where aqueous solubility was high, very little could be encapsulated into PLA. However, above pH 10, loading was maximised at an incorporation efficiency greater than 67%, although detrimental changes in microsphere surface morphology resulting from polymer damage were also observed (Bodmeier and McGinity, 1987b). Diazepam showed a similar pH-sensitive loading; at pH 2 the microsphere drug content was 14.5%, increasing to 21.1% at pH 7 (Bodmeier and McGinity, 1987a).

The choice of the dispersed phase solvent has also been shown to have effects on microsphere drug loading. A high entrapment efficiency of quinidine sulphate into PLA microspheres was favoured by dissolution of drug and polymer in water-immiscible solvents with significant water solubility. It was considered that such solvents caused rapid precipitation of polymer at the droplet interface, thereby creating a barrier to drug diffusion out of the forming microsphere. The solvent able to achieve the highest drug loading (23% w/w) was dichloromethane, which had the highest aqueous solubility (2% w/w). On the other hand, insignificant drug loading (0.4% w/w) was achieved with chloroform, which had an aqueous solubility of just 0.8% w/w. If water-miscible solvents were used, polymer agglomerates were formed on mixing, although it was possible to produce discrete microspheres with a high drug loading by using a dispersed phase containing 30% of a water-miscible solvent (Bodmeier and McGinity, 1988).

B. Emulsifier

The role of the emulsifier in solvent evaporation processes is the short term stabilisation of the suspended polymer droplets.

Many of the published o/w emulsification techniques utilise polymeric stabilisers such as gelatin, PVA and methylcellulose and the increase in solution viscosity that these polymers can produce may affect microsphere properties. For example, the use of methylcellulose 400 as a stabiliser produced a high viscosity external phase that resulted in distorted, ovoid-shaped microparticles (Cavalier et al., 1986). In another system, for a given set of mixing conditions, microsphere size was found to increase with increasing PVA concentration (Benita et al., 1984). On the other hand, other workers have produced smaller microspheres with 1% sodium alginate as an emulsifier than with a lower viscosity 1 or 2% gelatin solution (Wakiyama et al., 1981; Kojima et al., 1984).

Other o/w stabilisers used have included the polysorbates (TweensTM) (e.g. Bodmeier and McGinity, 1984b; Smith and Hunneyball, 1986), sodium oleate (Fong et al., 1986) and sodium dodecyl sulphate (SDS) (Suzuki and Price, 1985).

Typical emulsifiers for o/o systems are the sorbitan esters (SpansTM) (e.g. Huang and Ghebre-Sellasie, 1989) and lecithin (e.g. Wada et al., 1988).

An unfortunate effect of emulsifiers is their ability to enhance the solubility of drugs. When attempting to encapsulate lomustine and progesterone in PLA, crystals appeared both on the microsphere surface and in the aqueous phase as a result of enhanced solubilisation by the emulsifiers, PVA and methylcellulose. The crystals could be eliminated and drug loading enhanced by removal of the emulsifier solution halfway through solvent evaporation and

resuspension of the partly solidified microspheres in water (Benita et al., 1984b).

The use of PVA as an emulsifier has also been found to have dramatic effects on the release of insulin from PLA microspheres. The emulsifier was thought to promote the growth of insulin crystals, by solubilisation, at the microsphere surface, and this resulted in a marked burst effect with instantaneous release of up to 88% of the encapsulated drug on in vitro testing. However, the use of 1% gelatin solution as an emulsifier resulted in an initial release of only 26% of the encapsulated drug. This difference in behaviour may have resulted from gelatin being a less efficient solubiliser than PVA of insulin (Kwong et al., 1986).

In another paper, an increase from 0 to 2% in the concentration of Tween 20 in the aqueous phase caused a small reduction in microsphere quinidine content. Apart from enhanced drug solubilisation, another reason attributed to reduced drug content was stabilisation of the drug-polymer interface by the surfactant; It was proposed that this would reduce the rate of solvent loss, thereby reducing the polymer precipitation rate and allowing more drug to escape from the forming microsphere before an adequate polymeric diffusional barrier could be formed (Bodmeier and McGinity, 1987c).

C. Control of microsphere size

The principal parameters controlling microsphere size are the speed, equipment, and technique used for mixing the two phases, and the concentration of polymer in the dispersed phase.

The microsphere size tends to decrease exponentially with increasing mixing speed, accompanied by a narrowing in the particle size distribution (Benita et al., 1984b; Babay et

al., 1988; Barkai et al., 1990).

The design of the mixing vessel can affect both the size and yield of microspheres. Inclusion of baffles in the mixing vessel eliminated vortex formation, and as a result the microsphere yield increased from 50 to 90 %. In addition, break-up of the drug-polymer droplets on the baffles reduced the average microsphere size from greater than 75 μm to less than 30 μm (Bodmeier and McGinity, 1987b).

The microsphere size, in general, tends to increase with polymer concentration. For example, microspheres made from a 2% w/v solution of EudragitTM polymers had a mean diameter of 140 μm , whereas microspheres produced with a 5% w/v solution had a mean diameter of 295 μm (Pongpaibul et al., 1984). There are two contributing factors here: 1) By increasing the concentration of polymer in the dispersed phase, the solution viscosity will increase and so for a given set of mixing conditions the droplet size and so final microsphere size will tend to be larger; 2) An increase in the concentration of polymer inside the droplet increases the volume it occupies when the solvent has evaporated, although this will be offset to some extent by a reduction in microsphere porosity with increasing polymer concentration. An increase in the density of poly(anhydride) microspheres was observed when the concentration of polymer solution used for preparation was increased (Mathiowitz et al., 1990).

1.1.3. Polymers used for microsphere fabrication

There are two main classes of polymer used for producing microspheres by solvent evaporation, biodegradable and non-biodegradable. In general, microspheres produced from biodegradable polymers are for potential parenteral administration whereas microspheres produced from non-biodegradable polymers are for potential oral

administration.

1.1.3.1. Biodegradable polymers

A. Polyesters

The most important class of biodegradable polyesters are those based upon lactic and glycolic acids: poly(lactic acid) (PLA), poly(glycolic acid) (PGA) and lactic/glycolic acid copolymers (PLGA). In vivo, these polymers degrade by hydrolysis to their constituent acids which are non-toxic and easily excreted. Excellent biocompatibility has been demonstrated through their use as resorbable sutures and prostheses. The other major attraction of the polyesters is their ability to achieve prolonged release of drug. Drug permeability is low and release is measured in days, weeks or even months, and results from a combination of diffusion and polymer erosion (Juni and Nakano, 1987; Wise et al., 1979).

A large number of drugs have been encapsulated into polyester microspheres using emulsification-solvent evaporation including anticancer agents (e.g. Spenlehauer et al., 1988; Tsai et al., 1986; Wada et al., 1988), insulin (Kwong et al., 1986), corticosteroids (e.g. Cavalier et al., 1986; Fong et al., 1986; Smith and Hunneyball, 1986), steroid hormones (e.g. Beck et al., 1979, 1981; Benoit et al., 1986), narcotic antagonists (Cha and Pitt, 1988, 1989), and neuroleptics (e.g. Fong et al., 1986; Maulding et al., 1986; Suzuki and Price, 1985).

Proteins have also been encapsulated into polyester microspheres. PLGA microspheres have been produced containing bovine serum albumin and horse radish peroxidase (Cohen et al., 1991), human serum albumin (Hora et al., 1990), and ovalbumin (O'Hagan et al., 1991).

PGA has not been widely used as an encapsulating polymer because of its poor solubility in common solvents. One

example is the encapsulation of prednisolone-21-acetate by codissolution of drug and polymer in hexafluoroacetone sesquihydrate, followed by emulsification into carbon tetrachloride containing sorbitan sesquioleate as surfactant (Redmon et al., 1989). In this system, solvent evaporation was carried out by two different methods. The solvent was partially evaporated to produce a suspension of part-formed microspheres. Complete removal was then carried out by either stirring the dispersion in 1,4-dioxane and allowing solvent to evaporate or by freeze-drying the part-formed microspheres. The microspheres completed by stirring released drug more rapidly than those completed by freeze-drying. The difference in release was thought to reflect differences in microsphere porosity, since the surface area of the microspheres completed by stirring was two to three times greater than the freeze-dried microspheres.

Other biodegradable polyesters utilised in solvent evaporation processes have been poly(β -hydroxybutyrate) (PHB) (Bissery et al., 1984; Juni et al., 1987), and poly(carbonates) (Kojima et al., 1984).

PHB microspheres less than 200 nm in diameter have been prepared by dispersion of a 1.6% w/v solution of polymer in chloroform into 0.2% w/v aqueous SDS solution. Following initial mixing of the two phases by homogeniser, the emulsion was sonicated for 30 minutes followed by evaporation of solvent (Koosha et al., 1989).

B. Poly(anhydrides)

Poly(anhydrides) are hydrophobic polymers which undergo surface erosion via water-labile anhydride linkages. By choosing different backbone structures, a wide range of degradation and thus drug release rates can be achieved (Leong et al., 1986). Good biocompatibility has been demonstrated, and drug-containing poly(anhydride) implants for treatment of brain cancer are undergoing human clinical

trials (Domb et al., 1991).

Drugs microencapsulated into poly(anhydrides) using solvent evaporation have included insulin (Mathiowitz et al., 1988, 1990) and bethanechol (Howard et al., 1989).

Insulin-containing microspheres were produced by both an o/w and o/o emulsification procedure. On implantation into rats, the rate of insulin release from the microspheres produced by the o/w procedure was so fast that most of the animals died within a day from hypoglycaemia, whereas a prolonged lowering of serum glucose was seen for the microspheres produced by the o/o procedure. The rapid release of insulin from the o/w microspheres was considered to be due to high porosity and possibly accelerated polymer degradation during microsphere preparation (Mathiowitz et al., 1990).

1.1.3.2. Non-biodegradable polymers

A. Acrylic polymers

i). Eudragits

The main group of pharmaceutically important acrylic polymers are the Eudragits (trade mark of Röhm Pharma, Darmstadt, Germany), based upon acrylic and methacrylic acids. There are five different Eudragit polymers and their chemical structures are detailed in table 1.2. They are available as solids or ready-to-use solutions and latexes.

Eudragit E is a so-called "reverse enteric" which dissolves at acidic pH, but is insoluble at higher pH levels. One of the uses of this material is for coating tablets to provide improved stability or taste masking whilst allowing rapid disintegration in the stomach (Handbook of Pharmaceutical Excipients, 1986; Eudragit technical data).

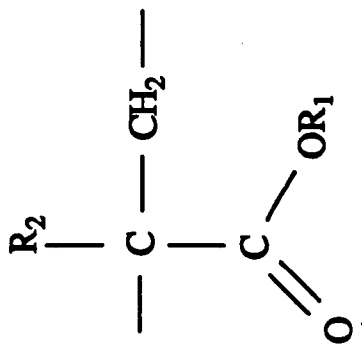
Eudragits L and S are enteric polymers which dissolve above

Table 1.2.

Chemical structure of

Eudragit copolymers

(from Davies et al., 1989).



Type and frequency of polymer side-group R₁ (R₂ = CH₃, except for ^{*}, when R₂=H).

Eudragit	H	CH ₃	C ₂ H ₅	C ₄ H ₉	CH ₂ CH ₂ N(CH ₃) ₃	CH ₂ CH ₂ N ⁺ (CH ₃) ₃ Cl ⁻
S	1	2	-	-	-	-
L	1	1	-	-	-	-
E	-	1	-	1	2	-
RL	-	2	1*	-	-	0.2
RS	-	2	1*	-	-	0.1

pH 6.0 and 7.0 respectively to form polymeric salts. Eudragit L dissolves at the lower pH since it contains the greater proportion of soluble poly(methacrylic acid) functions. Below the critical pH values, the polymers are water-impermeable (Handbook of Pharmaceutical Excipients, 1986; Eudragit technical data).

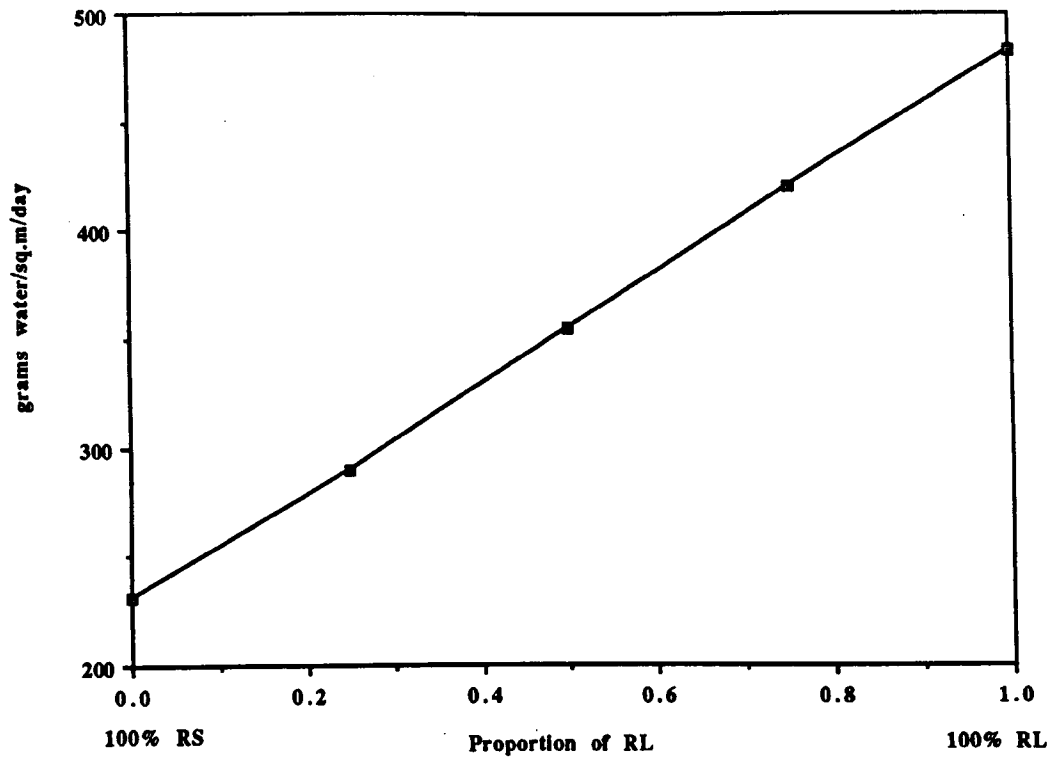
Eudragits RL and RS are both insoluble in the pH range of the gastrointestinal tract, yet are permeable. The permeability is conferred by the trimethyl ammonioethyl chloride functions ($\text{CH}_2\text{CH}_2\text{N}(\text{CH}_3)_3^+\text{Cl}^-$) which are present as fully dissociated salts in the pH range 2 to 8. The proportion of these groups is greatest in Eudragit RL and so this polymer has the higher permeability to water and drugs (see figure 1.3, adapted from Eudragit technical data). The materials are commonly used as coatings to produce sustained-release tablets and pellets (Handbook of Pharmaceutical Excipients, 1986; Eudragit technical data).

There are a number of reports on the use of Eudragits for manufacturing microspheres by the solvent evaporation technique. The majority have focused on the encapsulation of non-steroidal antiinflammatory drugs (NSAIDs).

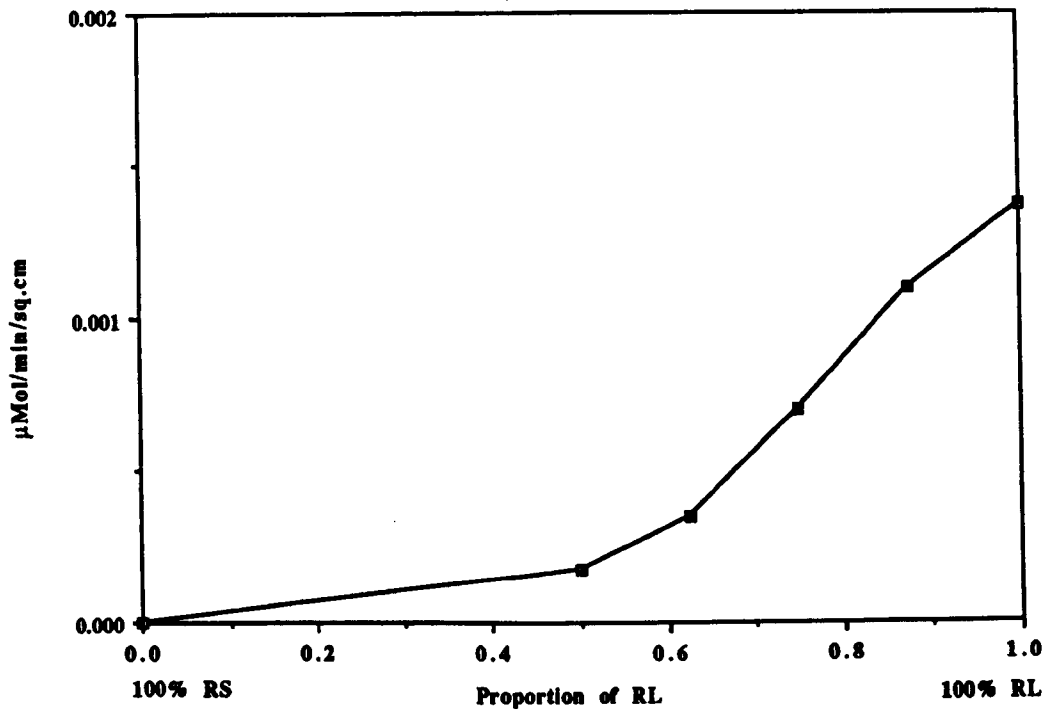
The first report of Eudragit microspheres being produced by emulsification-solvent evaporation appeared in 1985 (Goto et al., 1985). An attempt was made to encapsulate 42 different drugs in Eudragit RS by dispersion of drug, polymer and magnesium stearate (stabiliser) in dichloromethane into water. Using this technique, only three of the drugs could be successfully encapsulated, sulphamethizole, frusemide and piretanide. Following solvent evaporation it was claimed that the microspheres were highly swollen, and removal of water, under reduced pressure, took several days. On drying, microspheres were found to be very fragile.

Figure 1.3

a) Permeability of Eudragit RL/RS mixtures to water vapour



b) Permeability of RL/RS mixtures to trifluoperazine HCl, 0.00025M, pH 5, 37 °C.



Microspheres with improved physical properties were produced using an o/o technique. Ketoprofen (a NSAID) and aluminium tristearate as stabiliser were dispersed into a solution of Eudragit RS dissolved in acetone. This mixture was emulsified into liquid paraffin, the acetone evaporated by warming, and the completed microspheres washed with hexane prior to drying. A marked sustaining of drug release was observed (Kawata et al., 1986).

Further work investigated ketoprofen encapsulation into the entire range of Eudragit polymers. Eudragit E, L, and S microspheres containing up to 40% w/w ketoprofen were produced. In an acidic medium, Eudragit E microspheres dissolved rapidly and released their encapsulated drug, whereas the L and S microspheres resisted release until pH 6.06 and pH 6.74 respectively (Goto and Kawata, 1986a). RL microspheres containing 40% w/w ketoprofen released all of their drug within 1 hour, while equivalent RS microspheres had released less than 50% of encapsulated drug within 8 hours. Microspheres produced from a 50:50 blend of RL and RS provided an intermediate rate of drug release (Goto et al., 1986b). All of these Eudragit microspheres were between 0.25 and 1 mm in diameter.

Other workers have successfully produced Eudragit RS and RL microspheres containing indomethacin using o/w techniques. In one case, microspheres were produced by dispersion of 5-10 ml of polymer solution in methylene chloride into 1.4 L of 0.25% w/v PVA solution. RL microspheres (105-180 μ m in diameter) released about 70% of drug within 8 hours, while equivalent RS microspheres had released less than 10% (Bodmeier and Chen, 1989a). In another report, Eudragit RL microspheres were produced by emulsification of 20 ml of 10% w/v polymer in dichloromethane into 250 ml of 0.8% w/v PVA solution. Sustained release of drug was demonstrated (Babay et al., 1988).

A comparison has been made between Eudragit RL/RS-indomethacin microspheres produced by o/w and o/o techniques. In the first instance, microspheres were produced by emulsification of polymer and drug dissolved in 75 ml of dichloromethane into 300 ml of 0.5% aqueous PVA solution. The second set of microspheres were produced by emulsification of drug and polymer in ethanol into an external phase consisting of 270 ml liquid paraffin, 30 ml of silicone oil and 3 g of Span 85 as emulsifier. Microspheres produced using the o/w system were more porous, had a higher drug content, and released drug more rapidly than microspheres produced using the o/o system (Malamataris and Avgerinos, 1990).

Indomethacin microspheres have also been produced from a blend of Eudragits RS and L using an o/o technique. Dissolution testing was carried out at pH 6.5, and as the proportion of L increased, so did the drug release rate (Pongpaibul et al., 1984).

ii). Poly(methylmethacrylate)

Poly(methylmethacrylate) (PMMA) is a water-insoluble, water-impermeable polymer, and one of its uses is as a bone cement (Charnley and Pusso, 1968).

Using an o/o solvent evaporation procedure, theophylline has been microencapsulated in PMMA. As a result of the low permeability of the polymer, polyethylene glycol (PEG) 4000 was included in all formulations. In contact with water, the PEG dissolved to form pores in the microsphere matrix, and the higher the PEG content the more rapid the rate of drug release (Pongpaibul et al., 1988).

B. Celluloses

Ethylcellulose is a hydrophobic, highly water-insoluble polymer, widely used as a pharmaceutical excipient for orally administered dosage forms (Handbook of

Pharmaceutical Excipients, 1986). It has also been used to produce microspheres by solvent evaporation.

Using o/w techniques, ethylcellulose microspheres containing indomethacin have been produced. In one case, the drug release rate was increased by the addition of PEG to the microspheres, but it was still considered too low to be of practical use (Babay et al., 1988).

In another example, indomethacin-ethylcellulose microspheres (105-180 μm diameter) were prepared using either chloroform or dichloromethane to dissolve drug and polymer. Microspheres prepared from both solvents had the same drug content, but the drug release rates differed dramatically. The microspheres prepared using chloroform released more than 75% of encapsulated drug within two hours, whilst the microspheres prepared with dichloromethane had released less than 5% of drug within 24 hours. The differences were considered to be due to differences in the relative solubility of drug and polymer. When dichloromethane was used, polymer precipitated before drug, but with chloroform, drug precipitated before polymer and crystals were evident on the microsphere surface. The indomethacin release rate from the microspheres prepared using dichloromethane could be increased by incorporation of the more permeable polyester, poly(caprolactone) (Bodmeier and Chen, 1989a).

Addition of water-insoluble plasticisers to ethylcellulose microspheres containing diphenhydramine hydrochloride reduced the drug release rate, possibly as a result of reducing the porosity of the polymer matrix (Huang and Ghebre-Sellassie, 1989).

For the antibiotics cephadrine and cefadroxil, ethylcellulose microspheres containing up to 70% w/w drug were produced (Uchida and Goto, 1988).

Microspheres containing the diuretic, piretanide, have been produced from a mixture of ethylcellulose and hydroxypropyl cellulose. As the proportion of ethylcellulose was increased, the drug release rate decreased (Tsuyoshi et al., 1989).

Different sizes of theophylline crystals have been encapsulated into cellulose acetate propionate (Shukla and Price, 1989). For microspheres of similar size and drug loading, the release rate of theophylline was faster from microspheres containing medium and large drug crystals than from samples containing micronised drug crystals. The rapid release from the larger drug crystals was probably a result of incomplete coating by the polymer. When encapsulating large drug particles, the result will tend to be misshapen drug-polymer microparticles, where any imperfections in the polymer coat will expose a large proportion of the underlying drug, resulting in rapid dissolution. However, with small drug particles, the drug will be highly dispersed within the microsphere polymer matrix, leading to a lower rate of release.

1.1.4. Clinical use of microsphere-based delivery systems

Figure 1.4. outlines some of the potential clinical uses of microsphere-based drug delivery systems. In the next section, some of these concepts will be expanded.

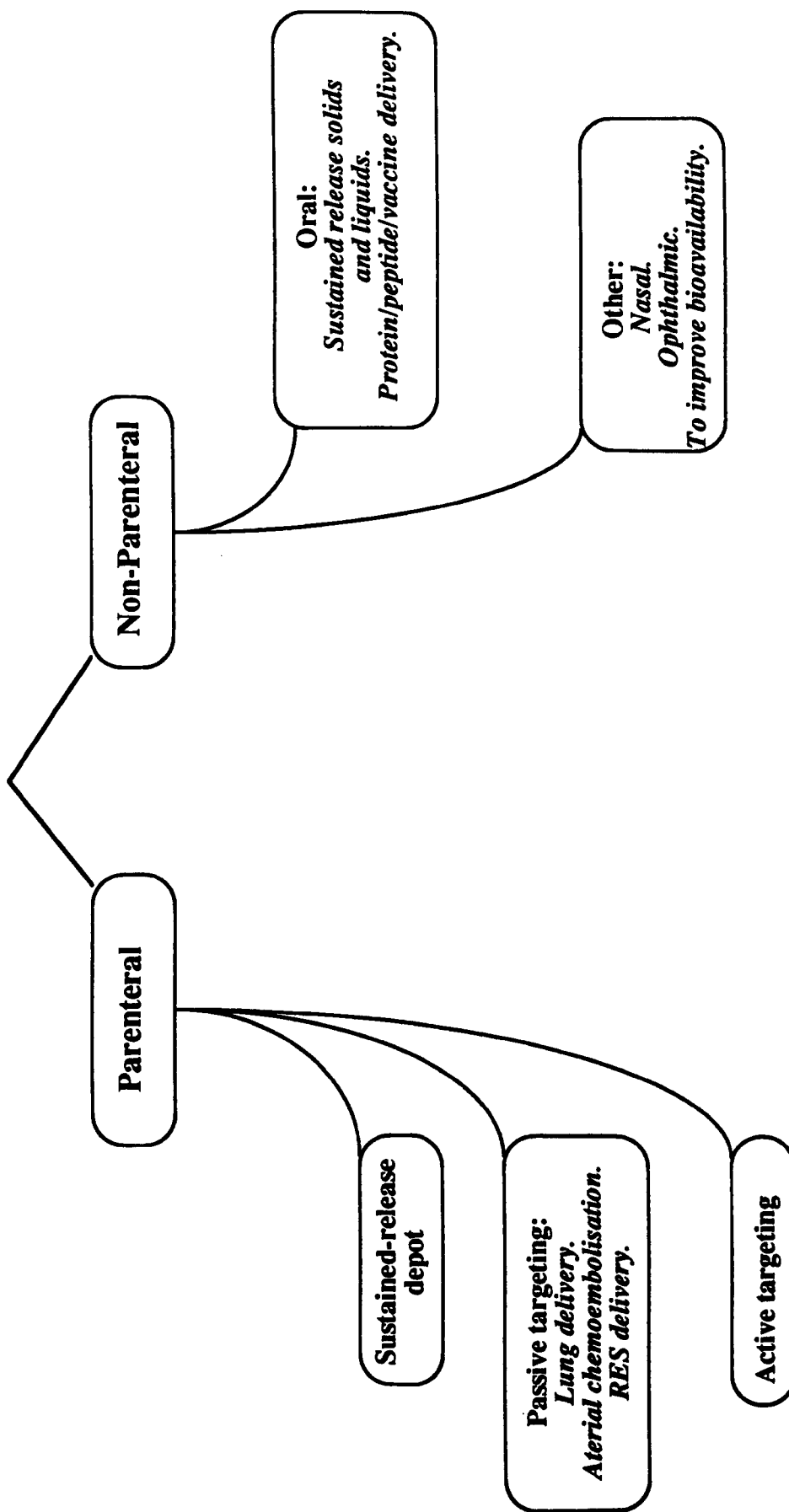
1.1.4.1. Parenteral drug-delivery

It is perhaps in the area of parenteral drug-delivery that microsphere-based drug delivery systems hold the greatest promise. There are two potential major applications:

A. Sustained-release depots

Parenteral sustained-release delivery systems based on biodegradable polymers have the potential for providing very long periods of drug release. One of the first systems to be clinically evaluated was norethisterone-containing

Figure 1.4. Potential Clinical Uses of Microsphere Drug-Delivery Systems



PLA microspheres, a potential long-acting contraceptive system. In female volunteers, release of drug for a period of up to six months was demonstrated (Beck et al., 1981). However, since complete biodegradation of the microspheres was thought to take a further six months, a more rapidly dissolving PLGA system was evaluated. On clinical testing, this system was shown to release norethisterone over a three month period (Beck et al., 1983).

More recently, testosterone-PLGA microspheres have undergone clinical evaluation. A biphasic release pattern was seen, and during week 1 and between weeks 6 and 11 postinjection, significant increases in plasma testosterone levels were measured (Burris et al., 1988).

Parenteral delivery is of particular interest for the delivery of therapeutic peptides and proteins (Pitt, 1990) since these molecules generally show very poor bioavailability by other routes. A monthly-administered depot of PLGA microspheres has been developed for the delivery of the peptide, leuprolide acetate (Toguchi et al., 1991) and is now marketed ("Prostap SR", Lederle, UK).

Other microsphere-based sustained-release parenteral depots have also progressed to the marketplace (Kissel et al., 1988).

B. Targetable drug carriers

There are envisaged to be two mechanisms by which targeting of microspheres can take place:

i). Passive targeting

Passive targeting applies to systems where no effort is made to circumvent the body's natural defence against injected foreign particulate material.

The simplest example would be the administration of

microspheres larger than the diameter of capillaries (3-11 μm). Material would be entrapped in the first capillary bed encountered, which in the case of intravenous injection would be the lungs (Tomlinson, 1983). This principle is used for diagnostic imaging of the lungs by administration of radiolabelled albumin microspheres (Rhodes et al., 1969). However, it is not clear whether lung entrapment could have any useful application in drug delivery (Davis and Illum, 1989). Selective arterial catheterisation can deposit material in the capillary bed of organs such as the liver or kidneys. This is the principle of arterial chemoembolisation (Kerr et al., 1991) in which microspheres containing anticancer agents have successfully been used to treat tumours (Nemoto and Kato, 1984; Fujimoto et al., 1985).

Particles small enough to flow through the capillaries will be trapped by cells of the reticuloendothelial system (RES). The RES consists of phagocytic cells found principally in the liver (Kupffer cells) but also in the spleen, lymph nodes, bone marrow, lungs and circulating in the blood and lymph (Altura and Saba, 1981). On entry into the circulation, foreign particles are rapidly coated with proteins (opsonins) that allow recognition and uptake by RES phagocytes. Thus, radiolabelled 1-5 μm PLG microspheres were primarily deposited in the liver of rats whether administered through the hepatic portal vein or jugular vein (Hazrati et al., 1989). Uses of RES targeting may include treatment of intracellular parasites and enzyme storage disorders (Davis and Illum, 1986). However, the treatment of liver cancer in this way may be limited; a study in man demonstrated minimal uptake of particulates by liver tumour cells (Poste, 1985).

ii). Active targeting

Active targeting applies to systems that are designed to elude capture by the body's natural defence mechanisms,

thereby allowing drug delivery to tissues outside the RES or the carrier to remain in the circulation for prolonged periods.

A major obstacle in achieving active targeting is the avoidance of RES uptake. It appears that the surface characteristics of the carrier are an important factor in determining its in vivo distribution. For example, coating microspheres with the surfactant, poloxamer 407, directed them away from the liver and spleen and toward the bone marrow, whereas a coating of poloxamine 908 increased retention in the vascular compartment. The presence of surfactant may have altered the profile of adsorbed opsonins or sterically inhibited interaction between the microspheres and phagocytic cells (Illum et al., 1987).

1.1.4.2. Oral drug-delivery

Multiparticulate carriers have been used for many years for the oral delivery of drugs, beginning with "Spansules" in the 1950s. Such systems are primarily used to provide sustained or delayed release of drug and technologies for their production were described in section 1.1.2.4.

As mentioned earlier, most of the publications concerned with production of microspheres for potential oral administration have involved encapsulation of NSAIDs. One of the major side-effects of NSAIDs is gastric irritation leading to bleeding, and in some cases ulceration (Woodbury and Finch, 1975). By administering the drug in a dispersed system, the risk of local high concentrations of drug and therefore gastric irritation is greatly reduced. However, it is unlikely that microencapsulation techniques such as solvent evaporation would offer any benefits over the more conventional mechanical methods for the manufacture of these systems.

A pharmacokinetic comparison of sustained-release

indomethacin administered as a commercially available pellet preparation or in Eudragit RL/RS microspheres has been reported. Both formulations demonstrated similar in vitro dissolution performance and were administered to 12 healthy male volunteers in a cross-over study. Relative to a conventional capsule formulation the microspheres demonstrated higher bioavailability than the pellets, although the difference was not statistically significant (94.6 ± 28.9 % and 84.8 ± 26.5 % respectively) (Avgerinos and Malamataris, 1990).

There are two potential areas of use for much smaller orally administered microencapsulated dosage forms which techniques such as solvent evaporation are able to provide.

The first is the production of sustained-release or taste-masked oral liquid preparations. The major problem in such formulations is to minimise the particle size of the drug carrier since the texture of the product in the mouth is important for patient acceptability. Leaching of drug from the microspheres when suspended in a liquid carrier is a major potential obstacle to the development of these systems. Most enteric polymers tend to be relatively impervious and so provided the suspending vehicle is at the correct pH, loss of drug should not be a problem. Indeed dosage forms with bitter drugs contained within Eudragit microspheres, produced by solvent evaporation, are under development (Colston and Crainich, 1990).

Sustained-release microparticulate suspensions of the poorly water-soluble drugs, indomethacin (Bodmeier and Chen, 1989a) and ibuprofen (Iwamoto et al., 1988), have been proposed. Leaching is more of a problem when developing sustained-release formulations for hydrophilic drugs, but can be overcome by the prior adsorption of the drug onto ion-exchange resin beads, which are then suspended in an ion-free vehicle (Raghunathan et al.,

1981).

Another potential application of orally-administered particulate carriers is for the delivery of vaccines and therapeutic proteins and peptides. There is increasing evidence for the intact uptake of very small (probably less than 5 μm) particulates when administered by the oral route, with the uptake considered to take place through the Peyer's patches in the intestine (Jani et al., 1989). The number of particles taken up in this way is probably small, but for therapeutic agents with very small dosage requirements, and in particular vaccines, this might prove to be a viable route of administration (O'Hagan et al., 1991).

1.1.4.3. Other routes

Systemic drug delivery by the nasal route is currently generating considerable interest, since it appears to be a suitable site for the absorption of peptides and proteins (Chien et al., 1989). However, without the use of absorption enhancers, the bioavailability of these molecules is invariably low, but has been shown to be increased by administering the drug in bioadhesive microspheres (Illum et al., 1990). The enhanced absorption from the bioadhesive formulation was probably a result of a reduced rate of nasal clearance.

Another route of administration in which rapid clearance reduces drug bioavailability is the eye. Here also, particulate drug carriers have been used in an attempt to prolong contact between drug carrier and eye (Harmia et al., 1986; Fitzgerald et al., 1987).

1.1.5. Summary

Microsphere-based formulations hold great promise for improving the therapeutic performance of drugs administered by a number of routes and such delivery-systems are now

beginning to reach the marketplace.

Of the various techniques available for microsphere production, the one chosen will depend on a number of factors including:

- a) The size of drug carrier required.
- b) The encapsulating polymer to be used.
- c) Solubility characteristics of drug.
- d) Physical stability of drug and polymer in different solvents.
- e) Practicality and economics of large scale-production.

The emulsification/solvent evaporation technique is suitably versatile that it can be adapted to meet most of these requirements and accounts for its widespread usage.

1.2. THE COLON AS A SITE FOR DRUG-DELIVERY

1.2.1. Introduction

There is currently intense interest in the colon as a site for drug absorption and targeted drug release. Until recently, this portion of the gastrointestinal (GI) tract was largely neglected when considering oral drug delivery, and interest was confined to rectally administered dosage forms i.e. enemas and suppositories.

There are primarily three reasons for the current interest in the colon as a site for drug-delivery:

1. With the advent of gamma scintigraphy for the study of the GI transit of dosage forms, it has become apparent that small intestinal transit times are significantly less than previously thought. As a consequence, many sustained release oral dosage forms may be spending a considerable period of their drug-releasing lifetime in the colon. Thus knowledge of the colon absorption characteristics of the drugs in question are crucial, to ascertain whether or not a sustained-release system is appropriate.

2. The second reason for an interest in the colon is as a site for local treatment of colonic disease. The major stimulus for research in this the area is the demand for dosage forms capable of delivering 5-aminosalicylic acid into the colon for topical treatment of inflammatory bowel disease. Targeted delivery is required since this drug is well absorbed from the small intestine and, as a result, not available for topical action in the colon.

3. A proliferation of novel molecules arising from biotechnology is injecting new impetus into research of the feasibility of oral peptide/protein delivery. The colon is of particular interest in this respect since the luminal pH and enzyme content are considered to be more favourable to

peptide/protein stability than the rest of the GI tract.

Later sections of the chapter will consider these issues in more detail, including strategies for targeting drugs into the colon.

1.2.2. Structure and function of the colon

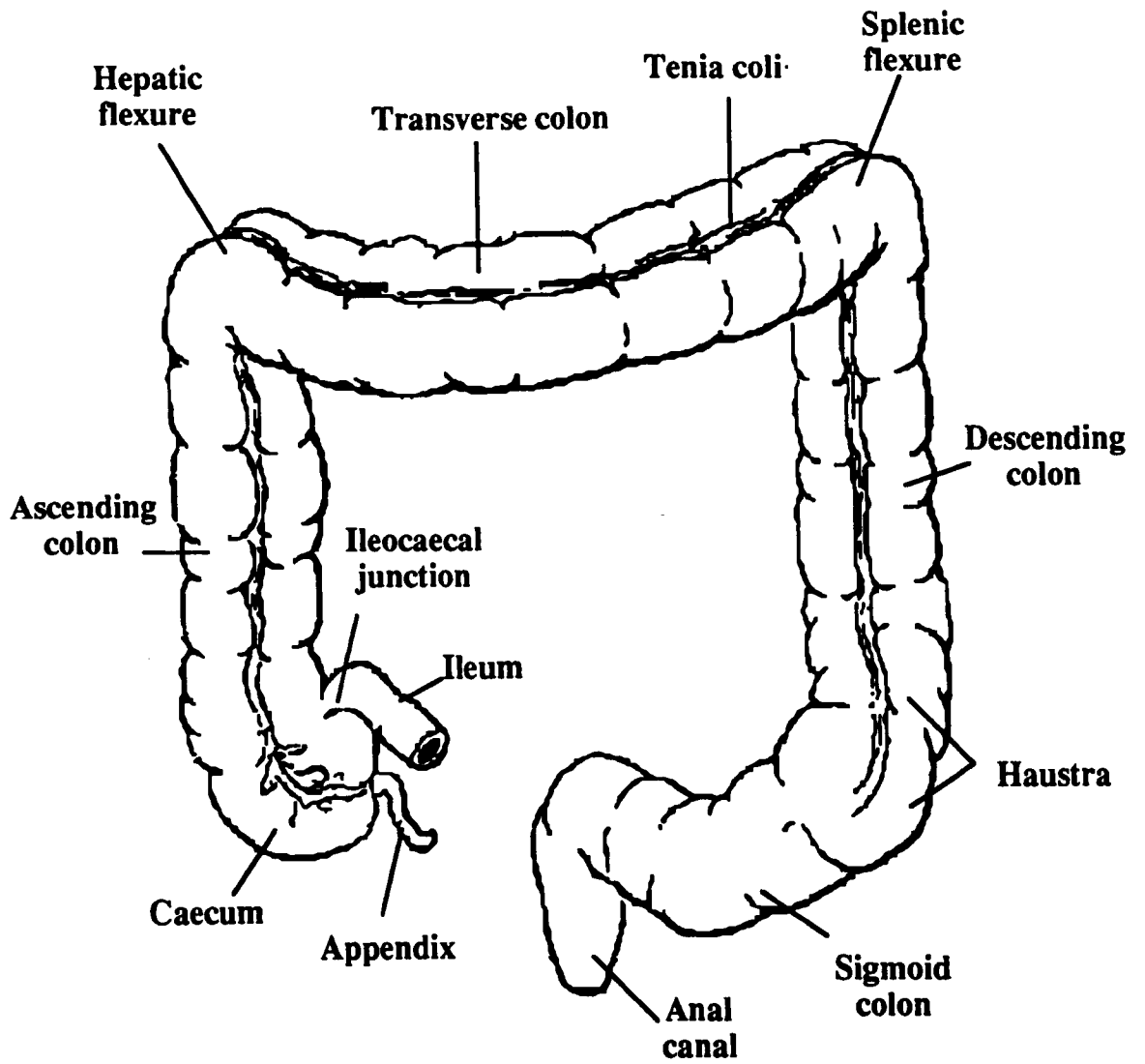
The colon forms the lower part of the GI tract, extending from the ileo-caecal junction to the anus. Its general function is to consolidate the intestinal contents into faeces by the absorption of water and electrolytes, and to store the faeces until excretion. The slow movement of materials through the colon also allows a large bacterial population to thrive, which has important nutritional implications in some mammals (Christensen, 1987).

The colon is divided into a number of anatomical regions, namely the caecum, the ascending colon, the hepatic flexure, the transverse colon, the splenic flexure, the descending colon, the sigmoid colon and the rectum/anal canal (figure 1.5).

The intestinal contents (chyme) enter into the colon from the ileum through the ileo-caecal junction. The caecum forms a pouch, about 6.5 cm long, above which lies the ascending colon, approximately 20 cm in length extending to the hepatic flexure. Between the hepatic and splenic flexures lies the transverse colon, 40-50 cm in length. The descending colon extends for 30 cm and then becomes the sigmoid colon, between 15 and 50 cm in length. The colon ends with the rectum and anal canal (Haubrich, 1985).

In common with rest of the GI tract, the colon wall contains three layers of muscle, two longitudinal and one circular which allow mixing and propulsive movements to take place (Ganong, 1981). In the colon however, the outer layer of longitudinal muscle is concentrated into three

Figure 1.5. Anatomy of the human colon.



bands, the teniae coli. Between these bands the longitudinal muscle is still present but it is very thin, which allows the inner layer of circular muscle to form outward bulges. At regular intervals, there are tight contractions of circular muscle resulting in formation of the haustra (Christensen, 1987)(see figure 1.5).

Activity in the colon consists of two modes, segmental and propulsive. Segmenting movements, effected by circular muscle and causing the appearance of haustra, predominate and result in mixing of the luminal contents (Steed et al., 1989). The mixing function has been demonstrated by a study involving administration of different-sized radiopaque discs 36, 24 and 12 hours before X-ray imaging of the colon. The images showed the discs to be out of chronological order with some of the most recently administered having travelled furthest (Halls, 1965). Significant propulsive activity, effected by longitudinal muscle, is less common and in humans occurs an average of three or four times daily (Steed et al., 1989). The predominant activity is considered to depend on the function of the different colon regions. Retrograde movements are common in the proximal portions of the colon and serve to increase the retention of material in the ascending colon and caecum. In the middle section of the colon, segmenting movements result in a slow progression of faeces towards the rectum, whereas in the distal portions of the colon propulsive activity, associated with defecation, predominates (Christensen, 1987).

Each day, approximately 1500 ml of chyme enter the colon from the ileum, from which more than 90% of the fluid is absorbed (Phillips and Giller, 1973). Fluid and salt absorption is assisted by the segmenting movements which circulate the chyme across the colonic mucosa. In the healthy human colon, sodium and chloride ions are usually absorbed, while potassium and bicarbonate ions are usually

secreted (Binder and Sandle, 1987).

The progressive absorption of water as material passes along the colon results in a progressively solidifying mass. Whereas the contents of the caecum and ascending colon are fluid and semi-solid, in the transverse colon solidification commences, while in the descending colon, solid faeces has formed (Steed et al., 1989).

1.2.3. Colon environment

1.2.3.1. Microorganisms

All parts of the GI tract contain microorganisms, but in the human the greatest population by far is found in the colon. Over 400 species of bacteria are present and a small number of fungi. Anaerobic bacteria predominate and the most prevalent species are Bacteroides, Bifidobacterium, and Eubacterium (Simon and Gorbach, 1987).

The principal source of nutrition for the colonic microflora are undigested polysaccharides. These include starch, lactose and various other di- and trisaccharides. Also digested by the bacteria for their energy content are some of the non-starch polysaccharides (dietary fibres). The main products of fermentation are short chain fatty acids, carbon dioxide, methane and hydrogen (Rubinstein, 1990).

1.2.3.2. pH in the colon

Radiotelemetry has been used to measure the gastrointestinal pH in healthy human subjects. The highest pH levels (7.5 ± 0.5) were found in the terminal ileum. On entry into the colon, the pH dropped sharply to 6.4 ± 0.6 . The pH in the mid-colon was measured at 6.6 ± 0.8 and in the left colon, 7.0 ± 0.7 (Evans et al., 1988). The drop in pH on entry into the colon is probably due to the presence of short chain fatty acids arising from the bacterial fermentation of unabsorbed polysaccharides.

Polysaccharide drugs and dietary content can affect the colonic pH. For example, the laxative, lactulose, a semi-synthetic disaccharide, is fermented by the colonic bacteria to produce considerable amounts of lactic acid. This results in acidification of the colon contents with the pH dropping to about 5 (Avery et al., 1972). The in vitro fermentation of two other pharmaceutical polysaccharides, ispaghula and guar gum, in the presence of faecal bacteria also resulted in a fall in pH (Tomlin and Read, 1988).

A diet high in dietary fibre would result in a high colonic concentration of unmetabolised polysaccharides and would presumably also cause a reduction in colonic pH.

1.2.3.3. Faecal content

By weight, faeces is typically 75% water. Of the solid material, about 30% is bacteria, 15% inorganic materials (principally calcium and phosphates), 5% fat, and the remainder mainly undigested plant fibres (Ganong, 1981).

1.2.4. Issues of importance to drug delivery

1.2.4.1. Transit of materials through the colon

Traditionally, GI transit has been measured by oral administration of a marker (e.g. radiopaque pellets) followed by monitoring of its appearance in the stools (Hinton et al., 1969). More valuable information on transit can be obtained by administration of radiopaque pellets followed by regular X-rays (Hossain et al., 1990), although the drawback of this technique is the high radiation exposure received by the subjects being examined.

Gamma scintigraphy has proved to be a more valuable method for measuring transit times through the GI tract (Digenis and Sandefer, 1991; Wilding et al., 1991; Wilson and Washington, 1988). A major benefit is the considerably reduced radiation dose received by the patient compared to

X-ray techniques; whereas when using radiopaque markers, images are generally only recorded daily to minimise radiation exposure, this problem is not encountered with gamma scintigraphic investigations. This allows frequent images to be recorded and yields considerably more information on the dynamics of GI transit.

The total transit of a dosage form through the GI tract can essentially be divided into three phases, gastric, small intestinal and large intestinal.

Gastric emptying of dosage forms is highly variable and depends principally on whether the subject is fed, and the physical properties of the dosage form such as size and density (Wilson and Washington, 1988). The emptying of non-disintegrating single units from the fasted stomach in one study varied from 15 minutes to more than three hours (Kaus et al., 1984). The presence of food may result in prolonged retention of the dosage form and in some cases, with regular feeding, dosage forms have been seen to reside in the stomach for periods in excess of 11 hours (Davis et al., 1984a; Wilson et al., 1989).

The small intestinal transit time is less variable. A summary of 201 gamma scintigraphic studies reported that the mean small intestinal transit time was 3-4 hours and appeared to be independent of the type of dosage form (single units, pellets, solutions) and whether the subject was in a fed or fasted state. The longest times recorded were in excess of 6 hours whereas the shortest were less than 1 hour (Davis et al., 1986).

Therefore, a non-disintegrating, orally administered dosage form can potentially arrive at the colon within less than four hours after administration.

In comparison to the other regions of the GI tract,

movement of materials through the colon is slow. The total time for transit tends to be highly variable and influenced by a number of factors such as diet, in particular dietary fibre content, mobility, stress, disease and drugs (Barrow et al., 1991).

A. Transit under normal conditions

There have been a number of detailed studies of transit through the colon. Using a radiopaque marker technique, transit times in a group of 73 healthy adults have been estimated. For the male subjects, mean time to the hepatic flexure was 8 h and to the splenic flexure, 14 h, with a mean total colon transit time of 31 h. For the female subjects, movement of markers was considerably slower with transit taking 11 h to the hepatic flexure and 21 h to the splenic flexure, with a mean total transit time of 39 h (Metcalf et al., 1987).

The effect of gender on transit is unclear since some studies have found slower transit in females (Abrahamsson et al., 1988; Metcalf et al., 1987) whereas others have shown no difference (Hinds et al., 1989; Wyman et al., 1978).

Five 5 mm radiolabelled non-disintegrating tablets were administered to six healthy subjects on three consecutive days. In all cases, the tablets were found to become widely dispersed on passage through the colon. The transit rates varied considerably, with the mouth to anus transit time for a group of five tablets varying from 18 hours to 72 hours. The mouth to colon component of total transit was between 2 h and >11 h (Khosla and Davis, 1989).

The GI transit of a non-disintegrating osmotic tablet ("Oros") has been measured in six subjects. On a fasted stomach, gastric emptying was rapid with a mean of 0.8 h. Mean small intestinal transit was 3.0 h. Movement through

the colon was considerably more variable with a median transit time of 20.9 h. In one of the subjects, colon transit was exceptionally fast at just 2.5 h, giving a whole gut transit time of just 6 h (Davis et al., 1988).

Findlay et al. (1974) suggested that under certain conditions the rate of transit of solid and liquid phases through the colon could differ. In a group of healthy volunteers receiving a 20 g/day bran supplementation, "streaming" of solid and liquid phase markers occurred with the liquid travelling faster than the solid. On the other hand, in patients with diverticular disease, the solid phase travelled more quickly than the liquid phase.

A number of more recent studies have also investigated the rate of transit of different phases and sizes of material through the colon.

The colonic transit rate of 0.5-1.8 mm indium-labelled beads, delivered as a bolus into the colon in an enteric-coated gelatin capsule, has been compared to a radiolabelled liquid phase. When the capsule containing the beads arrived at the colon, 10 ml of technetium-DTPA solution was infused into the colon through an oro-caecal tube at a rate of 1 ml/min. The two phases were seen to empty simultaneously from the ascending colon. The transit rate through the other regions of the colon was also identical, suggesting no discrimination between solid and liquid phases in normal subjects (Proano et al., 1991).

In a related study, the transit rate of 0.5-1.8 mm radiolabelled beads was compared to the transit rate of 6 mm diameter pieces of radiopaque tubing. The mean transit time of the radiopaque markers through the ascending colon was 9.9 ± 3.8 h and for the beads, 11.9 ± 2.0 h. This difference was statistically significant ($p < 0.05$) (Proana et al., 1990)

A study of the effects of capsule size and density on colon transit has been reported. Although capsule transit was found not to depend on density, there was a tendency for the transit rate to increase with size. However, intersubject variability was considerable and there was no significant difference in transit between the different sizes (0.3, 0.8 and 1.8 cm³). In general, 50% of the dosage forms reached the splenic flexure within 7 hours of entering the colon (Parker et al., 1988).

A comparison of the simultaneous colonic transit rate of a radiotelemetry capsule (25 mm long x 9 mm diameter) and radiolabelled ion-exchange resin beads (0.5-1.8 mm diameter) has been carried out. Although both the beads and the capsule entered the colon simultaneously, the transit of the capsule through the ascending colon appeared to be more rapid, reaching the hepatic flexure ahead of 86% of the beads, which became widely distributed. Whole colon transit of the capsule varied widely, ranging from 13 h to 68 h (Hardy et al., 1985).

From the studies described above, there is evidence to suggest that the rate of transit of material through the colon may be size-dependent.

B. Effects of disease on colon transit

Diseases affecting colon transit have important implications for drug delivery. Disorders which may cause diarrhoea and an increase in colon transit include the inflammatory bowel diseases (ulcerative colitis and Crohn's disease), irritable bowel syndrome, coeliac disease and lactose intolerance (Barrow et al., 1991).

Consequences of accelerated transit might be a reduction in the bioavailability of drugs generated by colonic bacterial metabolism and compromised performance from sustained-release formulations (Read and Sugden, 1987).

The effect of ulcerative colitis on gastrointestinal transit has been investigated using gamma scintigraphy. A group of six patients was used, two with active disease at the time of the study. The residence time of individual tablets in the ascending colon varied from as little as 0.8 hours to greater than 20 hours. Combined residence times in the ascending and transverse colon were about seven hours in the two subjects with active disease, and in excess of 17 hours in the remainder (Hardy et al., 1988).

C. Effects of diet

The principal component of diet which can influence colon transit is dietary fibre content. In general, dietary fibre supplementation increases faecal weight and reduces the colon transit rate. For example, addition of 20 g/day of bran to the diet of a group of healthy subjects increased stool weight by 127% and reduced whole gut transit from a mean of 73 ± 24 h to 43 ± 7 h (Cummings et al., 1978). In another study, the same level of bran supplementation reduced whole gut transit from 66 ± 18 h to 50 ± 11 h, with a 50 % increase in stool weight (Findlay et al., 1974).

A cross-over study investigating the effects of two levels of fibre intake on the GI transit of a radiolabelled tablet and radiolabelled beads has been reported. A group of four vegetarian and four omnivore subjects received diets containing 15 or 40 g/day dietary fibre for six days prior to the scintigraphic investigation. The results for colon transit were generally inconclusive. For the omnivores, the tablet residence time in the colon was similar at both fibre levels with a mean ascending colon residence time of 267 minutes for the high fibre and 245 minutes for the low fibre diet. Surprisingly, for the vegetarians, colon transit was in both cases slower than for the omnivores with mean ascending colon residence times for the tablet of 405 and 627 minutes for the high and low fibre diets respectively (Price et al., 1991a).

The intrinsic variability of colon transit has been assessed by administering radiolabelled tablets to a group of subjects receiving a controlled diet providing 25 g/day of dietary fibre. Despite the same food intake, colon transit times were extremely variable (Price et al., 1991b).

D. Effects of drugs

Many drugs are known to reduce or increase colonic motility (Beeley and Stewart, 1987).

An obvious cause of drug-induced diarrhoea is from laxative abuse. Magnesium-based antacids in large quantities may also cause diarrhoea as a side-effect.

Antibiotics, in particular those with a broad spectrum of activity, may cause diarrhoea, probably a result of effects on the colonic microflora leading to overgrowth of particular species. A less common, but more serious complication of antibiotic therapy is pseudomembraneous colitis. This condition is caused by overgrowth of Clostridium difficile which in turn produces a toxin which damages the colonic mucosa leading to diarrhoea. Other drugs which can cause colitis include vasopressin, oral contraceptives and non-steroidal antiinflammatory agents.

Drugs causing constipation include the opiates and anticholinergics and high doses of aluminium hydroxide and calcium carbonate antacids.

1.2.4.2. Colonic microflora

The colonic bacteria appear to have the ability to transform many drug substances.

Some drugs are converted into pharmacologically active species by the action of colonic bacteria. Examples include the glycoside cathartics, cascara and senna (Peppercorn and

Goldman, 1976), the disaccharide, lactulose (Avery et al., 1972), and sulphasalazine (Das et al., 1974). The colonic metabolism of sulphasalazine has been the prime stimulus for a variety of colon-targeting strategies, explained in detail in later sections.

The action of other drugs may be prolonged by colonic microflora. Many drugs are excreted into bile as inactive sulphate or glucuronate conjugates. Cleavage of the conjugating function by bacterial action will yield free drug which may then be reabsorbed from the colon. Drugs whose action may be prolonged in this way include stilboestrol, morphine, and indomethacin (Peppercorn and Goldman, 1976).

There is also the potential for the generation of toxic drug species by bacterial action. Drugs for which colonic metabolism has been implicated in causing toxicity include L-dopa and chloramphenicol. In the case of chloramphenicol, aplastic anaemia has only been reported in patients taking the drug orally. It has been suggested that this type of toxicity is confined to patients whose microflora contain organisms capable of converting chloramphenicol into suitable toxic metabolites (Holt, 1976).

Similarly, there are examples of drugs whose efficacy is reduced when exposed to colonic bacteria. A pharmacokinetic evaluation of an enteric-coated digoxin preparation revealed that in some subjects a large proportion of the drug was converted to its inactive dihydro- derivative. It was suggested that bacterial metabolism of the drug was responsible (Magnusson et al., 1982).

It has been suggested that atropine may also be subject to colon inactivation (Peppercorn and Goldman, 1976).

1.2.4.3. Absorption of drugs from the colon

On the surface, the colon would appear to have few desirable properties conducive to efficient drug absorption. In comparison with the small intestine, its surface area is small. Additionally the progressive absorption of water means that the further one travels around the colon, the more viscous the contents will become. This will theoretically reduce the dissolution rate of particulate drug and slow the diffusion of dissolved drug to the mucosa. Nevertheless, many drugs appear to be well absorbed from the colon. It is the slow transit rate that is the major compensatory factor in achieving good colonic drug absorption.

However, the colon is a more selective site for drug absorption than the small intestine. Drugs shown to be well absorbed include glibenclamide (Brockmeier et al., 1985), diclofenac (Gleiter et al., 1985), theophylline (Staib et al., 1986), ibuprofen (Wilson et al., 1989), metoprolol (Godbillon et al., 1986) and oxprenolol (Antonin et al., 1985).

Drugs whose absorption from the colon is reduced by comparison to other parts of the GI tract include frusemide (Bieck, 1989), piretanide (Brockmeier et al., 1986), buflomedil (Wilson et al., 1991), and lithium, which is not absorbed at all (Erlich and Diamond, 1983).

The absorption of digoxin was found to be reduced when the colon was diseased. In healthy subjects, relative bioavailability from the colon was found to be 85%. In a group of four patients suffering from ulcerative colitis, the bioavailability was reduced to 9% (Ochs et al., 1975).

The poor absorption of many drugs in the colon may be due to the fact that epithelial cell junctions are very tight (Powell, 1981) and as a consequence the predominant route

of absorption will be transcellular, which favours hydrophobic molecules. Thus in the rat, the rates of absorption of two hydrophilic drugs, hydrochlorothiazide and atenolol, were found to be uniform throughout the small intestine, but fell dramatically on entry into the colon (Taylor et al., 1989).

Less is understood about regional differences in drug absorption within the colon. However, absorption might be expected to be less efficient in the distal regions of the colon, where the luminal contents are viscous and have a low water content. The bioavailability of diclofenac was the same whether distilled into the colon at the caecum or at the splenic flexure, but since the colon was cleansed by enema prior to drug administration, the study merely demonstrated that the permeability of the mucosa to the drug was the same at both locations (Gleiter et al., 1985). A capsule containing ciprofloxacin was remotely triggered to release its contents into different portions of the gastrointestinal tract. Colonic absorption was poor compared to the small intestine. However, within the colon, drug absorption from the descending colon was reduced by comparison to the ascending colon (Staib et al., 1989).

Studies with an "Oros" system containing oxprenolol have demonstrated the importance of the colon in determining drug bioavailability from sustained release dosage forms. In a subject in which the device was resident in the colon for just 2.5 h, the absolute bioavailability of oxprenolol was 13.8%, with 79% of the dose remaining in the excreted tablet. On the other hand, in a subject where the device took 27.5 h to pass through the colon, the bioavailability was 54.3% with only 14.3% of the dose remaining in the excreted tablet (Davis et al., 1988).

Absorption from the majority of the colon is into the superior and inferior mesenteric veins. These veins become

part of the portal venous system and drain directly into the liver. Thus drugs absorbed by this route will be subjected to first pass metabolism. The lower rectum and anal canal ultimately drain into the vena cava and thus drugs absorbed here may avoid the first pass effect. However, there are many anastomoses between rectal veins and so even absorption from the lower rectum/anal canal may result in a first pass through the liver (Steed et al., 1989).

Since it now apparent that many sustained-release dosage forms rely on a degree of colonic absorption to remain therapeutically effective (Davis et al., 1988; Wilson et al., 1989), when designing such formulations it is clearly essential to establish the absorption characteristics of the drug in question. If the drug is only poorly absorbed from the colon, a sustained release dosage form may be wholly inappropriate. Knowledge of colon absorption may also be of importance when developing enteric-coated dosage forms. Poor bioavailability from a erythromycin tablet was thought to be a result of its enteric coat resisting dissolution until pH 6.5. This probably resulted in tablet disintegration beyond the proximal small intestine, the main absorption site for erythromycin (Watanabe et al., 1977).

1.2.5. Reasons for targeting drugs into the colon

1.2.5.1. Local treatment of colonic disease

A major stimulus for the development of delivery systems targeted at the colon has been to improve the treatment of colonic disease, in particular the inflammatory bowel diseases (IBD): Crohn's disease and ulcerative colitis.

A. Inflammatory bowel diseases

i). Clinical features

The inflammatory bowel diseases are principally diseases of Western societies and have a prevalence of 5-

7/100,000/year, with the incidence being greater in whites than non-whites. The cause is unknown, although infection, diet, immune disorders and genetic influences have all been suggested (Gaska and Sarafpour, 1989; Baker, 1988).

Crohn's disease most commonly involves the terminal ileum and colon, although any part of the GI tract may be affected. The disease is characterised by inflammation extending through all layers of the gut wall which may ultimately lead to the formation of fistulae. The inflammation is not continuous however, and healthy tissue may remain around the diseased areas. The clinical features of Crohn's disease depend upon its site but may include diarrhoea, abdominal pain and weight loss (Gaska and Sarafpour, 1989; Baker, 1988).

Ulcerative colitis generally remains confined to the rectum, although it can affect the whole colon. Unlike Crohn's disease, tissue inflammation and ulceration is confined to the mucosa. The most prominent clinical features are abdominal pain and the passage of bloody diarrhoea (Gaska and Sarafpour, 1989; Baker, 1988).

IBD tends to be associated with periods of illness interspersed with periods of remission, sometimes lasting months or years (Gaska and Sarafpour, 1989; Baker, 1988).

ii). Treatment

The mainstay of IBD treatment for many years has been sulphasalazine (salicylazosulphapyridine; SASP). The drug was originally developed as a treatment for rheumatoid arthritis and combines the sulphonamide antibiotic, sulphapyridine (SP), and 5-aminosalicylic acid (5-ASA), with the two molecules linked by an azo bond (-N=N-) (figure 1.6).

The rationale behind the design of SASP was based on two

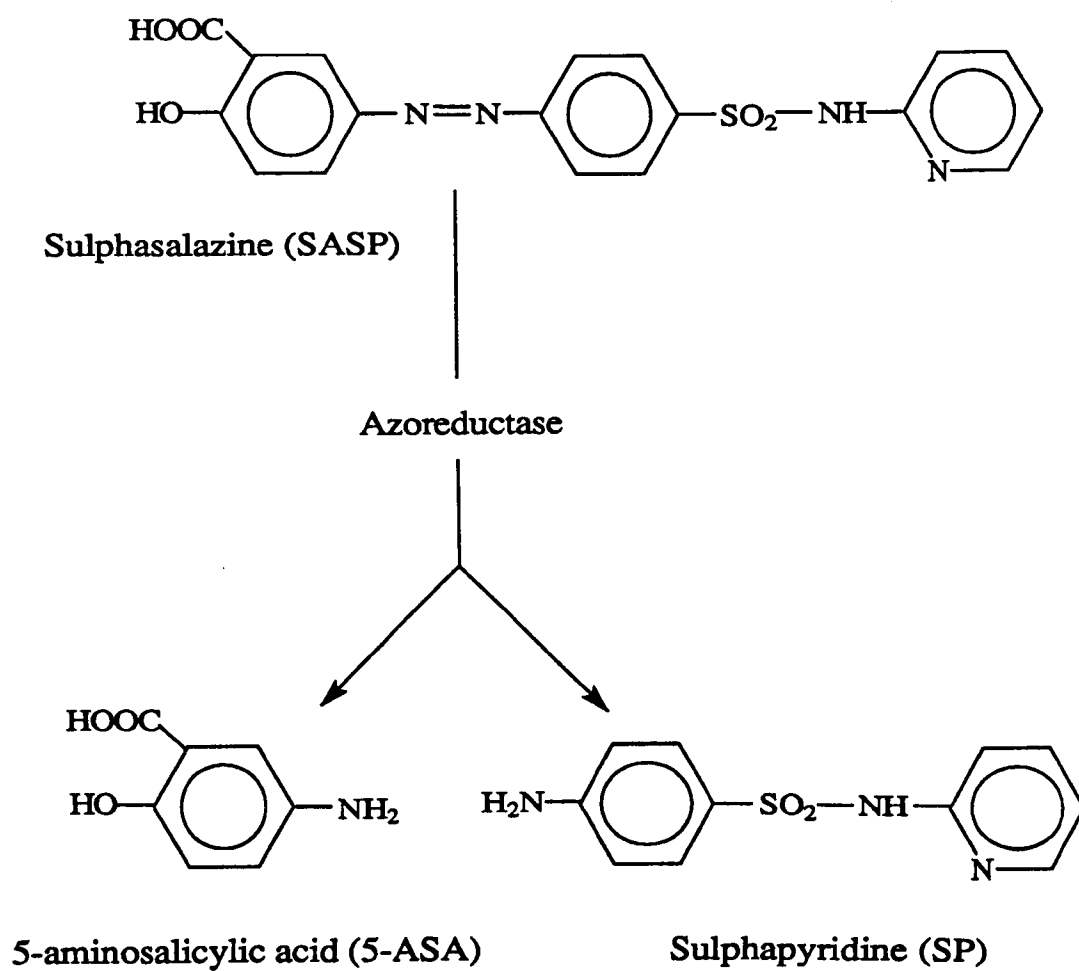
factors: i) rheumatoid arthritis was thought at the time to be bacterial in origin and, ii) it responded to treatment with the salicylate, aspirin. Thus a molecule was synthesized containing a salicylate and an antibacterial (Svartz, 1942).

Although the drug was reasonably successful in the treatment of rheumatoid arthritis, its effectiveness in patients with IBD was dramatic. However, it is only comparatively recently that its mechanism of action has been understood (Azad Khan et al., 1977).

SASP is essentially a prodrug and at least 85% of an oral dose passes unabsorbed into the colon (Klotz, 1985). In the colon, the action of azoreductase enzymes cleaves SASP into its two constituent molecules, 5-ASA and SP (figure 1.6). The azoreductase activity predominantly arises from bacteria, although tissue-based enzymes also play a minor role (Azad Khan et al., 1983). 5-ASA is largely unabsorbed from the colon where it is thought to exert topical antiinflammatory activity, whereas SP is largely absorbed and gives rise to side-effects (Klotz, 1985). SP-induced toxicity is a major problem, and as many as 30% of patients are unable to tolerate treatment with SASP (Peppercorn, 1984).

Although it is not universally accepted that its only role is as a carrier for 5-ASA (Hayllar and Bjarnason, 1991), because of the toxicity of SP, there has been considerable interest in the use of 5-ASA alone as a treatment for IBD. Unfortunately, since 5-ASA is well absorbed from the small intestine (Jarnerot, 1989), it is unavailable for topical action in the colon if administered in a conventional oral dosage form. It has been the desire to deliver 5-ASA directly into the colon by the oral route that has led to the development of a number of novel colon delivery systems, to be discussed later in this chapter.

Figure 1.6. Colonic metabolism of sulphasalazine.



The second major class of drugs used in the treatment of IBD are the corticosteroids. Whereas SASP and other 5-ASA based drugs are used for maintenance therapy and the treatment of mild attacks, corticosteroids are used for the treatment of more severe attacks (Piper et al., 1987). The major drawback of the corticosteroids are their wide-ranging side-effects (Haynes and Larner, 1975). Side-effects may also result from the systemic absorption of rectally applied drug (Farmer and Schumacher, 1970).

Corticosteroids with reduced systemic side-effects are under investigation. For example, beclomethasone dipropionate (Kumana et al., 1982) and tixocortol pivalate (Hanauer et al., 1986) are both rapidly metabolised on absorption into the systemic circulation and consequently side-effects are minimised.

Although drugs for topical action in the colon can be administered rectally, by enema or suppository, there are problems both in patient acceptability and in accessibility to the proximal colon.

The spread of rectally-administered dosage forms is limited. A 60 ml radiolabelled enema remained mainly confined to the rectum in healthy volunteers, though in subjects who had received a prior evacuation enema, spread as far as the ascending colon was seen (Jay et al., 1986). In another study, 50 ml enemas were mainly confined to the rectum and sigmoid colon, whilst with a 200 ml volume, spread as far as the transverse colon was observed. It was concluded that the optimum enema volume is probably 100 ml (Hardy et al., 1986). The spread of 5 ml of a radiolabelled foam enema was generally confined to the sigmoid colon in a group of IBD patients and was not significantly altered by increasing the volume to 50 ml (Farthing et al., 1979). The spread of enemas is probably greater in active colitis (Swarbrick et al., 1974; Campieri et al., 1986).

Thus for the treatment of inflammation in proximal regions of the colon, topically acting drugs need to be given by the oral route. Since many of these drugs are well absorbed from the small intestine (e.g. 5-ASA, corticosteroids), their effective use requires targeted delivery into the colon.

B. Other diseases

Other colon-targeting strategies might be for the delivery of anticholinergics for treatment of irritable bowel syndrome (IBS) or anticancer agents for treatment of colon cancer (Tozer, 1990).

1.2.5.2. Systemic delivery of drugs

The second major reason for wishing to target dosage forms into the colon might be to utilise the organ as a site for absorption of drugs for systemic therapy.

A. Conventional drugs

It was mentioned in section 1.2.4.3 that many sustained release oral dosage forms rely on colonic absorption to remain therapeutically effective in view of the relatively short period of residence in the small intestine. A number of drugs shown to be well absorbed from the colon were listed.

It is also conceivable that colon-targeted dosage forms containing absorbable drugs might offer novel therapeutic opportunities. For example, a colon-targeted device containing an antiinflammatory agent taken at bedtime might be useful in providing therapeutic levels of drug several hours later to relieve morning stiffness associated with arthritis.

B. Protein and peptides

A more elusive goal is to use the colon as a site for the oral delivery of therapeutic peptides and proteins.

Although there have been many reports of peptide and protein absorption following oral administration, bioavailability is invariably extremely low (Zhou and Li Wan Po, 1991; Lee and Yamamoto, 1990).

There are considered to be four barriers limiting the oral bioavailability of these molecules (Zhou and Li Wan Po, 1991):

1. Degradation in the acidic environment of stomach.
2. Enzymatic degradation in the GI tract.
3. Low mucosal permeability.
4. First pass metabolism by the absorbing membrane and the liver.

One of the attractive properties of the colon is often considered to be its relative lack of degradative enzymes compared to the stomach and small intestine. Although peptidase enzymes are present in the mucosal cells lining the colon, their level is very low compared to the small intestine (Longer et al., 1989). However the colon luminal contents contain large quantities of peptidase and protease enzymes produced by colonic bacteria (Woodley, 1991; MacFarlane et al., 1988). The stability of insulin and insulin B chain in the presence of luminal contents isolated from guinea pig colon has been examined (Ikesue et al., 1991). Whereas after eight hours incubation insulin showed minimal degradation, about 40% of the insulin B chain had degraded, suggesting that protein structure might be an important determinant of stability.

Even if peptide/protein stability could be ensured, by for example structural modification or coadministration of enzyme inhibitors, the molecule still needs to be absorbed. The use of penetration enhancers to increase mucosal permeability is being intensively investigated (Lee and Yamamoto, 1990) and colon-targeted protein/peptide delivery

systems employing these substances have been patented (e.g. Davies et al., 1986). Although penetration enhancers may indeed promote colonic absorption, they are unlikely to provide a practical solution since their action is generally non-specific and consequently many undesirable substances present in the luminal contents, such as bacterial enterotoxins, may also be absorbed, with potentially undesirable effects.

1.2.6. Methods for targeting drugs into the colon

There are essentially three practical mechanisms by which a delivery system can be targeted into the colon following oral administration, two of which rely on unique properties of the target organ.

The two unique properties of the colon which have been exploited are:

1. pH.
2. The presence of a large bacterial population.

The third, non-colon-dependent, mechanism which has been utilised is the time taken for the dosage form to travel to the colon.

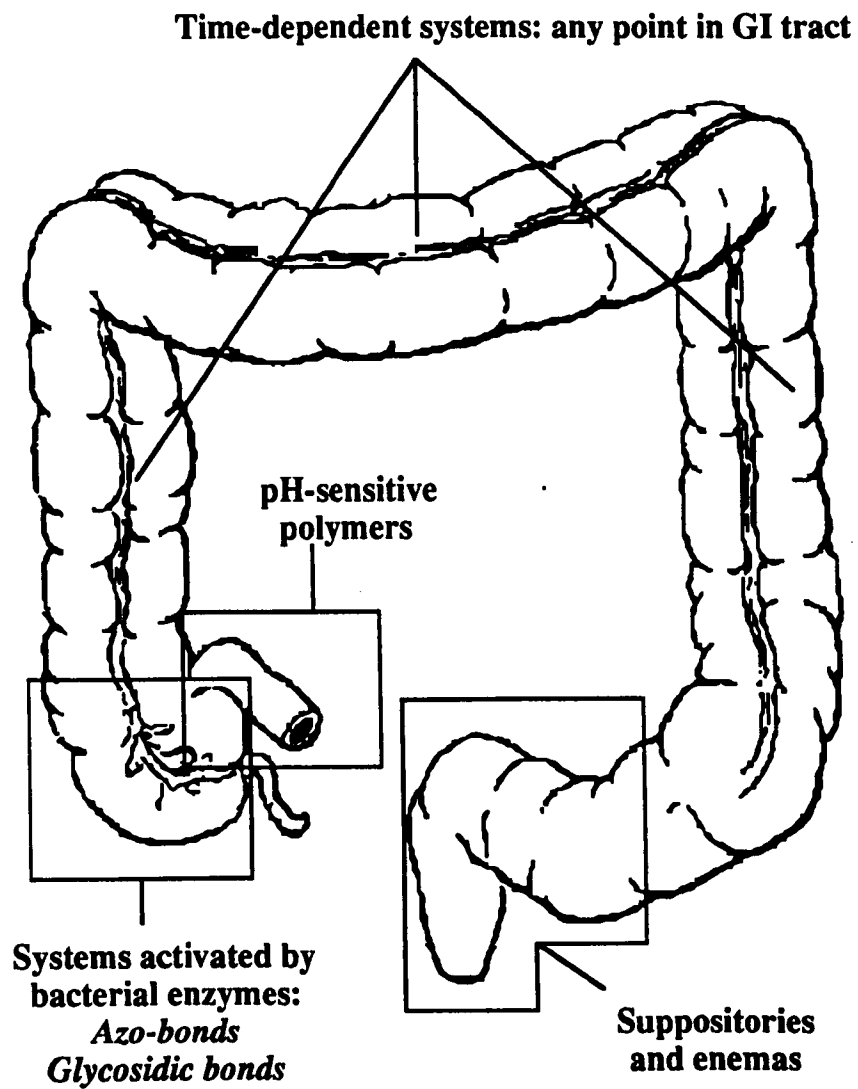
A summary of the different approaches to colon targeting is provided in figure 1.7 and will now be expanded in the following sections.

1.2.6.1. pH-triggered systems

Site-specific delivery into the small intestine has been achieved for many years by the use of enteric coatings. pH-sensitive coatings are also being utilised to achieve colon targeting of dosage forms.

As discussed in section 1.2.3.2, the pH in the terminal ileum and colon is higher than any other region of the GI

Figure 1.7. Strategies for targeting into the colon: the point of drug release from different delivery systems.



tract and thus dosage forms which disintegrate at suitably high pH levels have the potential for site-specific delivery into the colon.

The principal group of polymers utilised have been the Eudragits, and in particular Eudragits L and S, the properties of which were described in section 1.1.3.2.A. Eudragits L and S are enteric polymers which dissolve above pH 6 and 7 respectively.

Dew et al. first reported the use of Eudragit S as a colon-targetable coating in 1982. Hard gelatin capsules containing barium sulphate as a radiopaque marker and SP as a marker for drug release were coated with a 120 μm -thick coat of Eudragit S using an air suspension technique. Six subjects each swallowed six capsules. Twelve hours after administration, of the 36 capsules administered, 4 had broken in the distal ileum, 23 in the colon, and 9 remained intact. After 24 hours, four capsules remained intact.

This approach was extended to the evaluation of 5-ASA tablets, each containing barium sulphate and coated with an 80 μm -thick coat of Eudragit S. Eight patients received a total of 64 tablets. After 6 h, 24 tablets were in the stomach, intact, whilst the remaining 40 tablets were in the terminal ileum and ascending colon, and only two of these were intact. At 12 h, 20 tablets were in the stomach, and four tablets remained intact in the terminal ileum/colon. At 24 h, all tablets had reached the colon and had disintegrated (Dew et al., 1983). 5-ASA tablets coated with Eudragit S are now marketed for the treatment of mild to moderate ulcerative colitis (AsacolTM, SmithKline Beecham). (5-ASA is now commonly called mesalazine).

Since 5-ASA is well absorbed from the small intestine but poorly absorbed from the colon, urinary excretion of the drug is a good indicator of the quantity released at sites

proximal to the colon. Urinary excretion of about 20% of the dose of 5-ASA has been reported following administration of AsacolTM tablets, a quantity comparable to sulphasalazine administration (Dew et al., 1984). The colon-specificity of AsacolTM is also emphasized by the fact that stool dialysate concentrations of 5-ASA were twenty times higher than in subjects taking uncoated drug (Mardini et al., 1988).

The principal drawback of AsacolTM is from inadequate performance of the polymer coat; occasional failure of the tablets to disintegrate has been noted, with patients observing intact tablets in their stools (Schroeder et al., 1987). In addition, other drugs may affect the performance of AsacolTM. In particular, patients receiving AsacolTM tablets are warned not to take lactulose, since the acidification of the colon that it causes may prevent dissolution of the Eudragit S coat (Data Sheet Compendium, 1989).

Two 5-ASA tablets coated with Eudragit L are also available, ClaversalTM and SalofalkTM. These products are intended to deliver 5-ASA into the proximal small intestine and terminal ileum and as such are suitable for the treatment of Crohn's disease affecting these parts of the GI tract. A scintigraphic assessment indicated that in a group of 13 patients more than 70% of administered ClaversalTM tablets disintegrated in the small intestine, on average 3.2 h after gastric emptying (Hardy et al., 1987).

PentasaTM tablets consist of microgranules of ethylcellulose-coated 5-ASA. The tablets readily disintegrate in the stomach. The rate of release of 5-ASA from the dispersed granules is pH-dependent. In vitro, at pH 2 and pH 6, less than 90% of the drug was released after 24 hours, whilst at pH 7.5, an equivalent amount of drug

was released within 8 hours (Rasmussen et al., 1982). As for the Eudragit L-based tablets, Pentasa™ is particularly suitable for treatment of inflammation of the lower small intestine but not especially reliable for delivery of 5-ASA into the colon; with this preparation, about 50% of the administered dose of 5-ASA was excreted into the urine, indicating appreciable absorption proximal to the colon (Rasmussen et al., 1982).

Capsules coated with the enteric polymer, cellulose acetate phthalate (CAP) have been reported to enhance the delivery of the corticosteroid, beclomethasone dipropionate, to the terminal ileum. Ileostomy patients received drug-containing capsules that were uncoated, coated with shellac, or coated with CAP. The mean recovery of drug and active metabolite in ileostomy effluent was significantly greater when administered in CAP-coated capsules (43.0±24.1%) compared to shellac-coated (18.8±13.5%) or uncoated (13.5±8.5%) (Levine et al., 1987).

The Alza Corporation has patented osmotic pumps coated with pH-sensitive polymers for potential colon drug-delivery applications (Wong and Theeuwes, 1986, 1987).

1.2.6.2. Enzyme-triggered delivery systems

Both prodrugs and dosage forms from which the release of drug is triggered by the action of colonic bacterial enzymes have been devised.

A. Azo- bonds

The reduction of azo- bonds by the action of colonic azoreductase enzymes has been utilised to develop colon targeted prodrugs and polymers.

I. Prodrugs

The first azo- bond prodrug was, serendipitously, SASP. However, due to its toxicity, SP is not the ideal carrier

molecule for 5-ASA and consequently, a number of other 5-ASA prodrugs have been developed (figure 1.8).

The first of these to be introduced to the clinic is olsalazine (I), a dimer of 5-ASA (Campbell and Berglindh, 1988). This drug appears to be as effective as sulphasalazine in maintaining remission in ulcerative colitis (Sandberg-Gertzen et al., 1988) and in treating mild forms of the disease (Willoughby et al., 1988).

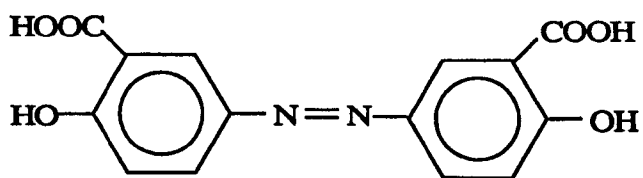
Other 5-ASA prodrugs include balsalazine (II) and ipsalazine (III). In these two molecules, 5-ASA is azo-linked to 4-aminobenzoyl- β -alanine and p-aminohippurate respectively (Chan et al., 1983).

5-ASA has also been azo-linked to polymers. One approach is based on a poly(vinylamine) backbone to which are attached benzenesulphonamide groups which in turn contain azo-bonded 5-ASA (termed as "polymer 7", IV). Release of 5-ASA from the polymer was demonstrated in vivo in rats and the compound was effective in reducing carrageenan-induced colon inflammation in guinea pigs (Brown et al., 1983).

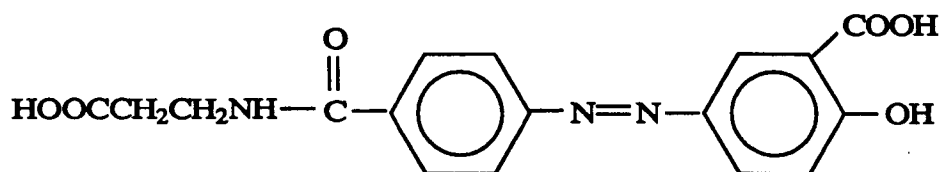
Polymeric prodrugs have also been produced by azo-bonding 5-ASA via a spacer group to poly(methyl vinyl ether-co-maleic anhydride), poly(vinyl-pyrrolidone-co-maleic anhydride) and to activated derivatives of dextran and poly[(2-hydroxyethyl)aspartamine]. When incubated with human colon contents, the dextran conjugate liberated 5-ASA at the same rate as sulphasalazine (Schacht et al., 1991).

Potentially bioadhesive polymeric 5-ASA carriers have been reported. To N-(2-hydroxypropyl)methacrylamide copolymers have been attached bioadhesive monosaccharides and, via azo bonds, 5-ASA. Copolymers containing fucosylamine monosaccharide moieties selectively bound to isolated guinea pig colon, with the degree of binding increasing

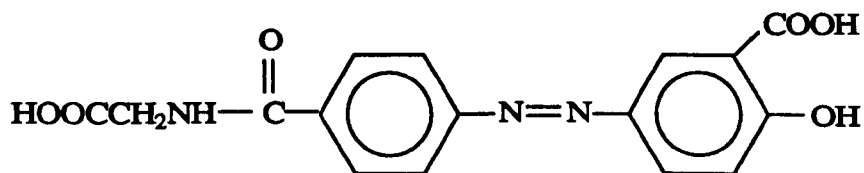
Figure 1.8. Structure of some 5-ASA prodrugs.



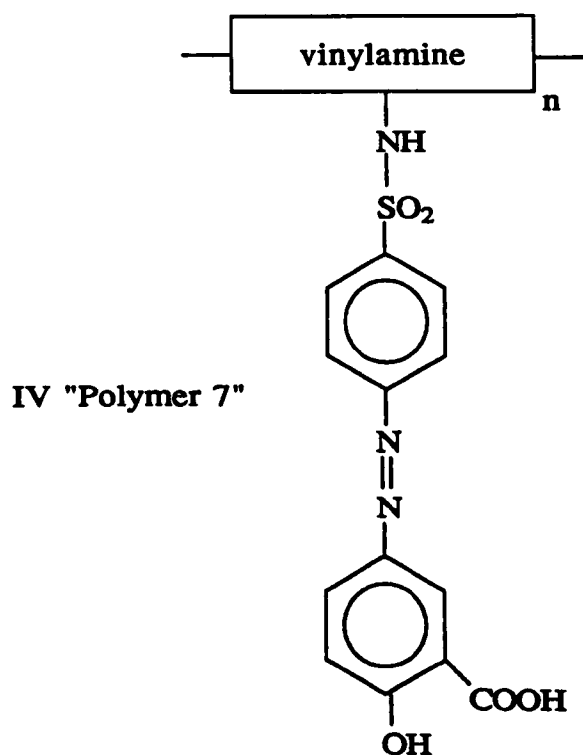
I Olsalazine



II Balsalazine



III Ipsalazine



IV "Polymer 7"

with fucosylamine content (Kopeckova et al., 1991).

II. Polymers

The first work in this field was published by Saffran et al. in 1986 and describes the synthesis of polymers of polystyrene and hydroxyethyl methacrylate cross-linked with divinylazobenzene. Insulin and vasopressin were administered to rats inside gelatin capsules and pellets coated with these polymers and delayed absorption was demonstrated.

Bronsted and Kopecek (1990) have produced hydrogels based on acrylic acid, N,N-dimethylacrylamide and N-ter-butyl-acrylamide crosslinked with 4,4'-di(methacryloylamino) azobenzene. At the low pH encountered in the stomach, the degree of swelling of the polymer is low. However, as it passes down the GI tract and the pH increases, the polymer begins to swell. By the time it has reached the colon, the hydrogel is sufficiently swollen to allow access to bacterial azoreductase enzymes. Cleavage of the azo-bonds should allow release of active compound included in the hydrogel matrix.

B. Glycosidic bonds

A number of delivery systems exploiting the saccharolytic abilities of colonic bacteria (mediated through glycosidase enzymes) have been reported.

I. Prodrugs

It was mentioned in section 1.2.4.2 that some commonly used laxative drugs are known to rely on colonic glycosidic activation to be therapeutically effective. More recently a number of glycosidic prodrugs have been designed in an attempt to achieve colon-specific delivery.

Friend and Chang (1984, 1985) have developed corticosteroid prodrugs by attachment to glycosidic carriers. The prodrugs

should theoretically pass unabsorbed into the colon where the glycoside bonds are cleaved by the action of bacterial glycosidase enzymes making the corticosteroid available for therapeutic action. A comprehensive review of the in vivo performance of these agents has been published (Friend, 1991). A degree of selective delivery of the corticosteroid into the caecum was achieved in the rat and guinea-pig. However, these animal models possess relatively high small intestinal glycosidase activity, and thus more selective delivery might be predicted in humans. Dexamethasone- β -D-glucoside was evaluated as a treatment for carrageenan-induced ulcerative colitis in guinea pigs. Compared to control, the number of large intestinal ulcers was significantly less in animals receiving the prodrug or unconjugated dexamethasone. A 0.65 $\mu\text{mol/kg}$ dose of prodrug was equieffective as 1.30 $\mu\text{mol/kg}$ dexamethasone supporting the hypothesis that the prodrug achieved higher caecal and colonic levels of free drug.

Colon targeted corticosteroids termed as "pro-antedrugs" have been reported. Corticosteroid derivatives which are readily metabolised into inactive metabolites following systemic absorption were synthesized ("ante-drugs"). To the ante-drugs were attached glycosidic functions to allow colon-targeting. Generation of free antedrug in the large intestine of guinea pigs and rats was demonstrated (Kimura et al., 1991).

The colonic microflora also possesses glucuronidase activity, thought to be responsible for prolonging the activity of some drugs (section 1.2.4.2). Glucuronide conjugates have been synthesized for two opiate antagonists, nalmefene and naloxone. Physiological effects concurrent with large intestinal activation of the prodrugs were reported (Simpkins et al., 1988).

II. Polymers

A number of delivery systems based on polysaccharides which are selectively degraded in the colon have been reported. One of the major problems in using these materials is that they are extremely hydrophilic and thus methods have to be devised to ensure that drug does not prematurely diffuse from the dosage form.

A potential colon-specific delivery system based on a poorly soluble pectate salt has been devised. The salt and indomethacin were compressed into a matrix and the release of drug evaluated in vitro. Under control conditions, release of indomethacin into pH 7 buffer was minimal. However, in the presence of pectinolytic enzyme or rat caecal content, release of indomethacin was significantly greater (Rubinstein and Radai, 1991).

Guar gum, locust bean gum, tragacanth and xylan have been mixed with Eudragit polymers and used to coat tablets. The in vitro release of drug from tablets coated with mixtures of Eudragit L and guar or Eudragit RL and guar was enhanced in the presence of glycosidic enzymes (Lehmann and Dreher, 1991).

Delivery systems based on the mucopolysaccharide, chondroitin, have also been proposed, with the solubility of the polymer being reduced by cross-linkage (Sintov et al., 1990).

1.2.6.3. Time-dependent delivery systems

The final major approach to colon targeting uses time as the release trigger. From gamma scintigraphic studies, the time of passage of dosage forms from mouth to colon is now well understood. As discussed earlier, although gastric emptying tends to be highly variable, small intestinal transit times are less so. Small intestinal transit rates would dictate that for successful colon delivery the device

should not release drug until 3-4 hours after leaving the stomach (section 1.2.4.1).

A delivery device using this basic concept has been developed. The PulsincapTM (Scherer DDS) is similar in appearance to a hard gelatin capsule, but the main body is water-insoluble. The contents are contained within the body by a hydrogel plug which is covered by a water-soluble cap. If necessary, the whole unit can then be coated with an enteric polymer. In vivo, once the cap has dissolved, the hydrogel begins to swell. When the swelling reaches a critical point, the plug pops out of the capsule body and the contents are released. Depending on the properties of the plug used, the time at which this occurs can be controlled (Pharmaceutical Journal, 1991).

A PulsincapTM has been used to assess the colonic absorption of captopril. A device with a 5 hour "pulse" was used, and in ten subjects the actual point of drug release ranged from 246 to 389 minutes (Wilding et al., 1991).

1.2.7. Summary

It is now appreciated that the colon can be an important site for the absorption of drugs from sustained release dosage forms. Although the surface area is low compared to the small intestine, this is compensated for by the markedly slower rate of transit. However, the colon is a more selective absorption site than the small intestine and tends not to favour hydrophilic compounds.

The colon has a number of features which allow site-specific drug delivery, the most important being the presence of a large bacterial population. This allows the design of enzyme-triggered delivery systems. Although pH- and time-dependent systems have also been designed these are inherently less reliable means of achieving colon-specific delivery.

Targeted dosage forms are of particular interest for the delivery of drugs that are well absorbed from the small intestine, yet are required for local topical action in the colon to treat IBD e.g. 5-ASA and corticosteroids.

For the future, the colon may become a viable site for the absorption of peptides and proteins although there are major obstacles to be overcome, in particular stability against bacterial protease and peptidase enzymes and diffusion through the poorly permeable colon epithelium.

1.3. AIMS OF THE THESIS

The aim of the work carried out in this thesis was to investigate the use of microspheres as potential colon drug-delivery systems.

Preliminary work was to focus on the development of microspheres using the solvent evaporation technique. It was planned to use the Eudragit family of polymers to encapsulate agents active in the treatment of inflammatory bowel diseases. It was hoped that characterisation of the microspheres using a number of different techniques would provide a further insight into their mechanism of formation.

There were primarily two reasons for the interest in microspheres for colon delivery. Firstly, multiparticulate dosage forms become widely dispersed in the small and large intestine. This characteristic might be useful for the treatment of widespread inflammatory disease. Secondly, there was evidence to suggest that small particles travel through the colon more slowly than large. There was thus a possibility that colon retention could be enhanced by using a multiparticulate-type dosage form.

To investigate size-transit rate phenomena, fundamental studies on the rate of transit of different-sized radiolabelled particles through the human colon were to be undertaken using gamma-scintigraphy. This work was planned in both healthy subjects and in patients suffering from diseases which increased colon motility.

Ultimately it was hoped that a biopharmaceutical evaluation of drug-polymer microspheres in the human colon could be undertaken. This would require the development of a technique for radiolabelling the microspheres.

CHAPTER 2.

PREPARATION OF MODEL EUDRAGIT NANOPARTICLES AND
MICROPARTICLES AND THE EFFECTS OF CHANGING MANUFACTURING
PARAMETERS ON THEIR PROPERTIES.

2.1. INTRODUCTION

The first experimental chapter in this thesis describes the development and use of two different emulsification-solvent evaporation procedures for the preparation of model (drug-free) Eudragit RL particulates. The first technique was used for the preparation of nanoparticles, whereas the second technique was used to prepare microparticles.

Eudragit RL was chosen as the encapsulating polymer for a number of reasons:

1. The polymer has sustained-release properties (see section 1.1.3.2).
2. Readily available pharmaceutical excipient.
3. Amenable to microencapsulation using solvent evaporation techniques (see section 1.1.3.2).

The aim of the work presented here was to establish how the alteration of basic preparation parameters can influence nanoparticle and microparticle properties, and in particular, size. The results should be broadly applicable to any solvent evaporation process.

2.2. EXPERIMENTAL

2.2.1. Materials

Eudragit RL100 (Dumas (UK), Tunbridge Wells, UK), sodium dodecyl sulphate (SDS) (biochemical grade)(Sigma, Poole, UK), Tween (polysorbate) 80 (BDH, Poole, UK), dichloromethane (GPR grade)(Rhône-Poulenc, Dagenham, UK).

2.2.2. Methods

2.2.2.1. Particle preparation

Both of the preparation techniques used a two stage

process. In the first stage, an emulsion of Eudragit RL-dichloromethane droplets was produced. In the second stage, the dichloromethane was evaporated from the polymer droplets at 50 °C in a water-bath, whilst the emulsion was gently agitated at a lower stirring speed.

Diagrams of the two basic preparation processes are shown in figure 2.1.

A. Nanoparticles

The required quantity of Eudragit RL was weighed into a 100 ml glass-stoppered conical flask and 10 ml of dichloromethane was added to dissolve the polymer pellets. Dissolution of the polymer was aided by gentle agitation of the flask.

The flask containing the polymer solution was then partly immersed in a beaker containing ice in order to minimise heating during the emulsification process. 25 ml of aqueous Tween 80 solution was slowly poured into the flask and the two liquids were allowed to cool for about a minute. An homogeniser (Silverson, Chesham, UK) was lowered into the polymer solution ensuring that the bottom section of the mixing head was completely covered with liquid. It was then switched on at the required speed for a predetermined time period (see following section for individual experimental conditions).

After emulsification, the dichloromethane was evaporated from the dispersion of Eudragit RL droplets by placing the flask on top of an underwater magnetic stirrer in a water bath at 50 °C. The solution was gently stirred by a magnetic flea as the solvent evaporated. Solvent evaporation was generally complete within 60 minutes. The nanoparticles were kept suspended in the emulsifier solution for subsequent characterisation.

The following experiments were carried out:

i). Effect of polymer concentration on particle size.

Eudragit RL was dissolved in dichloromethane at concentrations of 1, 4, 7.5, 10, 13 and 23% w/v. The polymer solutions were emulsified at half-maximum homogenisation speed (about 4000 rpm) into 1% w/v Tween 80 solution for a period of 5 minutes.

ii). Effect of mixing time on particle size.

A solution of 23% w/v Eudragit RL in dichloromethane was emulsified into 1% w/v Tween 80 solution for 5, 7.5, 10 or 20 minutes at maximum homogenisation speed (about 8000 rpm).

iii). Effect of surfactant concentration on particle size.

A solution of 23% w/v Eudragit RL was emulsified into 0.0025, 0.01, 0.25, 1 or 5% w/v Tween 80 solution for a period of 20 minutes at maximum homogenisation speed.

B. Microparticles

The required quantity of Eudragit RL was weighed into a glass bottle and dissolved in 20 ml of dichloromethane. The surfactant, SDS, was dissolved in 50 ml of distilled water in a 200 ml glass beaker. To prepare the microparticles, the beaker containing surfactant solution was partly immersed into ice to minimise solvent evaporation during emulsification. An overhead paddle stirrer (Stuart Scientific, Manchester, UK) was lowered into the polymer solution, the surfactant solution poured in, and the mixer switched on. After mixing at the required speed for the required period of time (see below), the beaker was transferred to a water bath (50 °C) and stirring continued at 200 rpm until evaporation of solvent was complete, which typically took about 60 minutes. All microparticle samples were kept in solution for subsequent characterisation.

The following experiments were carried out:

i). Effects of polymer concentration on particle size.

A solution containing 2.5, 5, 7.5 or 10% w/v Eudragit RL was emulsified into 1% w/v SDS solution for a period of 10 minutes at 350 rpm, followed by solvent evaporation at 200 rpm.

ii). Effects of mixing speed on particle size.

Two concentrations of polymer solution were used, 2.5% and 10% w/v Eudragit RL. Solutions were emulsified into 1% w/v SDS for a period of 10 minutes at 350, 500 or 700 rpm, followed by solvent evaporation. Two microparticle batches were produced for each polymer concentration/speed combination.

iii). Effects of stirring time on particle size.

Again, 2.5 and 10% w/v Eudragit RL solutions were used. The initial emulsification stage was carried out for 1, 2.5, 5, 10, 20, 30 or 40 minutes into 50 ml of 1% w/v SDS solution, at a mixing speed of 350 rpm. Two batches of microparticles were produced for each combination of polymer and surfactant solution.

iv). Effects of SDS concentration on particle size.

20 ml of 5% w/v Eudragit RL solution was emulsified into 50 ml of distilled water containing 0.5, 1.0, 1.5, 2.0, 3.0, 4.0, 4.5, 5.0, 6.0, 7.5 or 9.0 % w/v SDS, at 350 rpm. Two batches of microparticles were produced for each concentration of surfactant.

2.2.2.2. Particle size determination

The size of the nano- and microparticles was determined using laser light scattering techniques. Measurements were carried out by using either a Malvern photon correlation spectrometer or a Malvern Mastersizer (Malvern Instruments, Malvern, UK).

Photon correlation spectroscopy (PCS) is based upon the scattering of laser light by suspended particles undergoing Brownian motion. Laser illumination of the particle suspension generates a diffraction pattern which continuously changes as the particles diffuse. The rate of diffusion is dependent upon particle size. Therefore, measurement of the rate of change of the diffraction pattern (by a photomultiplier) enables an estimation of the particle size. Since PCS relies on Brownian motion of the particles being analysed, it is generally limited to measurements in the nanometre size range (Cummins and Pike, 1977; Ho, 1989).

The Malvern Mastersizer is also based upon laser light diffraction. Here however, particle size calculations are based upon the principle that the angle of diffraction is inversely proportional to particle size (Weiss and Frock, 1976; Ho, 1989). The diffraction pattern produced by illumination of the sample is focused by a lens onto a series of detector rings. The instrument measures the intensity of the diffraction pattern at the different rings and calculates a sample size distribution. Using different optical arrangements, the Mastersizer is capable of measuring particles from 100 nm to 600 μm in diameter (Malvern Mastersizer User Manual, 1988). The optical arrangement used for this work enabled measurement of particles over a 0.2-80 μm size range, although PCS is the preferred technique for sub-micron samples.

2.2.2.3. Light microscopy

Samples of microparticle suspension were viewed using a Nikon Optiphot light microscope (Nikon, Tokyo) at x20 or x40 magnification.

2.2.2.4. Scanning electron microscopy (SEM)

Onto an aluminium stub was mounted a piece of double sided-sticky tape. A drop of microparticle suspension was placed

onto the sticky tape and allowed to dry. The dried stub was sputter coated with gold in an argon atmosphere and then viewed with a Jeol JSM 35C scanning electron microscope (Jeol, Tokyo).

2.3. RESULTS AND DISCUSSION

2.3.1. Nanoparticle samples

2.3.1.1. Effect of polymer concentration

The mean particle size, measured by the PCS instrument, was seen to increase with polymer concentration, from a diameter of 196 nm at 1% w/v Eudragit RL to a diameter of 451 nm at 13% w/v Eudragit RL (table 2.1). Size values in table 2.1 are the mean of five measurements for each sample. Using 23% w/w polymer solution, many of the particles were greater than 1 μm in diameter, and so an accurate size could not be obtained by PCS.

The PCS instrument also provided data on sample polydispersity (the polydispersity index). Although in monodisperse systems the value of the polydispersity index approaches zero, a value below 0.1 is considered to represent a relatively narrow size distribution. The majority of the samples had a polydispersity index below 0.3, although the polydispersity of the 451 nm sample was markedly higher (table 2.1).

Factors responsible for increases in particle size with polymer concentration when using solvent evaporation processes were described in section 1.1.2.5.C and apply here.

2.3.1.2. Effect of mixing time

Here, the particle size was determined using the Malvern Mastersizer. The Mastersizer generates a comprehensive breakdown of the percentage of the sample within 64 size increments between 0.1 and 80 μm . The particle size

Table 2.1. Effect of polymer concentration on the size and polydispersity of Eudragit RL nanoparticles.

Eudragit RL conc. (% w/v)	Mean particle size (nm)	Polydispersity
1	196	0.23
4	227	0.11
7.5	290	0.25
10	354	0.27
13	451	0.45

distribution was in all but one case bimodal, with the main body sized below 5 μm and a second, smaller group close to 50 μm . An example is presented in figure 2.2. The most likely explanation for these two distinct groups is incomplete mixing, since a second population of particles was not seen for the batch mixed for 20 minutes.

The presence of a bimodal distribution complicated data interpretation. Therefore, a meaningful comparison of the effect of mixing time on particle size was made by comparing the mode (or median) diameters of the samples (see figure 2.2). As might be expected, the particle size was seen to fall with mixing time (table 2.2).

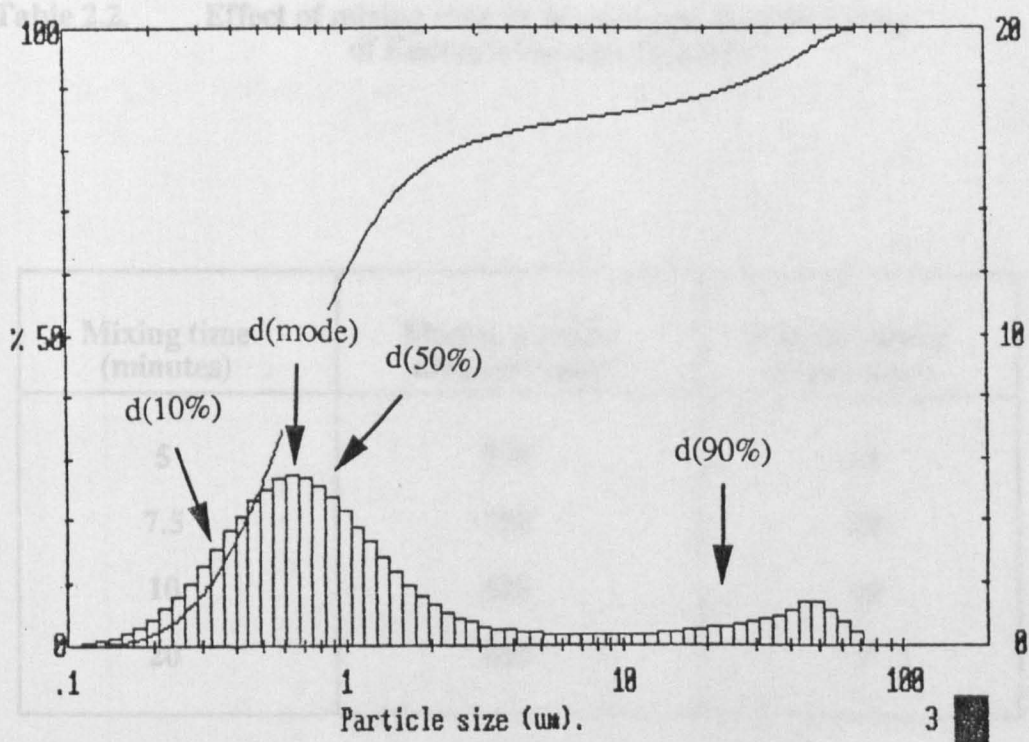
The Mastersizer also provides a measure of the particle polydispersity, termed the "span". The span is equal to the difference between the d90% and d10% diameters divided by the d50% diameter. Polydispersity values are recorded in table 2.2 and fell with increasing mixing time. The dramatic drop in polydispersity between 15 and 20 minutes was due to the replacement of the bimodal distribution with a unimodal one.

2.3.1.3. Effect of surfactant concentration

The particle size using 0.0025 and 0.01% w/v Tween 20 as surfactant was similar, but with a further increase in concentration, the particle size declined (table 2.3). All of the samples were found to be unimodal in distribution, probably a consequence of the prolonged, high speed mixing.

An important factor to be considered when evaluating the effects of surfactant on the size of Eudragit RL (and RS) nano- and microparticles, is that this polymer already possesses intrinsic surface active properties due to the quaternary ammonium groups in its structure. The successful production of Eudragit RL and RS nanoparticles by a solvent evaporation process without using surfactant has been

Figure 2.2. Bimodal distribution of Eudragit RL nanoparticles.



$$d(90\%) = 23.95 \mu\text{m}$$

$$d(50\%) = 0.80 \mu\text{m}$$

$$d(\text{mode}) = 0.68 \mu\text{m}$$

$$d(10\%) = 0.32 \mu\text{m}$$

Table 2.2. Effect of mixing time on the size and polydispersity of Eudragit RL nanoparticles.

Mixing time (minutes)	Median particle diameter (nm)	Polydispersity (span value)
5	790	62
7.5	750	53
10	680	30
20	610	2

Table 2.3 Effect of Tween 80 concentration on the size of Eudragit RL nanoparticles.

Tween 80 conc. (% w/v)	Mean particle diameter (d50%)(nm)
0.0025	720
0.01	730
0.25	620
1	600
5	520

reported (Bodmeier and Chen, 1989b). As a consequence, the effect that surfactant will have on particle size may be diminished.

2.3.2. Microparticle samples

2.3.2.1. Effect of polymer concentration

The effect on microparticle size of changing the polymer concentration is recorded in table 2.4. As seen with the nanoparticles, size increased with polymer concentration.

The dramatic difference in the particle size generated between the two preparation techniques is clearly demonstrated. Whereas the high-speed homogenisation technique resulted in particles of around 350 nm diameter using 10% w/v Eudragit RL, the gentler overhead stirrer method produced particles of 25 μm diameter using the same concentration of polymer solution.

2.3.2.2. Effect of stirring speed

The influence of mixing speed on microparticle size is shown in figure 2.3. Although there was a large difference in size between the two polymer concentrations when stirred at 350 rpm, the difference at the two higher mixing speeds was only small. The slower decline in size with the 10% w/v polymer solution reflected its higher viscosity.

In view of the small size difference between the samples stirred at 500 and 700 rpm, it is likely that the 10% w/v polymer solution produced denser microparticles than the 2.5% w/v solution.

2.3.2.3. Effect of stirring time

A similar pattern was seen as the mixing time increased. Thus the decline in microparticle size was most rapid for the lower polymer concentration, with the two groups approaching in size as the mixing time increased (figure 2.4). With 10% polymer solution, after 1, 2.5 and 5 minutes

Table 2.4 Effect of polymer concentration on the size of Eudragit RL microparticles.

Eudragit RL conc. (% w/v)	Mean particle diameter (d50%)(μm)
10	24.6\pm2.0
7.5	19.1\pm1.8
5.0	15.1\pm0.3
2.5	7.3\pm0.3

Figure 2.3. Effect of mixing speed on size of Eudragit RL microparticles

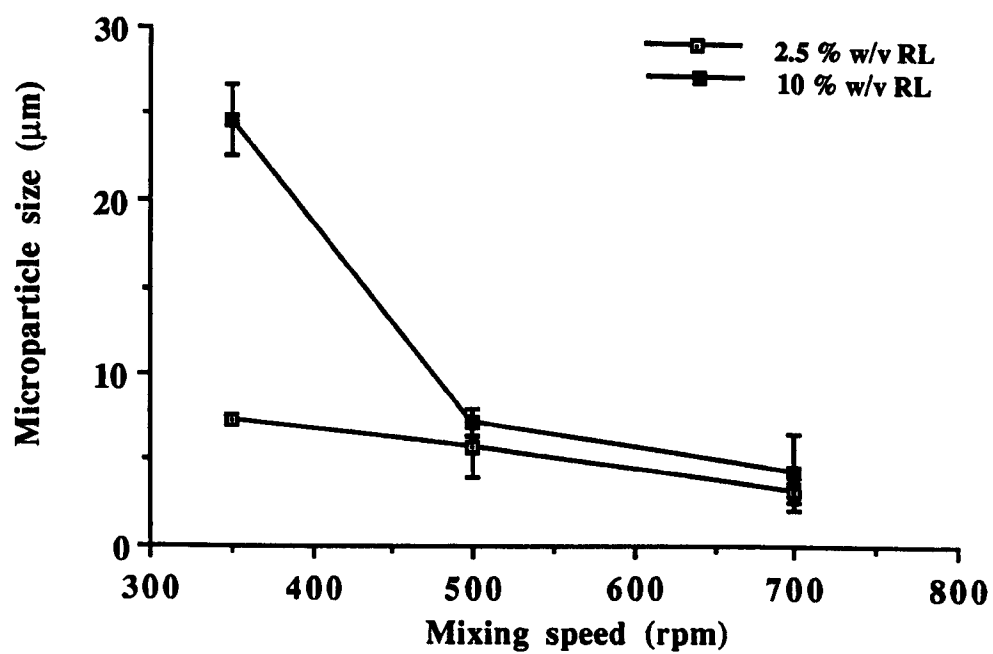
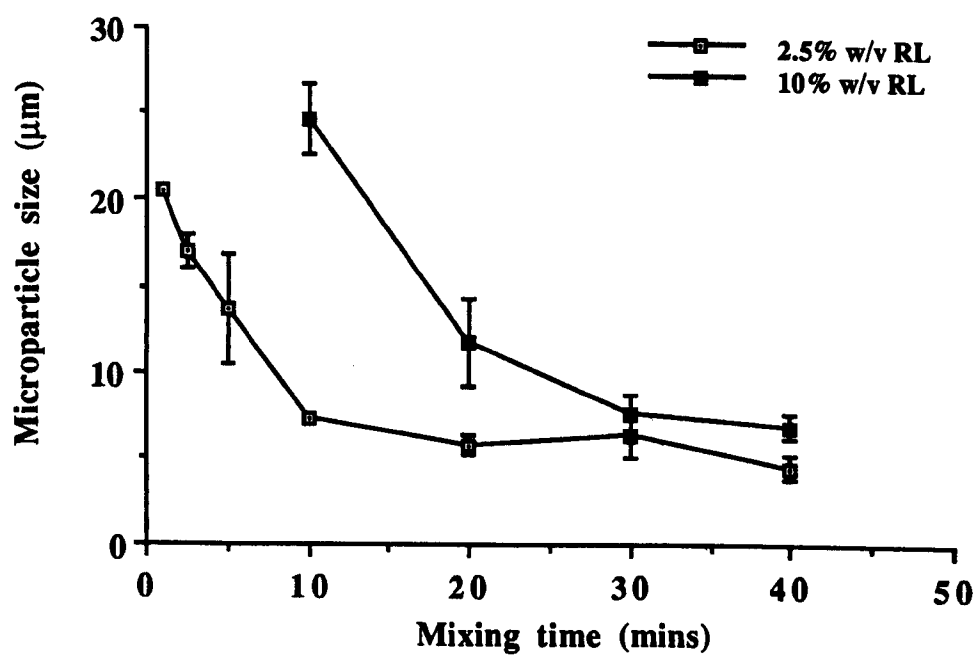


Figure 2.4. Effect of mixing time on size of Eudragit RL microparticles



mixing, the majority of the microparticles were in excess of 80 μm (the upper size-limit of the Malvern Mastersizer). As for the previous section, it is likely that there were density differences between the two sets of microparticles.

2.3.2.4. Effect of surfactant concentration

The effect of surfactant concentration on microparticle size is shown in figure 2.5. An initial rapid decline in size with increasing surfactant concentration was followed by a sudden, marked increase in size at 4 and 5% w/v SDS. Light microscopy revealed that at these two concentrations, the microparticles had formed aggregates, appearing to have partly fused into larger bodies.

Aggregation phenomena have been reported for aqueous emulsions of benzene and paraffins (Cockbain, 1952; Higuchi et al., 1962). In 10% benzene emulsions, globule aggregation was observed between SDS concentrations of 0.36 and 0.8% w/v. At 0.97% SDS, globules were disaggregated, but further increasing the surfactant concentration resulted in the reappearance of aggregates. It was speculated that aggregation at the lower SDS concentration might have resulted from attractive forces between exposed hydrophobic surfactant groups residing at the droplet surface, while at the higher SDS concentration, aggregation may have resulted from forces of attraction between adsorbed micelles (Cockbain, 1952).

2.3.3. Scanning electron microscopy

SEM micrographs of a sample of Eudragit RL microparticles are shown in figures 2.6 a) and b).

There appeared to be two distinctly different types of microparticle. Although both types were roughly spheroidal in shape, some contained surface pores and were whole spheres, whereas others appeared not to contain large pores but were markedly misshapen, and contained large surface

Figure 2.5. Effect of SDS concentration on size of Eudragit RL microparticles

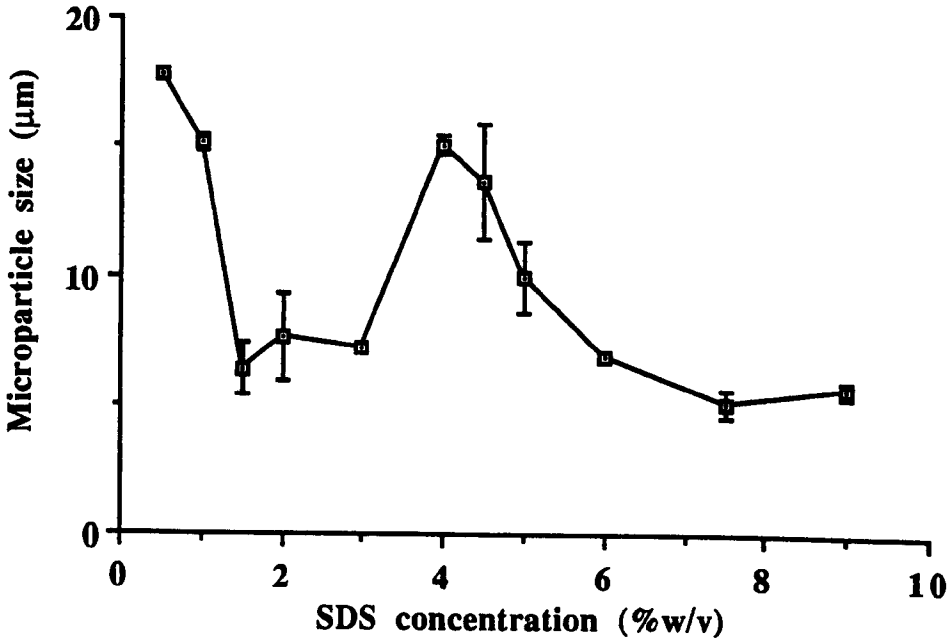
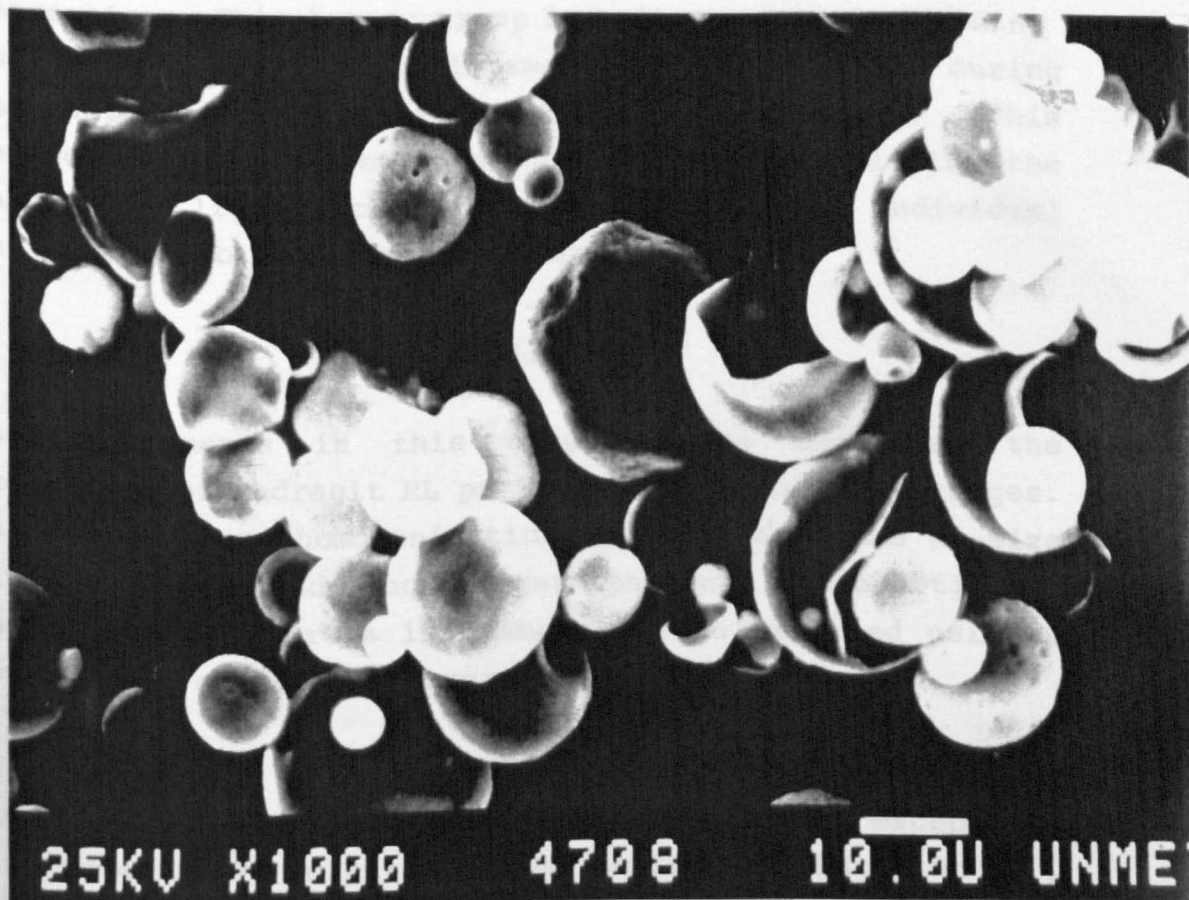
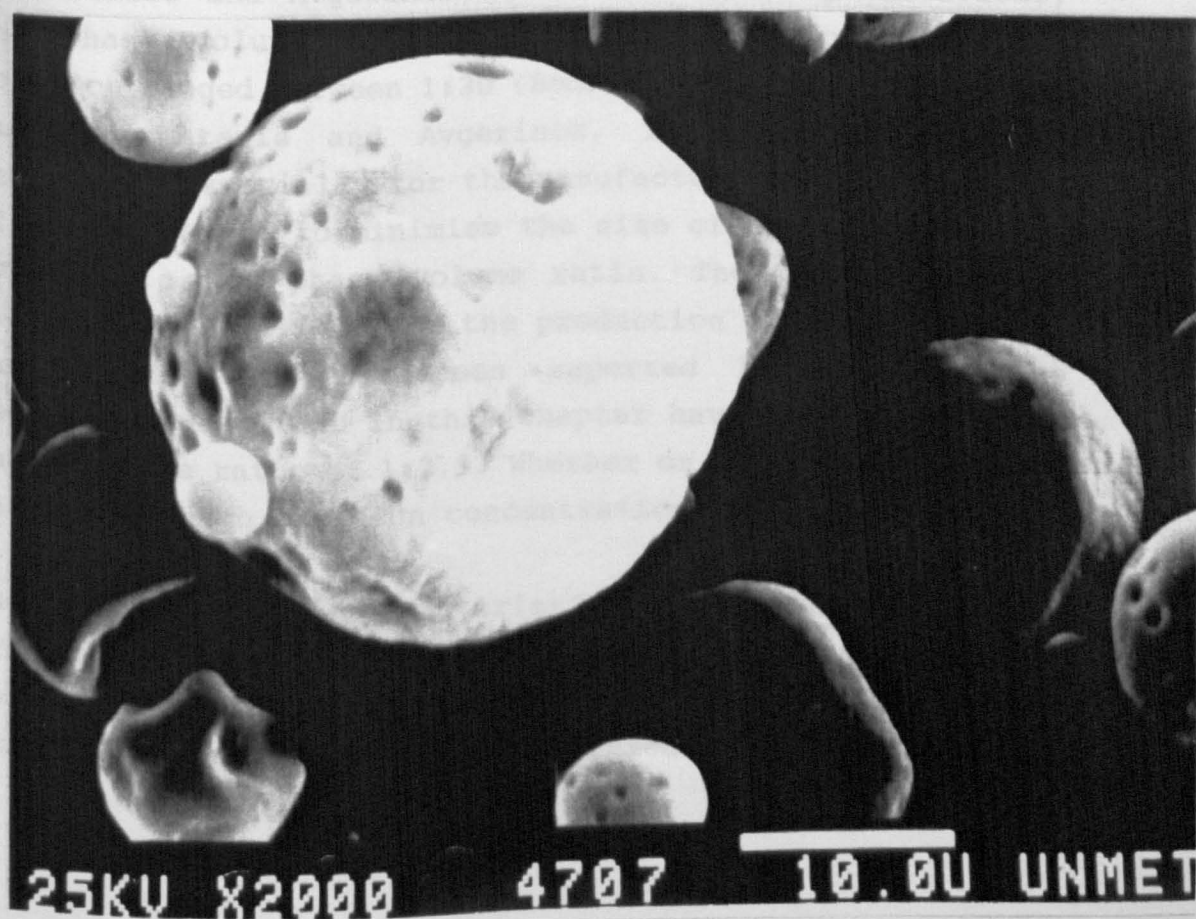


Figure 2.6. Electron micrographs of Eudragit RL microparticles.

a) Magnification x1000.



b) x2000.



depressions. This latter group had the appearance of being hollow and having collapsed at some stage during manufacture or preparation for microscopy. This heterogeneity in appearance was confirmed by viewing the samples by light microscopy, and many of the individual particles also appeared to be transparent.

2.4. CONCLUSIONS

The experiments in this chapter have described the production of Eudragit RL particulates in two size ranges. Using high-speed homogenisation, particles in the nm-size range were produced. Much larger spherical microparticles, up to tens of microns in diameter, were produced using a lower-speed overhead stirrer.

In the past, using o/w procedures, Eudragit RL/RS microspheres have been produced, almost without exception, with aqueous PVA solution as the emulsifier (Babay et al., 1988; Barkai et al, 1990; Bodmeier and Chen, 1989a; Malamataris and Avgerinos, 1990). In these publications, the phase volume ratio of polymer solution:surfactant solution ranged between 1:30 (Bodmeier and Chen, 1989a) and 1:4 (Malamataris and Avgerinos, 1990). It is clearly desirable, especially for the manufacture of large batches of microspheres, to minimise the size of the mixing vessel by using a low phase volume ratio. The use of SDS and Tweens as emulsifiers for the production of Eudragit RS/RL particulates has not been reported before, and the techniques described in this chapter have used a far lower phase volume ratio of 1:2.5. Whether or not PVA can achieve an equally high emulsion concentration is not clear.

The effects on size-characteristics of changing a number of production parameters was assessed. The ability to closely control the size of particulate carriers is in many cases critical to their successful clinical use. For example,

systems for parenteral administration need to be sufficiently small to pass through a hypodermic needle. In addition, as discussed in section 1.1.4.1.B, the size of a particulate is one factor determining its in vivo distribution following parenteral administration. More fundamentally, as the size of a microparticle is decreased, the more rapidly drug will be released (e.g. Suzuki and Price, 1985; Pongpaibul et al., 1984).

From the experiments undertaken in this chapter, for a given set of manufacturing equipment, the most useful parameters for controlling particle size would appear to be the time and speed of mixing. Although surfactant concentration and polymer concentration were also able to influence size, these are probably of less practical use:

- There was an initial sharp decrease in particle size with increasing surfactant concentration. However, thereafter further increases in surfactant had relatively minor effects on particle size and, in the case of SDS, aggregation was observed.

- Using prolonged and/or high speed mixing, the effects of polymer concentration on particle size were not dramatic. It is probable that as the concentration of polymer decreases, so does particle density. Since decreased density means increased porosity, changes in polymer concentration will affect particle drug release characteristics.

The microparticles were far from homogeneous in appearance. Many were markedly misshapen and must bring into question their ability to reliably retard the release of any drug encapsulated within. Whilst undertaking this work, a few test batches were produced using Eudragit RS. The appearance, under the light microscope of these microparticles was very different. In contrast to the

transparent, misshapen appearance of the Eudragit RL samples, microparticles produced from Eudragit RS were more uniformly round and appeared to be considerably denser. It was partly for this reason that subsequent work investigating drug incorporation concentrated on Eudragit RS as the encapsulating polymer. Differences in appearance between Eudragit RL and RS microparticles presumably reflect differences in polymer structure i.e. the proportion of trimethyl ammonioethyl methacrylate functions is greater in RL and results in the polymer having a higher permeability.

CHAPTER 3.

THE ENCAPSULATION OF 5-AMINOSALICYLIC ACID INTO
EUDRAGIT RS MICROSPHERES.

3.1. INTRODUCTION

The work carried out in chapter 2 had established basic techniques for the production of microspheres from Eudragit RL. The next stage of the project was to adapt these methodologies and attempt to encapsulate 5-aminosalicylic acid (5-ASA) into Eudragit RS microspheres to produce a potential sustained-release system for drug delivery into the colon.

The use of 5-ASA as a therapeutic agent for the treatment of inflammatory bowel diseases was discussed in detail in sections 1.2.5 and 1.2.6. A number of the strategies used to optimise its delivery into the colon were outlined. Since Eudragit RS does not possess intrinsic colon-specific release characteristics, 5-ASA containing microspheres would require delivery within a colon-targeted device to be of maximum therapeutic use.

On the face of it, the rationale for developing a colon-targeted sustained-release form of 5-ASA might be questionable. Since the colonic absorption of 5-ASA is very poor, any dose released into the colon will theoretically remain available for therapeutic action until excreted in the faeces. However, degradation or metabolic conversion to inactive derivatives by colonic bacteria cannot be discounted. 5-ASA encapsulated within microspheres should be protected from potential inactivation until released.

Another major benefit of delivering 5-ASA within a sustained-release dosage form is the avoidance of dose dumping prior to entry into the colon. It is recognised that significant systemic absorption of 5-ASA may result in renal toxicity (Hayllar and Bjarnason, 1991). This may arise when a dosage form designed to release its contents into the colon disrupts prematurely and releases drug into the proximal small intestine. Unwanted absorption of 5-ASA

will also reduce the amount available for local action in the colon. With a sustained-release preparation, the potential for dose dumping is avoided.

An additional benefit of sustained release 5-ASA may be in the treatment of GI tract inflammation proximal to the colon e.g. Crohn's disease of the small bowel. Here, the dosage form would ideally release 5-ASA for topical action but at the same time minimise the amount of drug available for systemic absorption and, indeed, such a product is in clinical use (PentasaTM see section 1.2.6.1).

It was apparent, at an early stage in the development of the 5-ASA microspheres, that the concentration of surfactant used in the production procedure might be able to influence the microsphere physical properties, most clearly evident in the drug release rate. This work was extended to investigate a range of concentrations of two surfactants and their effects on microsphere properties. These experiments are described in this chapter.

3.2. EXPERIMENTAL

3.2.1. Materials

Eudragit RS100 (Dumas (UK)), 5-ASA (95-98 % purity)(Sigma), sodium dodecyl sulphate (GPR grade)(Sigma), polysorbate (Tween) 20 (Sigma), dichloromethane (GPR grade)(Rhône-Poulenc).

3.2.2. Methods

3.2.2.1. Microsphere production

Preliminary experiments investigating the encapsulation of 5-ASA employed minor modifications of the technique described in section 2.2.2.1.B. 5-ASA powder was suspended in 20 ml of a 10% w/v solution of Eudragit RS in dichloromethane (5-ASA is insoluble in dichloromethane). The drug:polymer mixture was then dispersed into 100 ml of

1% w/v aqueous SDS solution at 500 rpm for 5 minutes using an overhead stirrer (Stuart Scientific, Manchester, UK). The dichloromethane was evaporated at 40 °C in a water-bath, whilst stirring at 350 rpm. During solvent evaporation, the drug:polymer droplets coalesced to form large agglomerates. The agglomeration was probably heat-induced, and so in all subsequent encapsulation experiments solvent evaporation was carried out at room temperature.

Using room temperature evaporation, the encapsulation process was successful. However, the drug and polymer formed into misshapen, elongated microparticles. This was a result of the polymer precipitating around the long, needle-shaped crystals of 5-ASA. Examination by light microscope indicated that the 5-ASA was in the form of needle-shaped crystals up to 100 μm in length.

By finely grinding the drug powder using a pestle and mortar, to produce particles less than 20 μm in diameter (measured by light microscopy), microspheres could be produced.

As a result of these preliminary experiments, the following production procedure was used for the microencapsulation of 5-ASA:

To 20 ml of a 10% w/v solution of Eudragit RS in dichloromethane was added 1 g of finely-ground 5-ASA powder. The dispersibility of the ground 5-ASA was poor and was aided by placing the bottle containing polymer solution and drug into an ultrasonic bath (Decon FS100, Decon, Hove, UK) for a period of 20-30 minutes.

With the dispersion complete, the drug-polymer mixture was poured into a 250 ml glass beaker containing 100 ml of an aqueous solution of one of two surfactants, SDS or Tween 20. A range of surfactant concentrations were employed: 0,

0.05, 0.075, 0.10, 0.175 and 0.25% w/v SDS and 0.025, 0.05, 0.25, 0.5, and 1% w/v Tween 20. The drug-polymer mixture was emulsified into the surfactant solution with the overhead paddle stirrer set at 200 rpm. Stirring was continued, at room temperature, until evaporation of the dichloromethane was complete, which typically took 4-5 hours.

In all cases of 5-ASA encapsulation, two distinct groups of particles were observed. Some of the material formed into microspheres which sunk to the bottom of the beaker when the stirrer was stopped. The remainder of the drug and polymer floated on the liquid surface as misshapen agglomerates. These agglomerates were separated from the microspheres by decantation at the end of solvent evaporation. The remaining microspheres were collected by passing through a Buchner funnel containing a 20 µm paper filter (Whatman, Maidenhead, UK). After washing with 200 ml of distilled water, the microspheres were transferred to a small glass beaker which was then covered with pierced Parafilm™ (American Can, CT, USA).

The microspheres were then frozen by plunging the beaker into liquid nitrogen and freeze-dried overnight (Edwards Modulyo, Crawley, UK). After freeze-drying, the weight of microspheres was recorded. Finally, a 250-500 µm sieve-fraction was collected for further experiments. Each microsphere batch was produced at least in duplicate.

3.2.2.2. Assay for drug content

The microspheres were finely ground using a pestle and mortar and an accurately weighed quantity, estimated to contain up to 5 mg of 5-ASA, was placed into a 100 ml volumetric flask. 100 ml of pH 7 phosphate buffer (appendix 1) was added to the flask and the powdered microspheres dispersed by sonication in an ultrasonic bath (Decon FS100) for 10 minutes. The flask was then left to stand, with

occasional shaking, for up to 6 hours to allow the 5-ASA to fully dissolve from the ground microspheres. A sample of the flask contents was then drawn into a syringe, passed through a 1 μm membrane filter (Whatman) to remove particulate material and the UV absorbance at 330 nm measured (Uvikon 860, Kontron Instruments, Switzerland). The concentration of drug present was calculated by reference to a calibration curve of 5-ASA dissolved in pH 7 phosphate buffer.

3.2.2.3. Drug release studies

Profiles of drug release from the microspheres were obtained using a USP (apparatus 2) dissolution tester (Erweka model DT-D6, Heusenstamm, Germany). Samples were released into 500 ml of pH 7 phosphate buffer at 37 °C, containing 0.02% w/v Tween 20 to aid microsphere wetting, and agitated at 100 rpm with paddles. Approximately 120-140 mg of microspheres containing about 40-45 mg of 5-ASA were placed into each vessel. The solubility of 5-ASA was estimated to be in excess of 1 g/ 500 ml at 37 °C/pH 7, and so the amount of drug present in each dissolution vessel was always well below saturation level. At 30, 60, 120, 180, 240, 300, and 360 minute intervals a 10 ml sample of dissolution fluid was drawn into a syringe, filtered to remove any microspheres (1 μm membrane filter) and the UV absorbance at 330 nm measured. Any microspheres retained on the filter were returned to the dissolution vessel with 10 ml of fresh buffer. Concentrations of 5-ASA were calculated from the calibration curve of drug in pH 7 phosphate buffer. The dissolution rate of unencapsulated 5-ASA powder was assessed in the same way.

3.2.2.4. Low temperature scanning electron microscopy

Electron micrographs were obtained of two microsphere samples, those produced with no surfactant and those produced using 0.25% w/v SDS.

The electron microscope stage was maintained at $-180\text{ }^{\circ}\text{C}$ using liquid nitrogen in order to minimise damage to the samples from electron beam irradiation. Using this technique (low temperature/cryogenic SEM) it is possible to obtain electron micrographs of heat sensitive materials such as margarine and chocolate (Sargent, 1988a,b).

The samples were mounted on a holder using carbon cement and then immediately frozen by plunging into nitrogen "slush" at $-210\text{ }^{\circ}\text{C}$. Samples were initially placed in a preparation chamber (Hexland CT1000A cryotransfer system, Oxford, UK) and then moved through onto the electron microscope stage (Philips SEM 505). They were examined at a low kV while the temperature was raised to $-80\text{ }^{\circ}\text{C}$ to allow sublimation of any surface water. The sample was then moved back into the preparation chamber, sputter coated with gold in an atmosphere of argon, and finally returned to the stage for imaging. To obtain an internal surface for imaging, the sample was moved back into the preparation chamber, fractured with a knife and recoated with gold.

3.3. RESULTS AND DISCUSSION

3.3.1. Microsphere production

Eudragit RS microspheres containing 5-ASA could be produced successfully over the entire concentration range of Tween 20 and SDS investigated, with the sole exception of 0.175% SDS.

With 0.175% SDS, microspheres could not be produced, and the dispersed drug-polymer-solvent droplets rapidly coalesced into a single mass. This concentration of surfactant may represent a critical value for this system at which the emulsified droplets aggregate, in a phenomenon similar to the one reported in section 2.3.2.4.

The microsphere formulation details are recorded in table

3.1. Even in the complete absence of surfactant, microspheres were produced, although the yield was low, and only 20 to 30% of the added mass of drug and polymer had formed into microspheres at the end of solvent evaporation, with the remaining material forming misshapen agglomerates. The ability to produce Eudragit RL/RS microspheres without surfactant has been noted earlier in this thesis (section 2.3.1.3), although the presence of drug probably restricts this process. With SDS, yields were little different (varying between 20 and 40%) and were not related to surfactant concentration. Similarly, the yield of microspheres varied little over the range of concentrations used for Tween 20, although the efficiency of the process was considerably higher with 70-80% of the drug and polymer formed into microspheres.

The difference in microsphere yield between the two surfactants may be related to their critical micellar concentrations (cmc). The cmc for SDS is around 0.23% w/v at 25 °C, whereas for Tween 20 it is 0.006% w/v (Florence and Attwood, 1981). Consequently, while just one of the SDS formulations was made with a surfactant concentration close to or greater than the cmc, all Tween 20 concentrations exceeded the cmc.

To test this hypothesis, one batch of 5-ASA:Eudragit RS microspheres was produced using 1% w/v SDS solution as surfactant, a concentration which considerably exceeds the cmc. Although the emulsification efficiency was very high with very few agglomerates, the resulting product was not microspheres. Instead, a voluminous mass of extremely brittle drug-polymer particles had formed following solvent evaporation. Thus, it appeared that the low yield observed with SDS as surfactant was probably due to the fact that the concentrations were, with possibly one exception (0.25% w/v), below the cmc.

Table 3.1. Eudragit RS:5-ASA microsphere formulation details.

Surfactant concentration used to produce microspheres (% w/v)	Mean microsphere 5-ASA content (% w/v)(n=3)	Yield (by weight)
<p>No surfactant</p> <p><u>SDS</u></p> <p>0.05 0.075 0.10 0.25</p> <p><u>Tween 20</u></p> <p>0.025 0.05 0.25 0.5 1.0</p>	<p>29.3±1.3</p> <p>29.2±1.5 30.1±1.5 30.7±1.0 30.7±1.4</p> <p>29.5±1.3 30.1±1.4 28.9±1.4 29.2±0.4 29.6±2.0</p>	<p>20-30%</p> <p>) 20-40%</p> <p>) 70-80%</p>

The stirring speed used for microsphere production was chosen in order to maximise the proportion of microspheres between 250 and 500 μm in diameter. Typically 30-50 % (by weight) fell within the desired size range.

For both surfactants, the efficiency of drug encapsulation was high at around 30% w/w (table 3.1), reflecting the relatively low aqueous solubility of 5-ASA. (The theoretical maximum microsphere loading was 33% w/w). The final drug content of the microspheres did not appear to be related to the concentration of surfactant used.

3.3.2. Microsphere drug release characteristics

The drug release profiles from microspheres produced using SDS and Tween 20 as surfactants are shown in figures 3.1 and 3.2 respectively. The times for 50% of the encapsulated drug to be released ($t_{50\%}$) are presented in table 3.2.

For both SDS and Tween 20, the rates of drug release from the microspheres were found to be dependent upon the concentration of surfactant used in the production procedure. An increase in the concentration of surfactant was accompanied by an increase in the rate of drug release. The microspheres made without surfactant demonstrated the greatest retardation in drug release, with a $t_{50\%}$ in excess of 360 minutes. In contrast, microspheres made with the highest surfactant concentrations, 1% Tween 20 and 0.25% SDS, showed little or no retardation in availability over unencapsulated 5-ASA.

For SDS, the fact that microspheres could not be produced at a concentration of 0.175% w/v combined with the rapid jump in drug release rate between 0.1 and 0.25% w/v suggested that a structural change associated with the cmc may have occurred.

Figure 3.1. Effect of SDS concentration on rate of release of 5-ASA from microspheres.

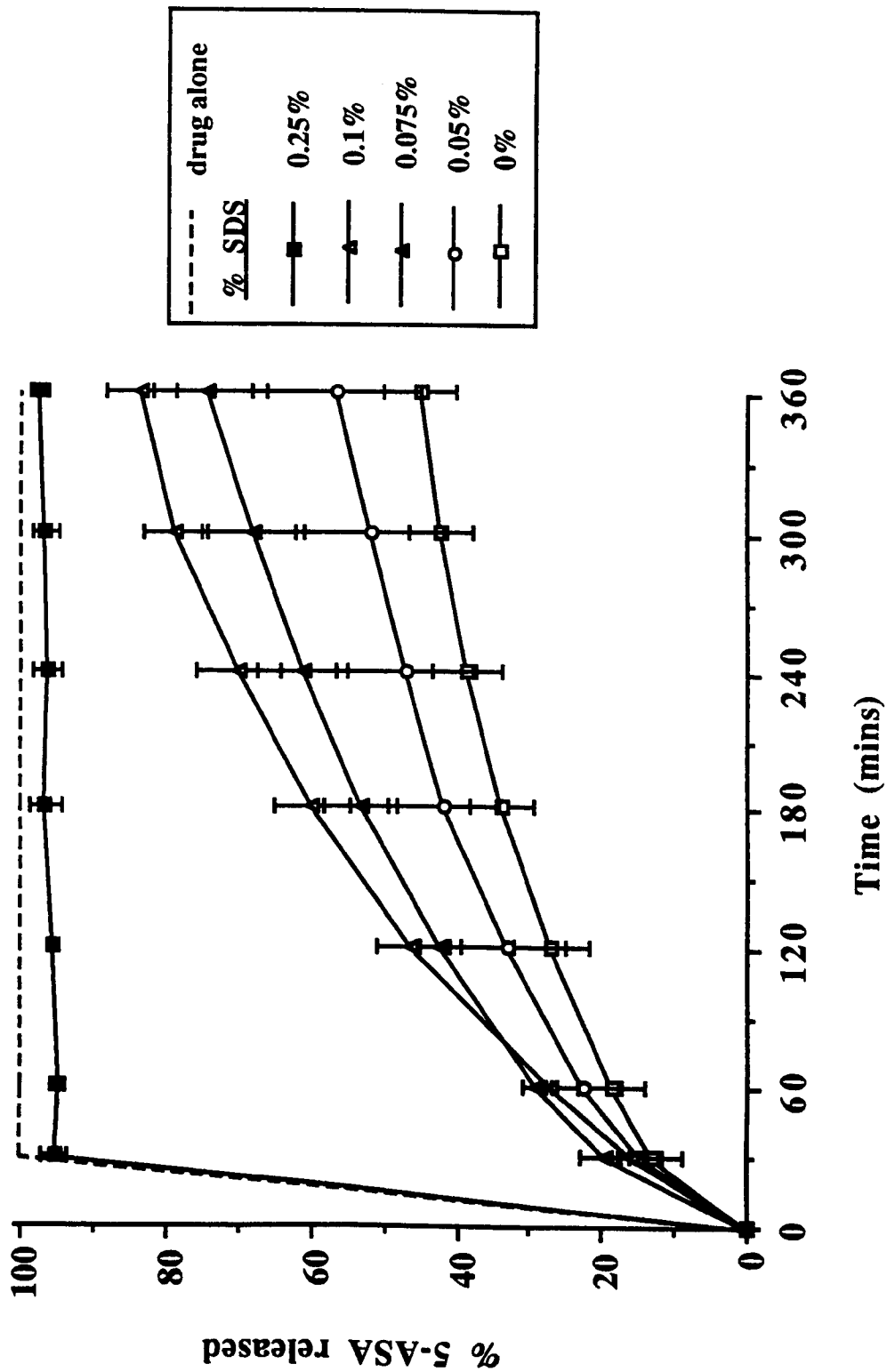


Figure 3.2. Effect of Tween 20 concentration on rate of release of 5-ASA from microspheres.

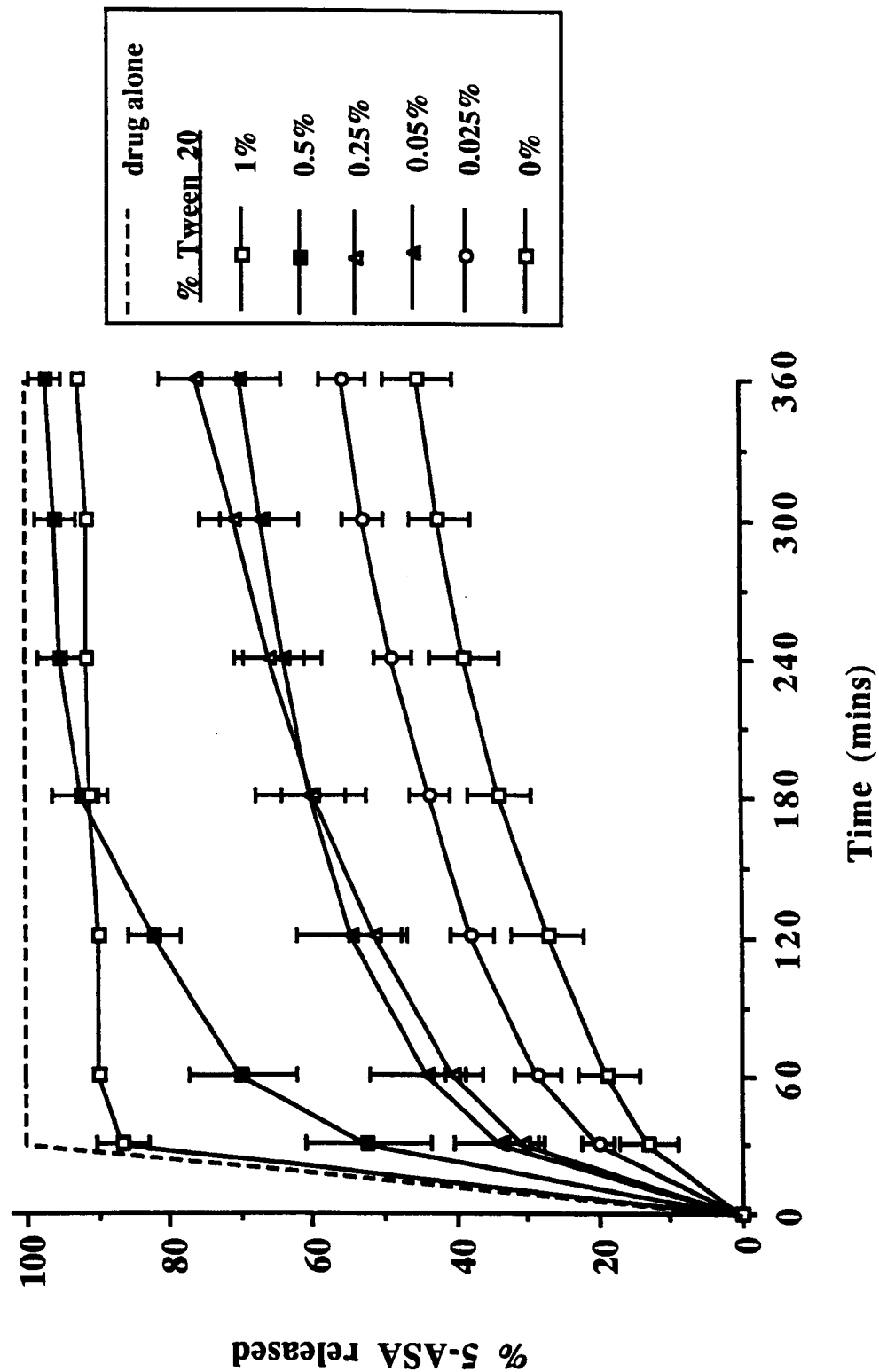


Table 3.2. Time for 50% of 5-ASA to be released from microsphere formulations.

Surfactant type and concentration (% w/v)	t50% for drug release (mins)
<u>SDS</u>	
0	>360
0.05	300
0.075	160
0.10	140
0.25	<30
<u>Tween 20</u>	
0	>360
0.025	300
0.05	120
0.25	100
0.5	30
1.0	<30

3.3.3. Low temperature SEM

Low temperature SEM was used to investigate the surface and internal structure of two microsphere formulations that represented the two extremes in drug release rate, i.e. the rapidly-releasing system produced using 0.25% w/v SDS and the sustained-release system produced without surfactant.

The surfactant-free system produced microspheres that were smooth and spheroid-shaped (figure 3.3a). At higher magnification, the smoothness and integrity of the surface was emphasized and only a few small surface pores were visible (figure 3.3b). In comparison, the microspheres produced with surfactant were less spheroidal in shape with an uneven outer surface (figure 3.4a). The surface was seen to contain areas of high porosity (figure 3.4b). Using the scale on the micrograph, the surface pores are estimated to be up to 2 μm in diameter.

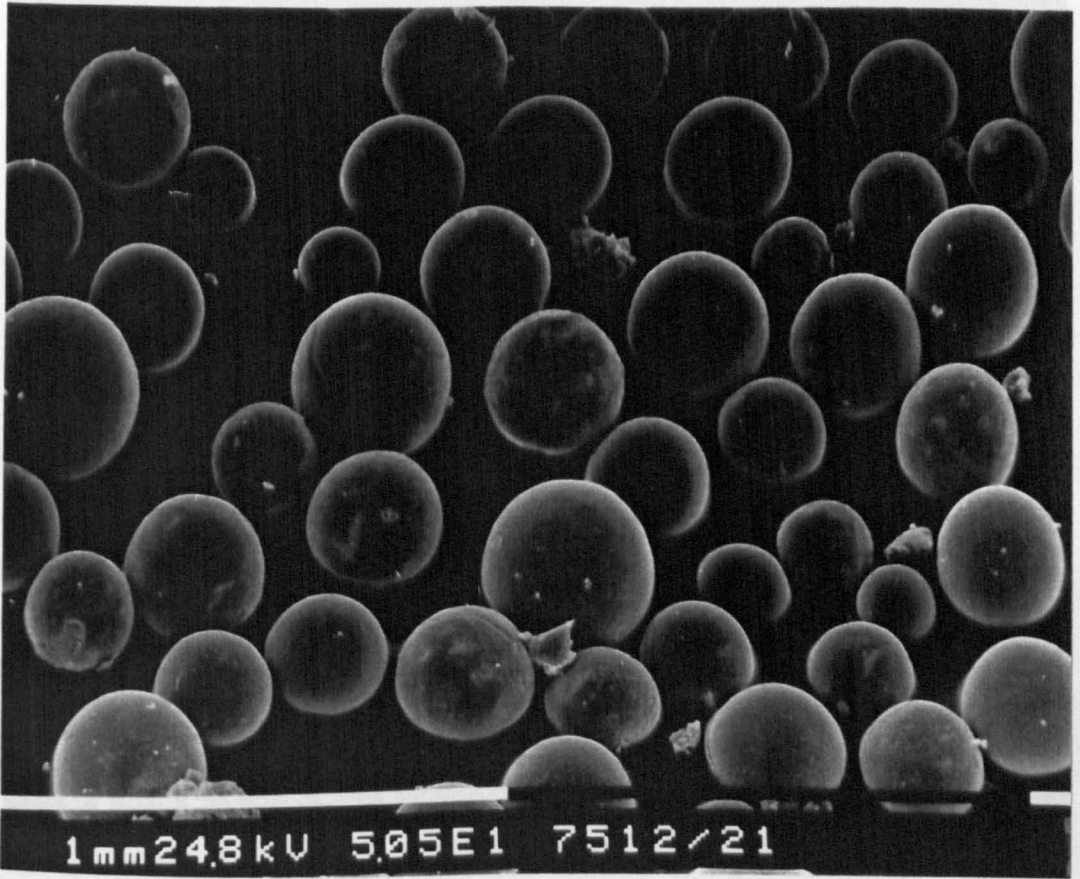
When freeze-fractured, more dramatic structural differences were revealed between the two systems. Figure 3.3c shows a sectioned view of a representative microsphere from the surfactant-free system. The drug-polymer matrix appeared generally dense with a number of large holes present. Figure 3.3d shows a magnified view of this section in which crystals of 5-ASA are visible.

In the microspheres produced with 0.25% SDS, the internal structure reflected the surface topography. The drug-polymer matrix was extremely open and porous, resulting in a sponge-like or honeycomb appearance (figure 3.4c). Figure 3.4d shows a crystal of 5-ASA suspended in this open framework of polymer. There are fewer crystals visible in the micrographs of the 0.25% w/v SDS system because, although the w/w drug loading is equivalent to the surfactant-free system, the bulk density is considerably lower due to their highly porous nature.

Figure 3.3. Electron micrographs of Eudragit RS:5-ASA microspheres prepared without surfactant.

c) Freeze-fractured section of microspheres (x260).

a) View of microsphere population (magnification x50).



d) Freeze-fractured section of microspheres (x260).

b) Detail of microsphere surface (x460).

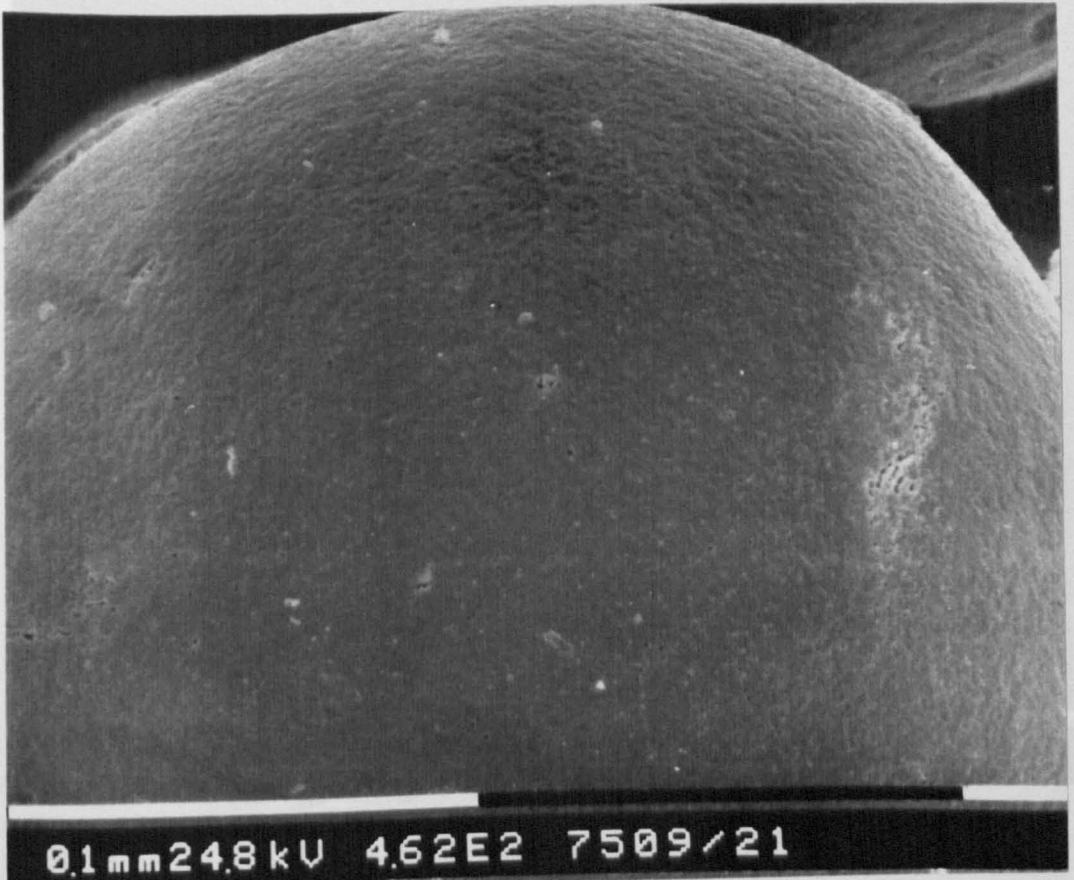
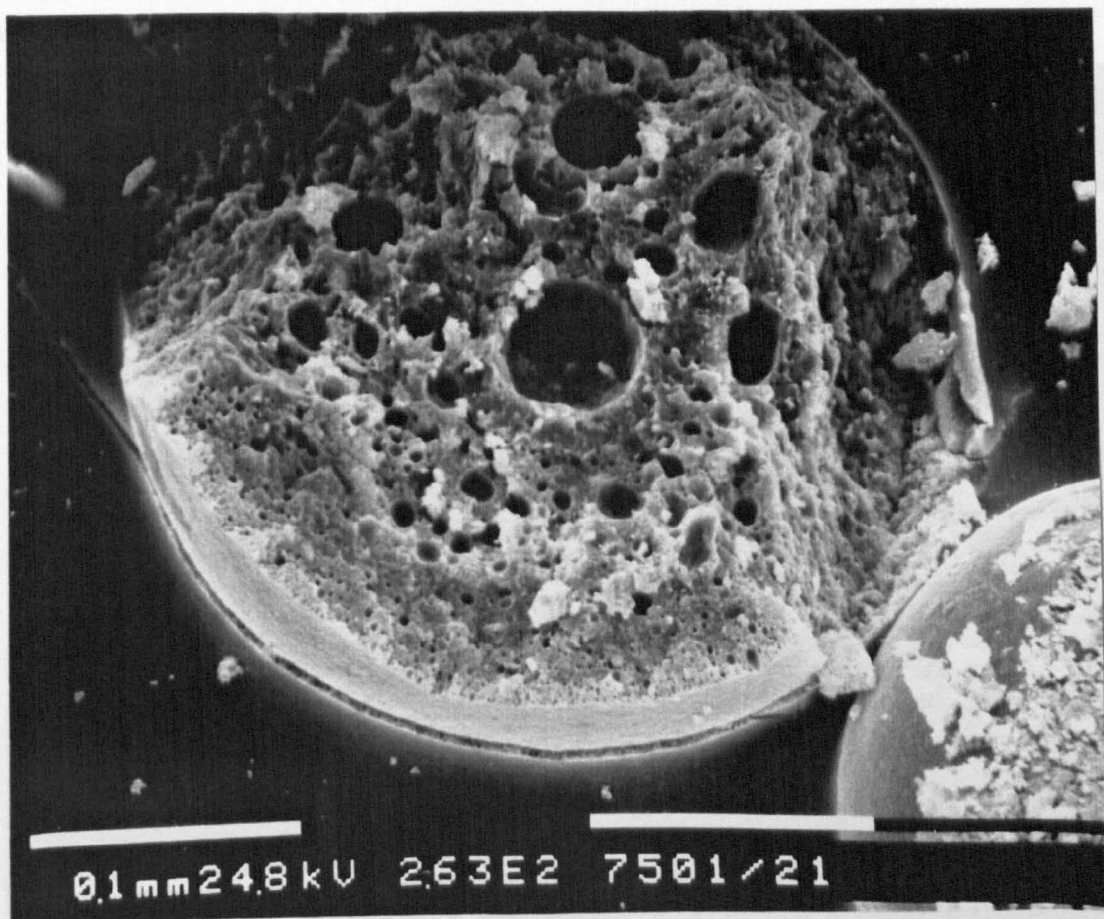


Figure 3.4. Electron micrographs of Dextran 250,000 microspheres prepared with 0.1% w/v SDS as surfactant.
c) Freeze-fractured section of microsphere (x260).



d) Freeze-fractured section of microsphere (x2600).

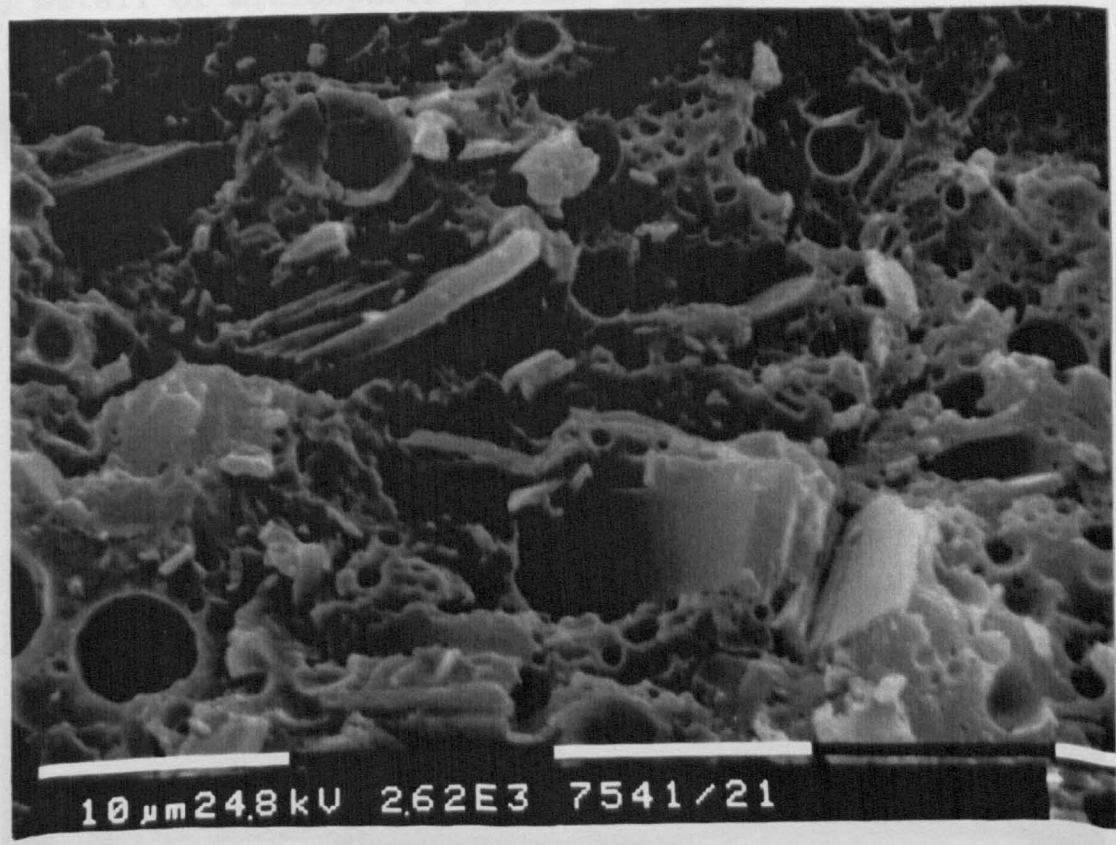
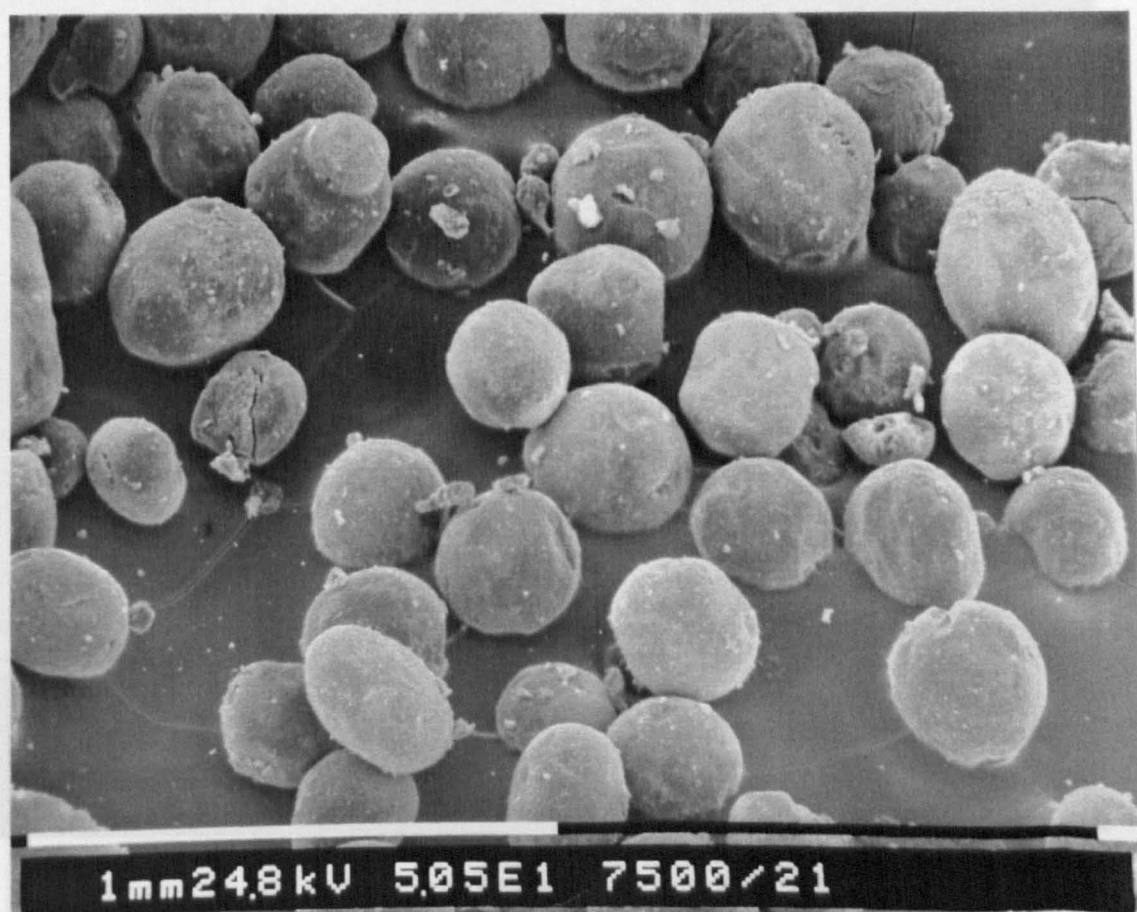


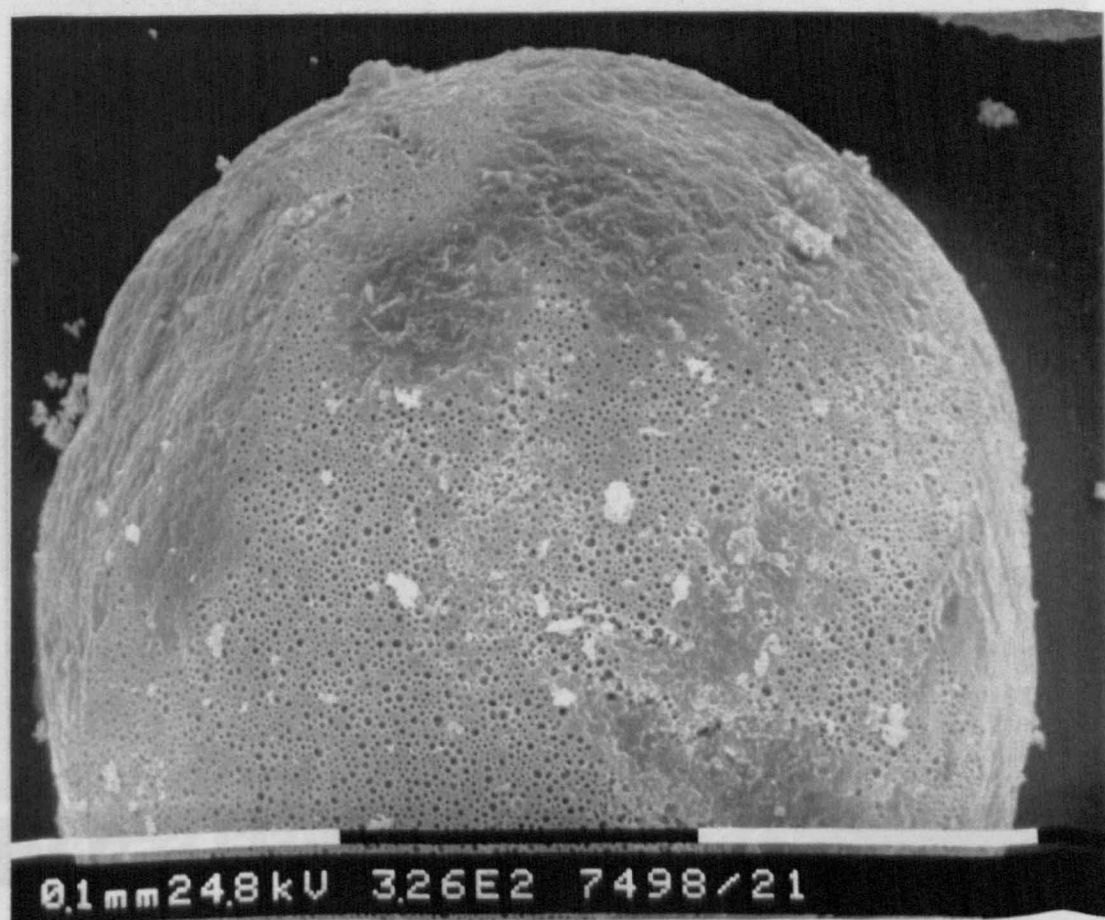
Figure 3.4. Electron micrographs of Eudragit RS:5-ASA microspheres prepared with 0.25% w/v SDS as surfactant.

c) Freeze-fractured section of microspheres (x340).

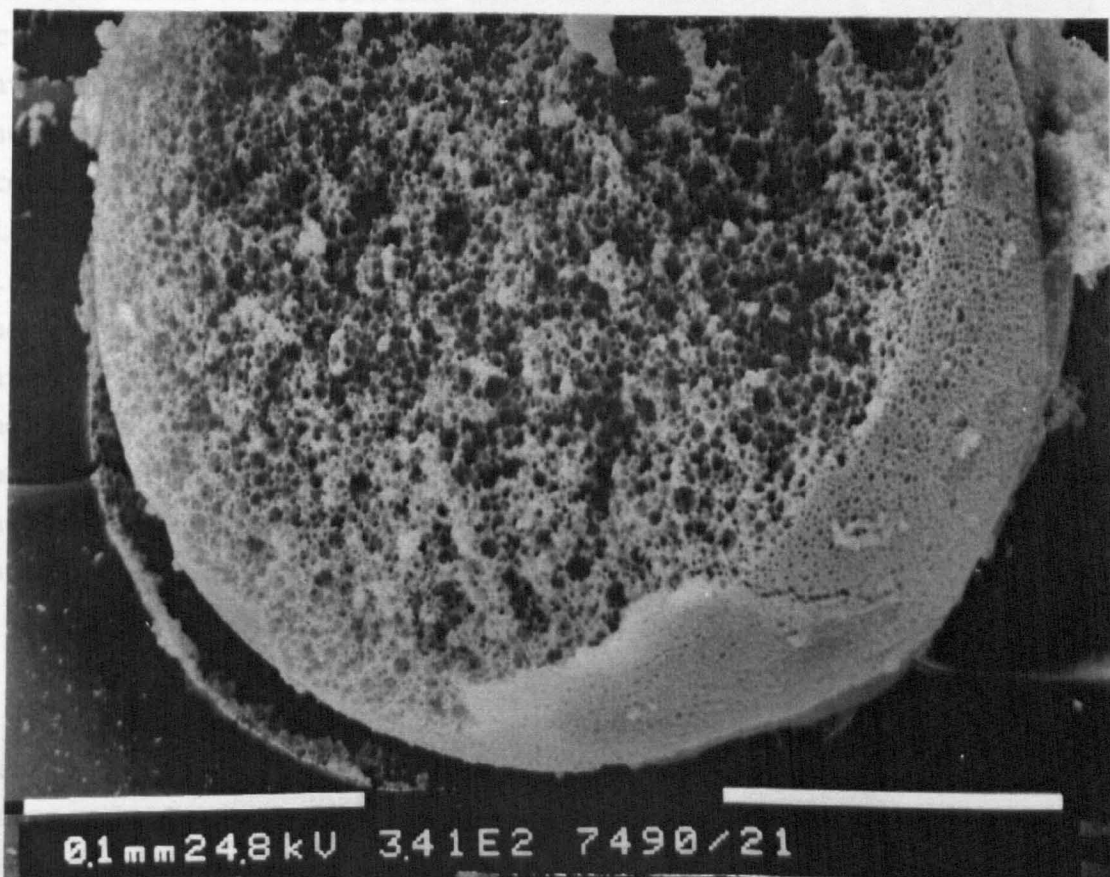
a) View of microsphere population (magnification x50).



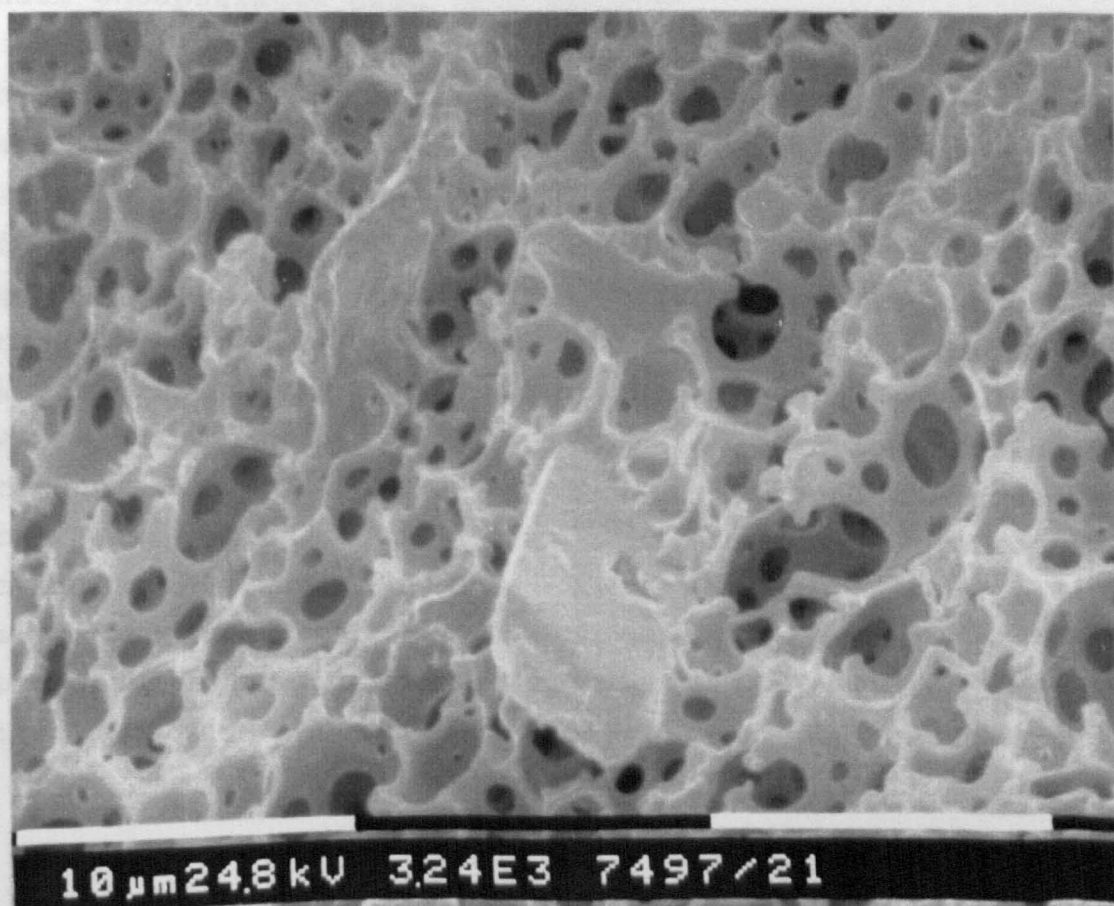
b) Detail of microsphere surface (x330).



c) Freeze-fractured section of microsphere (x340).



d) Freeze-fractured section of microsphere (x3200).



The SEM work demonstrated that the dramatically contrasting drug release characteristics of the two systems investigated was a result of changes in the structure of the drug-polymer matrix. Thus, for the microspheres produced using 0.25% SDS, the highly porous structure allowed rapid entry of dissolution fluid and rapid exit of dissolved drug. Conversely, in the surfactant-free system, the 5-ASA was embedded in a more dense, lower porosity matrix, and as a result diffusion of dissolution fluid into and dissolved drug out of the matrix would be slower, and to a greater extent through the hydrated polymer itself, rather than primarily through pores as was the case for the rapidly releasing system.

3.4. CONCLUSIONS

This chapter has demonstrated that 5-ASA can be successfully encapsulated with high efficiency into Eudragit RS microspheres. By using different concentrations of surfactant, the rate of drug release can be modulated to provide sustained-release systems or systems which release their encapsulated drug very rapidly.

The mechanism responsible for an increase in drug release rate with increasing surfactant concentration is unclear, although for SDS at least, it could be due to the formation of pores in the microsphere matrix. This could result from aqueous droplets of surfactant solution entering into the drug-polymer-solvent droplets during the early stages of microsphere formation, to effectively form a multiple (w/o/w) emulsion system. As solvent evaporation proceeds, drug and polymer would be precipitated around the aqueous droplets. Removal of water from the microspheres by freeze-drying would leave a matrix containing pores. Looking at the micrographs showing the internal structure of the microspheres produced with 0.25% SDS (figures 3.4c and d) it is easy to imagine that the cavities seen could arise

from the deposition of polymer around aqueous droplets.

It is also possible that the mechanism responsible for the surfactant-induced enhancement in drug release is not the same for Tween 20 and SDS. With Tween 20, the enhancement in drug release rate was progressive over the concentration range investigated. With SDS, the enhancement was gradual to a point, but the difference in drug release rate between 0.1% and 0.25% SDS was marked. In addition, all of the concentrations of Tween 20 used exceeded the cmc, yet sustained-release microspheres could be produced. With SDS however, the one concentration that may have exceeded the cmc (0.25% w/v) produced microspheres that released drug instantaneously. When an even higher concentration was used, it was not possible to produce discrete microspheres.

An important point to be considered when evaluating the effects of these two surfactants is that Tween 20 is non-ionic, whereas SDS is anionic. Consequently with SDS, there is the potential for an interaction between the negatively charged dodecyl sulphate ions and the positively charged trimethyl ammonioethyl groups in Eudragit RS. Inactivation of the positively charged polymer functions would certainly alter the microsphere formation process, since they are responsible for its weak surface active properties. But, how such an interaction would influence the final microsphere structure is unclear.

As discussed in section 1.1, in solvent evaporation processes a number of parameters can be used to control the drug release rate. Examples include the drug-loading, the encapsulating polymer, the inclusion of additives such as plasticisers, and the microsphere size. This work has demonstrated, in addition, that the concentration of surfactant may be used as a controlling factor for the rate of drug release from Eudragit RS microspheres. For the system investigated here, it appeared that Tween 20 was a

suitable surfactant for this task.

It is not clear if surfactant-enhanced drug release applies to other encapsulating polymers, although for toxicological reasons the presence of high concentrations of surfactant in microspheres for parenteral administration would probably be undesirable.

CHAPTER 4.

BULK CHARACTERISATION OF EUDRAGIT RS-SULPHASALAZINE
MICROSPHERES USING FOURIER TRANSFORM-RAMAN SPECTROSCOPY.

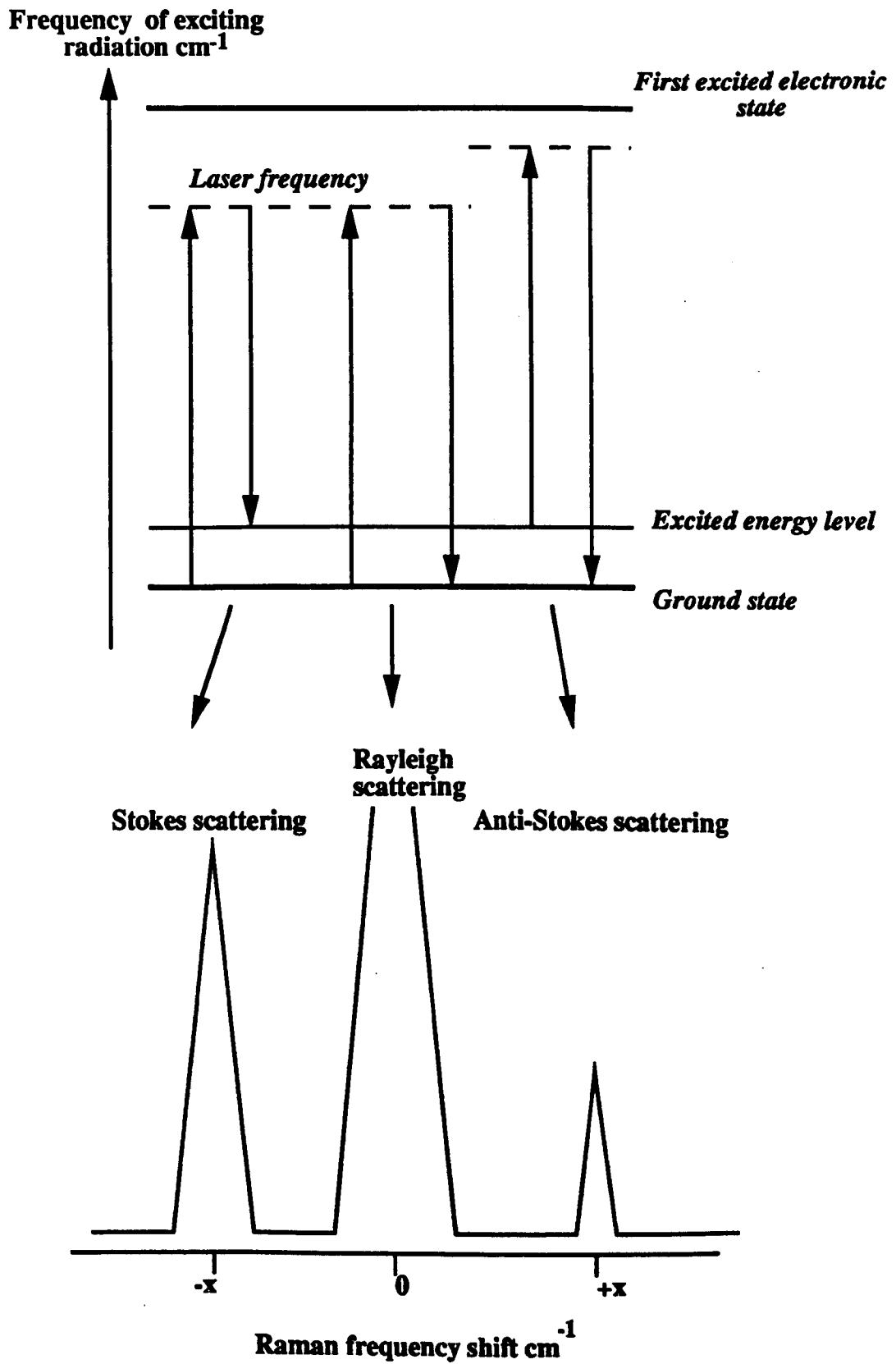
4.1. INTRODUCTION

Raman spectroscopy was discovered in 1928 by C.W.Raman. Although widely used through the 1930s, it was rapidly overtaken by developments in infrared (IR) spectroscopy after this time and largely passed out of use as a routine analytical technique (Ellis et al., 1989).

Raman and infrared spectroscopy are complementary techniques and provide information on both molecular vibrational and rotational changes. Raman spectra arise from the inelastic scattering of light, and are associated with changes in molecular polarisability. Polarisability is defined as the ease with which a molecule can be polarised by an external force. In contrast, infrared spectra are generated by changes in the molecular dipole moment (Willard et al., 1988).

When a material is irradiated with a monochromatic light source the molecules present will be excited into a higher energy state, determined by the energy of the incident photons (see figure 4.1). The majority of the incident radiation will undergo elastic scattering and the molecules will fall back to ground state, with the energy and frequency of the emitted radiation unchanged. This process is called Rayleigh scattering. A very small proportion of the photon collisions, about one in a million, will be inelastic and result in net energy exchange between photon and scattering molecule. If the excited molecule falls back to an excited vibrational level (i.e. a different degree of polarisability), the energy and frequency of the emitted radiation will decrease. Such transitions result in Stokes lines, at frequencies lower than the incident radiation. On the other hand, if the molecule is already at an excited vibrational level when a photon interacts, energy of a higher frequency will be emitted if the molecule falls back to the ground state. This results in energy bands at

Figure 4.1. Energy changes involved in Rayleigh and Raman scattering (adapted from Willard et al., 1988).



frequencies higher than the incident radiation, so-called anti-Stokes lines. This type of interaction is less common and consequently anti-Stokes lines are less intense than Stokes lines (Willard et al., 1988; Ewing, 1975; Hendra and Mould, 1988). These interactions make up the Raman spectrum (see figure 4.1).

Although Raman spectroscopy can yield useful molecular structural information, complementary to IR spectroscopy, it does have a major limitation. Raman scattering is very weak in intensity, since the vast majority of the incident radiation undergoes elastic scattering. As a result, if the material under investigation absorbs at the exciting or Raman wavelength (e.g. coloured compounds) or if it fluoresces even at low levels, the Raman scattering is overwhelmed and analysis is impossible (Hendra and Mould, 1988). In addition, molecules may undergo photo-decomposition (Chase, 1987). Consequently, most materials are unable to yield useful Raman spectra (Hendra and Mould, 1988). In addition, alignment of the irradiating laser and sample need to be very precise and as a result spectral acquisition may take many hours (Ellis et al., 1989).

However, there is currently a renaissance in Raman spectroscopy following the introduction of near-infrared laser sources for sample irradiation combined with analysis of the Raman scatter using an FT-IR spectrometer modified to operate in the near-infrared region (Chase, 1987; Hendra and Mould, 1988). Fluorescence, absorption and photo-decomposition are all markedly reduced using near-infrared irradiation, and consequently most materials are able to yield useful FT-Raman spectra (Ellis et al., 1989). A number of Fourier transform Raman spectrometers are now commercially available and as a result, Fourier transform Raman spectroscopy (FTRS) is becoming established as an important and versatile technique in analytical chemistry. The instruments eliminate the need for tedious sample

alignment, and operation is straightforward and rapid with minimal sample preparation requirements. A major attraction of FTRS is the fact that it is non-destructive and so samples can be recovered after analysis (Ellis et al., 1989).

There have been a number of reports on qualitative and quantitative applications of FTRS to materials of pharmaceutical interest. It has been used to identify illicit drug substances (Hodges et al., 1990), and to distinguish between structurally related compounds (Tudor et al., 1990). FTRS also appears to be able to distinguish between different drug polymorphic forms, for example cimetidine (Tudor et al., 1991a) and chlorpropamide (Tudor et al., 1991b).

It has also been used to investigate the structure and biodegradation of poly(anhydrides) (Tudor et al., 1991c), materials suitable for implantation as drug-delivery systems (see section 1.1.3.1.B).

There is currently considerably less data on the application of FTRS to pharmaceutical dosage forms. One paper has reported the characterisation of drug-containing polymer matrices (Davies et al., 1990a). For a series of tablets containing 5-60% w/w diclofenac sodium in sodium alginate, a linear relationship was seen between the integrated area of two drug bands from the Raman spectra and the concentration of drug. The spectra also suggested a degree of drug-polymer interaction.

The general aims of the FTRS work described in this chapter were to assess:

- a) If drug and polymer could be distinguished in spectra of drug-polymer microspheres. If this were the case, information would be provided on the microsphere bulk

structure which might enable any interactions between drug and polymer to be identified.

- b) The possibility of using the technique to quantify levels of drug present in microsphere samples.

Although the initial work involving drug encapsulation, described in Chapter 3, concentrated on 5-ASA, this drug would be unsuitable for planned in vivo biopharmaceutical investigations because of low colonic absorption. For assessment of the in vivo colonic release characteristics of the Eudragit microspheres, a different drug candidate was chosen, sulphasalazine (SASP). The use of SASP for the treatment of inflammatory bowel diseases is well established, and was discussed in detail in section 1.2.5. SASP was chosen since its sulphapyridine portion, generated by colonic metabolism, is well absorbed and would act as a potential marker for drug released from the microspheres into the colon.

4.2. EXPERIMENTAL

4.2.1. Materials

As for chapter 3, but in addition: SASP (in place of 5-ASA) (Sigma), acetone (Analar grade)(Rhône-Poulenc).

4.2.2. Methods

4.2.2.1. Microsphere production

SASP-Eudragit RS microspheres were produced by the same basic technique described in chapter 3. The Eudragit RS and SASP were weighed into a glass bottle. 20 ml of dichloromethane was then pipetted into the bottle to dissolve the polymer. The SASP remained in suspension, being largely insoluble in dichloromethane. When dissolution of the polymer was complete, the drug-polymer mixture was poured into a 200 ml glass beaker containing 100 ml of 0.1% w/v aqueous Tween 20 solution and stirred

with an overhead stirrer at 200 rpm. In all cases, the total quantity of drug and polymer in the dichloromethane at the start of microsphere manufacture was 2 g. Stirring was continued until all of the solvent had evaporated. The completed microspheres were then filtered, washed, and freeze-dried as described in chapter 3. After drying, the microspheres which passed through a 500 μm sieve were collected.

11 batches of microspheres were prepared containing a range of concentrations of SASP in order to produce a calibration graph of drug concentration versus Raman peak intensity. The following drug:polymer ratios (by weight) were employed: 6:94, 10:90, 15:85, 20:80, 25:75, 30:70, 35:65, 45:55, 50:50, 55:45, and 60:40. In addition, a drug-free sample of microspheres was prepared and a sample produced for a dissolution study composed of a 33:67 drug:polymer mixture.

4.2.2.2. Microsphere assay

An accurately weighed quantity of microspheres, estimated to contain approximately 2 mg of SASP, were placed into a 100 ml volumetric flask. 5 ml of acetone was added to the flask to dissolve the microsphere polymer matrix. The flask was then made to volume with 0.05 N aqueous sodium hydroxide solution, resulting in dissolution of the SASP and precipitation of the Eudragit RS. The liquid was filtered through a 1 μm membrane filter and the UV absorbance at 458 nm measured. The concentration of drug present was calculated by reference to a calibration curve of SASP in 0.05 N aqueous sodium hydroxide containing 5% v/v acetone. Assays were carried out at least in duplicate.

4.2.2.3. Microsphere drug release study

The microspheres made using the 33:67 drug:polymer mixture were dissolved to provide a comparison of microsphere drug content obtained from drug release measurements and FTIR

analysis. 40 mg of the microspheres (250-500 μm) were placed into each of the six flasks in a dissolution apparatus (see chapter 3) containing 500 ml of pH 7 phosphate buffer (appendix 1). The buffer was maintained at a temperature of 37 °C and agitated by paddle stirrers at 100 rpm. At 1, 3, 6, 9, 12, and 24 hours, one of the six flasks was removed and the microspheres collected by passing the contents through a Buchner funnel containing a 20 μm filter. The filtrate was assayed spectrophotometrically for SASP content (359 nm). The microspheres were recovered from the filter and air dried at room temperature in preparation for FTRS analysis.

4.2.2.4. FTRS analysis

Samples were analysed using a Bruker IFS-88 FT-IR spectrometer coupled to an FRA-106 FT-Raman accessory (Bruker Spectrospin, Coventry, UK). A general layout of the instrument sample area is shown in figure 4.2.

The samples (microspheres and pure drug) were lightly packed into an aluminium sample cup of 10 mm overall diameter containing a 2 mm diameter bore to hold the sample. The samples were irradiated by a diode pump Nd:YAG laser, wavelength 1.064 μm (Adlas, Lubeck, Germany), focused to a spot size of 100 μm diameter onto the sample. The backscattered radiation was detected and the resultant Raman spectrum was collected after 50 scans of the sample. The signal/noise ratio of each FT-Raman spectrum was optimised by altering the parameters governing spectral acquisition, namely the resolution and laser power. Pure sulphasalazine and all of the calibration samples, apart from the four highest drug concentrations were analysed at a laser power of 180 mW and an instrumental resolution of 4 cm^{-1} . The remaining four samples were analysed at 140 mW and 4 cm^{-1} resolution. To achieve a comparable signal/noise ratio, the dissolution samples were analysed at 300 mW and 4 cm^{-1} resolution.

Spectral reproducibility was also examined, using a microsphere sample containing 100 particles (100 scans). To test both sample variability, single spectra were obtained for a single microsphere (100 scans) and 100 scans were obtained for a single microsphere (100 scans). Weighing between acquisition parameters.

4.3.1. Microsphere... Microspheres were... drug/polymer... microsphere spectra... the efficiency of drug... increasing with drug... above 34% w/w SASP

4.3.2. Drug release study... The results of the microsphere... presented in table 4.2. The... drug released in the... interval... content... released... microspheres... properties... with only... of the... SASP released after 12 hours... For comparison, an equivalent amount of unencapsulated SASP powder completely dissolved within 30 minutes under the same conditions.

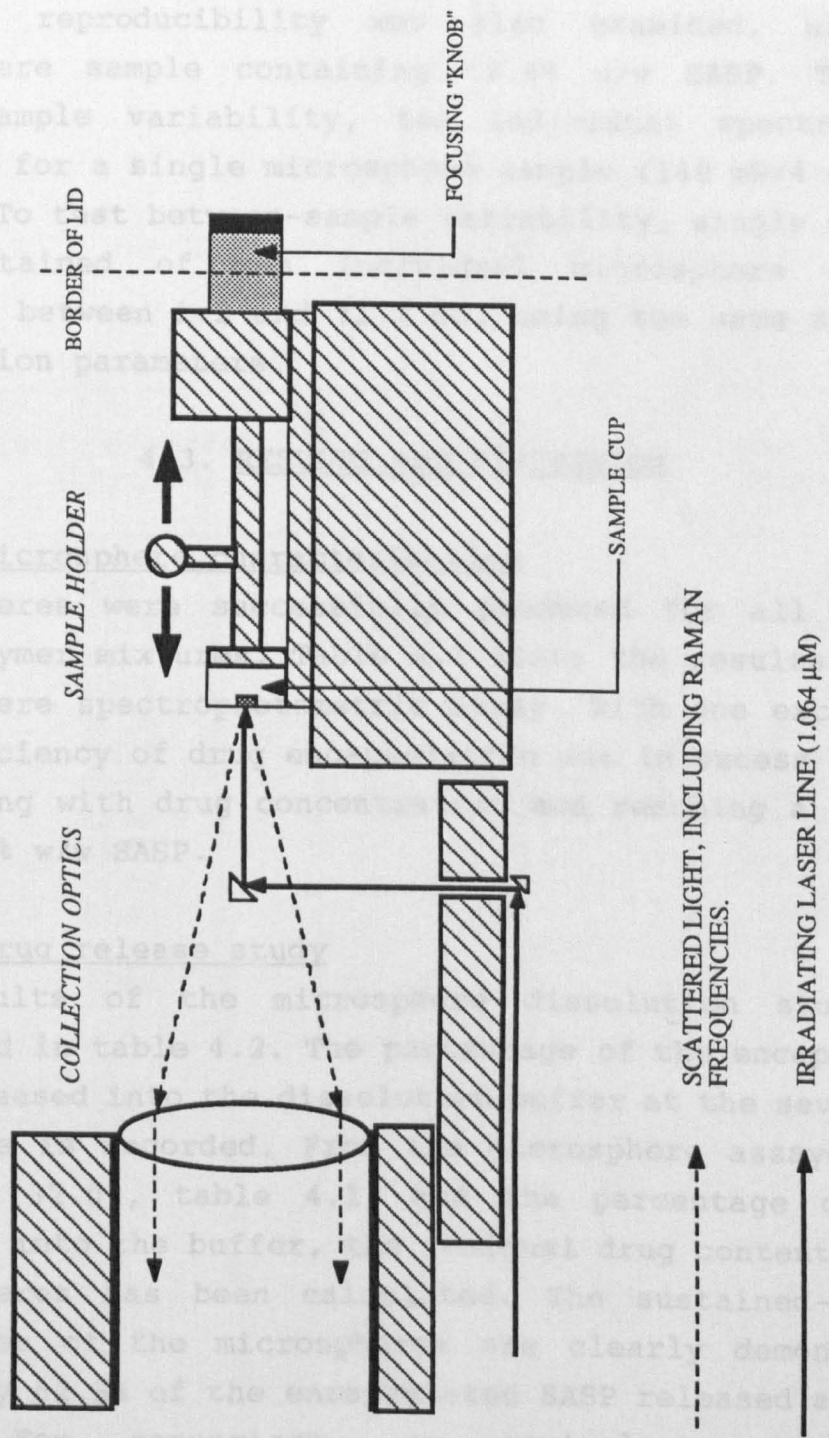


Figure 4.2. Schematic of Raman sampling area and collection optics.

Spectral reproducibility was also examined, using a microsphere sample containing 17.4% w/w SASP. To test within-sample variability, ten individual spectra were obtained for a single microsphere sample (140 mW/4 cm⁻¹/50 scans). To test between-sample variability, single spectra were obtained of ten individual microsphere samples weighing between 1.2 and 71.1 mg, using the same spectral acquisition parameters.

4.3. RESULTS AND DISCUSSION

4.3.1. Microsphere characterisation

Microspheres were successfully produced for all of the drug/polymer mixtures. Table 4.1 lists the results of the microsphere spectrophotometric assay. With one exception, the efficiency of drug encapsulation was in excess of 85%, increasing with drug concentration and reaching a plateau above 24% w/w SASP.

4.3.2. Drug release study

The results of the microsphere dissolution study are presented in table 4.2. The percentage of the encapsulated drug released into the dissolution buffer at the seven time intervals is recorded. From the microsphere assayed drug content (32.0%, table 4.1) and the percentage of drug released into the buffer, the residual drug content of the microspheres has been calculated. The sustained-release properties of the microspheres are clearly demonstrated with only 62.3% of the encapsulated SASP released after 12 hours. For comparison, an equivalent amount of unencapsulated SASP powder completely dissolved within 90 minutes under the same conditions.

Table 4.1. Details of Eudragit RS:sulphasalazine microsphere formulations.

Drug:polymer ratio (by weight)	Assayed drug content (%w/w)	Encapsulation efficiency (%)
6:94	5.1	85
10:90	8.9	89
15:85	11.7	78
20:80	17.3	86
25:75	24.0	96
30:70	28.5	95
35:65	33.8	97
45:55	42.9	95
50:50	47.3	95
55:45	51.2	93
60:40	54.6	91
33:67	32.0	96

Table 4.2. *In vitro* release of sulphasalazine from Eudragit RS microspheres over a 24 hour period.

Time after dissolution (h)	% w/w of encapsulated drug released	Microsphere drug content (% w/w)
0	0.0	32.0
1	12.4	28.0
3	29.6	22.5
6	39.8	19.3
9	54.7	14.5
12	62.3	12.1
24	73.2	8.6

4.3.3. FT-Raman spectra

4.3.3.1. Qualitative interpretation

The chemical structures of SASP and Eudragit RS are shown in chapter 1 (figure 1.6 and table 1.2 respectively).

Pure SASP produced an intense and complex Raman spectrum (figure 4.3). The intensity of the spectrum is a result of the three aromatic ring structures in the SASP molecule, since these functions are strong Raman scatterers (Willard et al., 1988).

In Raman spectroscopy, each form of ring substitution produces a specific pattern of bands. The scattering peaks at 1395, 1148, 1077 and 708 cm^{-1} may originate from the 1,2,4-trisubstituted benzene ring, whereas the peaks at 1246, 803 and 645 cm^{-1} may arise from the 1,4-disubstituted ring. The strong peak at 1584 cm^{-1} could originate from any of the three rings. Other prominent peaks in the spectrum arise from specific functions within the SASP molecule, such as the sulphonamide group ($-\text{SO}_2\text{NH}-$) at 1155 cm^{-1} and the 2-substituted pyridine which probably results in the peak at 1453 cm^{-1} and the broad shoulder at 1437 cm^{-1} . The relatively weak band at 3067 cm^{-1} arises from the aromatic C-H stretching vibrations. (For information on peak assignments, see Colthup et al., 1975).

Figure 4.4 is the FT-Raman spectrum of drug-free Eudragit RS microspheres. In comparison to SASP, the spectrum of the polymer was weaker in intensity and considerably less complex. Three major bands dominated the spectrum, at 1728, 1449 and 2949 cm^{-1} . The band at 1728 cm^{-1} arises from the carbonyl bond of the polymer ester functions. Stretching of the methyl and methylene groups results in the band at 2949 cm^{-1} , while deformation of these groups results in the band at 1449 cm^{-1} .

In Raman spectroscopy, aromatic, heterocyclic and

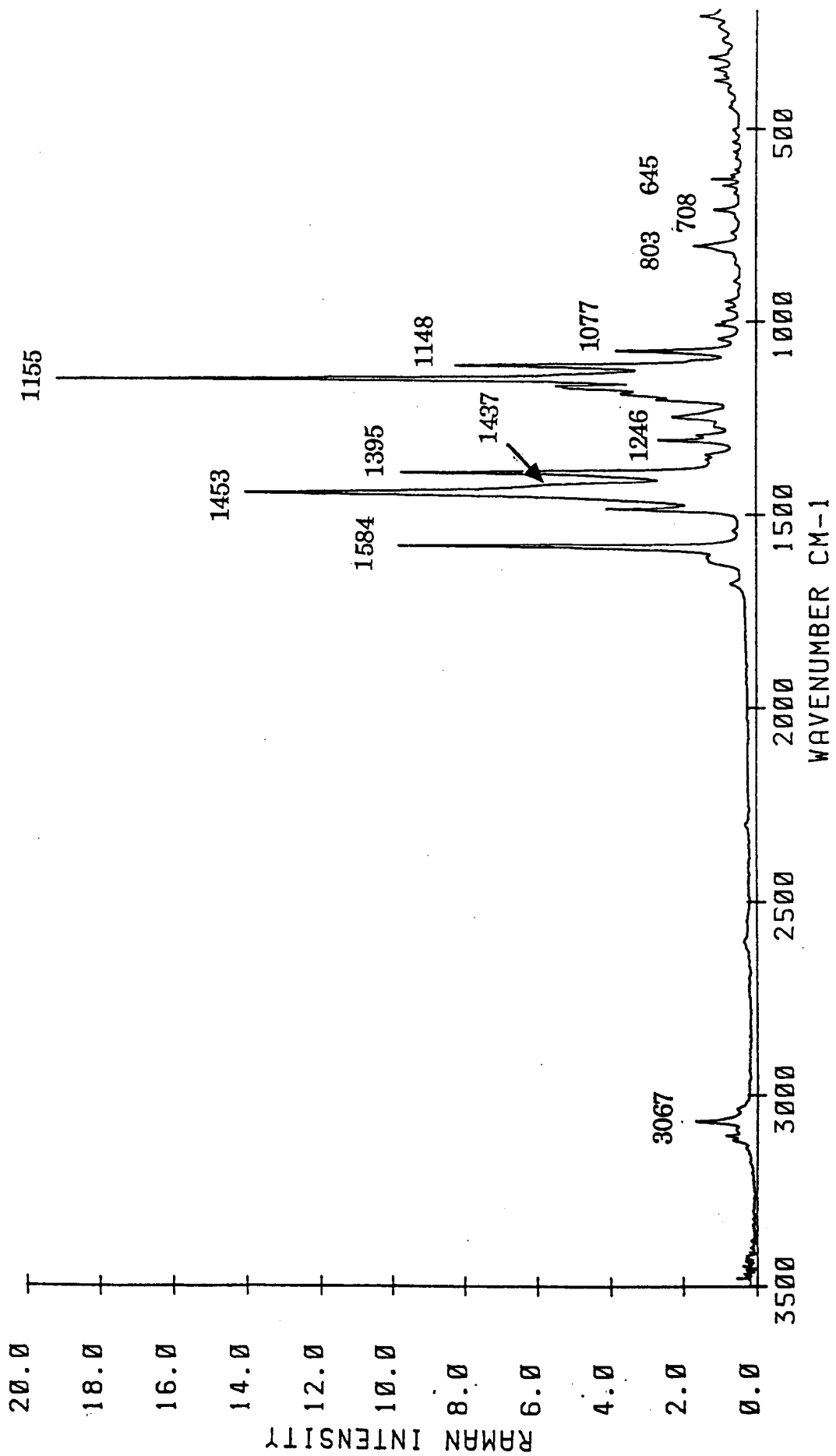


Figure 4.3. FT-Raman spectrum of sulphasalazine.

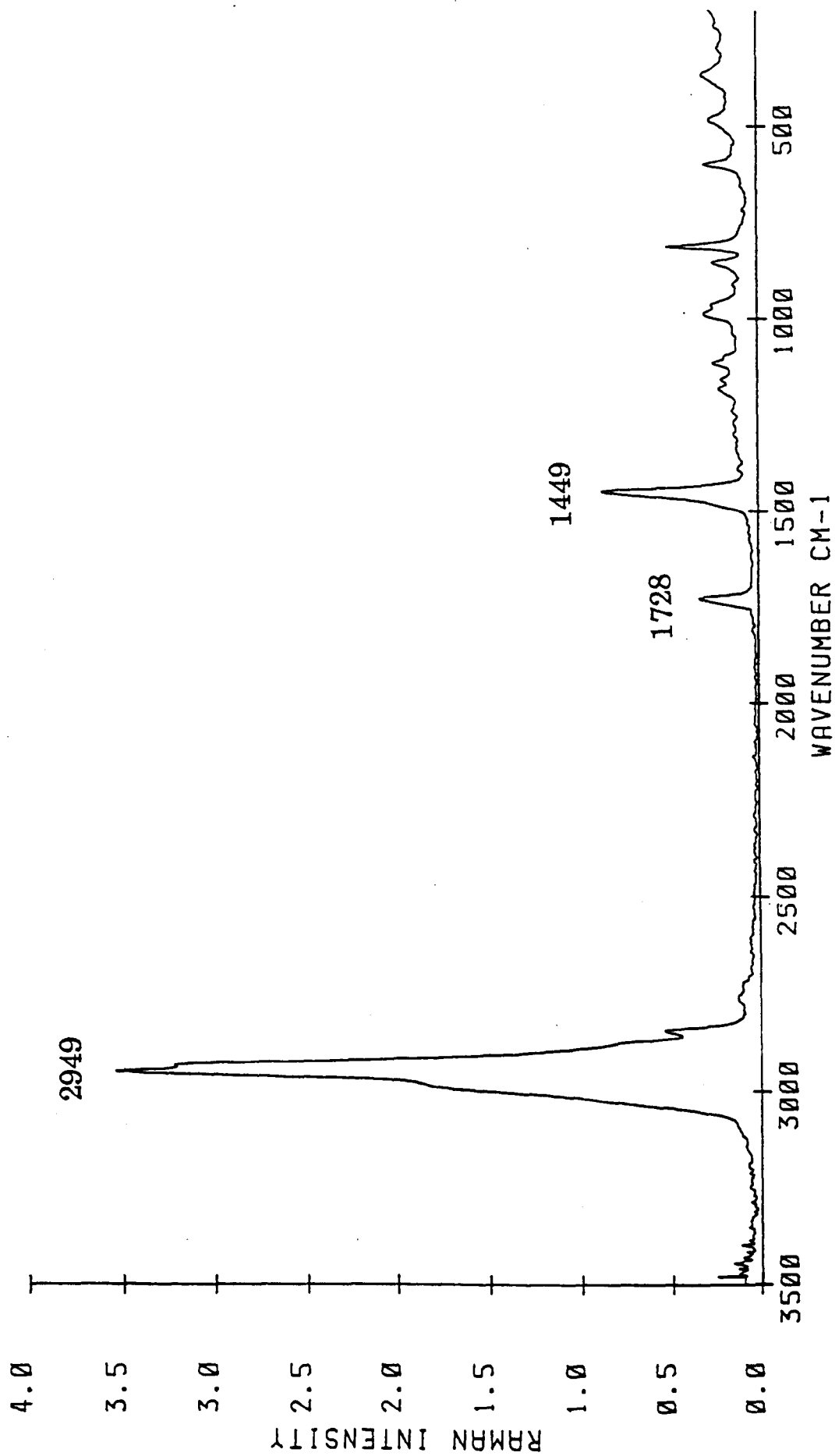


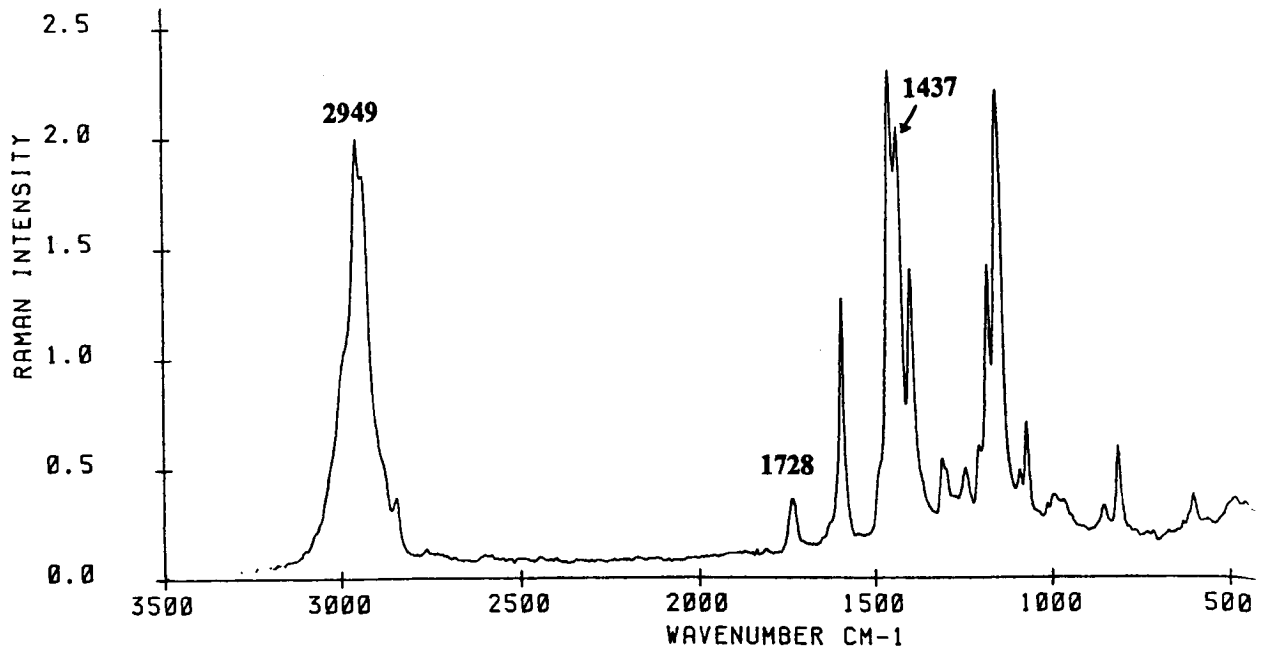
Figure 4.4. FT-Raman spectrum of drug-free Eudragit RS microspheres.

crystalline materials usually give intense Raman spectra. In contrast, randomised molecular systems, particularly if aliphatic tend to result in a complex vibrational pattern (Hendra, P.J., personal communication). As a consequence, the numerous bands overlap producing a broad, diffuse, weak spectrum. SASP and Eudragit RS are good examples of a good and poor scatterer respectively and illustrate this principle well.

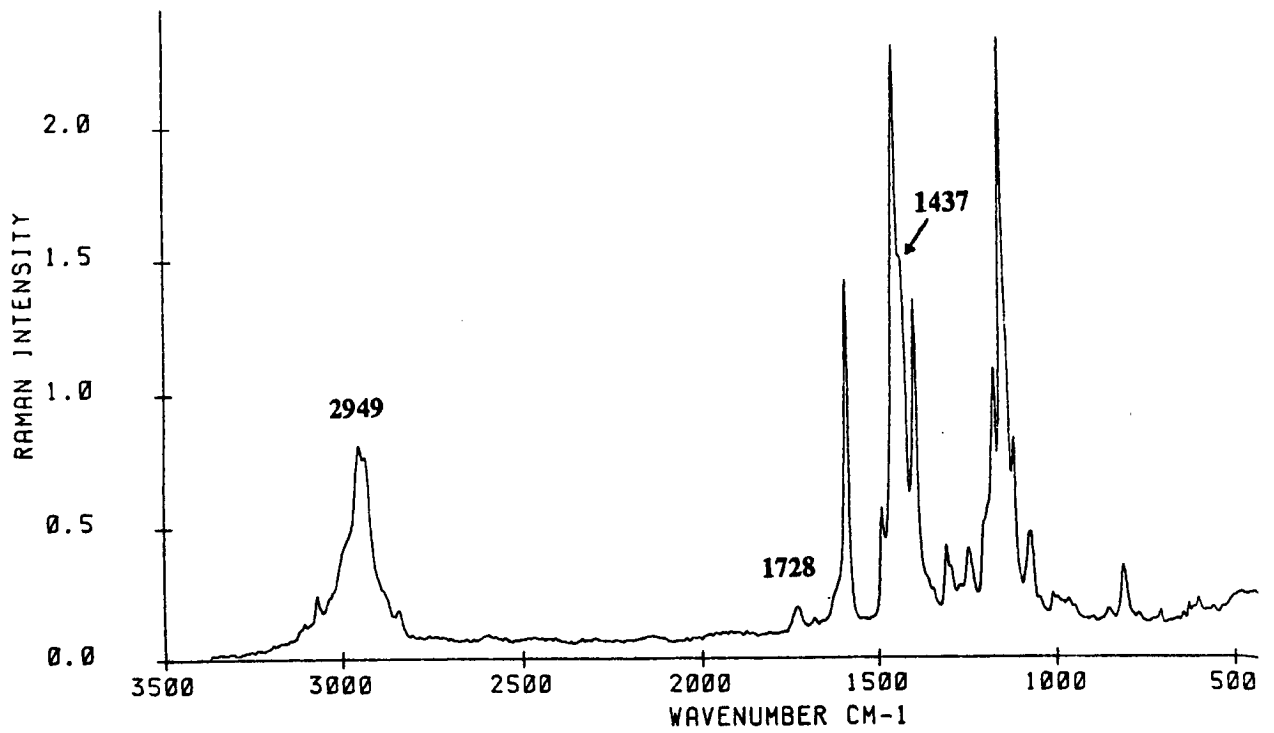
Figures 4.5a-d show the spectra of four of the drug:polymer microsphere formulations containing 5.1, 11.7, 28.5 and 54.6% w/w SASP respectively. In figure 4.5a (5.1% w/w SASP) the Eudragit RS bands at 2949 and 1728 cm^{-1} can clearly be seen, although the 1449 cm^{-1} band has been masked by SASP bands. The characteristic SASP bands are clearly evident (e.g. 1584, 1453, 1395, 1148 and 1077 cm^{-1}) and are of equivalent intensity to those from the polymer which reflects the high scattering intensity of the drug despite its low bulk concentration. As the concentration of SASP increases, the relative intensity of the polymer bands at 2949 and 1728 cm^{-1} diminishes. In fact at 54.6% w/w SASP, the 1728 cm^{-1} band is no longer visible. Figures 4.5a-d clearly demonstrate the ability to distinguish Eudragit RS from SASP in this mixed system.

An interesting observation in these spectra is the appearance of the 1437 cm^{-1} SASP band. In the pure drug this band appears as a shoulder on the larger 1453 cm^{-1} band (figure 4.3). However, in the spectrum of microspheres containing 5.1% w/w drug (figure 4.5a), the 1437 cm^{-1} band appears resolved. As the microsphere SASP content increases, the resolution of this band decreases and it becomes a shoulder (figures 4.5b-d). This behaviour may be indicative of a degree of drug-polymer interaction. It is perhaps the case that the drug dissolves to a small extent in the dichloromethane phase during microsphere production and as a result is able to interact with the polymer as

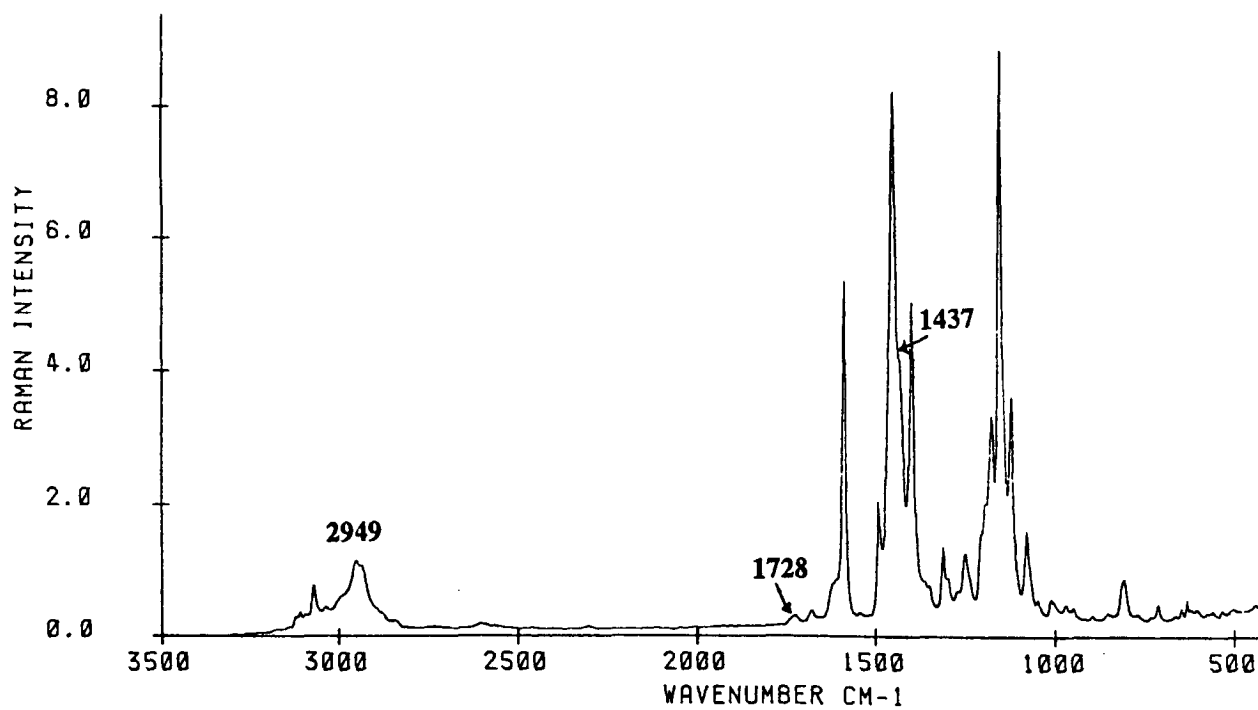
Figure 4.5. FT-Raman spectra of Eudragit RS-sulphasalazine microspheres.



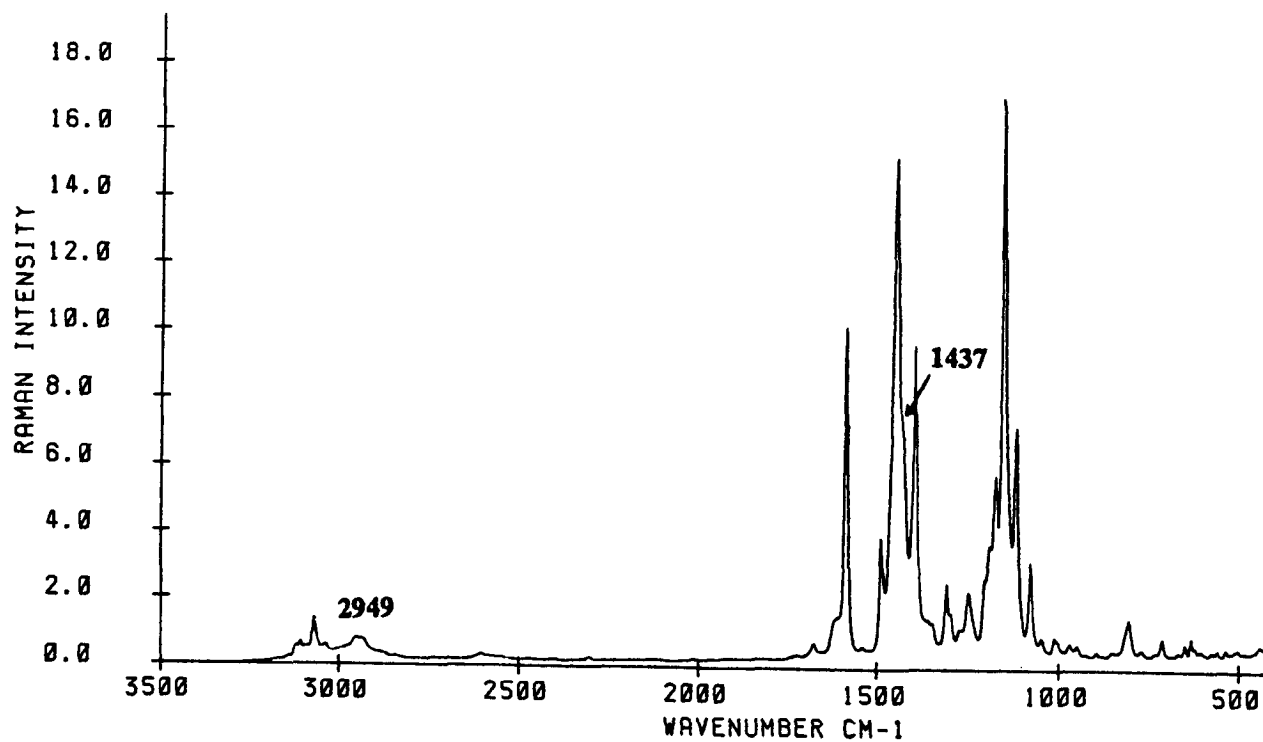
a) 5.1% w/w sulphasalazine.



b) 11.7% w/w sulphasalazine.



c) 28.5% w/w sulphasalazine.



d) 54.6% w/w sulphasalazine.

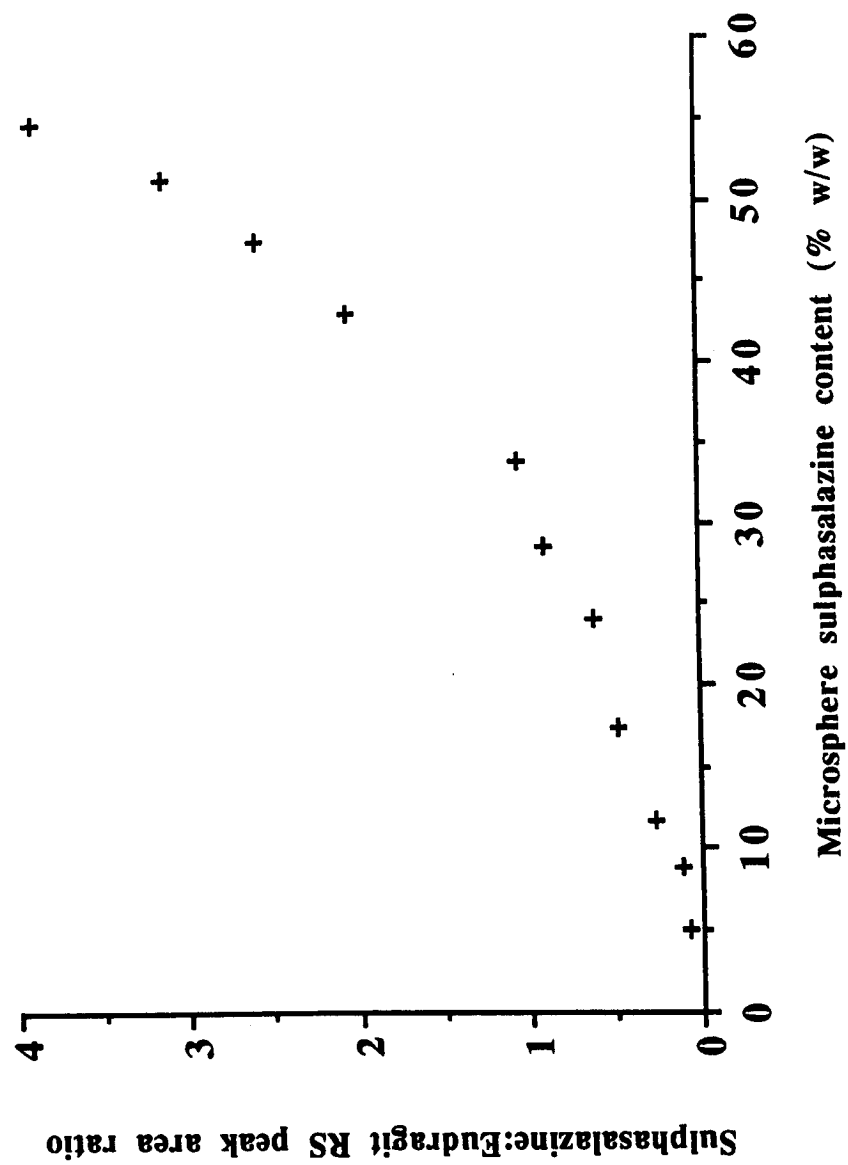
solvent evaporates. Since the quantity of drug dissolving and interacting in this way will be constant, depending only on its solubility in dichloromethane, the relative intensity of the affected peak will decrease as the microsphere SASP content increases. It should be noted that there appear to be no changes in the other major peaks in the SASP spectrum and so the degree of interaction is probably small.

4.3.3.2. Quantitative interpretation

A quantification of drug content based on SASP peak intensities was undertaken. Although the intensity of Raman scattering from the drug and polymer in each sample will be dependent on the quantity present within the area irradiated by the laser, due to variations in density and packing within the sample holder, the absolute intensity of the drug peaks within the Raman spectrum cannot be directly related to the concentration present. In order to eliminate problems arising from variations in sample packing and density, a peak area ratio was calculated between SASP (1584 cm^{-1} band) and Eudragit RS (2949 cm^{-1} band) for each spectrum. For SASP, the peak area was determined between 1600 and 1557 cm^{-1} and for Eudragit RS, between 3047 and 2857 cm^{-1} , thereby avoiding the small SASP band at 3067 cm^{-1} . Peak areas were directly obtained by manipulation of stored spectral data by the FT-Raman spectrometer.

For each spectrum, the peak area ratio (SASP:Eudragit RS) was calculated and plotted against the SASP content assayed spectrophotometrically (from table 4.1). This relationship, shown in figure 4.6, is not a simple one, since as the concentration of drug increases, so the concentration of polymer decreases. Thus, even if the intensity of scattering from polymer and drug were linear with concentration, the relationship in figure 4.6 would not be so.

Figure 4.6. Relationship between peak area ratio and microsphere drug content.



To simplify data interpretation, a plot of $\log[\text{peak area ratio}]$ vs. $\log[\%SASP/(100-\%SASP)]$ has been produced (figure 4.7). The derivation of this relationship is described in figure 4.8. A linear relationship was shown between the two parameters ($r=0.995$), with the y axis intercept corresponding to the relative difference in scattering intensity between the chosen drug and polymer peaks (figure 4.7). If the area of the drug and polymer peaks increased in a linear fashion with concentration, the gradient of the line would be 1.0 (figure 4.8), and so the actual gradient of 1.26 in figure 4.7 might indicate some deviation in linearity between peak intensity and drug or polymer concentration.

For each of the spectra from the dissolution samples, the SASP:Eudragit RS peak area ratio was also calculated. The ratio values were substituted into the figure 4.7 calibration equation and the concentration of SASP calculated. In figure 4.9, the microsphere drug content values calculated in this way and from the spectrophotometric data (table 4.2) are plotted versus time for comparison. For the 1, 3, and 6 hour samples, the Raman and UV-calculated values were in excellent agreement. However, for the 9, 12 and 24 hour samples, the Raman-calculated drug content values were all higher than the spectrophotometrically-based data, perhaps indicating deviations from linearity in the calibration curve at low SASP levels.

The same drug:polymer peak area ratio was employed to assess spectral reproducibility. For the within-sample test (ten spectra of the same sample), the standard deviation of the calculated peak area ratio was $\pm 3.0\%$ ($n=10$). For the between-sample test (one spectra from each of ten different samples) the standard deviation was $\pm 4.4\%$ of the mean peak area ratio. In fact, one of the samples began to burn during spectral acquisition as a result of laser damage,

Figure 4.7. Linear relationship between peak area ratio and microsphere drug content

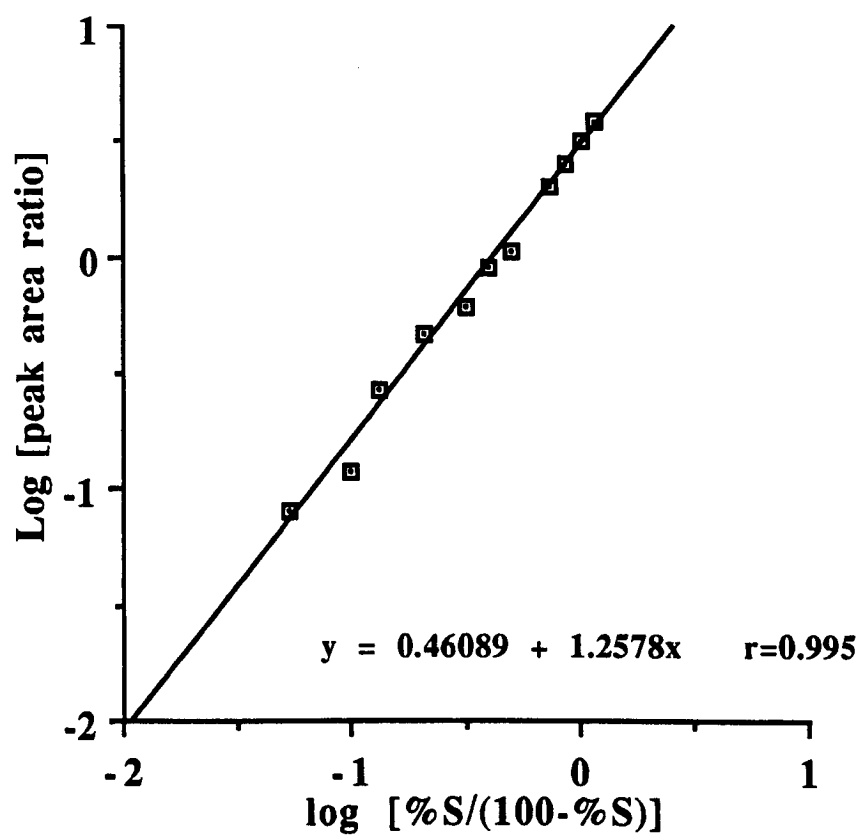


Figure 4.8. Derivation of a linear relationship between drug concentration and peak area ratio.

For a system containing two components, A and B,

$$\text{Drug:polymer peak area ratio, } R = \frac{f_A \times a}{f_B \times b}$$

Where, f = fraction of component, and a and b = peak area of 100% A and B respectively.

$$\text{Since } f_B = 100 - f_A$$

$$R = \frac{f_A \times a}{(100 - f_A) \times b}$$

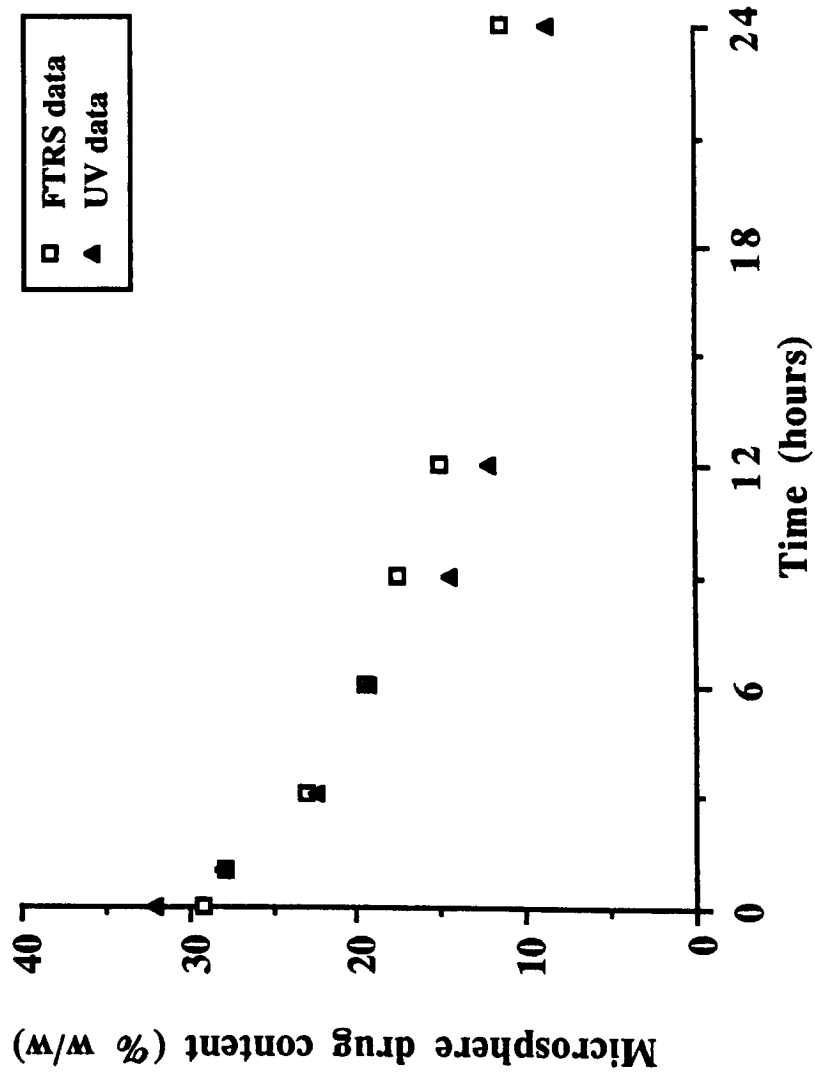
If the relative difference in peak intensity between a and b is y , i.e. $a = b \times y$, then,

$$R = \frac{f_A \times a \times y}{(100 - f_A) \times a} = \frac{y \times f_A}{100 - f_A}$$

Therefore, $\log R = \log y + \log [f_A/(100 - f_A)]$.

A graph of $\log R$ vs. $\log [f_A/(100 - f_A)]$ will therefore produce a straight line where the y axis intercept represents the relative difference in intensity between components A and B.

Figure 4.9. Microsphere sulphasalazine content determined by FTRS and UV-spectrophotometry



but the peak area ratio was not affected. The shape of figure 4.6 suggests that errors in peak area ratio will have the greatest effect at low concentrations of SASP. Thus, by substitution into the figure 4.7 calibration equation, a 3.0% variation in peak area ratio would produce a $\pm 0.6\%$ w/w error in concentration at 50% w/w SASP, whereas the error in concentration at 5% w/w SASP would be $\pm 0.1\%$ w/w. The between-sample variation of $\pm 4.4\%$ would result in a $\pm 0.9\%$ w/w error in concentration at 50% w/w SASP and a $\pm 0.15\%$ w/w error at 5% w/w SASP.

4.4. CONCLUSIONS

The work presented in this chapter has demonstrated that FTRS can yield both useful qualitative and quantitative information on Eudragit RS-SASP microspheres.

Analysis by FTRS was rapid, and for each sample the acquisition of the spectrum and determination of its peak area ratio took no more than 5 minutes. In fact, compared to UV-spectrophotometry, the assay of samples by FTRS was technically simpler and faster, with the only sample preparation being loading of the material into the sample holder.

In spectra of drug-polymer microspheres, peaks attributable to Eudragit RS and SASP could be identified. There was evidence to suggest a degree of drug:polymer interaction although this would need to be substantiated by further work.

The ability to distinguish drug from polymer in spectra of the Eudragit RS-SASP microspheres allowed FTRS to be used quantitatively. This appears to be one of the first examples of the successful quantitative application of FTRS to a two component system where the peak areas of both components need to be taken into consideration. Although

FTRS has been used to quantify levels of drug in a tablet, the tablets were of uniform size and density and thus the drug peak area could be directly correlated to drug content (Davies et al., 1990a). For the microspheres described in this chapter, this could not be done due to variations in sample density and packing. With a straightforward mathematical treatment, a linear relationship between drug:polymer peak area ratio and drug content was derived. Reproducibility of the peak area ratio both within- and between-samples was high. Drug content results showed good agreement with a conventional spectrophotometric assay.

Although FTRS cannot yet be considered as a routine analytical technique, this study demonstrates that it has considerable future potential as a non-destructive technique for the qualitative and quantitative characterisation of drug-delivery systems.

CHAPTER 5.

SURFACE CHARACTERISATION OF EUDRAGIT RS-SULPHASALAZINE
MICROSPHERES USING X-RAY PHOTOELECTRON SPECTROSCOPY
(XPS).

5.1. INTRODUCTION

This chapter describes the use of a surface-specific analytical technique, X-ray photoelectron spectroscopy (XPS), for the characterisation of Eudragit RS-SASP microspheres. XPS is also known as Electron Spectroscopy for Chemical Analysis (ESCA).

Much of the pioneering development work in XPS was carried out at the University of Uppsala in the 1940s and 1950s, but it was only during the 1970s that XPS equipment became commercially available (Christie, 1989). Since then, XPS has become a well established technique for the surface characterisation of a wide variety of materials, including those of biomedical interest. Some biomaterials which have been analysed by XPS include polyurethanes (Hearn et al., 1988), polyesters (Davies et al., 1990b), polyorthoesters (Davies et al., 1990c), polyanhydrides (Davies et al., 1990d), and the Eudragits (Davies et al., 1989). The technique has been the subject of a number of books and reviews (e.g. Briggs and Seah, 1983; Christie, 1989; Clark, 1977; Miller and Peppas, 1986; Paynter, 1988; Ratner; 1983).

The XPS process is based upon the photoelectric effect. The material under investigation is irradiated with a monochromatic source of X-rays. As a result, the atoms in the sample undergo photoionisation. If the photoelectrons generated in this process have sufficient energy, they will be able to escape from the sample surface in a process called photoemission.

The photoemission process can be described by the Einstein equation:

$$KE = hv - BE$$

Where, KE is the kinetic energy of the emitted photoelectrons, $h\nu$ is the energy of the incident X-ray photons and BE is the binding energy of the orbital from which the photoelectron is emitted (Paynter, 1988).

Figure 5.1 presents a diagrammatic representation of an XPS spectrometer. Sample irradiation is most commonly provided by AlK_{α} or MgK_{α} X-rays (1486.6 and 1253.6 eV respectively). The sample depth from which the detected photoelectrons are emitted varies with the properties of the sample and the angle at which the X-rays strike, but in general they arise from no greater than 10 nm below the surface. The emitted photoelectrons are separated by an analyser according to their kinetic energy, and the number falling into each energy band is amplified and counted. The photoemission process takes place under high vacuum to minimise contamination, and also because many of the components of the spectrometer will only function under these conditions. To generate an XPS spectrum, the emitted photoelectrons are scanned by the analyser, generally over a binding energy range of 0-1000 eV. The binding energy of the peaks in the spectrum are characteristic of specific orbitals within the atoms of specific elements. For example the $C1s$ binding energy is 285 eV, $N1s$ is 399 eV and $O1s$ is 532 eV (Paynter, 1988; Christie, 1989).

The binding energy values may be shifted according to the environment that the atom is situated in. For example, whereas the peak of C bonded to C (single bond) or H occurs at 285 eV, the peak of C bonded to N occurs at 286.6 eV, and the peak of C in a carbonyl function occurs at 289.2 eV. If the peaks characteristic of the different bonding environments present in a molecule are incorporated in a deconvolution of the $C1s$ peak, their relative proportions may be estimated. This may be employed to provide information on whether any of the functionalities in a polymer show preferential surface orientation (Clark, 1977;

Davies et al., 1990c,d).

XPS may also be used to quantify the elemental composition of a surface. Since the areas of the photoelectron peaks in the XPS spectrum are directly proportional to the elemental surface composition, by calculating peak area ratios, the relative proportions of the atoms present at the surface can be estimated. The data provided gives a breakdown of surface composition in terms of the percentage, by number, of the different atoms present, excluding hydrogen (Paynter, 1988).

The application of XPS to drug delivery systems has been limited. Binns et al. (1989) used the technique to characterise tablets compressed from blends of the drug, diclofenac sodium with either sodium alginate or calcium phosphate. Surface concentrations of two elemental markers for diclofenac sodium, chlorine and nitrogen, were higher than predicted, indicating surface drug enrichment.

In this chapter, XPS has been used to investigate the surface atomic composition of Eudragit RS-SASP microspheres to determine:

- a) How the surface drug concentration changes with different microsphere drug loadings.
- b) The changes in microsphere surface chemistry when microspheres are produced with and without surfactant.

5.2. EXPERIMENTAL

5.2.1. Materials

See chapter 4.

5.2.2. Methods

5.2.2.1. Microsphere production

Eudragit RS-SASP microspheres were produced using the technique described in Chapter 4. This time however, the drug-polymer solution was emulsified into either 100 ml of 0.1% w/v aqueous Tween 20 solution or 100 ml of distilled water. The total quantity of drug and polymer dissolved in dichloromethane was in all cases 3 g. The following drug:polymer combinations (by weight) were used: 0:100, 10:90, 20:80, 33:67 and 50:50.

5.2.2.2. Microsphere assay

As described in chapter 4.

5.2.2.3. XPS analysis

XPS spectra were obtained for all of the microsphere samples and for pure SASP. The samples were mounted onto aluminium stubs using double-sided sticky tape and analysed using a VG Scientific ESCALAB Mk II spectrometer (VG Scientific, Crawley, UK) employing MgK α X-rays (1253.6 eV). A wide scan spectrum (0-1000 eV) and narrow scan spectra for Cls, O1s, N1s and S2p were recorded. The analyser was operated in fixed transmission mode with a pass energy of 50 eV. Data was acquired and analysed by a VGS-5000-S data system, based on a DEC PDP11/73 computer.

5.3. RESULTS AND DISCUSSION

5.3.1. Microsphere characterisation

Microspheres were produced for all of the drug:polymer combinations when emulsified into surfactant solution. However, in the absence of surfactant the emulsification

process was, not unexpectedly, considerably less efficient. As a result, using the 50:50 drug:polymer mixture microspheres were not produced, with a single agglomerated mass forming as solvent evaporation progressed.

The drug content and encapsulation efficiency of the different formulations is shown in table 5.1. The efficiency of encapsulation increased with drug content and was consistently higher in equivalent samples produced without surfactant.

5.3.2. XPS analysis

5.3.2.1. Qualitative analysis

The chemical structures of SASP and Eudragit RS are provided in chapter 1 (figure 1.6 and table 1.2 respectively).

Figure 5.2 shows the wide scan XPS spectrum of pure SASP. Peaks for C1s, O1s, N1s, and S2p environments were present at 286.5, 533.3, 401.7 and 169.9 eV respectively. The sample appeared to be free of contaminating elements.

In the wide-scan spectrum of drug-free Eudragit RS microspheres produced without surfactant, the only prominent peaks are C1s and O1s (figure 5.3). Although N and S were both detected, their surface concentrations were too low to be discernible on the wide scan spectrum.

In the spectrum of surfactant-free microspheres containing 31.1% w/w sulphasalazine (figure 5.4), C1s and O1s again predominate, although N1s and S2p peaks are just evident.

5.3.2.2. Quantitative analysis

A quantitative assessment of the XPS data was based upon a comparison of the theoretical surface composition of the microsphere samples and the experimentally determined atomic composition.

Table 5.1. Details of Eudragit RS:sulphasalazine microsphere formulations.

Drug:polymer ratio (by weight)	Assayed drug content (%w/w)	Encapsulation efficiency (%)
Produced with- out surfactant		
10:90	8.9	89
20:80	18.4	92
33:67	31.1	93
50:50	-	-
Produced with surfactant		
10:90	8.7	87
20:80	18.2	91
33:67	30.3	92
50:50	47.5	95

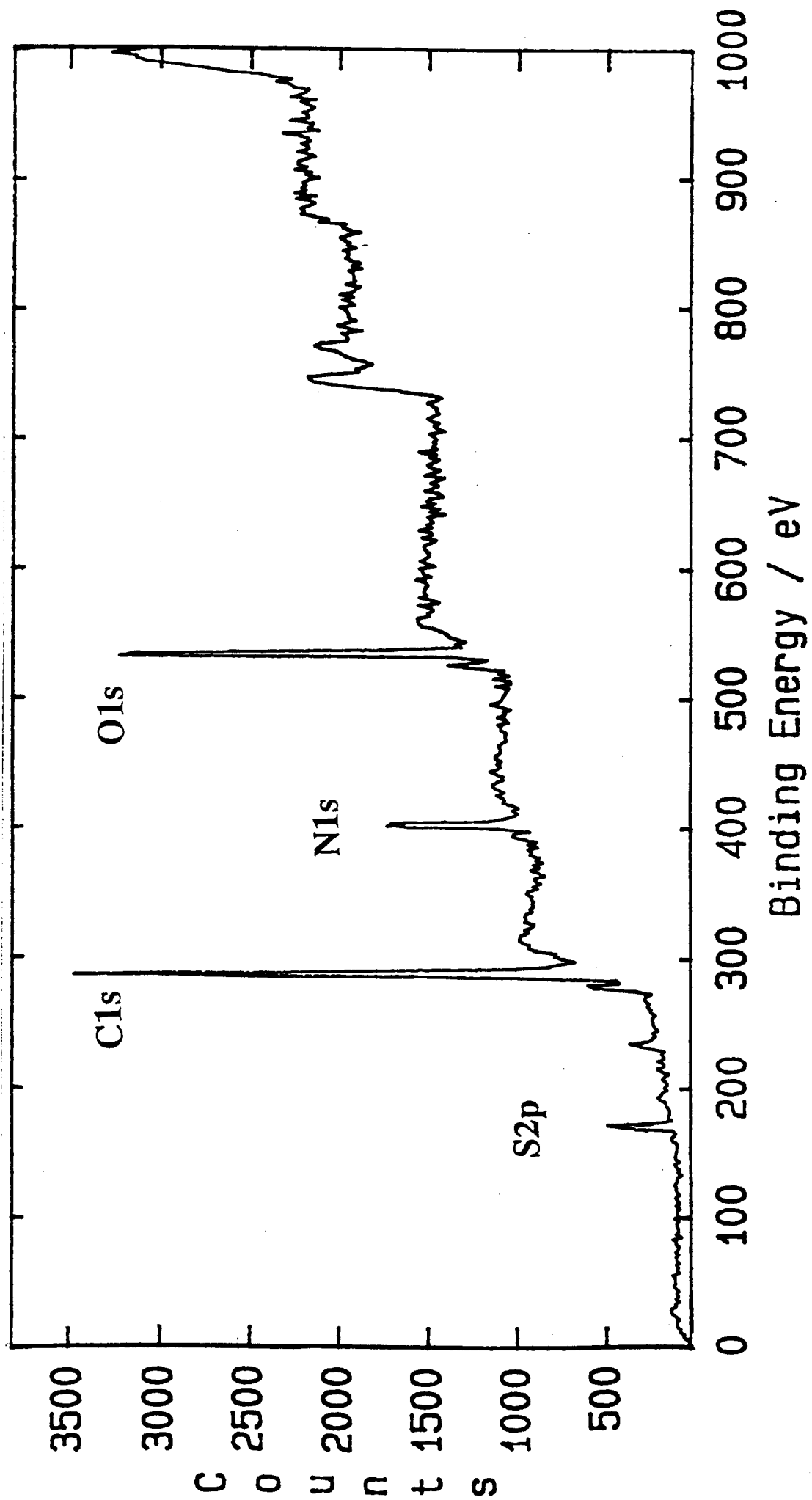


Figure 5.2. Wide-scan XPS spectrum of sulphasalazine.

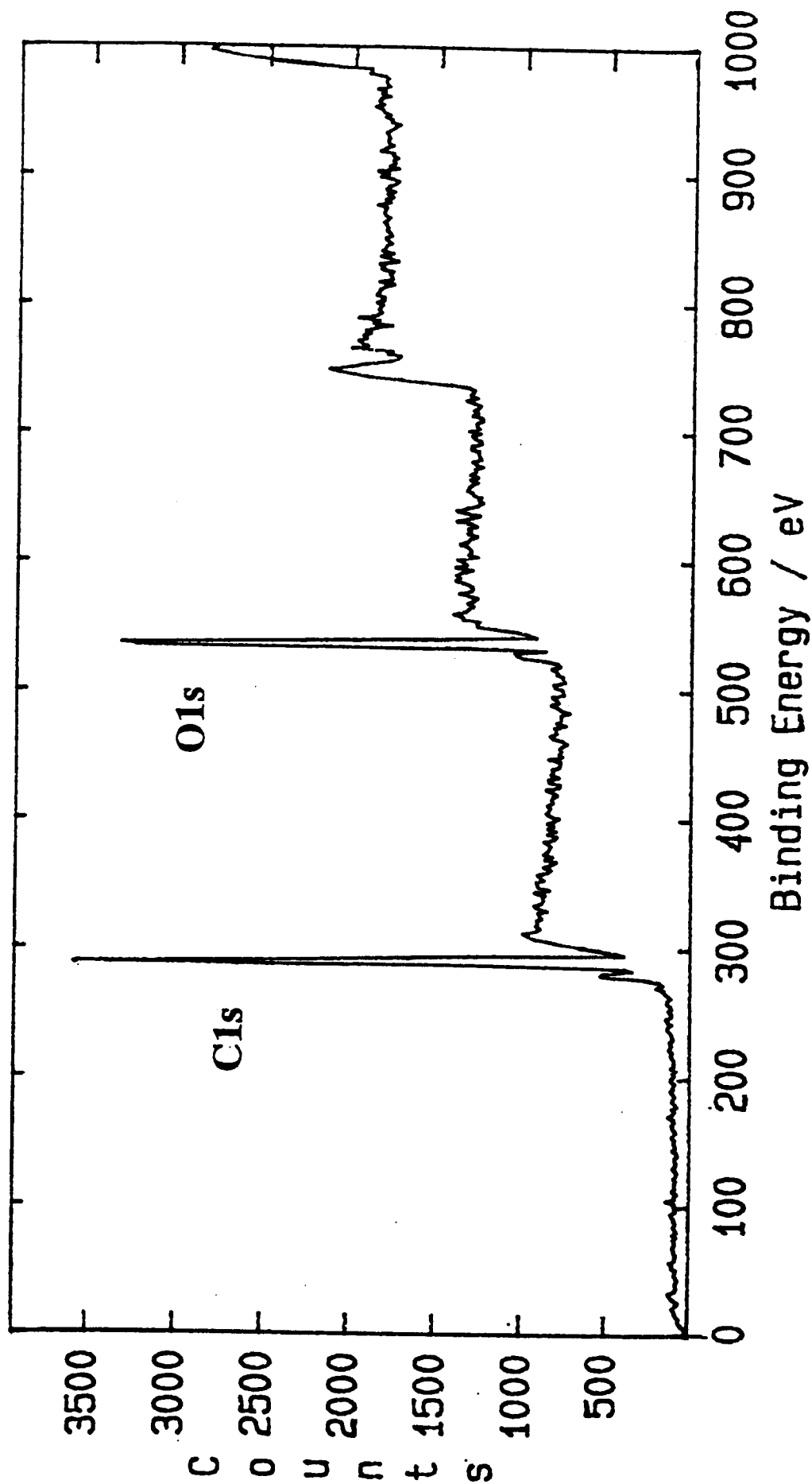


Figure 5.3. Wide-scan XPS spectrum of surfactant-free, drug-free Eudragit RS microspheres.

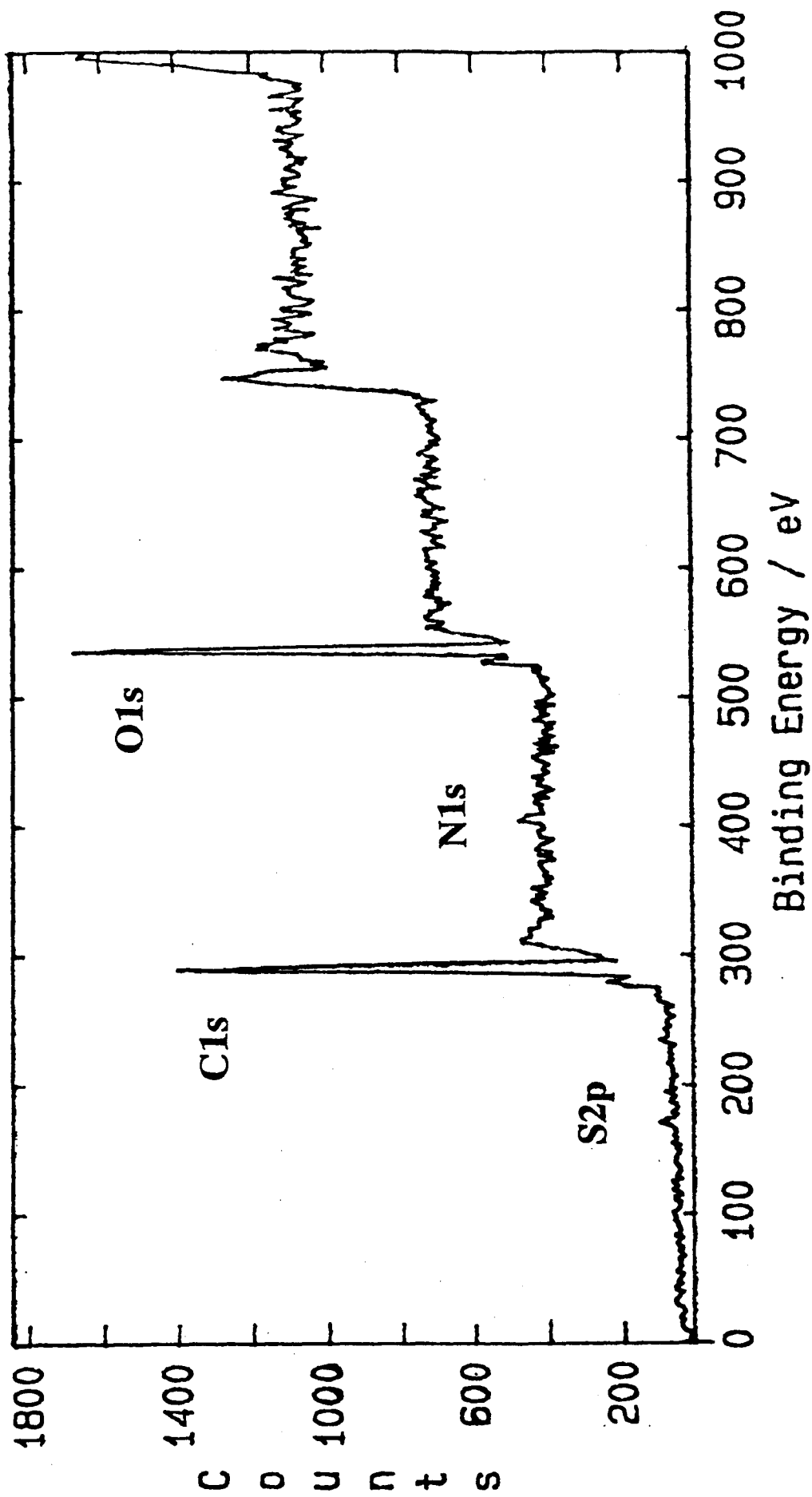


Figure 5.4. Wide-scan XPS spectrum of surfactant-free, Eudragit RS microspheres containing 31.1% w/w sulphasalazine.

To calculate the theoretical elemental surface composition of the samples, two assumptions had to be made:

- 1) The drug and polymer are present at the microsphere surface as a homogeneous molecular dispersion in proportion to their bulk composition.
- 2) There is no preferential surface orientation of either component.

Thus, for each of the microsphere samples the theoretical number of C, O, N and S atoms present per unit weight were calculated, and in turn the percentage of the total number of atoms present that each represented. Figure 5.5 provides details of the calculation of % atomic composition of SASP and Eudragit RS. The Eudragit RS composition is based upon a molar ratio of 2:1:0.1 of methyl methacrylate, ethyl acrylate and trimethylammonioethyl methacrylate chloride monomer units and a molecular weight of 150,000. In figure 5.6 is a sample calculation of the theoretical surface composition of one of the drug:polymer microsphere samples.

Table 5.2 records the theoretically derived and experimentally determined atomic compositions of the samples.

For pure SASP, the experimental and predicted atomic compositions were in excellent agreement. This suggests that the surface chemistry of the SASP crystals directly reflects the structure of the drug molecule.

For the surfactant-free, drug-free microspheres, the level of carbon was 3.7% higher than predicted. This was accompanied by a 3.9% fall in surface oxygen. The nitrogen level was close to predicted, although the accuracy of XPS below concentrations of 1% is not high. The very small quantity of sulphur detected (0.1%) may arise from a

Figure 5.5. Calculation of atomic % composition of microsphere components.

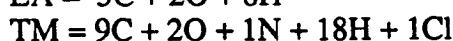
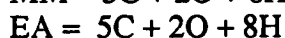
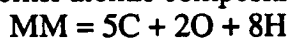
1. Eudragit RS

Eudragit RS = methyl methacrylate (MM), ethyl acrylate (EA), and trimethyl ammonioethyl methacrylate (TM) in a 2:1:0.1 ratio, respectively.

Monomer mol.wt: MM = 100, EA = 100, TM = 207

Mol.wt. of each RS "backbone unit" = $(2 \times 100) + (1 \times 100) + (0.1 \times 207) = 320.7$.

Monomer atomic composition:



Total atoms/backbone unit

$$\text{C} = (2 \times 5) + (1 \times 5) + (0.1 \times 9) = 15.9$$

$$\text{O} = (2 \times 2) + (1 \times 2) + (0.1 \times 2) = 6.2$$

$$\text{N} = (0.1 \times 1) = 0.1$$

$$\text{Cl} = (0.1 \times 1) = 0.1$$

$$\text{H} = (2 \times 8) + (1 \times 8) + (0.1 \times 18) = 25.8$$

Polymer mol.wt. = 150,000

$$= 150,000/320.7 = 467.7 \text{ backbone units/mole}$$

Therefore, total atoms/mole (excluding H)

$$\text{C} = 467.7 \times 15.9 = 7437$$

$$\text{O} = 467.7 \times 6.2 = 2900$$

$$\text{N} = 467.7 \times 0.1 = 47$$

$$\text{Cl} = 467.7 \times 0.1 = 47$$

Total atoms (excluding H) = $7437 + 2900 + 47 + 47 = 22498$

$$\text{Atomic \% C} = 7437/10431 \times 100 = 71.6\%$$

$$\text{Atomic \% O} = 2900/10431 \times 100 = 27.9\%$$

$$\text{Atomic \% N} = 47/10431 \times 100 = 0.5\%$$

2. Sulphasalazine

Mol.wt. = 398.

Atomic composition = 18C, 5O, 4N, 1S, 14H

Total atoms (excluding H) = $18 + 5 + 4 + 1 = 28$

$$\text{Atomic \% C} = 18/28 \times 100 = 64.3\%$$

$$\text{Atomic \% O} = 5/28 \times 100 = 17.9\%$$

$$\text{Atomic \% N} = 4/28 \times 100 = 14.3\%$$

$$\text{Atomic \% S} = 1/28 \times 100 = 3.6\%$$

Figure 5.6. Calculation of atomic % composition of Eudragit RS microspheres containing 18.2% w/w sulphasalazine (SASP).

SASP: Eudragit RS ratio (by weight) = 18.2:81.8.

Molar ratio = $(18.2/398):(81.8/150,000) = 0.046:0.00055$.

i) 100% SASP = 18 C atoms, 5 O atoms, 4 N atoms, and 1 S atom.

No. of C atoms from SASP = $18 \times 0.046 = 0.828$

No. of O atoms " " = $5 \times 0.046 = 0.230$

No. of N atoms " " = $4 \times 0.046 = 0.184$

No. of S atoms " " = $1 \times 0.046 = 0.046$

ii) 100% Eudragit RS = 7437 C atoms, 2900 O atoms, and 47 N atoms.

No. of C atoms from RS = $7437 \times 0.00055 = 4.090$

No. of O atoms from RS = $2900 \times 0.00055 = 1.595$

No. of N atoms from RS = $47 \times 0.00055 = 0.026$

Total no. of atoms (C, O, N, S) from SASP and Eudragit RS = 6.999

$$\text{Atomic \% C} = [(0.828 + 4.09)/6.999] \times 100 = 70.2 \%$$

$$\text{Atomic \% O} = [(0.23 + 1.595)/6.999] \times 100 = 26.1\%$$

$$\text{Atomic \% N} = [(0.184 + 0.026)/6.999] \times 100 = 3.0 \%$$

$$\text{Atomic \% S} = (0.046/6.999) \times 100 = 0.7 \%$$

Table 5.2. Experimental and (theoretical) surface atomic composition of Eudragit RS:sulphasalazine microsphere samples.

<u>Sample</u>	<u>% Carbon</u>	<u>% Oxygen</u>	<u>% Nitrogen</u>	<u>% Sulphur</u>
Pure S	65.6 (64.3)	16.9 (17.9)	13.6 (14.3)	3.8 (3.6)
MS* 0% S	75.3 (71.6)	24.0 (27.9)	0.6 (0.5)	0.1 (0.0)
MS* 8.9% S	72.9 (70.9)	23.3 (27.1)	3.2 (1.7)	0.6 (0.3)
MS* 18.4% S	72.0 (70.1)	24.4 (26.1)	2.8 (3.0)	0.8 (0.7)
MS* 31.1% S	73.2 (69.4)	22.8 (24.7)	3.1 (4.7)	0.9 (1.2)
MS 0% S	78.2 (71.6)	21.0 (27.9)	0.5 (0.5)	0.3 (0.0)
MS 8.7% S	73.9 (70.9)	24.5 (27.0)	1.3 (1.8)	0.4 (0.3)
MS 18.2% S	74.1 (70.2)	23.9 (26.1)	1.6 (3.0)	0.4 (0.7)
MS 30.3% S	75.4 (69.3)	22.3 (24.7)	1.7 (4.8)	0.5 (1.2)
MS 47.5% S	73.1 (68.1)	24.5 (23.0)	1.8 (7.2)	0.6 (1.7)

[(S = sulphasalazine, MS = microsphere, * = surfactant free)]

contaminant present in the raw polymer. For comparison, XPS analysis by Davies et al. (1989) of a film of Eudragit RS cast from methanol, yielded the following composition: C=72.8%, O=26.9% and N=0.3%. The discrepancy between predicted and experimental microsphere C and O contents could be a result of surface hydrocarbon contamination. Alternatively, it is possible that the difference is a result of an unexpected polymer orientation.

That Eudragit RS has surface active properties is clear, both from the work presented in this thesis, where microspheres have been produced without surfactant, and from the literature (Bodmeier and Chen, 1989b). Stabilisation of the polymer at an aqueous interface is most likely to arise from the trimethyl ammonioethyl functions orientating towards the interface. Although this might be expected to produce differences between the experimental and predicted surface composition, the magnitude of the effect is impossible to predict. For example, although the molar ratio of trimethyl ammonioethyl groups is only small in Eudragit RS (47 out of a total 1450 monomer units in each polymer chain), conformational changes in the polymer chains may produce a local high concentration of these groups at the surface.

For the drug-free microspheres produced with surfactant, the surface C content was 6.6% higher than predicted. This discrepancy might be expected to result in part from the presence of surfactant at the microsphere surface. However, Tween 20 (empirical formula $C_{58}H_{114}O_{26}$) has a C:O ratio of 69%:31% and thus significant amounts at the microsphere surface might also be expected to raise the level of detected oxygen. In fact the level of oxygen is 6.9% lower than predicted. Therefore, although Tween 20 would be expected to be present in this sample, it is also possible that the unexpected surface composition might be a result of preferential polymer orientation in the presence of the

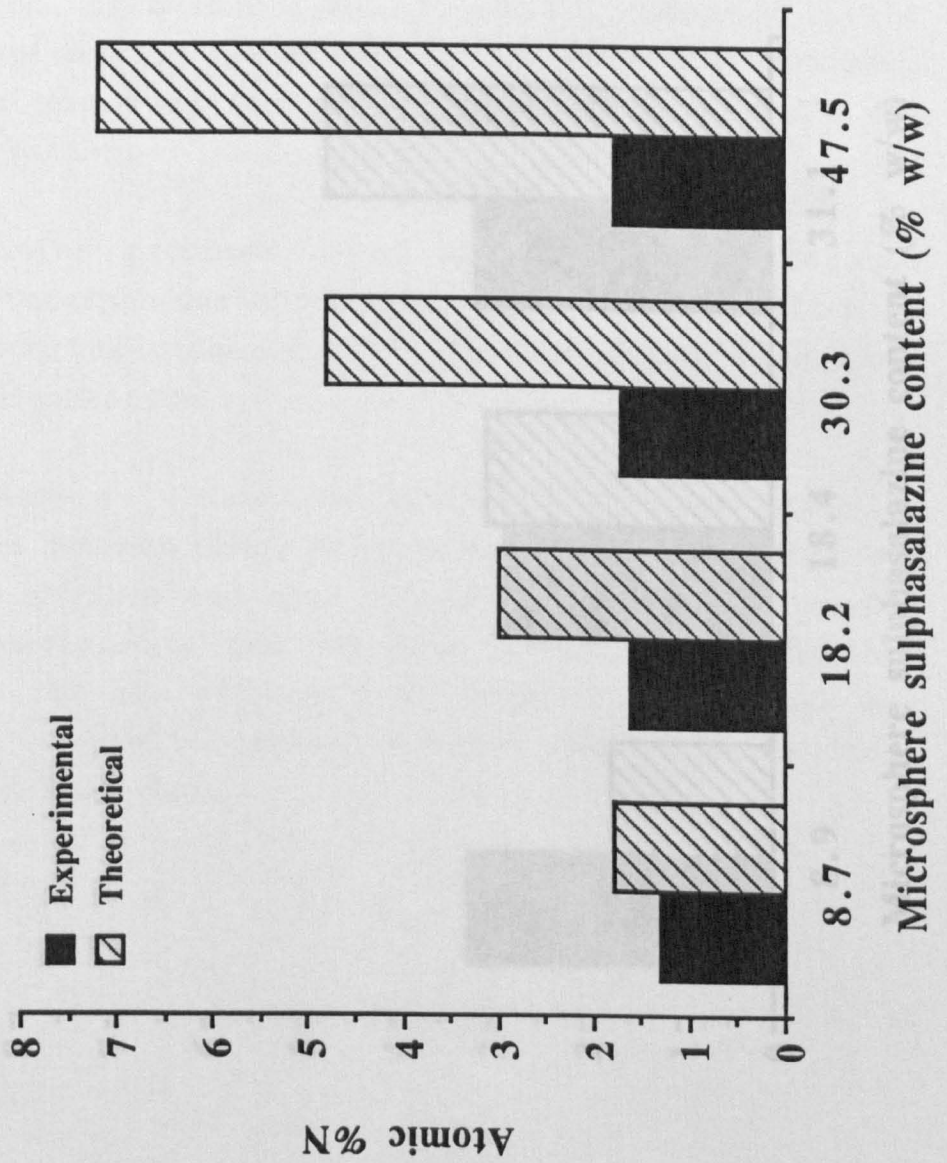
surfactant.

Sulphur was theoretically a unique marker for SASP in the drug-polymer microspheres. However, it was unsuitable for two reasons. Firstly, it unexpectedly appeared in the drug-free polymer samples, albeit at a low level, and secondly its predicted concentration was relatively low; Since 100% SASP only contains 3.8% S atoms and the accuracy of XPS below 1% is not high, there would be problems in accurately measuring the levels of S likely to be present in the microsphere samples. Nitrogen proved to be a better choice as a drug marker, since it was present in the polymer at only a low concentration, yet present in 100% SASP at 13.6%.

For each of the two sets of drug-containing microsphere samples (i.e. surfactant and no surfactant) the surface drug concentration, as measured by surface %N, remained relatively constant despite marked differences in bulk drug content. Thus, in the samples produced with surfactant, the surface N concentration was 1.3% for microspheres containing 8.7% w/w SASP, increasing to just 1.8% at a bulk drug content of 47.5% w/w SASP. The theoretical increase in % N over this range of SASP content was from 1.8 to 7.2% (table 5.2 and figure 5.7). As seen for the drug-free sample, carbon levels were generally considerably higher than expected, again suggesting surfactant contamination or preferential polymer orientation.

In the samples produced without surfactant, the surface N concentrations were again relatively constant but at a higher level, ranging from 2.8% to 3.2% (table 5.2 and figure 5.8). The relatively higher N concentrations in these samples are presumably a direct result of no surfactant being present.

Figure 5.7. Experimental vs. theoretical N content: surfactant containing microspheres



5.4. CONCLUSIONS

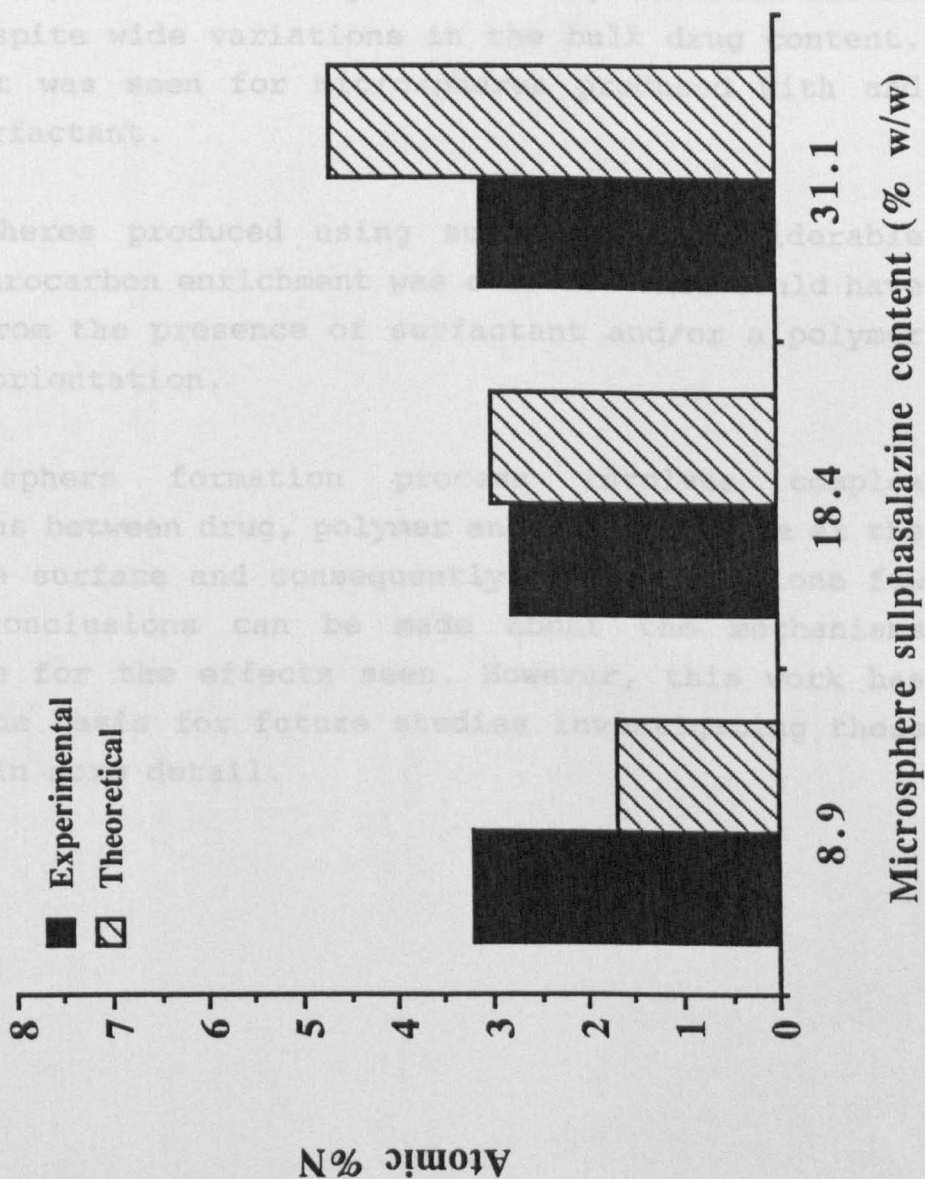
The work presented in this chapter has demonstrated that XPS is able to provide a valuable insight into the surface chemistry of microspheres manufactured by the solvent evaporation process under different conditions.

An unexpected finding was that the microsphere surface SASP concentration, as measured by surface N_1s , remained little changed despite wide variations in the bulk drug content. This effect was seen for microspheres with and without surfactant.

In microspheres produced using a surfactant, a considerable surface hydrocarbon enrichment was observed. This could have resulted from the presence of surfactant and/or a polymer surface reorientation.

The microsphere formation process involves complex interactions between drug, polymer and solvent. The microsphere surface and consequently the surface composition defined in this chapter can be made. However, this work has provided the basis for future studies into the microsphere formation in detail.

Figure 5.8. Experimental vs. theoretical N content: surfactant-free microspheres



5.4. CONCLUSIONS

The work presented in this chapter has demonstrated that XPS is able to provide a valuable insight into the surface chemistry of microspheres manufactured by the solvent evaporation process under different conditions.

An unexpected finding was that the microsphere surface SASP concentration, as measured by surface %N, remained little changed despite wide variations in the bulk drug content. This effect was seen for microspheres produced with and without surfactant.

In microspheres produced using surfactant, considerable surface hydrocarbon enrichment was evident. This could have resulted from the presence of surfactant and/or a polymer surface reorientation.

The microsphere formation process involves complex interactions between drug, polymer and aqueous phase at the microsphere surface and consequently, using XPS alone few definite conclusions can be made about the mechanisms responsible for the effects seen. However, this work has provided the basis for future studies investigating these phenomena in more detail.

CHAPTER 6.

THE DEVELOPMENT OF DOSAGE FORMS FOR THE ASSESSMENT
OF TRANSIT THROUGH THE COLON.

6.1. INTRODUCTION

One of the major aims of the work carried out for this thesis was to further investigate the phenomenon that the rate of transit of materials through the colon may depend on their size. A summary of some of the studies investigating the colonic transit rate of different-sized units was provided in section 1.2.4.1.

It was planned to undertake in vivo investigations in human subjects to compare the colonic transit rate of small particles with larger units. The chosen size of small particles was 0.2 mm, selected to represent a dispersed microparticulate type of dosage form. The larger units were non-disintegrating tablets of 5 mm or 8.4 mm diameter. By radiolabelling the two sizes with different radioisotopes, it would be possible to simultaneously measure their movement through the GI tract using gamma scintigraphy.

It was intended that the two sizes of particles should be administered together within a hard gelatin capsule, coated to resist disintegration until reaching the colon. If the two sets of particles were administered independently, there was the possibility of separation higher up the GI tract, resulting in one size of particle arriving at the colon well ahead of the other, and complicating data interpretation. In the event of separation occurring, it would be at the gastric emptying stage.

Delivery inside a coated gelatin capsule was considered to be most appropriate, since although direct placement of materials into the colon can be achieved by use of an oro-caecal tube (Krevsky et al., 1986; Proano et al., 1991) there are drawbacks. Apart from the fact that the intubation procedure is unpleasant for the subject, there is a limit on the size of material that can be passed down the tube. In addition, the presence of the tube may

stimulate colon motility, since in one study using this technique, transit through the ascending colon was abnormally rapid (Krevsky et al., 1986).

The standard method for radiolabelling oral dosage forms for scintigraphic investigations is to immobilise the radioisotope on an ion-exchange resin. The most commonly used radioisotopes for human scintigraphic investigations are technetium-99m (^{99m}Tc , half-life=6.0 hours) and indium-111 (^{111}In , half-life=67 hours) (Wilson and Washington, 1988). The most commonly used resins for isotope binding are the AmberlitesTM (Rohm & Haas (UK), Croydon), available in a number of different grades. AmberlitesTM IR120 and IRA410 resins are both cross-linked copolymers of styrene and divinylbenzene. IR120 is a cationic resin, and ion-exchange (In^+) takes place at sulphate functions (SO_3^-). IRA410 is an anionic resin, and ion-exchange (TcO_4^-) takes place at trimethylammonium functions ($\text{N}(\text{CH}_3)_3^+$) (Handbook of Pharmaceutical Excipients, 1986). Adsorption of the ions of large atoms such as Tc and In to the resins is very strong and desorption occurs only slowly (Proano et al., 1990).

This chapter describes the preparation of dosage forms to enable in vivo transit investigations to be undertaken, and in particular the development of a suitable colon-targetable coating. A review of strategies for targeting dosage forms to the colon was provided in section 1.2.6, the principal methods being the use of pH-dependent or bacterially metabolised coatings. The most appropriate coating formulation chosen from the work in this chapter was then used for in vivo investigations described in chapters 7 and 9.

6.2. EXPERIMENTAL

6.2.1. Materials

Amberlite™ IR120 ion-exchange resin (0.3-1.8 mm) (BDH), Amberlite™ IRA410 ion-exchange resin (0.3-1.8 mm) (BDH), ethylcellulose (Sigma), size 000 hard gelatin capsules (Farillon, Romford, UK), Eudragit S (Dumas (UK)), "Polymer A", low molecular weight poly(methylmethacrylate) (BDH), acetone (Analar grade)(Rhône-Poulenc), sodium hydroxide pellets (BDH), hydrochloric acid (36% w/v) (BDH), ¹¹¹In chloride (Amersham Int., Amersham, UK), sodium pertechnetate (^{99m}Tc) (Radiopharmacy, University Hospital, Nottingham).

6.2.2. Methods

6.2.2.1. Preparation of 0.2 mm particles

A. Cleaning and activation

The 0.2 mm particles were prepared from Amberlite™ IR120 resin. Prior to use, the resin was cleaned to remove any contaminants, and activated, according to instructions provided by the manufacturer (Rohm & Haas (UK)):

- i) Resin soaked for 20 minutes in 2 N hydrochloric acid.
- ii) Acid removed by filtration, resin rinsed with distilled water and left to soak in water for 30 minutes.
- iii) Water removed, resin soaked in 1.5 N sodium hydroxide solution for 20 minutes.
- iv) Wash as in step ii), and repeat steps i) to iv).
- v) Resin activated to H⁺ form by soaking in 2N HCl for 20 minutes.
- vi) Wash in water until eluent pH>4.

B. Size fractionation

A 0.18-0.25 mm sieve fraction of the resin was then prepared. Since ion-exchange resins swell when moist, the sieve fraction was prepared from wet resin. The wet resin was ground using a pestle and mortar and passed through a

0.25 mm sieve stacked onto a 0.18 mm sieve (Endecott, Crawley, UK). Resin which did not pass through the 0.25 mm sieve was returned to the mortar for further grinding. This process was continued until no resin >0.25 mm remained. The resin collected between the two sieves was dried at room temperature and stored until required.

C. Radiolabelling

To radiolabel the sieved resin, the required amount was placed into a glass beaker and moistened with water to form a paste. Sufficient ^{111}In chloride solution to leave 1 MBq/300 mg of resin at the time of dosing was then drawn by syringe and needle from its vial and gently mixed into the beaker contents. The radiolabelled resin was dried by heating the underside of the beaker with a hair-drier.

6.2.2.2. Tablet preparation

Tablets were required to remain intact for the duration of the in vivo study and were prepared from an insoluble polymer, ethylcellulose. Two different radiolabelling techniques were developed. The initial method (I) involved the incorporation of $^{99\text{m}}\text{Tc}$ labelled ion-exchange resin into the tablet blend prior to compression. Refurbishment of the radioisotope facilities containing the tablet press at a later stage in the programme necessitated the development of an alternative technique involving surface radiolabelling (II).

Method I

A. Cleaning and activation

AmberliteTM IRA410 resin was required for producing the tablets. Prior to use, the resin was cleaned and activated, as follows:

- i) Resin soaked for 20 minutes in 1.5 N sodium hydroxide solution.
- ii) Alkali removed by filtration, resin rinsed with

- distilled water and left to soak in water for 30 minutes.
- iii) Water removed, resin soaked in 2 N hydrochloric acid for 20 minutes.
 - iv) Wash as in step ii) and repeat steps i) to iv).
 - v) Resin activated to OH⁻ form by soaking in 2N NaOH for 20 minutes.
 - vi) Wash in water until eluent pH<9.

Prior to use, the resin was air-dried, and then very finely ground using a pestle and mortar.

B. Radiolabelling

For radiolabelling, the required amount of sodium pertechnetate solution was added to a paste of water and ground IRA410 resin. The activity was mixed with the resin paste and dried using a hair-drier.

C. Tabletting

Tablets of 5 mm diameter and approximately 3 mm depth were produced by direct manual compression of a blend of ethylcellulose containing 1% w/w of radiolabelled Amberlite IRA410 resin, using a Manesty F6 tablet press. The desired tablet hardness was at least 6 kg and the target weight, 55-65 mg. To ensure integrity was maintained in vivo, the tablets were painted with four coats of 5% w/v ethylcellulose in acetone. The radioactivity in each tablet at the time of dosing was 0.67 MBq.

Method II

5 mm or 8.4 mm diameter tablets were produced by the direct compression of ethylcellulose. Tablet hardness was adjusted to produce tablets with a breaking force of at least 6 kg (5 mm) or 12 kg (8.4 mm). Sodium pertechnetate solution was diluted with water such that the required amount of activity at the time of dosing (0.67 MBq) would be present in 10 µL. Using a 10 µL micropipette (Gilson), the activity was carefully placed onto the tablet surface and allowed to

dry at room temperature. When dried, the tablet was coated with a solution of 10% w/v poly(methylmethacrylate) in acetone; First, a single drop of polymer solution was placed onto the dried sodium pertechnetate. Then gradually the whole tablet was painted with four coats of polymer solution.

In vitro dissolution testing (paddle stirrers at 100 rpm, pH 7 phosphate buffer, 37 °C (see also chapter 3)) indicated that the tablets produced by methods I and II remained intact for at least 24 hours.

6.2.2.3. Capsule coating

A dipping technique was employed for coating of the hard gelatin capsules (figure 6.1). A length of cotton was tied around the middle of each capsule. Of the two loose ends of cotton left after tying, one was cut and the other, at least 5 cm in length was used to suspend the capsule for drying. To coat, the capsules were dipped (complete immersion for about 5 seconds) into a bottle containing a solution of the coating polymer. Between dips, the capsules were suspended by attaching the end of the piece of cotton with sticky tape to a ruler fixed between two retort stands. When coating was complete and the coat dry, the suspending cotton was cut at the capsule body.

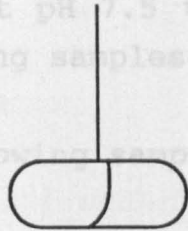
6.2.2.4. Preliminary in vitro experiments

In vitro coating experiments were based upon the use of two enteric polymers, Eudragit S which dissolves above pH 7 (section 1.1.3.2.A) and "Polymer A". Initial experiments used the two polymers alone, with later work adopting a dual coating procedure. Coating performance was evaluated using a tablet/capsule disintegration apparatus (Copley). The coating integrity was tested by approximately half-filling the capsules with dry beads of Amberlite resin. This allowed easy detection of capsule leakage, since when moistened, the smooth flow of the resin beads would be

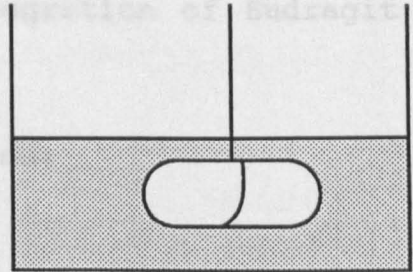
Figure 6.1. Procedure for dip-coating gelatin capsules.

interrupted. Disintegration testing was carried out according to an adaptation of the British Pharmacopoeial procedure for testing enteric coated tablets/capsules (British Pharmacopoeia, 1988).

1. Cotton tied around hard gelatin capsule.



2. Capsule completely immersed into a solution of coating polymer in acetone for about 5 secs.

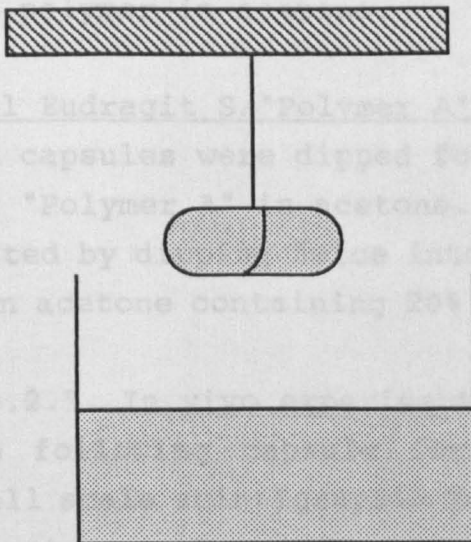


The following samples were evaluated:

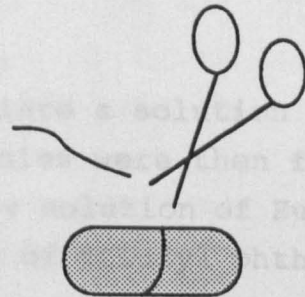
For Eudragit S

1. Three capsules dipped ten times into 10% w/v polymer in acetone.
2. Three capsules dipped six times into 10% w/v polymer in acetone containing 10% (by weight of polymer) dibutyl phthalate as plasticiser.

3. Between immersions, capsule allowed to dry.



4. Suspending cotton cut at capsule body.



Dual Eudragit S/Polymer A

Six capsules were dipped four times into a solution of 15% w/v "Polymer A" in acetone. The capsules were then further coated by dipping into a 10% w/v solution of Eudragit S in acetone containing 20% w/v dibutyl phthalate.

6.2.2. In vitro release

The following capsules and tablets were evaluated in a small scale *in vitro* release investigation using healthy human volunteers. For details of the technique of gamma scintigraphy, see chapter 4.

Formulation A: Five coats of 10% w/v "Polymer A" in acetone.

interrupted. Disintegration testing was carried out according to an adaptation of the British Pharmacopoeial procedure for testing enteric coated tablets/capsules (British Pharmacopoeia, 1988). Capsules were placed into 0.1 N hydrochloric acid for 2 hours, followed by pH 6 phosphate buffer (appendix 1) for 3 hours ending with a period at pH 7.5 to ensure disintegration of Eudragit S-containing samples.

The following samples were evaluated:

For Eudragit S

1. Three capsules dipped ten times into 10% w/v polymer in acetone.
2. Three capsules dipped six times into 15% w/v polymer in acetone containing 10% (by weight of polymer) dibutyl phthalate as plasticiser.

For "Polymer A"

Three capsules dipped three times into a solution of 15% w/v polymer in acetone.

Dual Eudragit S/"Polymer A" coatings

Six capsules were dipped four times into a solution of 15% w/v "Polymer A" in acetone. The capsules were then further coated by dipping twice into a 10% w/v solution of Eudragit S in acetone containing 20% by weight of dibutyl phthalate.

6.2.2.5. In vivo experimentation

The following capsule formulations were evaluated in a small scale scintigraphic investigation using healthy human volunteers. For more details on the technique of gamma scintigraphy, see chapter 7.

Formulation A: Five coats of 15% w/v "Polymer A" in acetone.

Formulation B: Five coats of "Polymer A" as above with a top layer of two coats of 10% w/v Eudragit S in acetone containing 20% (by weight of polymer) dibutyl phthalate and 5% v/v water.

Formulation C: Four coats of 15% w/v "Polymer A" with a top layer of four coats of 10% w/v Eudragit S in acetone containing 20% (by weight of polymer) dibutyl phthalate and 5% v/v water.

Six healthy volunteer subjects (age 23-40) undertook the study. Before coating, each capsule was filled with 150 mg of ¹¹¹In-labelled 0.2 mm Amberlite IR120 resin (1 MBq of activity/capsule at time of dosing). Each coating formulation was evaluated in two volunteers, with each subject receiving two capsules.

Subjects arrived for the study at 8 am having fasted from 10 pm the previous evening. Radioactive markers (see chapter 7) were attached to the subjects anterior and posterior over the right lobe of the liver to allow alignment of sequential scintigraphic images. The two capsules were swallowed, with a glass of water. Subjects received breakfast after the capsules had left the stomach.

Anterior and posterior scintigraphic images were recorded immediately after dosing and thereafter at 30-60 minute intervals throughout the day (IGE Maxicamera II/Star computer system, IGE, UK).

The point of capsule break-up, as evidenced by the dispersion of radioactivity, was determined from analysis of the stored scintigraphic images.

6.2.2.6. Further characterisation of "Polymer A" coatings
Ten empty 000-sized gelatin capsules were weighed and the mean weight determined. Each capsule was then dip-coated

three times into a solution of 15% w/v "Polymer A" in acetone. The capsules were then reweighed to determine the mean weight of coating applied.

To determine the thickness of the capsule coating, thin slices of the coated capsules were cut using a scalpel. The slices were placed onto a microscope slide and examined at x20 magnification (Nikon Optiphot). It was possible to distinguish the coat from the capsule shell which enabled the thickness of the coating polymer to be measured using a graticule.

6.3. RESULTS AND DISCUSSION

6.3.1. In vitro capsule evaluation

6.3.1.1. Eudragit S alone

The studies using Eudragit S alone as a capsule coating proved disappointing. After the 2 hour period in 0.1 N HCl, the capsules containing ten coats of Eudragit S had all allowed ingress of liquid and were beginning to spill the resin contained within. It was noted, before dissolution, that the capsule coatings had a crazed appearance.

Eudragit S forms brittle coatings and the routine use of plasticisers is recommended by the manufacturer. Plasticiser concentrations of up to 25% by weight of Eudragit S are considered not to adversely affect the polymer performance (Eudragit technical data).

Thus, the next set of coatings included 10% w/w dibutyl phthalate as a plasticiser. After 2 hours in acid, only one of the three capsules remained wholly intact. One of the capsules had spilled most of its contents and was removed. After three hours at pH 6, both capsules were spilling contents.

Therefore, even with the inclusion of plasticiser, coating

integrity remained a major problem.

6.3.1.2. "Polymer A" alone

After 2 hours in acid, all of the capsules coated with "Polymer A" appeared to have resisted moisture ingress. At pH 6, capsules were spilling resin after 30 minutes. After 45 minutes about half of each capsule body had dissolved away and after 60 minutes just small fragments of the thickest sections of polymer coating remained.

6.3.1.3. Dual "Polymer A"/Eudragit S coatings

Although the "Polymer A"-coated capsules showed excellent acid resistance in vitro, from their rapid dissolution at pH 6 it was considered that they would not remain intact as far as the colon in vivo. As a result, the strategy adopted was to coat with a base layer of "Polymer A", to provide improved integrity in the stomach and small intestine, and a top layer of S. In theory, the Eudragit S would dissolve in the colon exposing the coating of "Polymer A" which would then rapidly dissolve.

After 2 hours in acid, there was evidence of slight moisture ingress in two of the six capsules. No resin had been lost. After 2 hours at pH 6, some of the capsules showed evidence of moisture ingress, but no resin had been lost. At 3 hours, more liquid had entered the capsules, although no resin had been lost. After a half hour at pH 7.5, resin particles could be seen in the beaker containing the disintegration medium. Finally, after 1 hour at this pH, resin was spilling from all but one capsule.

6.3.2. In vivo evaluation of capsule coatings

Capsules arrived at the colon between 1 and 4 hours after administration to the human volunteers. Any delays were a result of retention in the stomach. Small intestinal transit time was only brief (less than 90 minutes).

Surprisingly, in the two subjects taking capsules coated with "Polymer A" alone (formulation A), disintegration did not occur until reaching the ileo-caecal/base of ascending colon region.

Formulation B capsules were resident in the ascending colon for some time before disintegration was apparent.

In one of the subjects taking Formulation C, disintegration did not begin until the hepatic flexure, whilst in the other subject the capsules travelled intact as far as the sigmoid colon. In the latter case, intestinal transit was very rapid.

6.3.3. Further characterisation of "Polymer A" coating

Before coating, the mean weight of the ten empty capsules was 163 ± 4 mg. The dip coating technique proved remarkably reproducible with a mean capsule weight following coating of 229 ± 3 mg. Since the piece of cotton remaining attached to each capsule weighed about 1 mg, the mean weight of polymer coating was approximately 65 mg.

Light microscope analysis of the coating indicated that it was between about 50 and $100 \mu\text{m}$ in thickness. The coat was thickest on the underside of each capsule and thinnest on the capsule ends.

6.4. CONCLUSIONS

Somewhat unexpectedly, "Polymer A" achieved the desired effect of delivering the capsules intact into the colon. Although capsules coated with this polymer disintegrated relatively rapidly in vitro, this behaviour was not evident in vivo. A combination of at least two factors may have been responsible for the unexpected in vivo behaviour. Firstly, the small intestinal transit time in all of the subjects was relatively short. Secondly, all subjects were

fasted and so levels of dissolution liquid in the small intestine to which capsules would have been exposed may have been low. Performance in fed subjects, where levels of liquid in the small intestine might be greater, or in subjects with a longer small intestinal transit time, could be very different.

The delayed disintegration of the Eudragit S-containing formulations, B and C, could be a result of a number of factors, including the colonic pH in the subjects investigated and the overall thickness of the coating. In one subject, capsule break-up in distal portions of the colon was almost certainly a result of a rapid intestinal transit rate.

Recently-published investigations from the Mayo Clinic into colon transit have also used radioisotope delivered within gelatin capsules (Proano et al., 1990, 1991). The capsules were coated with a solution of 13% w/v Eudragit S by a dipping technique. In vitro and in vivo disintegration of the Eudragit S coatings was generally slow, as demonstrated from the work in this chapter. The time for capsule disintegration to begin in vitro increased with coating thickness. For example, with one coat the capsule began disintegrating after 0.22 h at pH 7.4, whereas with five coats disintegration did not begin until 2.3 h. In vivo, capsules with four and five coatings passed through the colon intact, with two to three coatings disintegrated in the caecum and ascending colon, whilst with one coating, capsules disintegrated in the ileo-caecal region (Proano et al, 1990).

Since the "Polymer A"-based formulation developed in this chapter performed as required, this was selected for further in vivo investigations. In subsequent chapters it will be seen that this coating carried out its desired task with a high degree of reliability.

CHAPTER 7.

THE TRANSIT OF MODEL DOSAGE FORMS THROUGH THE COLON,
MEASURED USING GAMMA SCINTIGRAPHY.

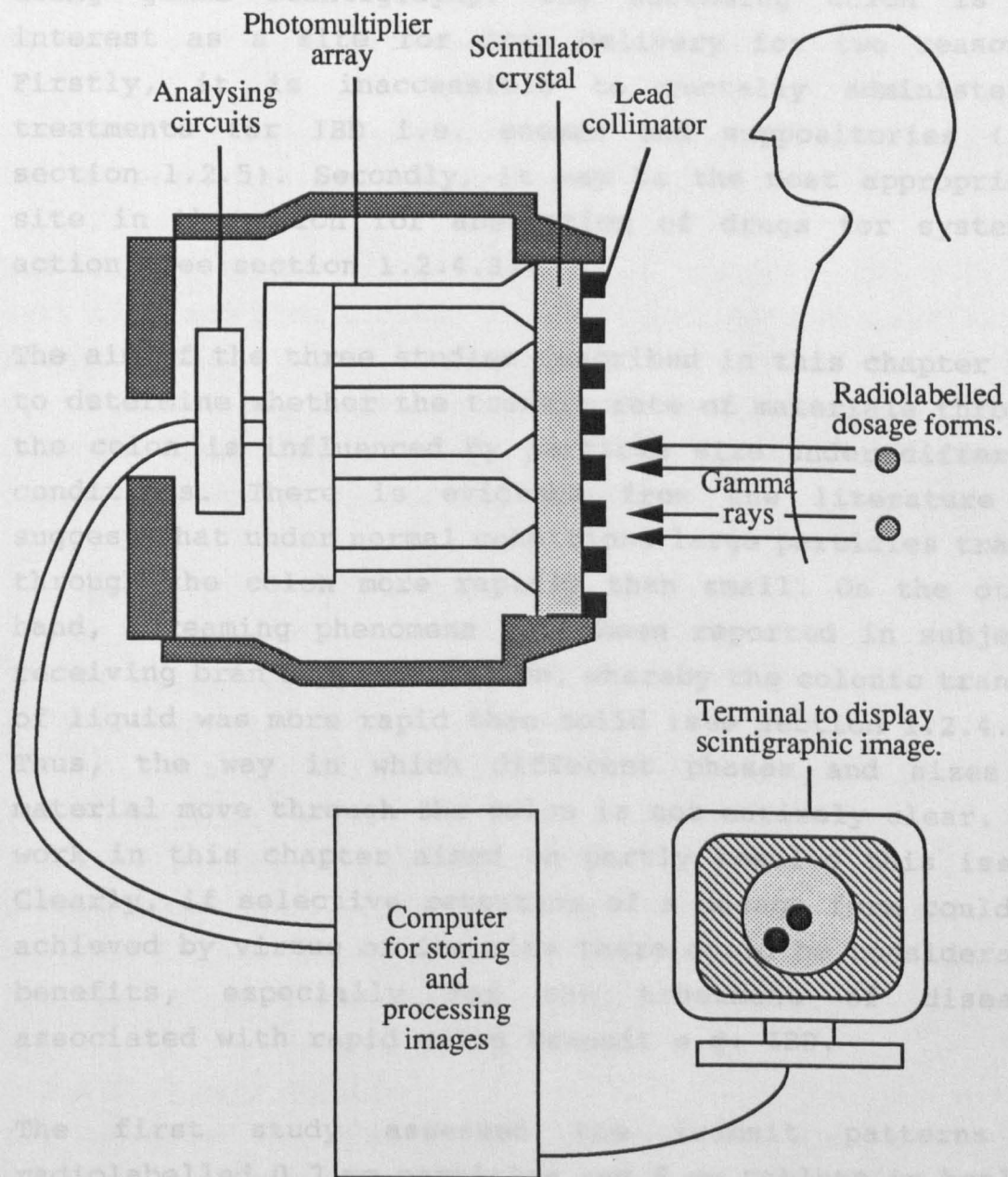
7.1. INTRODUCTION

The application of gamma scintigraphy for measuring the in vivo performance of dosage forms is now well established (Wilson and Washington, 1988). Although the technique has been applied to a wide variety of dosage forms administered by many routes, including buccal (Christrup et al., 1991; Washington and Wilson, 1988), rectal (Hardy et al., 1986; Jay et al., 1986), inhaled (Farr et al., 1985; Harnor et al., 1990), parenteral (Love et al., 1990) and ophthalmic (Fitzgerald et al., 1987), the majority of scintigraphic investigations have concerned the evaluation of oral drug-delivery systems (Digenis and Sandefer, 1991; Wilding et al., 1991; Wilson and Washington; 1988).

In gamma scintigraphy, the dosage form under investigation is radiolabelled by incorporation of a gamma-emitting radioisotope. Following administration of the radiolabelled dosage form to the subject, it can be located and followed externally by a gamma-camera (see figure 7.1). At appropriate intervals, the subject is positioned in front of the collimator. The gamma-rays emitted from the dosage form pass through the body of the subject, through the lead collimator located on the camera face and fall onto a thallium-doped sodium iodide crystal lying underneath. Interaction of the gamma rays with the crystal causes the emission of light photons. The photons are detected by photomultiplier tubes, positioned behind the scintillator crystal, which convert the light signal into an electrical signal. The energy of the electrical signal is proportional to the photon energy, and so photons from different radioisotopes can be simultaneously detected. The pattern of energy across the crystal face can be stored on a minicomputer for later analysis (Wilson and Washington, 1988).

The work undertaken in chapter 6 had demonstrated the

Figure 7.1. The Gamma-Camera.



feasibility of delivering materials into the colon inside hard gelatin capsules coated by a simple dipping technique. The next stage was to use these coated capsules to deliver the 0.2 mm and 5 mm and 0.2 mm and 8.4 mm radiolabelled particles (see chapter 6) into the colon and to follow their movement, through the ascending colon in particular, using gamma scintigraphy. The ascending colon is of interest as a site for drug delivery for two reasons. Firstly, it is inaccessible to rectally administered treatments for IBD i.e. enemas and suppositories (see section 1.2.5). Secondly, it may be the most appropriate site in the colon for absorption of drugs for systemic action (see section 1.2.4.3).

The aim of the three studies described in this chapter was to determine whether the transit rate of materials through the colon is influenced by particle size under different conditions. There is evidence from the literature to suggest that under normal conditions large particles travel through the colon more rapidly than small. On the other hand, streaming phenomena have been reported in subjects receiving bran supplementation, whereby the colonic transit of liquid was more rapid than solid (see section 1.2.4.1). Thus, the way in which different phases and sizes of material move through the colon is not entirely clear. The work in this chapter aimed to partly resolve this issue. Clearly, if selective retention of a dosage form could be achieved by virtue of its size there could be considerable benefits, especially for the treatment of diseases associated with rapid colon transit e.g. IBD.

The first study assessed the transit patterns of radiolabelled 0.2 mm particles and 5 mm tablets in healthy subjects under normal conditions and with coadministration of the laxative, lactulose. The selective colonic metabolism of lactulose was described in section 1.2.3.2. The laxative action is due largely to the retention of

extra water in the colon by osmotic means, although acidification of the colon probably also directly stimulates peristalsis (Avery et al., 1972). The aim of lactulose administration was twofold. Firstly it would provide data on particle movement in a hypermotile colon and secondly it could be established whether it provides a good model for the motility patterns seen in colonic diseases such as irritable bowel syndrome (IBS).

The second study investigated the differential transit of 0.2 mm particles and 8.4 mm tablets in healthy subjects.

The final study investigated the transit of 0.2 mm particles and 5 mm tablets in a group of patients suffering from irritable bowel syndrome. The results of this study would reveal any differences in particle behaviour in the diseased colon and whether lactulose is able to reflect these differences in healthy subjects.

7.2. EXPERIMENTAL

7.2.1. Materials

As for chapter 6.

7.2.2. Methods

7.2.2.1. Dosage form production

Dosage forms were produced using the methods described in chapter 6. All capsules received three coats of 15% w/v "Polymer A" in acetone as described previously.

7.2.2.2. Study design

All studies had the prior approval of the Nottingham University Medical School ethical committee. The administration of isotope was authorised by the Department of Health. The studies were conducted in accordance with the Declaration of Helsinki Guidelines for Ethics in Research and subjects were at all stages free to withdraw.

Study 1.

12 healthy human volunteers (7 male and 5 female, age 20-22) were recruited from the Nottingham University student population.

Each volunteer had to meet the following criteria:

- a) Absence of gastrointestinal symptoms.
- b) Non-vegetarian diet.
- c) Free from medication likely to alter GI motility.
- d) Non- or low-smoker.
- e) Alcohol intake within accepted limits.
- f) Female volunteers not pregnant. In addition, they were required to take a pregnancy test on the day before the study.

Study 1 was carried out in two parts, A and B, separated by a period of two weeks. All subjects undertook both parts of the study.

Part A.

During the four days prior to the investigation, each volunteer was requested to follow dietary guidelines in order to provide approximately 20 g of dietary fibre/day. The guidelines excluded certain high fibre foods and cathartics such as spicy foods, and were used to provide a degree of standardisation to the group.

On the morning of the study, volunteers arrived having fasted from 10 pm the previous evening. Radioactive markers were attached to each subject anterior and posterior over the right lobe of the liver to assist in alignment during scintigraphic imaging. Markers were produced by applying ^{99m}Tc solution to a small piece of filter paper attached to a length of sticky tape. When the solution had dried, the tape was wrapped into a small square with the filter paper concealed inside.

Each volunteer then swallowed three "Polymer A"-coated 000-sized capsules with 150 ml of water. Each capsule contained two 5 mm ethylcellulose tablets each radiolabelled with 0.67 MBq of ^{99m}Tc and 100 mg of 0.18-0.25 mm Amberlite IR120 resin labelled with 0.33 MBq of ^{111}In .

Immediately after swallowing the capsules, the subjects stood in front of the gamma camera for scintigraphic imaging. An anterior and posterior image of 30 seconds duration was recorded. Imaging was continued at 30-60 minute intervals throughout the day for a period of 12-14 hours with a final image 24 hours post-dose. Images were recorded using an IGE Maxicamera II gamma camera fitted with a medium energy parallel collimator (300 keV maximum energy). Images were acquired using the 140 keV photopeak for ^{99m}Tc and the 245 keV photopeak for ^{111}In . Data was stored on and processed by a Star computer system (IGE).

Once the three capsules were seen to have left the stomach, subjects received breakfast (10-11 am) and thereafter lunch (1 pm), coffee/tea and biscuits (4 pm and 9 pm) and dinner (6 pm) as follows:

Breakfast: Glass of orange juice.
 Two to four slices of toast with butter and
 jam or marmalade.
 Cup of decaffeinated coffee or tea.

Lunch: Sandwiches (four slices of bread).
 Packet of crisps.
 Piece of fruit.
 Tea, decaffeinated coffee or cold drink.

Dinner: Prawn cocktail.
 Fried steak, chips and mixed vegetables.
 Piece of sponge cake or cheesecake.
 Decaffeinated coffee.

Part B.

This was identical to part A, but in addition each subject also ingested lactulose solution (Duphar, Southampton, UK) 10-20 ml, three times daily for four days prior to the study and on the study day itself. The dose of lactulose was adjusted by the subjects themselves in order to approximately double their stool frequency.

Study 2.

12 healthy student volunteers were recruited (8 male and 4 female, age 18-24 years). The protocol was identical to study 1A described above. Here however, each capsule contained two 8.4 mm, ^{99m}Tc -labelled, ethylcellulose tablets (0.67 MBq/tablet) in place of the 5 mm tablets.

In this study, and in study 3, the scintigraphic data was stored on a Nuclear Diagnostics computer system (Nuclear Diagnostics, Gravesend, UK).

Study 3.

7 patients suffering from IBS were recruited from a gastroenterology clinic (2 female and 5 male, age range 27-53). Two suffered predominantly from diarrhoea, two from constipation whereas the other three alternated between diarrhoea and constipation. The same basic protocol as in study 1A was followed. The patients were advised to follow their normal diet for the period prior to the study, but to avoid cathartic foods and pulses.

7.2.2.3. Data analysis

The position of capsule break-up was determined visually from the images.

From the set of stored scintigraphic images, an outline picture of the colon could be developed for each subject. Using a variable region of interest program, the colon images were divided into four regions and the number of

counts in each recorded. The four regions were the ileo-caecal junction (ICJ), the ascending colon, the transverse colon and the descending colon/rectum (figure 7.2). On each image, background counts were also recorded. Distribution of the tablets could be determined visually by simply counting the number in each region.

Data analysis of the counts recorded in the colon regions was undertaken using a spreadsheet program (Microsoft Excel) run on an Apple Macintosh microcomputer. The spreadsheet was set-up to make corrections for background radiation and radioactive decay, and to present results as the geometric mean of anterior and posterior counts. The geometric mean = $\sqrt{\text{anterior counts} \times \text{posterior counts}}$, and partially overcomes errors due to tissue attenuation of the gamma rays (Hardy and Perkins, 1985).

The percentage of the administered dose in the whole colon was calculated by addition of the percentage values in the ascending colon, transverse colon and descending colon/rectum regions. By plotting the activity-time course in the whole colon and [whole colon-ascending colon] on the same graph it was possible to estimate the residence time of the activity in the ascending colon. The difference between the two curves at the 50% activity level represented the residence time of 50% of the administered activity in the ascending colon and was defined as the mean residence time (MRT) (figure 7.3). In addition, the percentage of activity remaining in the whole colon and ascending colon after 24 hours was estimated.

Tests for statistical significance (Wilcoxon signed rank sum test) were undertaken using "Statworks" program run on an Apple Macintosh.

Figure 7.2. Divisions of colon used for scintigraphic analysis.

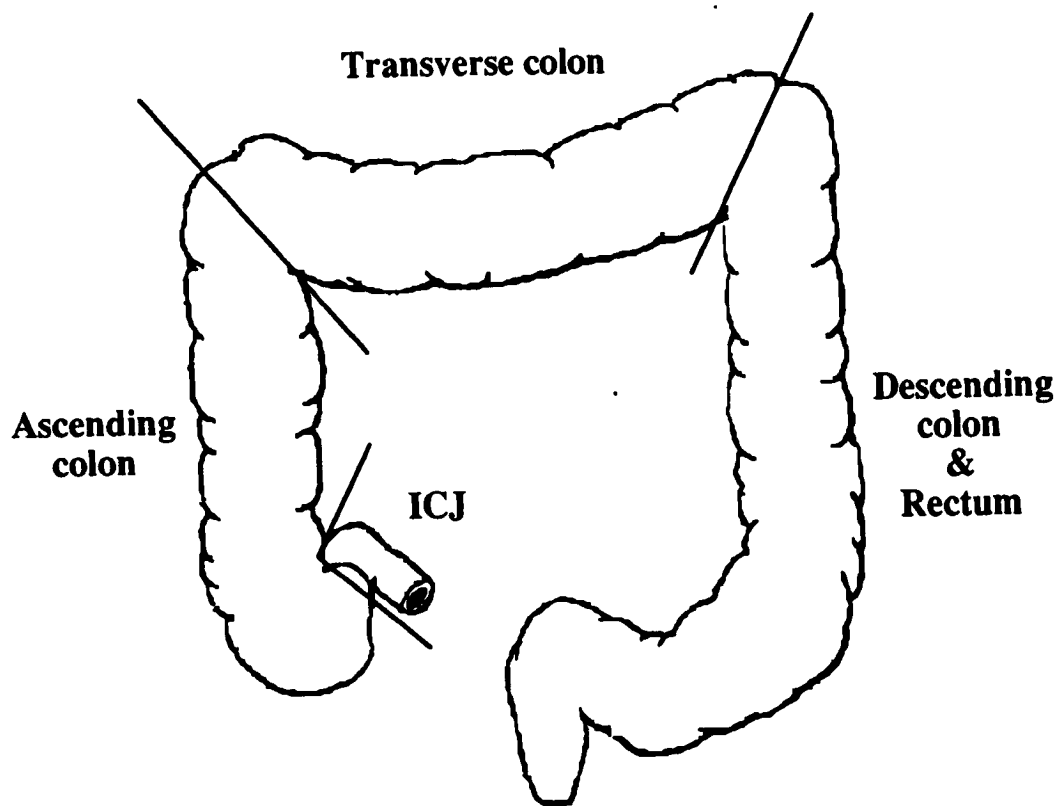
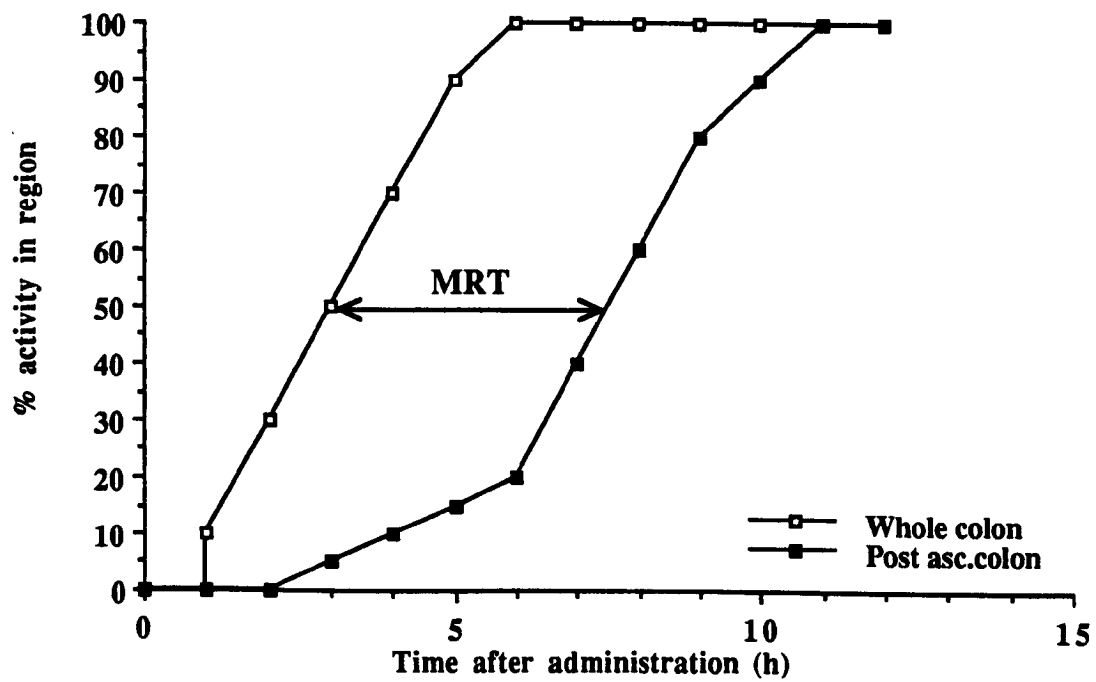


Figure 7.3. Graph to define ascending colon mean residence time (MRT).



7.3. RESULTS

7.3.1. Study 1.

Data is presented for 11 subjects; the data from one subject was excluded due to abnormally rapid colon transit.

7.3.1.1. Part A

The scintigraphic images showed reproducible delivery of the intact capsules into the ileocaecal region, from where they proceeded to disintegrate. Mean ICJ arrival time was 2.2 ± 1.3 h, with the principal source of variation in arrival being the time for gastric emptying. Small intestinal transit was invariably rapid and, although it was not measured precisely, in most instances it was probably less than 90 minutes. A period of stasis was often observed in the ICJ or caecum/base of ascending colon, with the body of activity sometimes residing there for a considerable length of time (2-3 hours) with very little spread evident. Activity generally moved from the ICJ into the colon as a single bolus. Material then commenced a gradual spread through the ascending colon and into the transverse and eventually descending colon.

Table 7.1 presents the colon transit data for study 1 A. The mean residence time for 50% of the 5 mm tablets in the ascending colon (MRT) was 14.1 ± 4.7 h and for the 0.2 mm resin, 12.9 ± 3.7 h. A wide variation was seen in the residence time values. For example the shortest residence time for the tablets was 7.5 h, but the longest was 23.5 h.

There was no significant difference between the residence time of the 0.2 mm particles and the 5 mm tablets ($p=0.07$).

After 24 hours, the majority of the administered dose of 0.2 mm particles ($80.7 \pm 18.6\%$) still resided in the colon. The percentage of the administered radioactivity resident in the ascending colon at 24 hours was $23.1 \pm 12.8\%$. As a

Table 7.1. Colon transit data for study 1A (healthy controls).

Subject	Ascending colon MRT (h)		% of administered 0.2 mm particles remaining after 24 h	
	5 mm tablets	0.2 mm particles	Ascending colon	Whole colon
1	7.50	10.75	18.6	31.2
2	23.50	23.25	56.0	94.7
3	18.75	13.25	9.6	85.4
4	15.75	13.50	28.0	90.2
5	14.75	10.50	15.2	75.9
6	11.25	10.25	14.9	85.6
7	14.75	13.00	28.2	100
8	16.25	14.25	26.0	89.5
9	11.25	11.00	26.9	86.2
10	7.50	9.75	20.2	80.8
11	13.75	12.25	10.6	68.0
Mean	14.11	12.89	23.1	80.7
SD	4.67	3.75	12.8	18.6

result of the short-half life of the ^{99m}Tc label, it was not possible to accurately assess the number of tablets resident at 24 hours.

7.3.1.2. Part B

With lactulose administration, the time of capsule arrival at the ICJ was 2.1 ± 1.0 h. The point of capsule break-up appeared to be unaffected, despite the fact that lactulose produces acidification of the colon.

The rate and extent of spread of radioactivity was considerably greater than for part A. In many of the subjects the 0.2 mm particles rapidly outlined the entire ascending colon. Retrograde movement of large areas of activity within the ascending colon was observed in some subjects.

The increase in colon motility after lactulose administration was reflected in the transit rate data (table 7.2). For both particles and tablets, a marked reduction in residence time in the ascending colon was seen. The MRT value for the 5 mm tablets was 8.7 ± 3.4 h, and for the 0.2 mm particles 7.0 ± 2.5 h. These values represented respectively a 37% and 46% reduction in residence over non-lactulose treatment and were statistically significant ($p=0.012$ and 0.002 respectively). Figures 7.4a) and b) show the transit profiles of the 5 mm tablets in one subject without and with lactulose administration and the change in colon motility is clear.

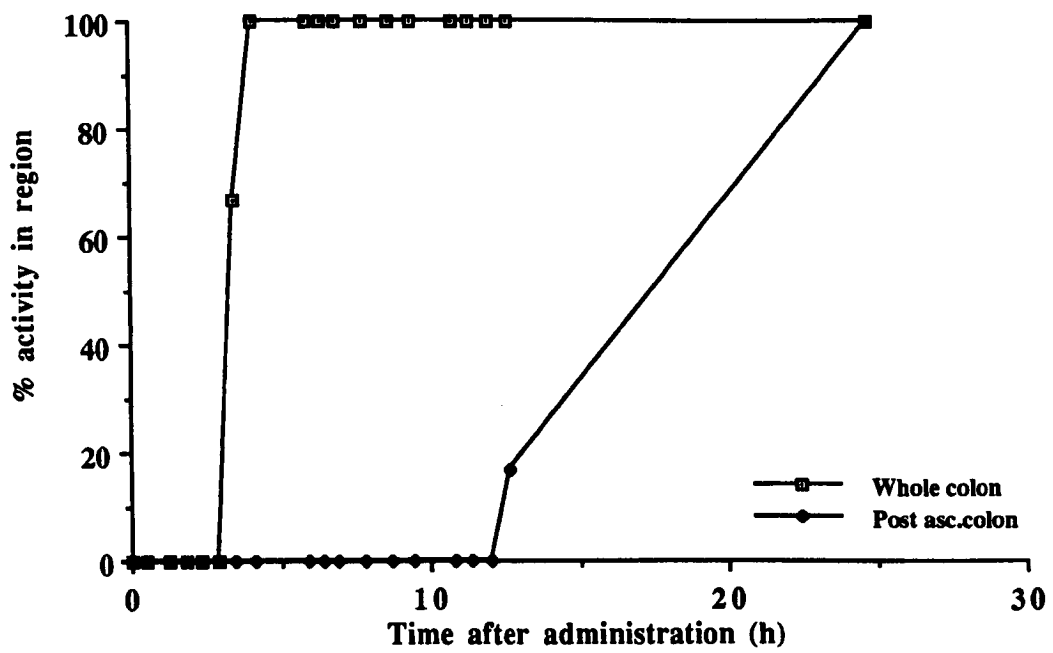
The MRT of the 5 mm tablets was significantly longer than for the 0.2 mm particles ($p=0.03$). However, looking at the individual data (table 7.2) there is no clear trend, with the 0.2 mm MRT being either greater than, or about the same as, the 5 mm MRT in 5 of the 11 subjects.

Lactulose administration did not significantly reduce the

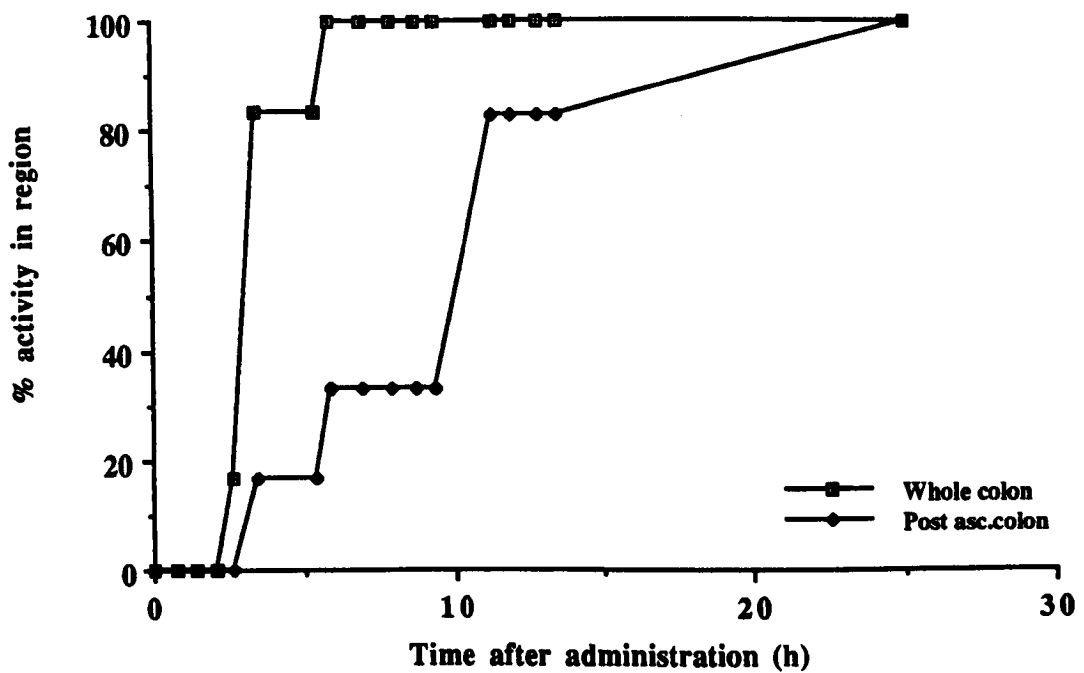
**Table 7.2. Colon transit data for study 1B
(coadministration of lactulose)**

Subject	Ascending colon MRT (h)		% of administered 0.2 mm particles remaining after 24 h	
	5 mm tablets	0.2 mm particles	Ascending colon	Whole colon
1	9.00	7.50	3.5	51.8
2	8.25	9.25	4.0	100
3	7.25	7.25	11.2	49.9
4	9.50	9.25	22.7	97.6
5	8.75	4.50	7.5	83.5
6	6.75	4.25	4.5	79.8
7	6.25	3.75	2.4	51.4
8	16.00	8.50	5.6	62.7
9	13.00	10.75	18.2	80.4
10	3.00	3.50	6.3	94.2
11	7.50	8.25	42.7	87.0
Mean	8.66	6.98	11.7	76.2
SD	3.44	2.55	12.2	19.1

Figure 7.4. a) Activity time-profile in healthy subject.



b) Activity-time profile in same subject receiving lactulose.



activity present in the whole colon after 24 hours ($76.2 \pm 19.1\%$), although the amount of activity remaining in the ascending colon was reduced by almost 50% from $23.1 \pm 12.8\%$ to $11.7 \pm 12.2\%$ ($p=0.025$).

7.3.2. Study 2

Data from the study investigating the differential transit of 0.2 mm particles and 8.4 mm tablets is presented in table 7.3. The data is for 10 subjects, since in two subjects one of the capsules was resident, intact, in the stomach for the whole of the study day.

The MRTs of the 0.2 mm particles and 8.4 mm tablets were 8.9 ± 3.2 h and 8.6 ± 3.7 h respectively. There was no significant difference between these values. Activity (from 0.2 mm particles) in the whole colon at 24 hours was comparable to Study 1 A at $79.3 \pm 10.4\%$, although the activity residing in the ascending colon was much lower ($12.6 \pm 8.5\%$).

Surprisingly, MRT values for both sizes of particles were markedly reduced compared to study 1, although this may simply reflect the small numbers of subjects used and the inherently large intersubject variation in colon residence. Presumably, with lactulose administration the residence times of the subjects in study 2 would have been reduced still further.

7.3.3. Irritable bowel syndrome

Table 7.4 presents data from the investigation with the seven IBS patients (study 3). This was a fairly disparate group in terms of disease state and no overall pattern emerged.

The MRT of the 5 mm tablets in the ascending colon was 6.2 ± 2.4 h and for the 0.2 mm particles, 8.5 ± 3.6 h. There was no significant difference between these two values.

Table 7.3. Colon transit data for 0.2 mm particles vs. 8.4 mm tablets in healthy subjects.

Subject	Ascending colon MRT (h)		% of administered 0.2 mm particles remaining after 24 h	
	8.4 mm tablets	0.2 mm particles	Ascending colon	Whole colon
1	8.75	11.00	12.1	69.3
2	14.00	9.75	10.3	81.3
3	15.75	15.75	29.8	87.6
4	6.75	10.00	16.5	82.6
5	6.00	7.50	2.5	65.3
6	7.50	8.25	9.1	83.1
7	9.75	5.75	2.6	73.3
8	6.25	9.25	20.5	86.2
9	3.50	3.75	16.2	97.9
10	7.75	8.00	6.6	66.9
Mean	8.60	8.90	12.7	79.3
SD	3.21	3.21	8.5	10.4

Table 7.4 **Colon transit data for IBS patients.**

Subject	Ascending colon MRT (h)		% of administered 0.2 mm particles remaining after 24 h	
	5 mm tablets	0.2 mm particles	Ascending colon	Whole colon
1	8.75	8.50	15.2	42.9
2	3.25	16.50	52.2	92.8
3	7.00	12.50	30.9	75.3
4	8.50	7.50	19.7	81.1
5	2.75	5.75	7.8	81.0
6	7.00	4.25	0.4	20.0
7	6.50	6.50	1.8	4.4
Mean	6.20	8.50	18.3	56.8
SD	2.40	3.60	18.4	34.4

Both of the MRTs were considerably shorter than for the normal controls in study 1 and compare favourably with the lactulose-treatment. However, the 0.2 mm mean MRT does not differ greatly from study 2.

Again, there were individual instances where very great differences in MRT between the two sizes of particles were seen, but again there was no clear trend. The most extreme examples are subject 2, where the MRT values for 0.2 mm and 5 mm particles were 16.5 h and 3.25 h respectively, and subject 3 (12.5 h and 7 h). On the other hand, in three of the subjects (1, 4, and 7) there was no great difference, and in another (6) the 5 mm MRT was greater than the 0.2 mm MRT.

There was no obvious relationship between disease state and ascending colon MRT. For example in subject 7, whose disease condition was predominantly diarrhoeal, although whole colon transit was rapid (4% activity remaining after 24 hours) the ascending colon transit was not excessively fast (MRT = 6.5 h).

7.4. CONCLUSIONS

These studies have demonstrated a versatile, non-invasive technique for simultaneously assessing the movement of different sizes of particles through the colon.

Combining the 0.2 mm data from studies 1 A and 2, an ascending colon mean residence time of 11.0 ± 4.0 h is obtained (n=21). This value is in good agreement with other studies which have reported transit times through the ascending colon of 10-12 h (Proano et al., 1990) and 8-11 h (Metcalf et al., 1987).

One of the aims of this work was to assess whether lactulose provided a good model for the transit patterns

associated with diseases such as IBS. Since the group of patients studied was only small and were not all diarrhoea predominant, it is difficult to draw definite conclusions. However from study 1, the ability of lactulose to significantly increase the transit of materials through the ascending colon in healthy volunteers was clearly demonstrated.

A comparison between the transit rate of the 0.2 mm particles and the tablets indicated that although there were a few individual instances where a marked difference in transit between the sizes was observed, overall there was no clear effect. Therefore, these studies suggest that in healthy human subjects, materials in the 0.2 mm to 8.4 mm size range are resident for the same period of time in the ascending colon. Marked enhancement in transit of the 5 mm tablets was noted in two of the IBS patients and may warrant further investigation. The more rapid passage of solid compared to liquid in a group of patients with diverticular disease has been reported by Findlay et al. (1974) (see section 1.2.4.1.A).

Proano et al. (1990, 1991) have recently reported that the transit through the ascending colon of 0.5-1.8 mm pellets was the same as a liquid phase, but slower than the transit of 6 mm pellets. This implied that the "cut-off" point below which a separation by size does not occur lies between about 1 and 6 mm. The work presented in this chapter conflicts with this finding and indicates that the ascending colon transit is the same for particles between 0.2 mm and 8.4 mm. A general problem when interpreting the results of colon studies is the inherent inter- and intrasubject variability in transit, which may be large. Consequently, a definitive relationship between particle size and colon transit may only become clear when many more similar studies have been undertaken.

However, the long period of residence of materials in the colon supports the premise that this part of the GI tract may represent a good site to achieve sustained local action or absorption of drug from dosage forms resident there. Furthermore, dispersed dosage forms such as microspheres, pellets, and mini-tablets are probably the most appropriate type of sustained-release dosage form for colon delivery for two reasons:

1. Such dosage forms become widely dispersed in the colon and may allow maximisation of drug absorption especially in distal regions where close contact with absorbing surfaces is desirable because of probable poor diffusion through viscous faecal contents.

2. The phenomenon of spread within the ascending colon followed by gradual emptying maximises the residence of a dispersed dosage form; some of the drug carriers will empty rapidly, some will be resident for much longer. Equally, a single unit dosage form under the same conditions could be resident for a relatively long period, yet on the other hand it may empty very rapidly. Depending on the intended use of the dosage form, rapid ascending colon emptying could compromise therapeutic efficacy, but this effect would be minimised by administering the drug in dispersed form.

CHAPTER 8.

RADIOLABELLING OF DRUG:POLYMER MICROSPHERES USING NEUTRON
ACTIVATION TECHNIQUES.

8.1. INTRODUCTION

The experiments described in chapter 7 established that under normal conditions, there was no difference in the colonic transit rate of model dosage forms in the size range 0.2 to 8.4 mm. However, it was considered that multiparticulate dosage forms may have benefits over single units for sustained drug delivery into the colon.

The next stage of the work was to investigate the rate of transit and release characteristics of drug-containing Eudragit RS microspheres in the human colon. Since the transit rate was to be assessed using gamma scintigraphy, a method for radiolabelling the microspheres had to be devised and the chosen technique was neutron activation.

Conventionally, dosage forms are radiolabelled by incorporation of isotopes such as ^{99m}Tc or ^{111}In during manufacture as described in Chapter 6. There are however a number of drawbacks in using this technique for radiolabelling:

1. The short-lived nature of some of these isotopes (e.g. half-life of ^{99m}Tc = 6 hours) means that the time for production of the dosage form may be limited. Although this can be partly overcome by simply incorporating more radioisotope into the dosage form, this has the disadvantage of exposing manufacturing personnel to higher levels of radioactivity.
2. The manufacture of radiolabelled dosage forms requires designated radioisotope facilities. One consequence is that radiolabelling dosage forms produced in a conventional pharmaceutical production environment is impractical.
3. If specialised manufacturing equipment is needed (e.g. extruder/spheroniser for pellet manufacture or a freeze-

drier) it could become contaminated with radioisotope, putting it out of use until the isotope has decayed.

4. If problems are encountered during manufacture of the dosage forms, or the final dosage forms fail to meet the required specifications, the investigation for which they were produced would have to be cancelled until a new batch could be made.

Many of these problems can be overcome by the use of neutron activation techniques. The application of neutron activation for the radiolabelling of dosage forms was developed at the University of Kentucky and Oakridge National Laboratory in the early 1980s (Parr et al., 1985). The fundamental difference between neutron activation and conventional radiolabelling is that in the former process, the isotope incorporated is not radioactive at the time of dosage form manufacture. When required for the scintigraphic study, the dosage form containing the isotope is exposed to a neutron source in a nuclear reactor. The incorporated isotope absorbs neutrons and is converted into a gamma-emitting radioisotope (see figure 8.1).

When bombarding an isotope with neutron radiation it is possible to estimate the amount of radioactivity generated (Krane, 1983). The rate of isotope production,

$$R = \phi \sigma (m/M) N_a$$

Where,

ϕ = neutron flux ($n \text{ cm}^{-2} \text{ s}^{-1}$ produced by reactor).

σ = neutron capture cross-section ($\text{cm}^2/\text{nucleus}$). This represents the probability of the isotope conversion taking place. $10^{-24} \text{ cm}^2 = 1 \text{ barn}$.

m = mass of target nuclide.

M = mass number/molecular weight of target nuclide.

N_a = Avogadro's number.

$[(m/M) \times N_a = \text{the number of target atoms}]$.

When the irradiation time, t , is considerably less than the half-life of the isotope being generated ($t_{1/2}$), the activity generated,

$$A = R \lambda t$$

Where, $\lambda = \text{decay constant} = 0.693/t_{1/2}$

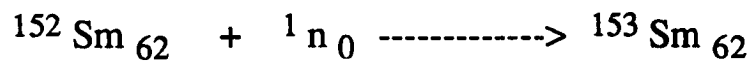
Thus, for a given target nuclide, the amount of radioactivity generated during neutron activation is dependent only upon: i) the neutron flux; ii) the mass of target nuclide; iii) the irradiation time.

Materials for activation that are suitable for incorporation into dosage forms should meet certain requirements. The parent isotope should have low toxicity and be chemically inert, whereas the daughter isotope, generated upon neutron irradiation, should produce gamma rays of a suitable energy (ideally 100-300 keV), have a relatively short half-life, produce no alpha activity, and decay to a stable, non-toxic isotope. Materials which meet these requirements include the oxides and nitrates of ^{152}Sm (samarium) and ^{170}Er (erbium) and the carbonate, nitrate, chloride and sulphate of ^{138}Ba (barium) (Digenis and Sandefer, 1991), and some of their properties are summarised in table 8.1.

The effects of isotope incorporation and subsequent irradiation have been reported for a number of dosage forms. Concentrations of Ba sulphate greater than 0.33% w/w and Sm oxide and Er oxide greater than 10% w/w were found to significantly reduce the hardness of lactose tablets. When these tablets were irradiated at a neutron flux of $4.4 \times 10^{12} \text{ n cm}^{-2} \text{ s}^{-1}$ for 15 minutes, their hardness increased, whilst the hardness of tablets containing no isotope was

Figure 8.1. Neutron irradiation of Samarium-152 (Sm).

1. Sm-152 absorbs neutrons and is converted to Sm-153:



2. Sm-153 is unstable and decays with a half-life of 46.7 hours to Europium-153, a stable isotope. The decay is accompanied by the emission of beta particles and gamma rays:

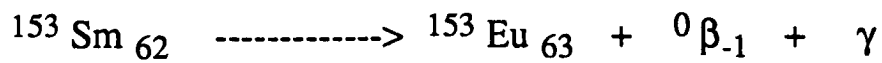


Table 8.1. Physical properties of some materials suitable for neutron activation and incorporation into dosage forms (from Digenis and Sandefer, 1991).

<u>Isotope</u>	<u>Neutron capture cross-section (barns)</u>	<u>Half-life of activated isotope</u>	<u>Chemical form</u>	<u>Water solubility (g/100ml)</u>
Sm-152	210	46.7 h	Oxide Nitrate	0.000054 58.95
Er-170	5.7	7.5 h	Oxide Nitrate	0.000222 Soluble
Ba-138	0.4	84 min	Carbonate Nitrate Chloride Sulphate	0.002 8.7 37.5 0.000222

unaffected following the same treatment. For tablets with and without isotope, a direct correlation was observed between the irradiation time and the time for tablet disintegration. This emphasized the importance of minimising the total radiation exposure of the dosage form and the amount of incorporated target nuclide (Parr and Jay, 1987).

The performance of enteric-coated erythromycin pellets containing Er oxide has been assessed before and after neutron irradiation. The amount of erythromycin released in vitro after 30 minutes was significantly reduced compared to non-irradiated pellets, although there was no difference in release after 60 minutes. Irradiation also caused a small decrease in the acid resistance of the pellet coating, which may have resulted from an increase in coat porosity (Parr et al., 1990).

Sustained-release matrix tablets containing ibuprofen have been radiolabelled by incorporation of Er oxide followed by neutron irradiation. The in vitro drug release rate was found to increase slightly following irradiation, but the tablets still met the required specifications (Parr et al., 1987).

A number of human scintigraphic studies using neutron activation techniques for radiolabelling have been reported. Dosage forms labelled with Er oxide have included ibuprofen tablets (Parr et al., 1987) and naproxen pellets (Hardy et al., 1991) while erythromycin pellets have been labelled with Sm oxide (Digenis et al., 1990). A study investigating the performance of enteric-coated 5-ASA pellets involved the incorporation of both Sm and Er oxides, one into the pellet core and one into the pellet coat (Digenis and Sandefer, 1991).

Sm chelates of EDTA, DTPA and HIDA have been produced by

dissolution of Sm oxide in acid followed by addition to a solution of the chelating agent. The chelates were incorporated as model drugs into matrix tablets, the tablets irradiated, and the in vitro release of activity monitored. It was suggested that this technique could be used to scintigraphically assess the in vivo dissolution performance of a formulation (Coupe et al., 1990).

A technique for radiolabelling microspheres produced by solvent evaporation has recently been reported. The target nuclide, $^{165}\text{holmium}$ acetylacetonate, was codissolved with a biodegradable polyester in chloroform. Microspheres were produced by emulsification into aqueous PVA solution followed by solvent evaporation, and were then irradiated. Formulations could be designed which demonstrated prolonged retention of the nuclide. It was considered that these microspheres could have use in the therapy of diseases including cancer and rheumatoid arthritis (Mumper and Jay, 1991).

A technique involving the incorporation of a soluble target nuclide would not be suitable for the radiolabelling of Eudragit RS microspheres due to the relatively high permeability of the polymer. Therefore for the studies carried out for this thesis a poorly water-soluble, particulate material was required as the target. The material chosen was Sm oxide (Sm_2O_3). Although Sm_2O_3 is extremely water-insoluble (table 8.1), it does dissolve in acidic solutions, and so may not be suitable for radiolabelling dosage forms in which it comes into direct contact with gastric juice.

Another attraction of Sm_2O_3 is its high neutron capture cross-section (table 8.1) which enables non-enriched material to be used to generate adequate levels of radioactivity with reasonably short irradiation times. Naturally occurring Sm_2O_3 contains seven different isotopes

(see table 8.2) of which the isotope of interest, ^{152}Sm , constitutes just 26.6%. The only factor that will preclude the use of this material for human investigations is the generation of undesirable activity from any of the other six isotopes. The only conversion of interest in this respect is the conversion of ^{154}Sm to ^{155}Sm . ^{155}Sm is a high energy beta-emitter, but fortunately since its half-life is just 22 minutes (CRC Handbook of Chemistry and Physics, 1987), it will rapidly decay to insignificant levels. The benefit of being able to use non-enriched Sm_2O_3 is that it is readily available. In contrast, the low cross-sectional area of ^{170}Er (5.7 barns) (table 8.1) and its low natural abundance (15 %) mean that artificially enriched material (95%+ ^{170}Er) has to be used (Digenis and Sandefer, 1991).

A further factor to be considered when planning to use neutron activation for radiolabelling is whether the dosage form contains any other elements that may be activated to undesirable isotopes. Two examples of pharmaceutical interest are sodium and potassium. The products of the irradiation of these elements, ^{24}Na and ^{42}K , are both long-lived ($t_{1/2} = 15$ h and 12 h respectively) (CRC Handbook of Chemistry and Physics, 1987), high energy gamma-emitting isotopes whose presence in the final dosage form in even small quantities would be undesirable. For the Eudragit RS microspheres, the only element present that can be activated, apart from samarium, is chlorine, present as chloride ions in Eudragit RS (see chapter 1, table 1.2). ^{37}Cl absorbs neutrons and is converted to ^{38}Cl , a beta-emitter, $t_{1/2} = 47$ minutes (CRC Handbook of Chemistry & Physics). The very small neutron capture cross-section of ^{37}Cl (0.2 barns) and its short half-life should ensure that only minor amounts of ^{38}Cl will be present in irradiated Eudragit RS microspheres at the time of dosing (at least 18 hours after irradiation).

Table 8.2. Composition of naturally occurring samarium oxide.

Isotope atomic number	% abundance
144	3.1
147	15.1
148	11.3
149	13.9
150	7.4
152	26.6
154	22.6

The work described in this chapter will be divided into two main sections. The first part describes the incorporation of Sm_2O_3 into SASP-containing Eudragit RS microspheres and the effects of irradiation on their physical properties.

Following preliminary investigations with SASP as a colon absorption marker, studies were switched to its absorbed colonic metabolite, sulphapyridine (SP). There were two drawbacks to using SASP. The first was its dosage requirement. Since it was estimated that at least 900 mg of SASP would need to be administered to generate adequate plasma levels of SP, this would require administration of a considerable volume of microspheres. In addition, the rate of absorption of SP would be dependent not only upon the rate of SASP release from the microspheres, but also upon its rate of generation from colonic metabolism of the parent molecule. It was observed that the incorporation of Sm_2O_3 into Eudragit RS-SP microspheres had interesting effects on their physical properties. These phenomena are described further in the second section of this chapter.

8.2. INCORPORATION OF SAMARIUM OXIDE INTO EUDRAGIT RS-SASP MICROSPHERES

8.2.1. EXPERIMENTAL

8.2.1.1. Materials

See chapter 4, but in addition, Sm_2O_3 (Sigma), chloroform (HPLC grade)(Rhône-Poulenc), methanol (HPLC grade)(Rhône-Poulenc), SpecpureTM samarium oxide (Johnson Matthey, Royston, UK), SpectrofluxTM 121A (Johnson Matthey).

8.2.1.2. Methods

A. Microsphere production

Microspheres were produced by the same basic method described in chapter 4. Briefly, Eudragit RS (4 g) was dissolved in 40 ml of dichloromethane in a glass bottle.

SASP (2 g) and Sm_2O_3 (0, 10, 20, 40 or 60 mg) were added to the polymer solution to form a suspension. The mean particle size of Sm_2O_3 was estimated to be about 10 μm using a laser diffraction technique (chapter 2) and it could generally not be completely dispersed by shaking alone. Therefore, the bottle containing drug, polymer and Sm_2O_3 was placed into an ultrasonic bath for 5-10 minutes to aid dispersion. The resulting mixture was emulsified into 200 ml of 0.1% w/v aqueous Tween 20 solution (overhead stirrer at 250 rpm) and stirring continued until all of the dichloromethane had evaporated. Then, any unemulsified drug-polymer agglomerates were decanted from the beaker, the microspheres filtered, washed with 150 ml of distilled water, and freeze-dried overnight. The weight of microspheres produced was recorded and a 250-500 μm sieve fraction collected.

B. Microsphere drug content

See chapter 4.

C. Efficiency of Sm_2O_3 entrapment

The concentration of Sm_2O_3 entrapped within the microspheres was determined using X-ray fluorescence spectroscopy (XRF). With this technique, the material of interest is irradiated with high energy X-rays. The X-rays eject electrons from the inner shells of the atoms of interest. When the electrons fall back from the outer shells to the vacant inner shells, X-rays are emitted and the X-ray spectrum is characteristic of the element. The intensity of the lines in the X-ray spectrum is proportional to the amount of the element present and can be measured on a suitable detector (e.g. scintillation counter) (Willard et al., 1988).

There are a number of different ways of presenting samples to the XRF spectrometer depending on the particular instrument used and on the properties and quantity of

sample available. The technique used in this study was to isolate the Sm_2O_3 from the microspheres by incineration, followed by fusing the residue with a flux. For each sample, 400 mg of microspheres were placed into a Pt/Au crucible. The crucible was ignited at 500 °C for 12 hours followed by further heating at 1000 °C for 15 minutes. This removed all of the organic matter from the microspheres, i.e. drug and polymer. The crucible was cooled, 2.6 g of SpectrofluxTM 121A added, and the sample fused at 1000 °C for 1 hour. The molten sample was then poured into a 32 mm die maintained at 225 °C, and pressed with a brass plunger. Standards containing 0, 0.15, 0.30, 0.55, 0.75 and 1.0 % w/w Sm_2O_3 were prepared by direct fusion with SpectrofluxTM 121A.

Concentrations of Sm_2O_3 were determined using a Philips PW1400 XRF spectrometer fitted with a Rh X-ray tube. The Sm concentration was determined using the $L_{\alpha 1}$ line, a LiF200 diffracting crystal and a scintillation counter. X-ray emissions for both peak and background were counted for 200 sec. The Sm_2O_3 content of the samples was determined from the net intensities (peak minus background) by reference to the calibration performed with the six prepared standards. The calibration plot of corrected counts against concentration for the Sm_2O_3 standards was linear over the concentration range used ($r = 0.999$).

D. Microsphere drug release rate

For apparatus and experimental details, see chapter 3. Samples were taken at 30, 60, 120, 180, 240, 300 and 360 minutes. Microsphere drug-release characteristics were assessed before and after irradiation. The post-irradiation tests were carried out after radioactivity had decayed to background levels.

E. Microsphere irradiation

500 mg samples of each of the five microsphere batches were

taken to the Universities Research Reactor, Risley, Cheshire for irradiation. Each sample was placed into a polypropylene tube and irradiated at a neutron flux of 10^{12} n cm⁻² s⁻¹ for a period of 90 minutes.

The radioactivity generated (MBq) was measured 21 hours after irradiation using a gamma-counter (Isotope Calibrator, Type 238, D.A.Pitman, Surrey, UK) set to detect ¹⁵³Sm. The delay between irradiation and measurement of activity allowed time for the decay of any short-lived isotopes present in the sample, in particular ³⁸Cl ($t_{1/2}$ =47 minutes) present in the polymer and ¹⁵⁵Sm ($t_{1/2}$ =22 minutes).

F. Leaching of radioactivity from the microspheres

In gamma scintigraphy, where the position of a dosage form is followed by means of its incorporated radiolabel, it is clearly desirable that the majority of label stays with the dosage form for as long as possible. For the Eudragit RS microspheres, Sm₂O₃ is insoluble at the pH encountered in the large intestine and therefore any loss of radiolabel will be in the form of particulate material.

To assess the extent of loss of particulate Sm₂O₃ from the microspheres during in vitro drug release, 45 mg of microspheres (containing theoretical Sm₂O₃ content of 1% w/w) were placed into 500 ml of pH 7 phosphate buffer (appendix 1) in the tablet dissolution apparatus (37 °C and 100 rpm). This study was undertaken six days after irradiation so that the level of radioactivity present in the microspheres was not too high to be measured on the laboratory gamma counter (Mini-Assay Type 6-20, Mini-Instruments, Essex, UK), yet high enough to allow detection of the loss of only small quantities of activity.

At hourly intervals over an eight hour period, the paddle in the dissolution vessel was stopped. Microspheres were allowed to sink to the bottom of the vessel and a 1 ml

sample of buffer drawn into a syringe. Prior to this it was ascertained that the sedimentation of Sm_2O_3 was very much slower than the microspheres, due to its very small particle size. Thus this technique avoided sampling of microspheres, but allowed sampling of any Sm_2O_3 that had become dissociated from the microspheres. The 1 ml sample was transferred to an Eppendorf tube and the counts recorded for a 10 second period. Each sample was counted five times. At each time interval, the counts from a reference sample of buffer solution were also recorded. Loss of activity was assessed by comparing dissolution buffer and reference buffer counts.

G. Drug stability

The stability of SASP to neutron irradiation was assessed by HPLC analysis of drug extracted from the microspheres before and after irradiation.

To extract the drug, an accurately weighed sample of the microspheres was placed in a 100 ml volumetric flask and 10 ml of methanol added to dissolve the Eudragit RS matrix. The polymer was precipitated and the drug dissolved by making to volume with 0.001 N sodium hydroxide solution. Prior to analysis, the samples were passed through a 0.1 μm membrane filter (Whatman) to remove precipitated polymer.

20 μL samples were injected manually (valve injector, Rheodyne, Cotati, CA) onto the HPLC column (25 mm x 4.6 mm ODS, Hichrom, Reading, UK). A mobile phase of 47.5% v/v methanol in pH 6 phosphate buffer (appendix 1) was used at a flow rate of 1.3 ml/min (Kontron LC pump, Kontron, Switzerland). The UV detector (Kontron Uvikon 720 LC) was set at 254 nm. Peaks were detected using a Spectra-Physics SP4270 integrator (Spectra-Physics, San Jose, CA). The pre- and post-irradiated samples of all five microsphere batches were analysed. Drug concentrations were calculated by reference to a calibration curve of SASP concentration

(dissolved in 0.001 N sodium hydroxide solution containing 10% v/v methanol) versus integrated peak area.

H. Polymer molecular weight analysis

The effect of irradiation on polymer molecular weight was assessed. The molecular weight of pre- and post- irradiated polymer was carried out using an ultracentrifugation technique. To extract the polymer, the microspheres were placed in a test tube and dissolved in methanol. This dissolved the polymer whereas most of the SASP remained in suspension. The tubes were centrifuged (MSE Centaur) at 2000 rpm for 10 minutes to separate SASP from polymer solution. The clear solution was pipetted into an evaporating glass and the methanol left to evaporate. The precipitated polymer was then redissolved in chloroform at an approximate concentration of 2 mg/ml in preparation for molecular weight analysis.

The relative polymer molecular weight was determined at the School of Agriculture, Nottingham University, by a sedimentation equilibrium ultracentrifugation technique (Beckman Model E analytical ultracentrifuge), described in detail elsewhere (Morgan et al., 1990).

I. Electron microscopy

The effect of irradiation on microsphere structure was assessed by low-temperature scanning electron microscopy, using the methods described in chapter 3.

8.2.2. RESULTS AND DISCUSSION

8.2.2.1. Before irradiation

A. Microsphere characterisation

Table 8.3 records the details of Sm₂O₃ incorporation into the SASP-Eudragit RS microspheres measured by XRF. Sm₂O₃ was successfully encapsulated and the incorporation efficiency appeared to increase with concentration. Since

Table 8.3. Samarium oxide incorporation efficiency into Eudragit RS:sulphasalazine microspheres.

Microsphere samarium oxide content (% w/w)		% incorporation efficiency
Theoretical	Assayed	
0	-	-
0.17	0.08	47
0.33	0.24	73
0.67	0.61	91
1.00	0.80	80

the aqueous solubility of Sm_2O_3 is minimal, the efficiency of incorporation must reflect factors other than partitioning from the polymer solution phase to the emulsifier phase. One important factor could be the difficulty in ensuring complete dispersion of the Sm_2O_3 into the drug-polymer mixture before emulsification; In all of the samples small agglomerates of Sm_2O_3 could be seen in the drug-polymer mixture before mixing into the surfactant solution, despite prior sonication.

Incorporation of Sm_2O_3 into the microspheres did not appear to significantly affect their formation or composition. Table 8.4 records yield and drug content values. The proportion of drug and polymer formed into microspheres was in all cases in excess of 80 % of the total material added. Typically, at least 30 % by weight of any given microsphere batch fell between 250 and 500 μm in size. Drug levels were similar at all Sm_2O_3 levels at between 31 and 32 % w/w, the high efficiency of encapsulation reflecting the low aqueous solubility of SASP with only small amounts dissolving from the drug-polymer solution into the surrounding emulsifier phase during microsphere production. (The aqueous solubility of SASP at 37 °C was estimated to be approximately 0.2 g/L).

All of the microsphere batches had a similar texture, colour and shape. Surface and internal SEM micrographs of the Sm_2O_3 -free batch of SASP microspheres are shown in section 8.2.2.2.F.

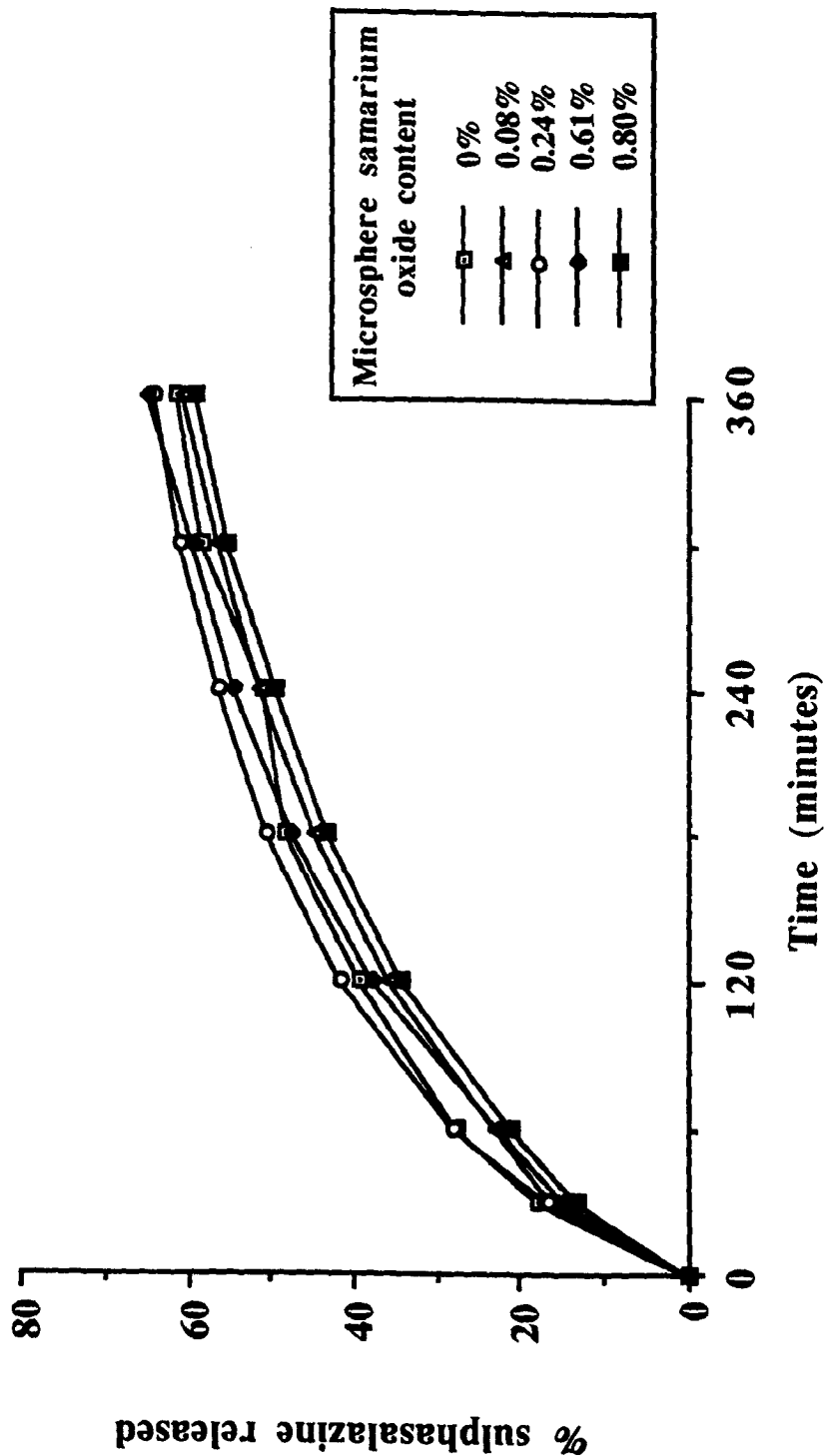
B. Drug release characteristics

Figure 8.2 shows the SASP release characteristics of the five microsphere batches. The rate of release was similar for all of the samples, with approximately 60% of encapsulated drug released after 6 hours, and thus appeared to be unaffected by the incorporation of Sm_2O_3 .

Table 8.4. Drug content and yield of Eudragit RS:sulphasalazine microspheres.

Samarium oxide content (% w/w)	Microsphere yield (g)	Sulphasalazine content (% w/w)	Sulphasalazine incorporation efficiency (%)
0	5.1	31.8	95.5
0.08	4.9	31.1	93.4
0.24	5.4	31.8	95.5
0.61	5.0	31.5	94.6
0.81	5.4	31.9	95.8

Figure 8.2. Effect of samarium oxide incorporation on sulphasalazine release rate.



8.2.2.2. After irradiation

A. Microsphere characterisation

There were obvious physical changes in the irradiated microspheres apparent on removal from the reactor. All of the samples had lightly caked into a single mass. Although this mass could be largely broken up by gentle shaking of the sample containers, all of the microspheres were passed through a 500 μm sieve prior to further evaluation. The microspheres had also appeared to have undergone some darkening and shrinkage which may have resulted from the effect of the heat of the reactor; the samples would have been exposed to a temperature of about 50-60 °C for the 90 minute period of irradiation.

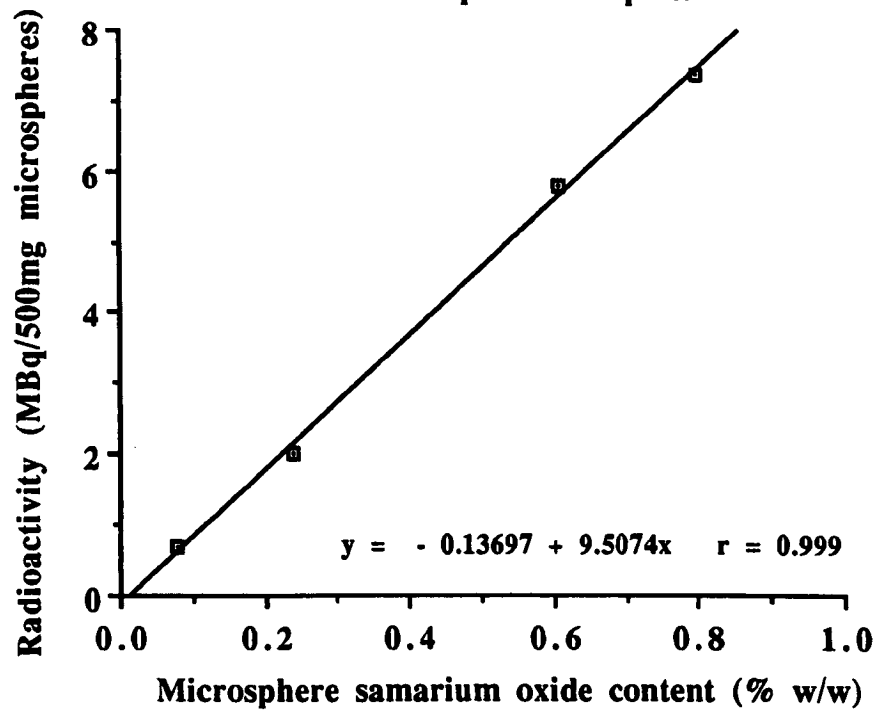
In figure 8.3, the radioactivity generated in each of the four Sm_2O_3 -containing samples is presented. The excellent correlation ($r=0.999$) between assayed Sm_2O_3 content and activity generated suggested that the precision of the XRF assay was high.

B. Leaching of radioactivity

The activity present in the 45 mg of microspheres to be dissolved was estimated as 1.57×10^6 counts/10 secs at the start of the experiment.

Throughout the 8 hour period of the dissolution experiment the counts in the dissolution buffer remained at the same level as the reference buffer (between 40 and 50 counts/10 secs/ml). Loss of counts due to radioactive decay would have been minimal over this period due to the 46.7 h half-life of ^{153}Sm . To demonstrate the sensitivity of this technique, if only 5% of the 1.57×10^6 counts had been lost into the surrounding buffer, the counts/10 secs/ml would have increased to 157 above the reference buffer. Although the total quantity of Sm_2O_3 present in the 45 mg of microspheres was only 0.36 mg (0.8% w/w), its small particle size should have ensured that any that became

Figure 8.3. Radioactivity generated from irradiation of microsphere samples.



dissociated would have become widely dispersed into the dissolution medium.

At the end of the 8 hour dissolution period, spectrophotometric assay of the dissolution buffer revealed that 75 % of the encapsulated SASP had been released. Therefore, it appeared that although a large proportion of the drug had dissolved from the microsphere matrix, the radiolabel remained in place.

The principal route for Sm_2O_3 to be lost would presumably be through pores and channels in the Eudragit RS matrix. The degree of porosity might be expected to increase as SASP dissolves. However, loss of particulate Sm_2O_3 would be prevented if the pores and channels were simply too small or if it was firmly "glued" to the polymer.

C. Drug stability

The results of the microsphere drug stability assay are presented in table 8.5. The SASP elution time was extremely sensitive to the buffer methanol content and was between 6.0 and 7.0 minutes using the chosen conditions.

For the pre-irradiated samples, there was generally good agreement with the drug content values obtained from the spectrophotometric assay (table 8.4).

Following irradiation, the assayed SASP contents were essentially unchanged. There were no additional peaks present in any of the irradiated samples and no change in the elution time of the SASP. For comparison, two potential degradative fragments of SASP, 5-ASA and SP, were found to elute at 2.1 and 2.9 mins respectively (see figure 8.4).

Therefore, SASP appeared to be stable to neutron irradiation. This is in general agreement with other neutron irradiation studies in which erythromycin (Digenis

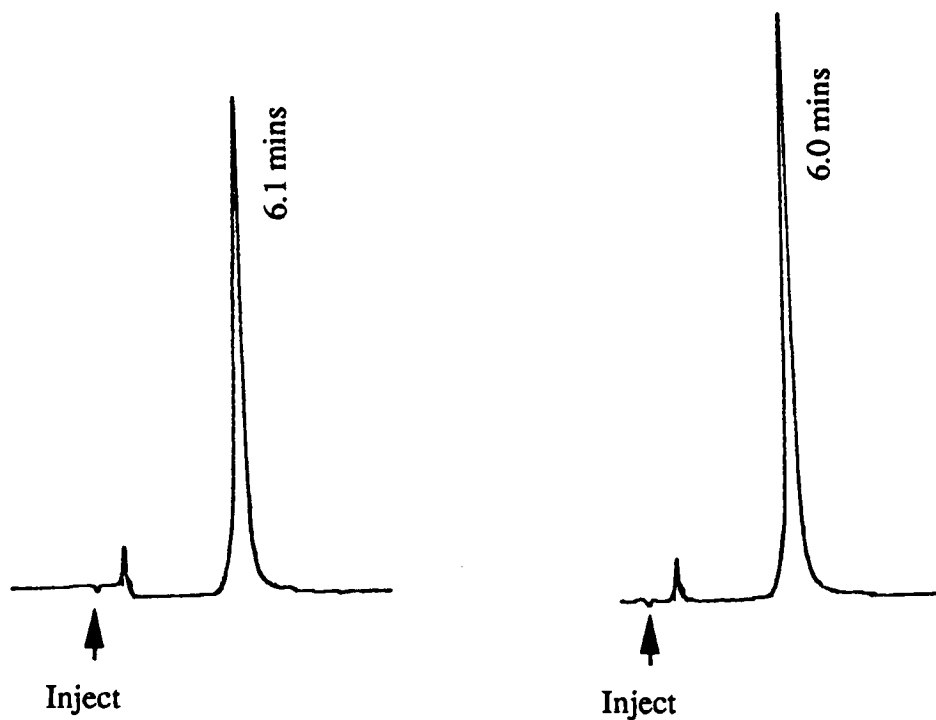
Table 8.5. Effect of neutron irradiation on assayed microsphere sulphasalazine content, measured by HPLC.

Microsphere samarium oxide content (% w/w)	Microsphere sulphasalazine content (% w/w)	
	Before irradiation	After irradiation
0	31.1±0.2	31.0±0.1
0.08	31.2±0.3	31.3±0.1
0.24	31.8±0.3	31.3±0.6
0.61	31.0±0.4	30.3±0.2
0.80	30.3±0.7	29.8±0.2

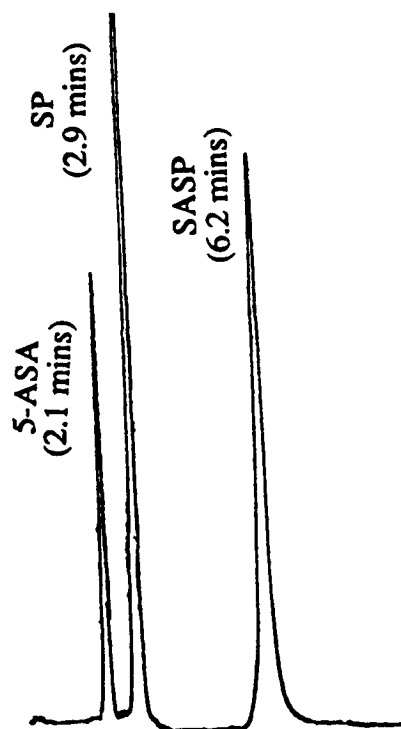
Figure 8.4. Radiation stability of sulphasalazine, measured by HPLC.

a) Extracted from microsphere sample (0.8% Sm oxide) before irradiation.

b) After irradiation.



c) Elution of sulphasalazine, sulphapyridine and 5-ASA.



et al., 1990), ibuprofen (Parr et al., 1987b), 5-ASA (Digenis and Sandefer) and naproxen (Hardy et al., 1991) have been shown not to undergo radiolysis.

D. Drug release rate

Figures 8.5a)-e) compare the drug release profiles of the five microsphere samples before and after irradiation. In all cases, the drug release rate following neutron irradiation was markedly enhanced. With one exception, the $t_{50\%}$ time was at least halved (table 8.6). It was considered that the enhanced drug release rate was most probably a consequence of radiation-induced polymer damage.

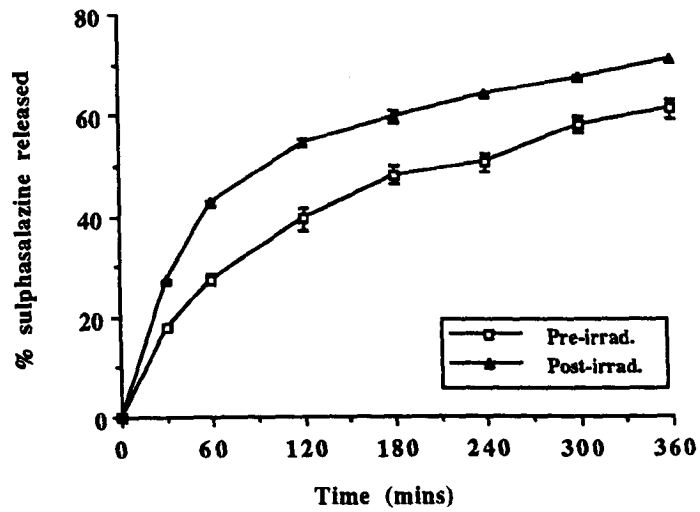
E. Polymer molecular weight analysis

For the Eudragit RS extracted from the microspheres before irradiation, the relative molecular weight, determined using ultracentrifugation, was 10,000. Following irradiation this had increased to 12,000. The margin of error of these values was approximately $\pm 10\%$ (Morgan, P., personal communication) and so it is possible that a small increase in molecular weight may have occurred during irradiation.

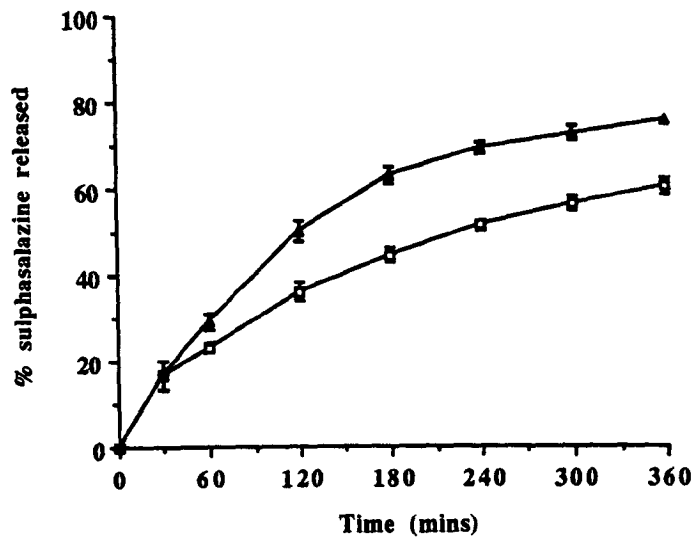
The potential effects of irradiation on polymers are complex and can result in backbone or side-chain scission and/or cross-linking (Swallow, 1973). In addition, the degree of damage can be influenced by many other factors such as the oxygen and moisture content of the sample (Swallow, 1973; Hartas et al., 1991). Consequently, further work would be needed to provide more definitive data on the effects of neutron irradiation on the structure of Eudragit RS.

Figure 8.5. Effect of irradiation on sulphasalazine release rate.

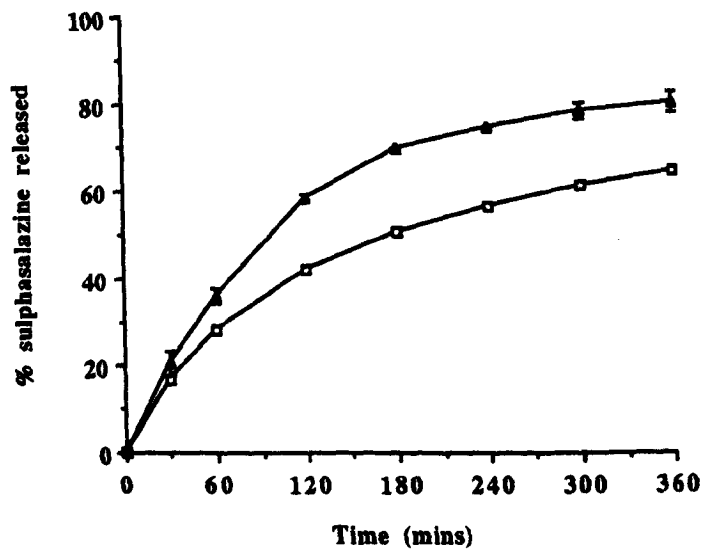
a) 0% w/w samarium oxide.



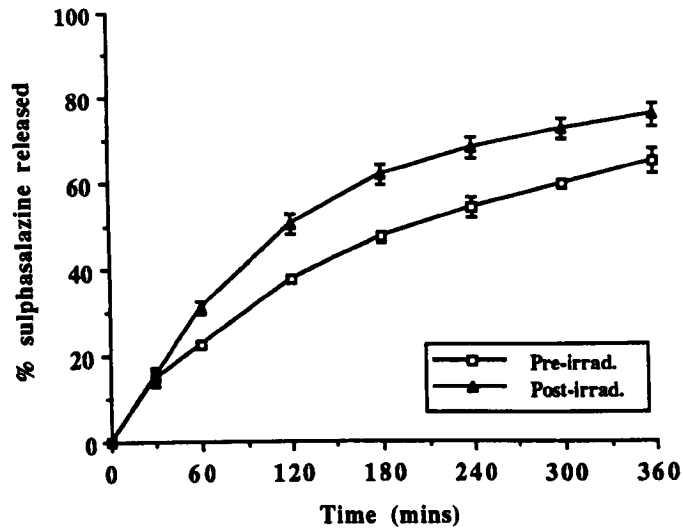
b) 0.08 % w/w samarium oxide.



c) 0.24 % w/w samarium oxide.



d) 0.61 % w/w samarium oxide.



e) 0.80 % w/w samarium oxide.

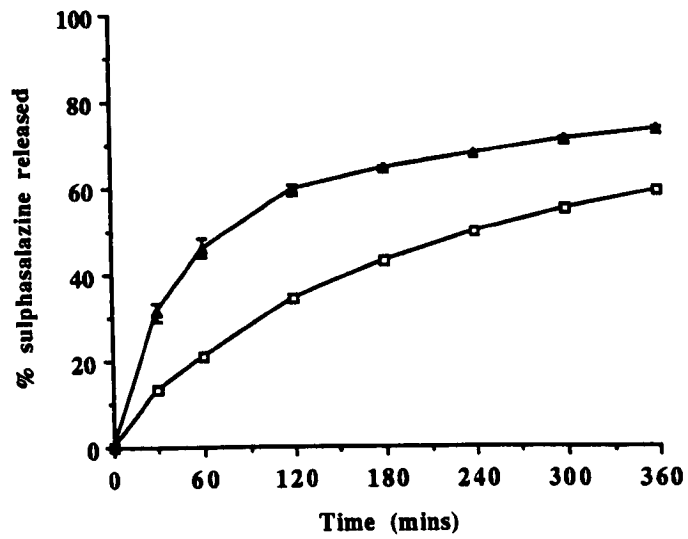


Table 8.6. Time for 50% of sulphasalazine to be released from microspheres (t50%) before and after irradiation.

Microsphere samarium oxide content (% w/w)	t50% (mins)	
	Before irradiation	After irradiation
0	240	90
0.08	240	120
0.24	180	90
0.61	210	120
0.80	260	80

F. Electron microscopy

Low temperature/cryogenic SEM micrographs of both the microsphere surface and internal structure were recorded for one of the microsphere samples before and after irradiation. Figures 8.6a)-d) compare the surface structures of the Sm_2O_3 -free batch at 220x and 1000x magnification.

The surface of the pre-irradiated microspheres was smooth and contained many pores (figures 8.6a and b). Following irradiation the smooth surface had been replaced by a softened/melted appearance (figures 8.6c and d). It is difficult to say whether a change in pore size or density had occurred following irradiation. In the irradiated sample, details of the structure underlying the microsphere surface are visible, possibly a result of shrinkage of the microsphere matrix.

Freeze-fracture of the microspheres revealed two distinct types of structure. Some were solid, whereas others were capsular with a large interior void, although in both cases the appearance of the drug-polymer matrix was similar. Before irradiation, the drug-polymer matrix had a porous, honeycombed appearance (figure 8.7a). High magnification views revealed a granular, possibly particulate, deposit on the internal matrix (figure 8.7b).

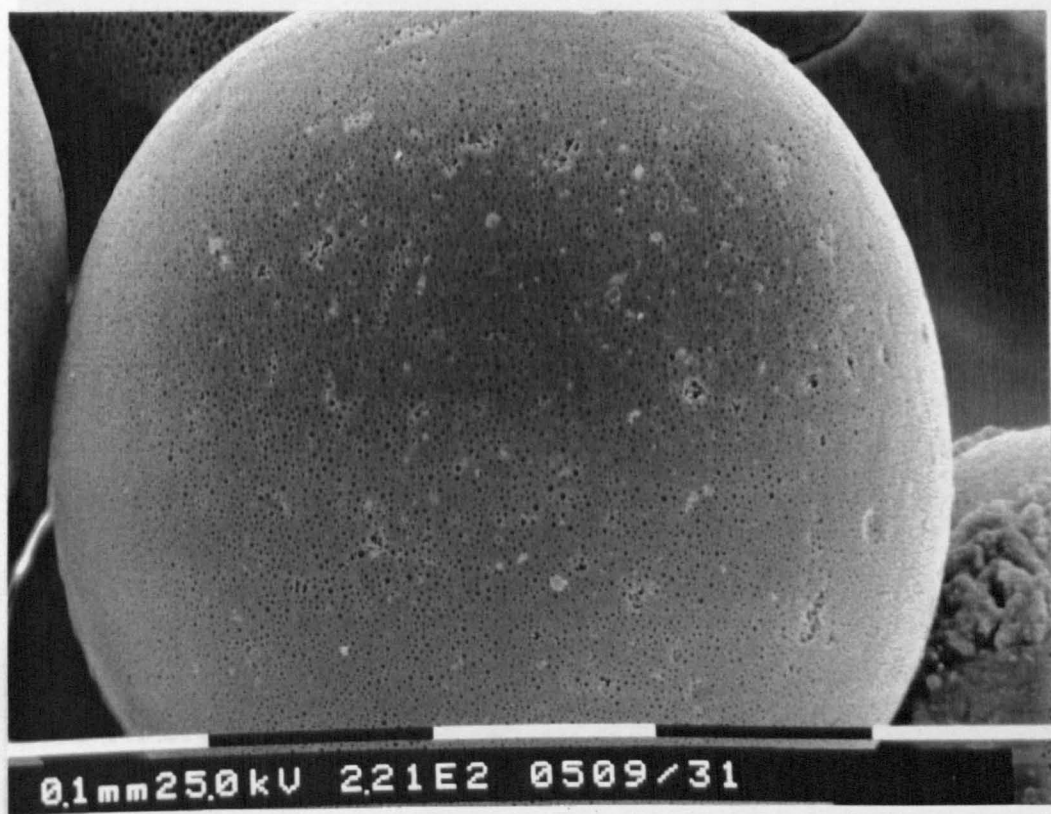
The honeycombed internal structure still appeared to be intact in the irradiated microspheres (figures 8.7c and d). Figure 8.7d also emphasizes the bumpy microsphere surface.

The softened appearance of the irradiated microspheres is probably a result of the glass transition temperature of Eudragit RS (42 °C)(Jones et al., 1991) being exceeded during irradiation.

Figure 8.6. Electron micrographs of surface of Eudragit RS:sulphasalazine microspheres.

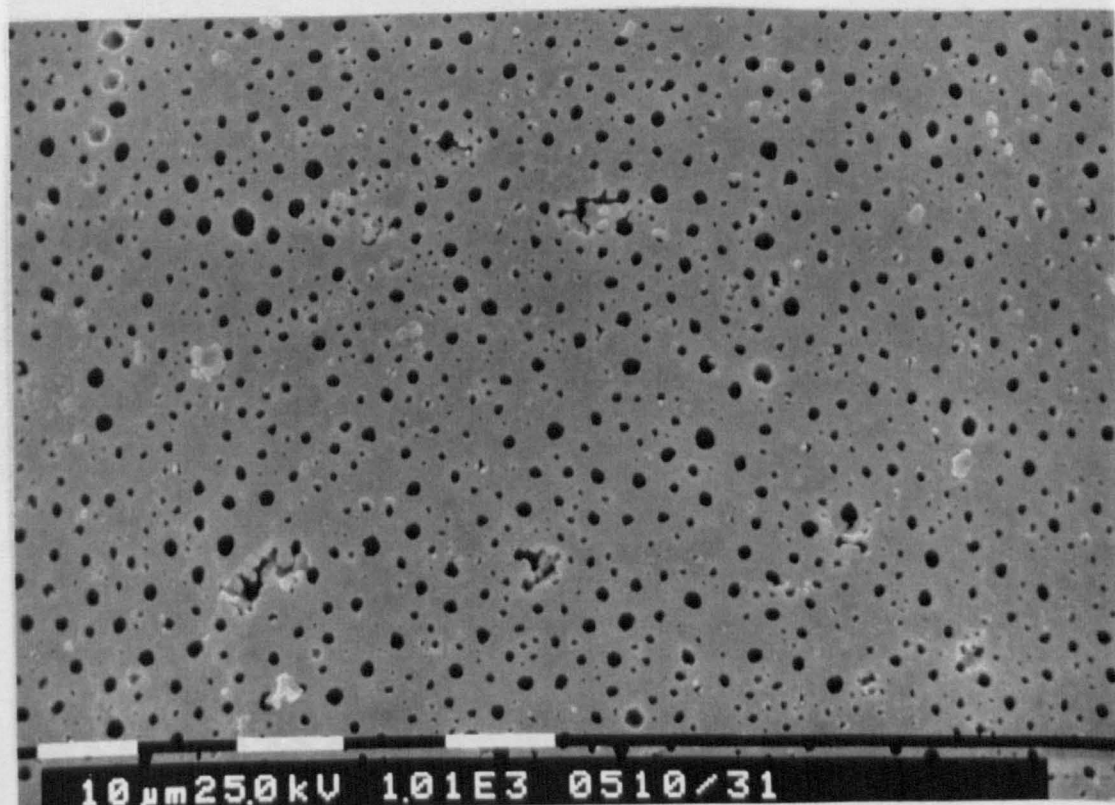
c) Irradiated microsphere (x220).

a) Non-irradiated microsphere (magnification x220).

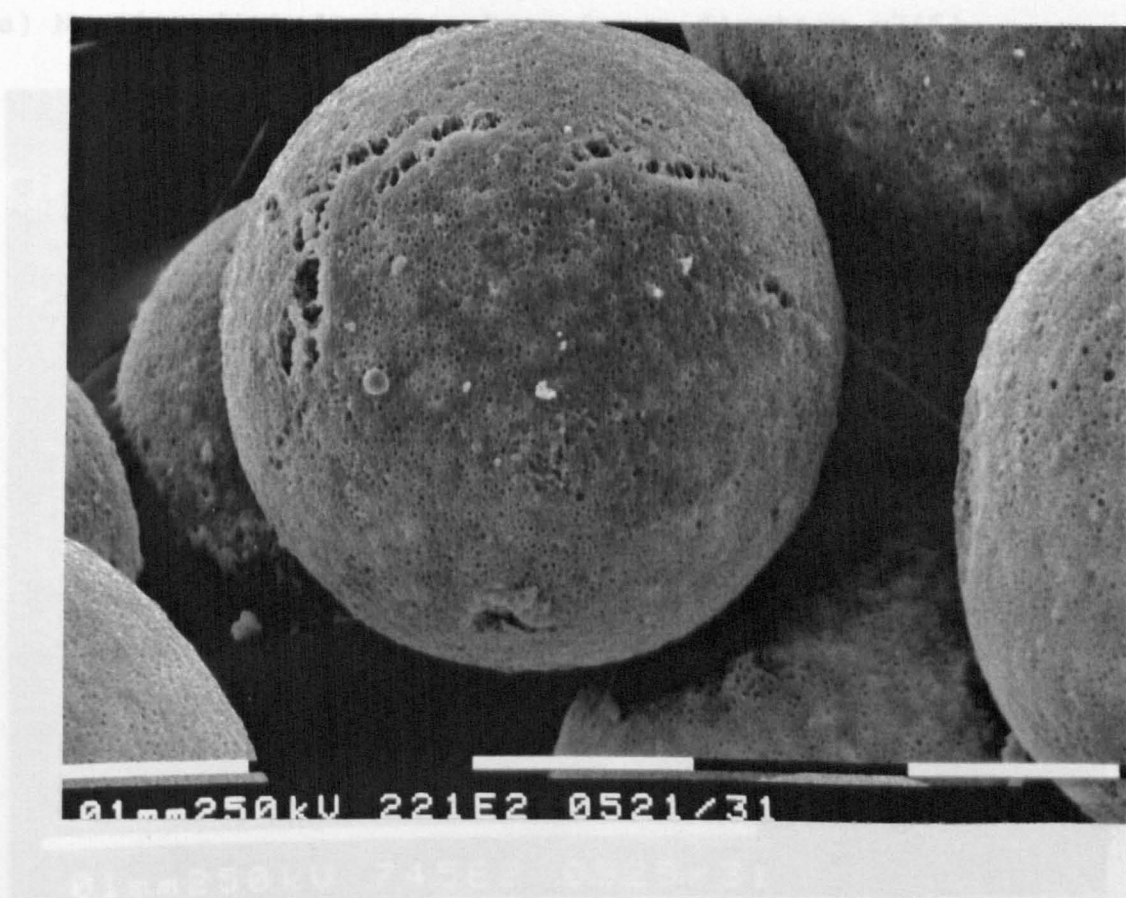


d) Irradiated microsphere (x1000).

b) Non-irradiated microsphere (x1000).



c) Irradiated microsphere (x220).



d) Irradiated microsphere (x1000).

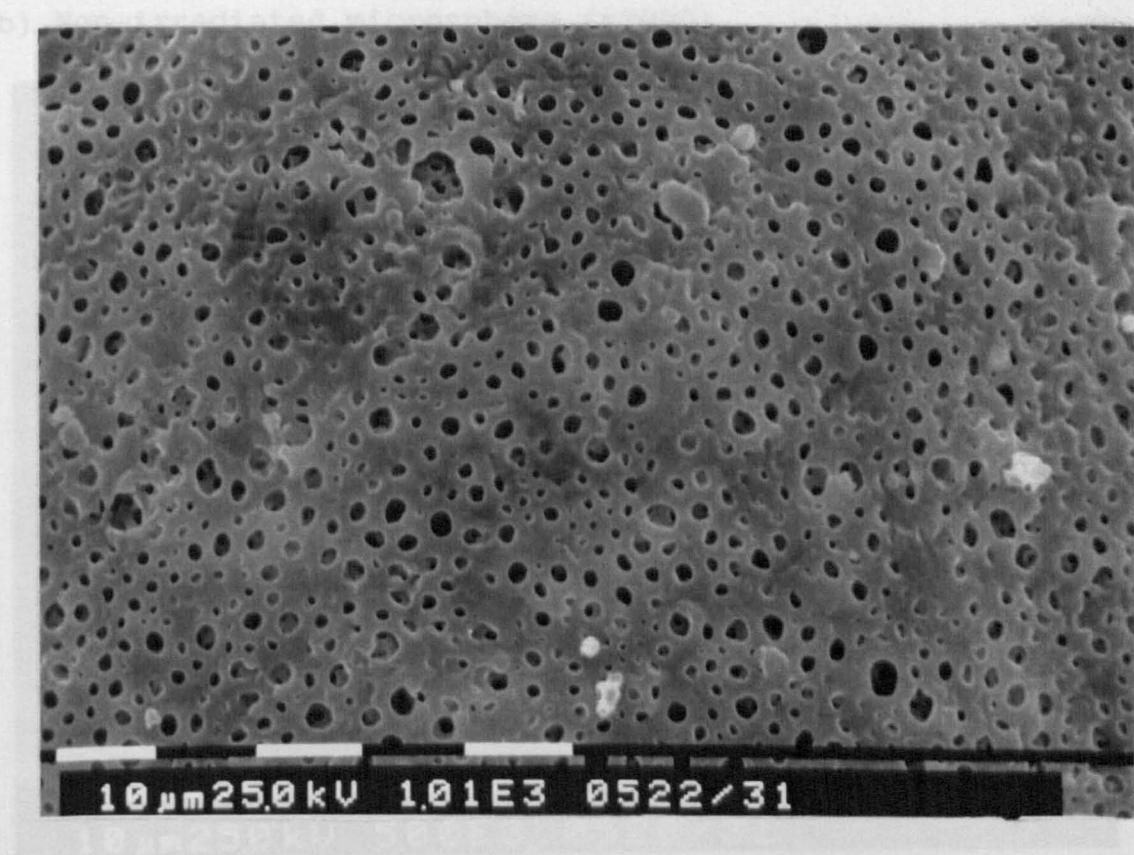


Figure 8.7. Electron micrographs of internal structure of Eudragit RS:sulphasalazine microspheres.

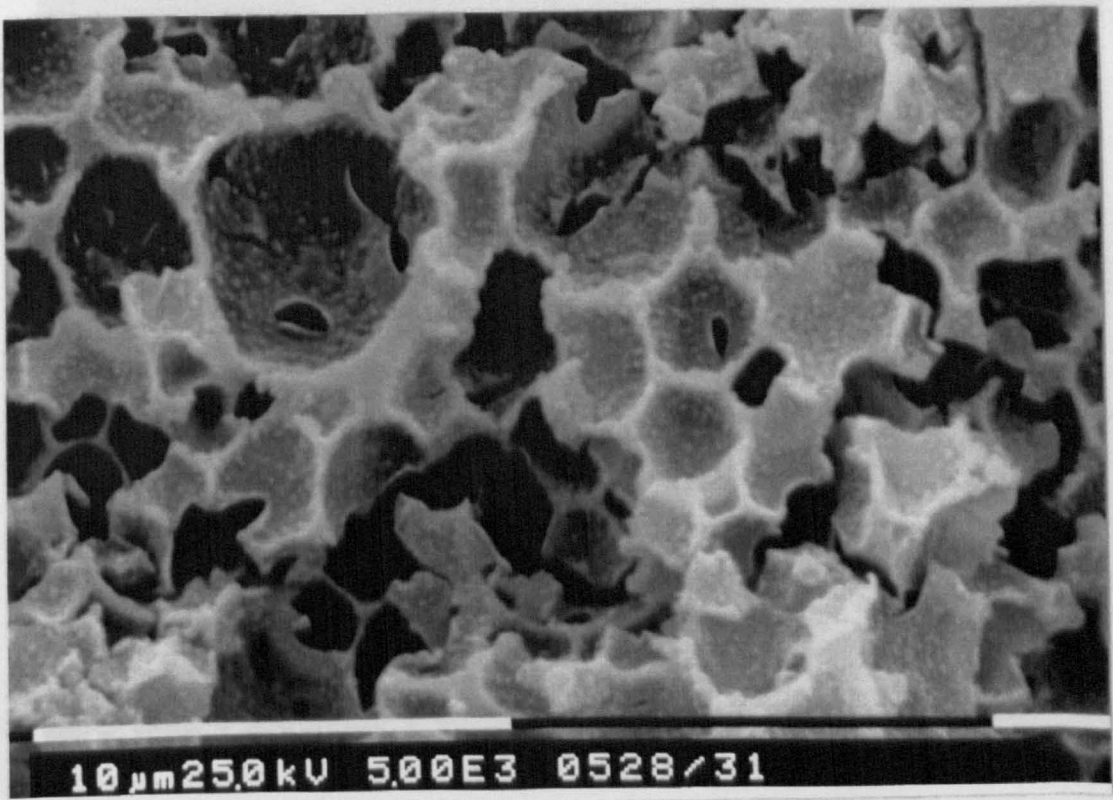
c) Irradiated microsphere (x745).

a) Non-irradiated microsphere (magnification x745).

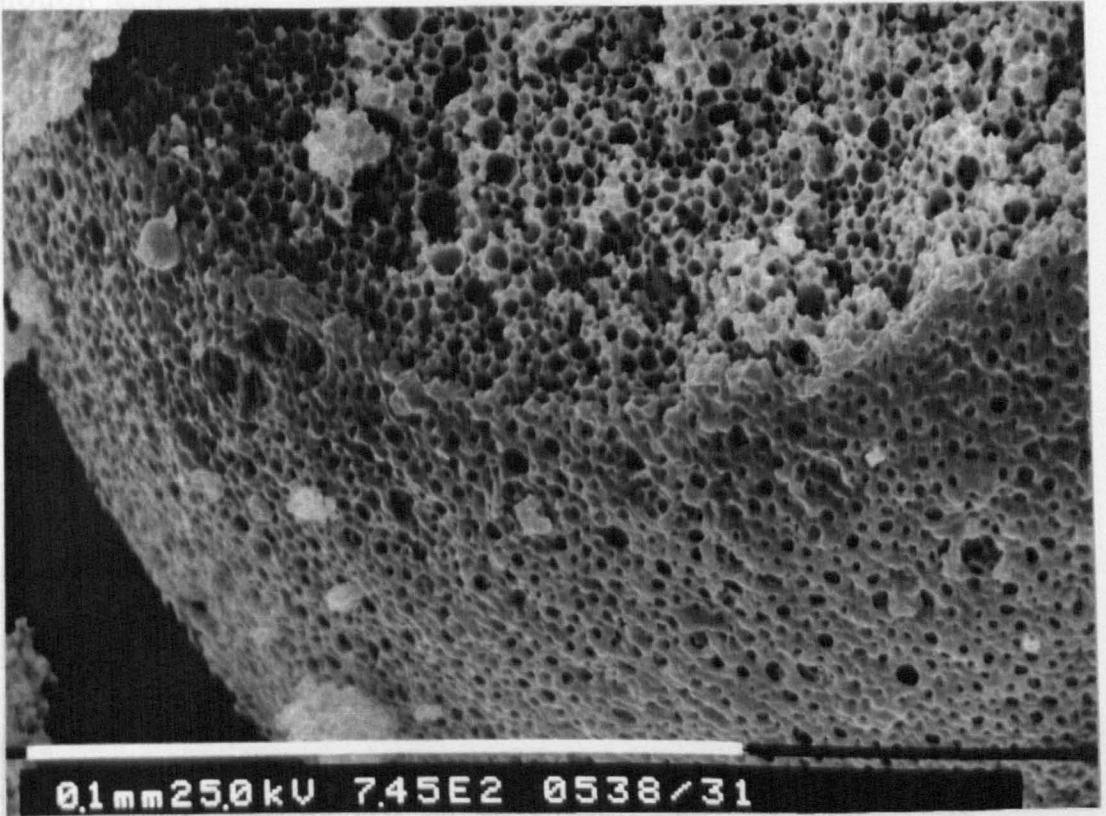


d) Irradiated microsphere (x5000).

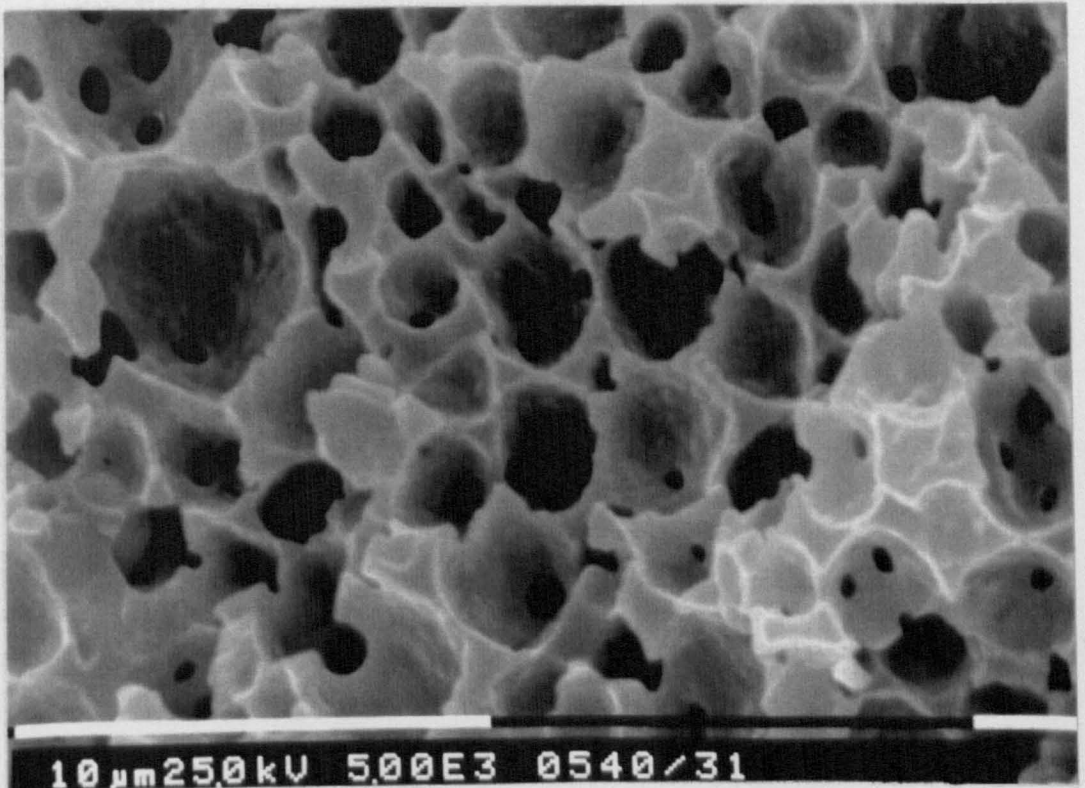
b) Non-irradiated microsphere (x5000).



c) Irradiated microsphere (x745).



d) Irradiated microsphere (x5000).



Although electron microscopy revealed that the irradiation process had clear effects on the physical structure of the microspheres, how these might have affected the rate of drug release is unclear.

8.3. INCORPORATION OF SAMARIUM OXIDE INTO EUDRAGIT RS-SULPHAPYRIDINE MICROSPHERES

8.3.1. EXPERIMENTAL

8.3.1.1. Microsphere production

To 3 g of Eudragit RS dissolved in 30 ml of dichloromethane was added 1.5 g of SP (gift from Rhône-Poulenc) and 0 mg or 67.5 mg of Sm_2O_3 . Being insoluble in the dichloromethane, SP and Sm_2O_3 formed a suspension. As for the SASP microspheres, dispersion of Sm_2O_3 was aided by sonication. This mixture was emulsified into 150 ml of 0.05% aqueous Tween 20 solution (overhead stirrer, 250 rpm). The production process was completed as described in section 8.2.1.2.A. Three batches were produced containing no Sm_2O_3 and three batches were produced containing 67.5 mg of Sm_2O_3 (1.5% w/w).

8.3.1.2. Microsphere size and density

Following drying, the weight of microspheres produced was recorded and the fraction in three size ranges determined by sieving: <250 μm , 250-500 μm and >500 μm .

Microsphere tap density was measured. A known quantity of microspheres was poured into a 10 ml glass measuring cylinder. The cylinder was lightly tapped twenty times and the volume of microspheres measured. The tap density was calculated by dividing the microsphere mass by its volume.

8.3.1.3. Sm_2O_3 content

Measured by XRF as described in section 8.2.1.2.B.

8.3.1.4. SP content

To assay for drug content, an accurately weighed quantity of microspheres estimated to contain 3-5 mg of SP was placed into a 100 ml volumetric flask. The polymer matrix was dissolved in 5 ml of methanol, followed by making to

volume with 0.05 N sodium hydroxide solution. 25 ml of this solution was further diluted to 100 ml with the 0.05 N NaOH, filtered (0.65 μm membrane filter, Whatman) and the UV absorbance measured (247 nm). SP concentrations were calculated with reference to a calibration curve of SP in 0.05 N NaOH.

8.3.1.5. Drug release rate

See section 8.2.1.2.D.

8.3.1.6. Electron microscopy

See section 8.2.1.2.I.

8.3.1.7. Effects of irradiation

A 9 g batch of Eudragit RS microspheres was produced containing theoretical SP and Sm_2O_3 contents of 33.3% w/w and 1% w/w respectively.

To establish whether a shorter period of irradiation would minimise damage to the microspheres, a sample was irradiated at a neutron flux of $10^{12} \text{ n cm}^{-2} \text{ s}^{-1}$ for 15 minutes as described in section 8.2.1.2.E.

The radiation stability of SP was assessed by extraction (section 8.3.1.4) followed by HPLC analysis. The HPLC equipment described in section 8.2.1.2.G was employed but with a mobile phase of pH 6 phosphate buffer containing 30% v/v methanol at a flow rate of 1 ml/min.

The drug release rate was measured for irradiated and non-irradiated microspheres.

In addition the loss of radioactivity from the irradiated microspheres was assessed by the technique described in section 8.2.1.2.F.

8.3.2. RESULTS AND DISCUSSION

8.3.2.1. Microsphere characterisation

Table 8.7 lists formulation details of the Eudragit RS-SP microspheres. There was little difference in yield between the two sets of samples. However, the tap density of the microspheres containing Sm_2O_3 was 30% higher than for the Sm_2O_3 -free samples. Differences in density were also apparent from handling the samples. Whereas the Sm_2O_3 -free samples were brittle and easily powdered between the fingers, for the samples containing Sm_2O_3 considerably more force was needed to break the microspheres.

The presence of Sm_2O_3 also appeared to affect microsphere SP content; The drug content of the samples containing Sm_2O_3 ($33.6 \pm 0.8\%$) was consistently higher than for those without ($31.3 \pm 0.3\%$).

There were also clear differences in the microsphere size distributions (figure 8.8). For microspheres containing Sm_2O_3 , the proportion $>500 \mu\text{m}$ was reduced compared to the Sm_2O_3 -free samples, with an increase in the proportion of smaller microspheres.

8.3.2.2. Drug release rate

Figure 8.9 shows the drug release profiles of the two sets of microsphere samples. The incorporation of Sm_2O_3 appeared to dramatically suppress the rate of drug release. For the samples containing no Sm_2O_3 , 54% of the encapsulated drug had been released after 6 hours, whereas in the same period of time, just 28% of encapsulated drug had been released from the samples containing Sm_2O_3 . The suppressed drug release rate of the latter samples may in part have been related to their higher density.

Table 8.7. Eudragit RS:sulphapyridine microsphere formulation details.

Samarium oxide content (%w/w)	Microsphere yield (g)	Microsphere tap density (g/ml)	Sulphapyridine content (%w/w)
0	3.7±0.2	0.26±0.01	31.3±0.3
1.15±0.8	3.5±0.3	0.34±0.02	33.6±0.8

Figure 8.8. Effects of samarium oxide incorporation on microsphere size distribution

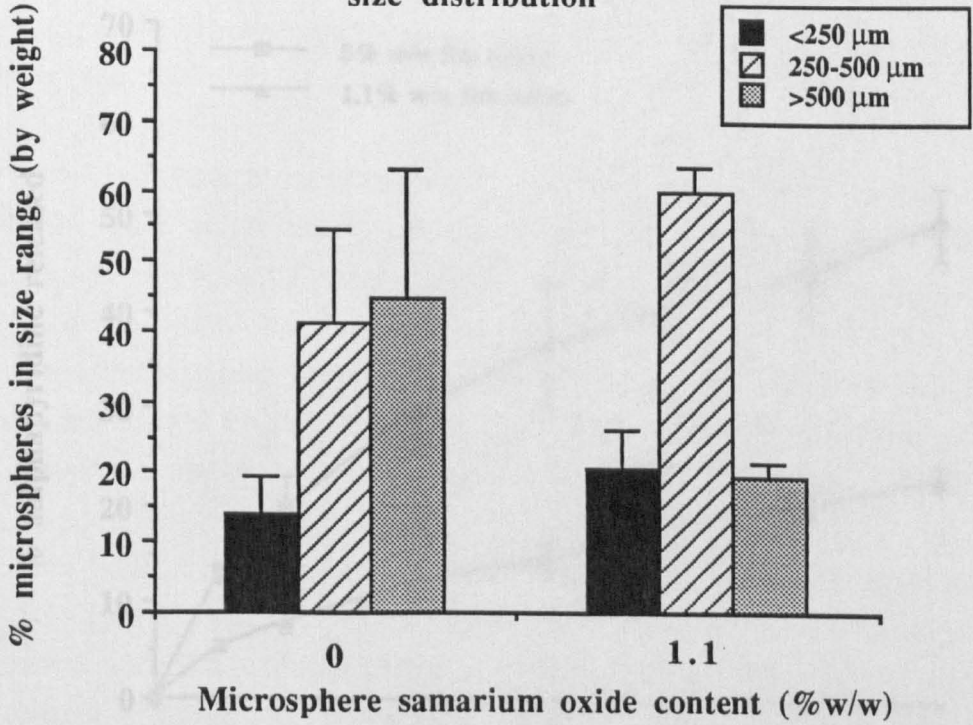
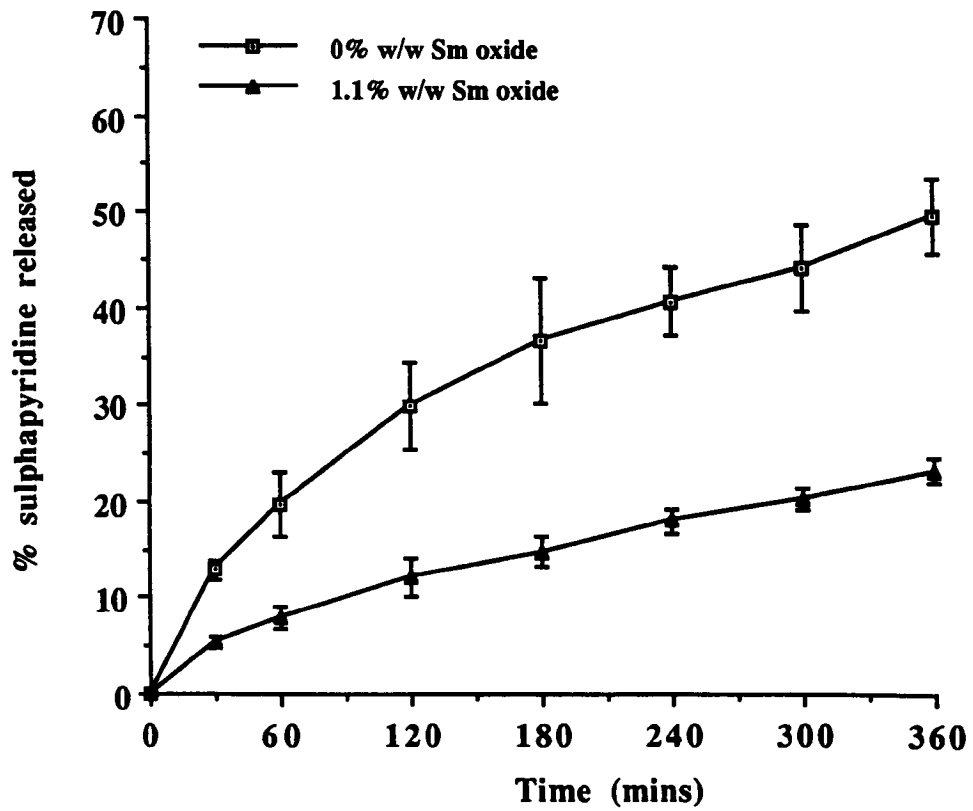


Figure 8.9. Effect of samarium oxide incorporation on microsphere drug release rate



8.3.2.3. Electron microscopy

It was clear that Sm_2O_3 was far from inert when incorporated into Eudragit RS-SP microspheres and appeared to be able to exert marked effects on their physical properties at only low concentrations. It was considered that these effects might have been a result of the accumulation of Sm_2O_3 at the organic:aqueous interface of the drug-polymer-solvent droplets during microsphere formation.

Surface electron micrographs of the microspheres produced without and with Sm_2O_3 are shown in figures 8.10a)-b) and 8.11a)-b) respectively. The Sm_2O_3 -free samples contained many large surface holes (8.10a) which were absent in the sample containing Sm_2O_3 (8.11a). Higher magnification views revealed that the size and number of pores was greater in the Sm_2O_3 -free samples (figure 8.10b vs. figure 8.11b).

The internal structure of the two sets of microspheres did not differ greatly. Both sets consisted of a spongy drug-polymer matrix containing a number of large cavities. The size and number of cavities appeared to be greater in the Sm_2O_3 -free microspheres (figure 8.12a) compared to the Sm_2O_3 -containing microspheres (figure 8.12b), which was consistent with the differences in density.

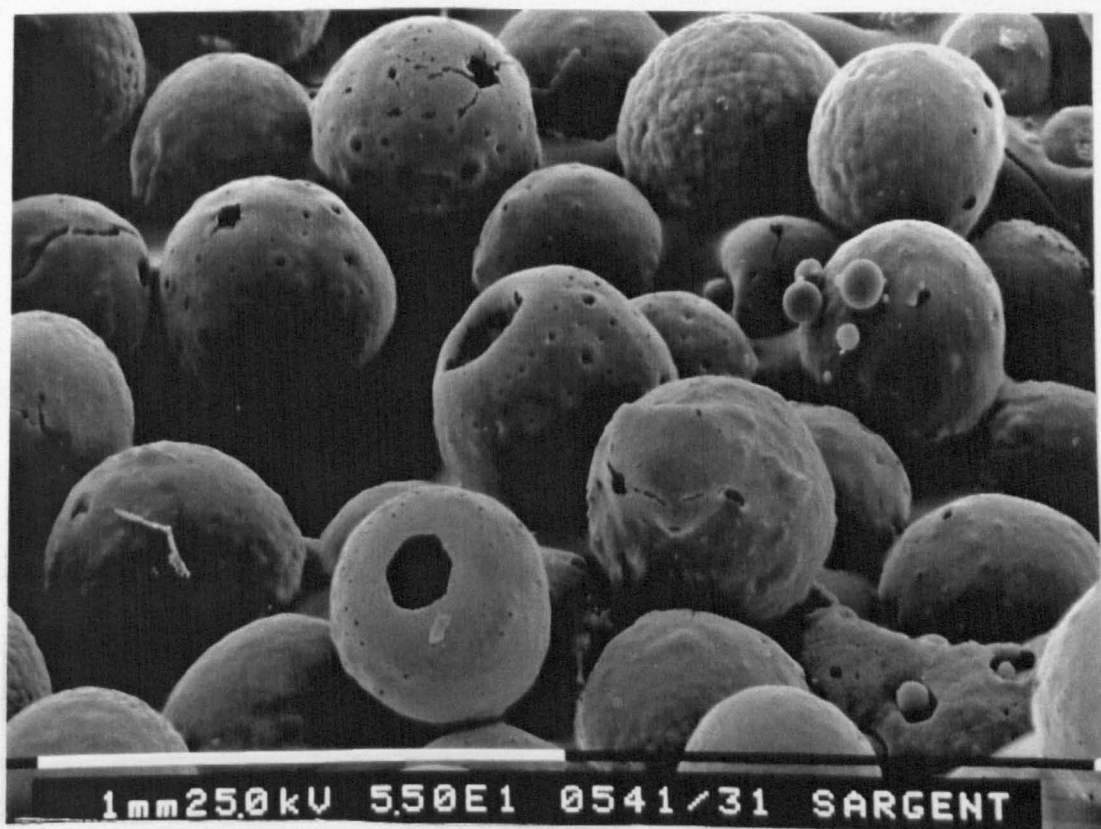
8.3.2.4. Effects of irradiation

The 9 g batch of Eudragit RS-SP microspheres had an assayed drug content of 35.0% w/w. This represents an incorporation efficiency of 105% and again points towards Sm_2O_3 having effects on microsphere drug content. The assayed Sm_2O_3 content was 0.7% (70% incorporation efficiency).

The SP content in the irradiated samples was identical to the non-irradiated, and no additional peaks were evident, indicating that the drug was stable to neutron irradiation.

Figure 8.10. Electron micrographs of Eudragit RS:sulphapyridine microspheres containing no samarium oxide.

a) View of microsphere population (magnification x55).



b) Microsphere surface (x1000).

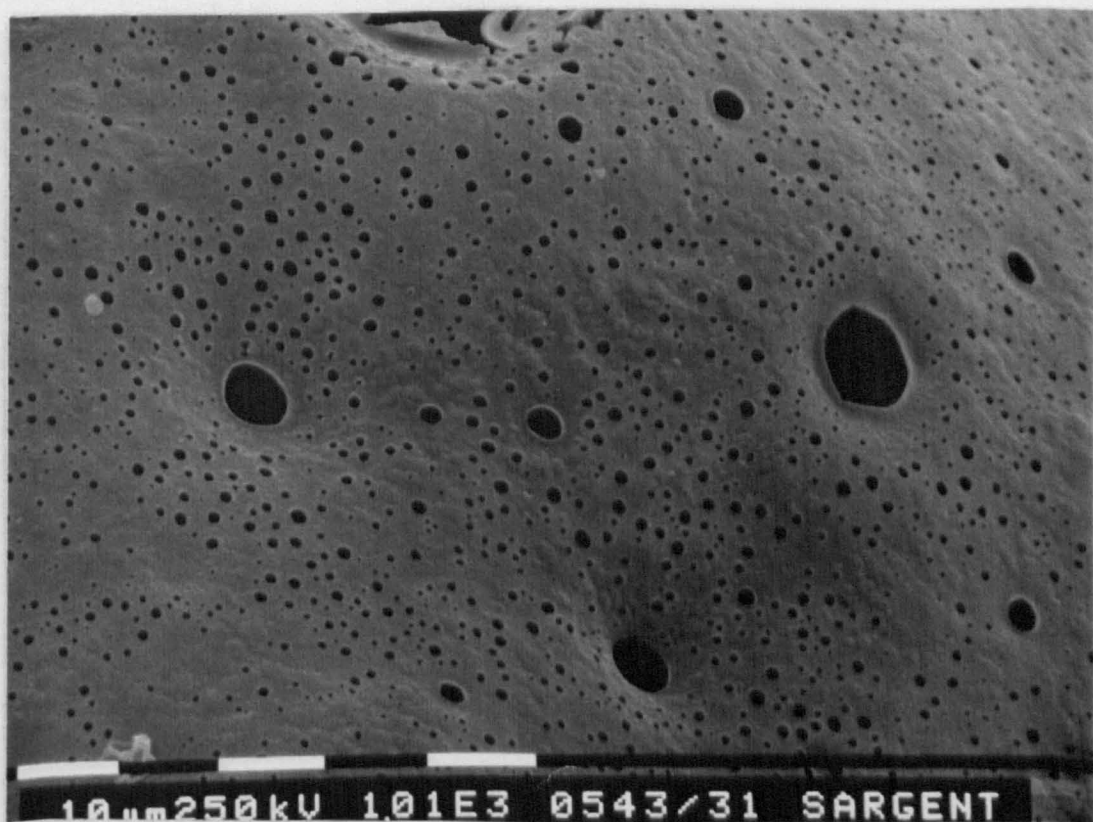
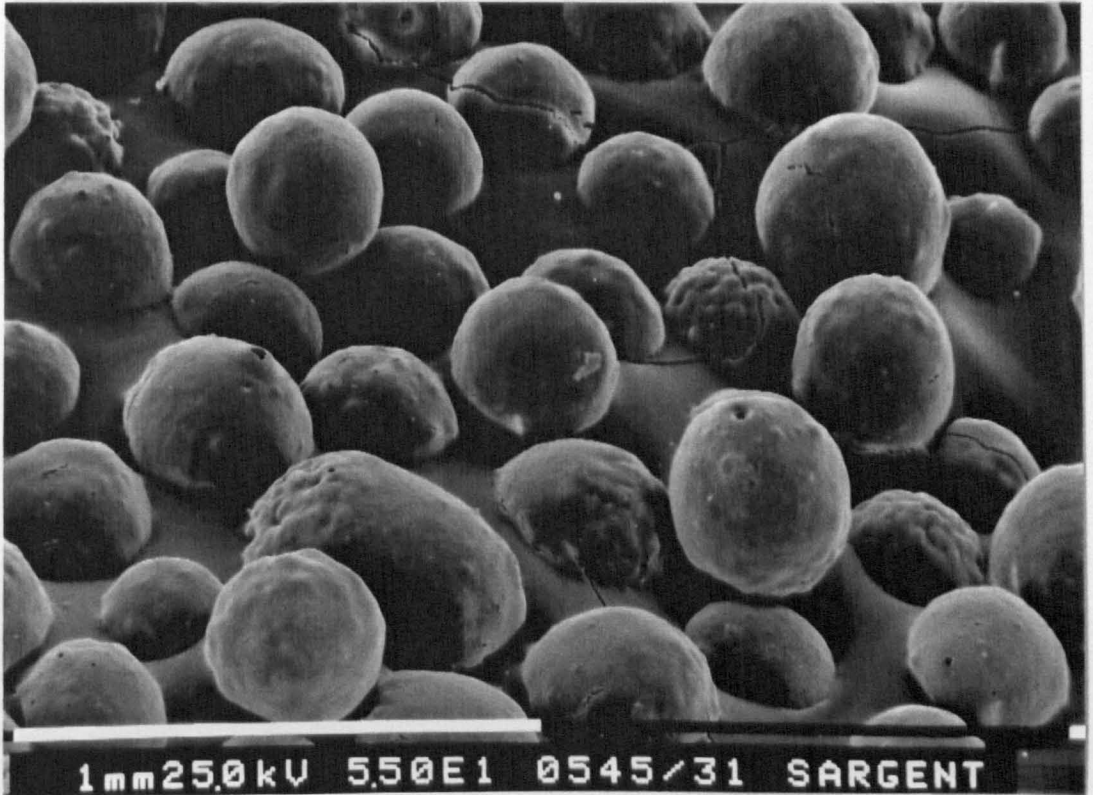


Figure 8.11. Electron micrographs of Eudragit RS:sulphapyridine microspheres containing 1.15% w/w samarium oxide.

- a) View of microsphere population (magnification x55).



- b) Microsphere surface (x1000).

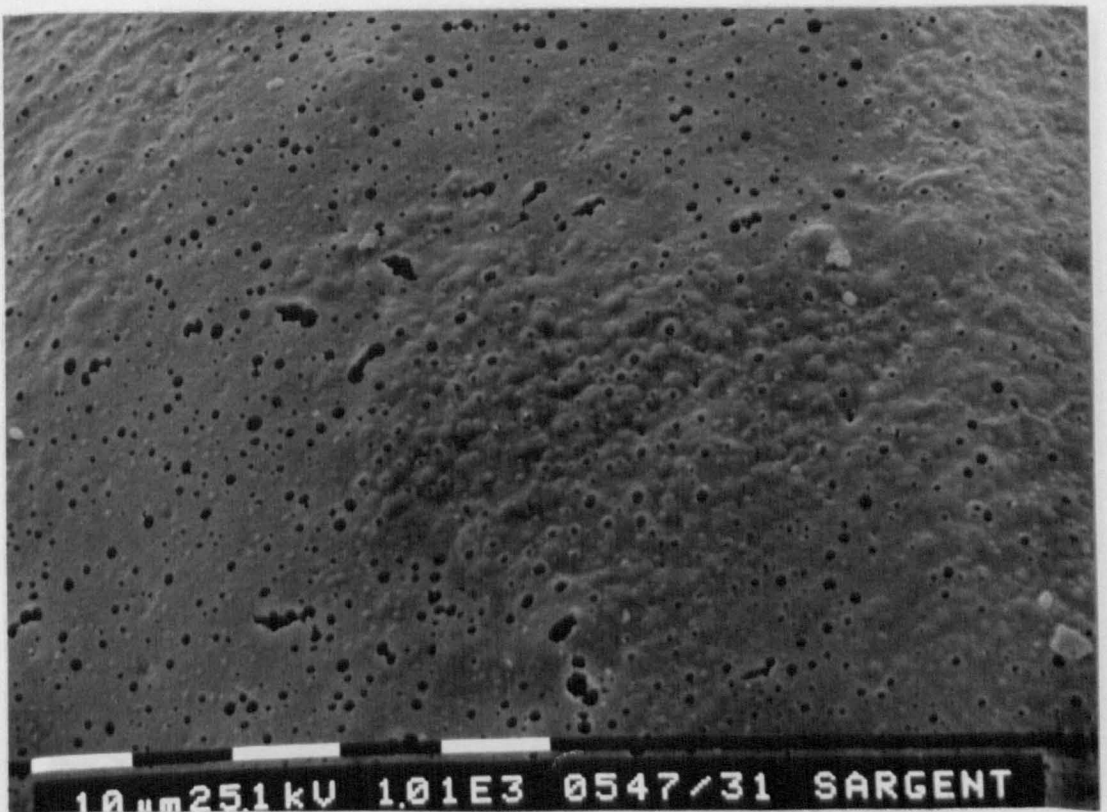
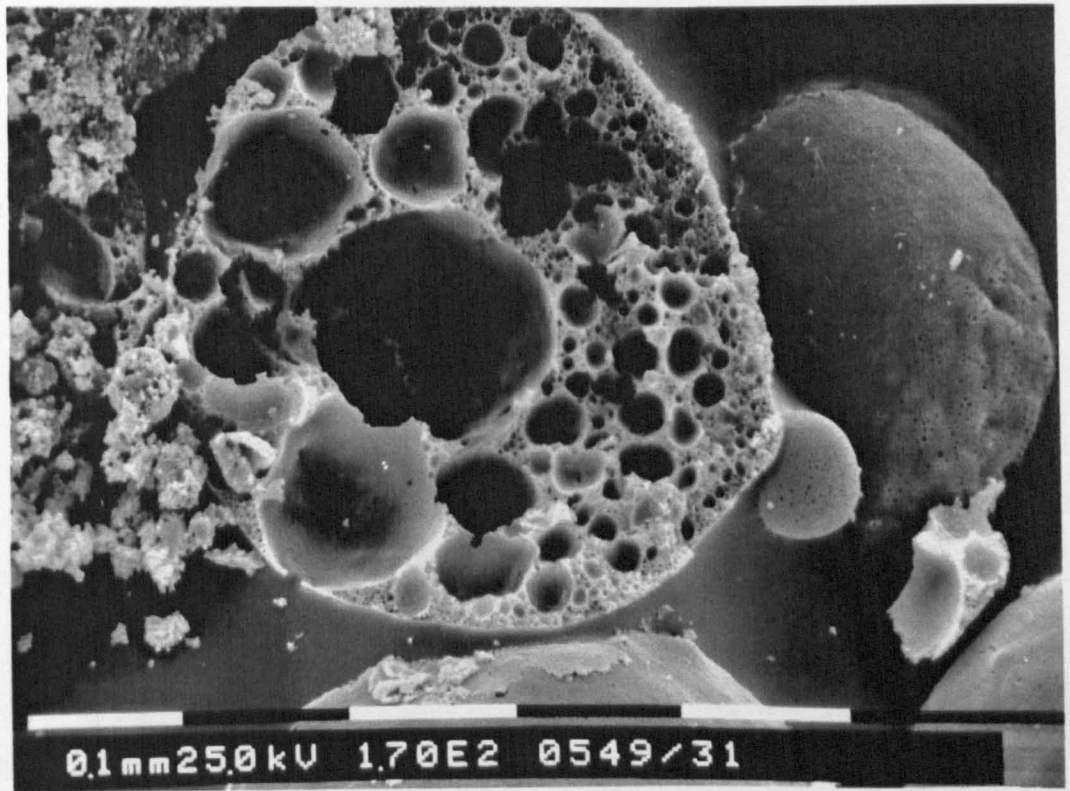


Figure 8.12. Electron micrographs of interior of Eudragit RS:sulphapyridine microspheres.

a) Containing no samarium oxide (magnification x170).



b) Containing 1.15% w/w samarium oxide (x170).

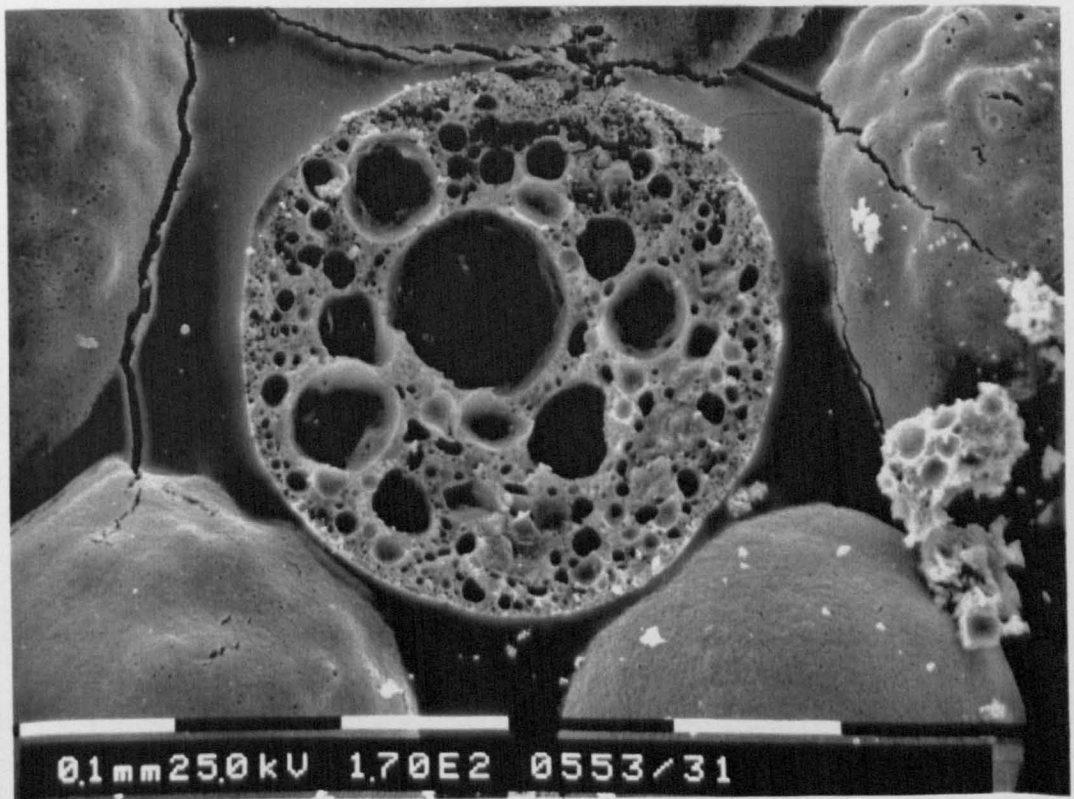
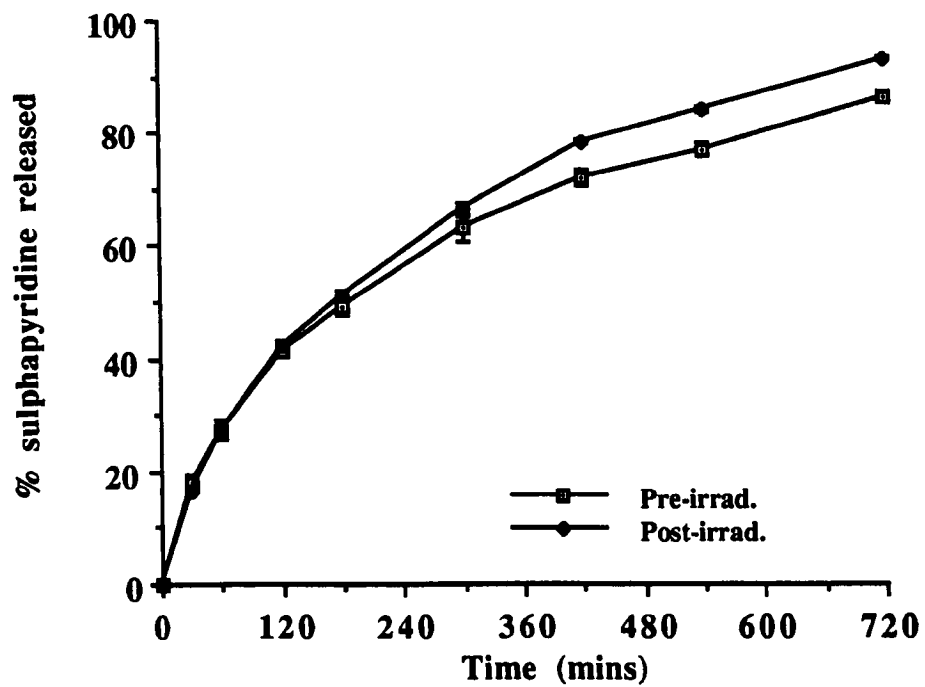


Figure 8.13. Effect of 15 minute irradiation on sulphapyridine release rate



Following a 15 minute irradiation, the rate of drug release from the microspheres was slightly increased, suggesting minor radiation damage (figure 8.13).

No leaching of radioactivity from the irradiated microspheres could be detected during in vitro dissolution.

8.4. CONCLUSIONS

The work described in this chapter has demonstrated that the incorporation of Sm_2O_3 followed by neutron irradiation is a viable method for radiolabelling microspheres produced by the solvent evaporation process.

Sm_2O_3 at concentrations up to 0.8% w/w had no apparent effect on the physical properties of Eudragit RS-SASP microspheres. However, following irradiation, physical changes were apparent both in Sm_2O_3 -containing and in Sm_2O_3 -free microspheres and a marked enhancement in the rate of drug release was seen. The physical changes observed as a result of irradiation were a softened/melted appearance to the microsphere surface, and possibly a small increase in polymer molecular weight. The mechanism responsible for the enhancement in drug release is unclear, and would require further investigation.

When incorporated into Eudragit RS-SP microspheres, Sm_2O_3 had marked effects on microsphere properties at a concentration not too dissimilar to that used in the SASP microspheres. Incorporation of 1.15 % w/w Sm_2O_3 caused an increase in microsphere density, a decrease in microsphere size, an increase in drug loading and a 50% reduction in the rate of drug release. It is probable that Sm_2O_3 was exerting these effects through accumulation at the microsphere surface, since electron microscopy revealed that the surface porosity was higher in the microspheres containing no Sm_2O_3 .

Irradiation of a sample of Eudragit RS-SP microspheres for a 15 minute period resulted in only a minor enhancement in drug release.

Following the finding that Sm_2O_3 -incorporation could affect microsphere properties, a single batch of Eudragit RS-SASP microspheres was produced containing 4% w/w Sm_2O_3 . The microsphere yield was lower, the density was increased, and only 11% of the encapsulated drug was released after 360 minutes. Thus the concentration of Sm_2O_3 at which changes in microsphere physical properties occur appears to be dependent upon the drug being encapsulated.

In conclusion, this work has emphasized the need for achieving a careful balance between the irradiation time and the level of incorporated Sm_2O_3 when developing a neutron activation technique for radiolabelling microspheres produced by solvent evaporation. Whereas the rate of drug release may be increased by long periods of irradiation, it may be suppressed by incorporating high levels of Sm_2O_3 . There could be clear benefits in using enriched material (95%+ ^{152}Sm) for this work, since the amount of radiolabel incorporated would effectively be reduced by almost 75%, and as a consequence, Sm_2O_3 -induced effects on microsphere physical properties would be minimised.

CHAPTER 9.

A BIOPHARMACEUTICAL EVALUATION OF EUDRAGIT RS-
SULPHAPYRIDINE MICROSPHERES IN THE HUMAN COLON.

9.1. INTRODUCTION

Investigations in the previous chapter had established that the incorporation of Sm_2O_3 followed by short exposure to neutron radiation was a suitable method for radiolabelling Eudragit RS microspheres. Although Sm_2O_3 had marked effects on the physical properties of Eudragit RS-SP microspheres, this was not considered to be a problem for the study described in this chapter, since the chosen manufacturing conditions and the level of incorporated label resulted in microspheres with a suitable drug release rate.

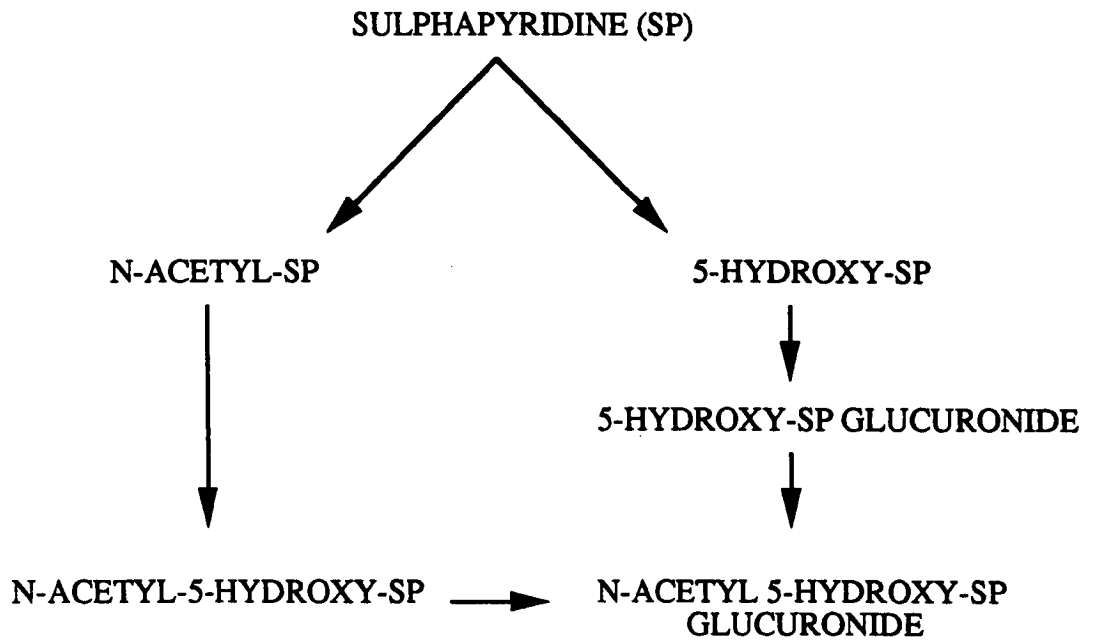
As discussed in the previous chapter, SP was the logical successor to SASP as a model drug for colon absorption studies. SP has now largely passed out of use as an antibiotic as a result of the introduction of newer treatments which are equally effective but with a lower incidence of side-effects. Consequently, most of the published pharmacokinetic data for SP has been generated from studies investigating the in vivo fate of SASP.

SP appears to be well absorbed from the colon and an absolute bioavailability of 70% has been quoted following SASP administration (Bieck, 1989).

Figure 9.1 shows the metabolic fate of SP. Elimination of SP is primarily by hepatic metabolism and the rate is dependent upon acetylator status. About 60% of caucasians are slow acetylators, and side-effects from SASP/SP are 2-3 times more frequent in this group. The elimination half-life is about 6 h in fast-acetylators and 14 h in slow acetylators (Klotz, 1985). In plasma samples from patients taking SASP, only SP and acetyl-SP (AcSP) could be detected in appreciable quantities by HPLC analysis (Astbury and Dixon, 1987; Fischer and Klotz, 1978).

The study undertaken in this chapter aimed to address two

Figure 9.1. Metabolic fate of sulphapyridine
(from Klotz, 1985).



main issues. The first was to establish the colonic transit rate of radiolabelled Eudragit RS-SP microspheres by carrying out scintigraphic experiments analogous to those in Chapter 7.

The second aim was to compare the colonic absorption characteristics of microencapsulated and unencapsulated SP. This would provide information on the suitability of the ascending colon as a target for sustained-release microparticulate dosage forms and might reveal in vitro/in vivo differences in dissolution performance.

Measurement of plasma SP levels would also reflect the exposure of the colonic mucosa to drug, an important measure of the suitability of microsphere drug-delivery systems for providing drug for local topical action.

It was considered that a microsphere formulation that released most of its encapsulated drug over a period of 12 hours would be most appropriate, taking into consideration the ascending colon residence times established in chapter 7. With release over longer periods, considerable amounts of drug would be released into areas of the colon beyond the hepatic flexure where the absorptive capacity may be more limited.

9.2. EXPERIMENTAL

9.2.1. Materials

As for chapter 8, but in addition, sulphadimidine sodium (Rhône-Poulenc), acetic anhydride (Rhône-Poulenc), Amberlite IRA410 resin, 000-sized hard gelatin capsules, "Polymer A", sodium pertechnetate solution.

9.2.2. Methods

9.2.2.1. Microsphere production

Two 15 g microsphere batches were produced for the clinical

investigation. For each batch, 10 g of Eudragit RS was dissolved in 100 ml of dichloromethane in a glass bottle. When the polymer had dissolved, 225 mg of Sm_2O_3 was added to form a suspension. Dispersion of Sm_2O_3 was aided by sonication of the bottle and contents for 10 minutes. Finally 5 g of SP powder was added to the bottle and dispersed by shaking. This mixture was immediately poured into 500 ml of 0.1% w/v aqueous Tween 20 solution and stirred at 250 rpm. Solvent evaporation took approximately 10 hours for each batch. Following filtration, washing and freeze-drying, a 120-500 μm sieve fraction was collected and weighed.

The collected sieve fractions from the two microsphere batches were placed in a single bottle and mixed together by gentle rotation.

9.2.2.2. Microsphere characterisation

Microsphere drug content, Sm_2O_3 content, drug release characteristics and electron micrographs were obtained using the techniques described in chapter 8.

9.2.2.3. Microsphere irradiation

1.5 g of the Eudragit RS-SP microspheres were placed into each of two polypropylene tubes. The tubes containing the microspheres were irradiated at the Universities Research Reactor, Risley for 15 minutes at a neutron flux of $10^{12} \text{ n cm}^{-2} \text{ s}^{-1}$.

Microsphere in vitro drug release characteristics were determined again after irradiation.

9.2.2.4. In vivo investigation

A. Dosage form assembly

Two types of dosage form were assembled for a two part in vivo investigation.

i) Into a 000-sized hard gelatin capsule was placed 500 mg of SP powder and 100 mg of finely-ground Amberlite IRA410 ion-exchange resin labelled with ^{99m}Tc as described in chapter 6. The capsule was coated by dipping three times into a solution of 15% w/v "Polymer A" in acetone (see chapter 6).

ii) 130 mg of irradiated and 320 mg of non-irradiated Eudragit RS-SP microspheres were placed into a 000-sized capsule. The capsule was coated as described above. Only part of the microsphere dose was radiolabelled to ensure that the radioactivity was not too diffuse following capsule disintegration. If the same amount of activity had been divided between all of the microspheres, the quality of scintigraphic images may have been unsatisfactory.

B. Study design

Six healthy male volunteers (age 23-29 years) were recruited for the biopharmaceutical study to evaluate SP administered as a powder and as sustained-release microspheres. The study received the prior approval of the Nottingham University Medical School ethical committee and was conducted in accordance with the Declaration of Helsinki Guidelines for Ethics in Research.

The investigation was carried out in two parts, separated by a period of two weeks.

On each occasion, subjects arrived at the study room at 7.30 am having fasted from 10 pm the previous evening. A forearm cannula was inserted to enable blood samples to be withdrawn during the study day and markers containing a small quantity of irradiated Sm_2O_3 powder were attached to the front and back over the right lobe of the liver to allow alignment during scintigraphic imaging. At approximately 8 am subjects were asked to swallow, with a glass of water, either one capsule containing SP powder or

three capsules containing SP microspheres. The former capsule contained 4 MBq of ^{99m}Tc whereas the latter three capsules contained a total of approximately 1.5 MBq of ^{153}Sm . The quantity of SP administered in each case was 500 mg.

Anterior and posterior scintigraphic images of 30 seconds duration were recorded at 30-60 minute intervals throughout the day as described previously (chapter 7). Once the capsules had left the stomach, subjects received breakfast and thereafter a set lunch, coffee/tea and biscuits, and dinner (chapter 7). Blood samples were withdrawn at 0 h and approximately 2, 4, 6, 8, 11, and 13 h post-dose and immediately placed into heparinised tubes to prevent clotting. Tubes were centrifuged for 15 minutes at 2000 rpm (MSE Centaur) and the plasma fraction removed and frozen at $-20\text{ }^{\circ}\text{C}$ for later analysis. Subjects returned for imaging (120 secs duration, microspheres only) and blood samples (by venipuncture) at 24 and 32 hours post-dose. Images were not recorded at 24 and 32 h for the drug-powder leg of the study due to the short half-life of the ^{99m}Tc -label.

C. Scintigraphic analysis

Stored scintigraphic images were analysed to determine the distribution of activity in the ICJ, ascending colon, transverse colon and descending colon/rectum using the methods outlined in chapter 7. This analysis enabled the residence time of 50% of the administered radioactivity in the ascending colon to be determined (MRT) and, for the microspheres only, the residual amount of activity remaining after 24 and 32 h.

Statistical comparisons between paired data (t-test) were undertaken using "Statworks" run on an Apple Macintosh computer.

D. Analysis of plasma samples

A number of HPLC methods for the analysis of SP and its metabolites have been reported (Astbury and Dixon, 1987; Fischer and Klotz, 1978; Shaw et al., 1983). For this study, a method was developed for the plasma assay of SP and its principal metabolite, AcSP. For assay development and generation of calibration graphs, AcSP was synthesized.

i) Synthesis of AcSP

1 g of SP was placed into a small glass beaker and approximately 1 g of acetic anhydride added. The top of the beaker was covered with foil, placed in a fume cupboard, and the contents stirred with a magnetic flea. After 1 hour, 50 ml of boiling water was added to the beaker to convert unreacted acetic anhydride into acetic acid and water. The beaker contents were cooled, the liquid removed by decantation and the sediment resuspended by adding distilled water. The beaker contents were then divided between two centrifuge tubes, spun down (2000 rpm/5 mins) and the liquid decanted off. Resuspension, centrifugation and decantation were repeated until the smell of acetic acid could no longer be detected. The sediment was then dried in an oven at 50 °C and stored in a desiccator.

ii) HPLC equipment

The following HPLC equipment was used for analysis of the plasma samples:

Knauer HPLC 64 pump (Knauer, Berlin, Germany), flow rate 1.2 ml/min.

Gilson 401/231 dilutor/autosampler (Gilson, Middleton, WI).
Hichrom Spherisorb ODS column (15 cm x 4.6 mm ID) fitted with a guard column (Upchurch).

Uvikon 720 LC detector (Kontron Instruments, Switzerland), 254 nm.

Spectra-Physics 4400 integrator.

Mobile phase: A solution of 6.8 g/L of potassium dihydrogen

phosphate in double distilled water was adjusted to pH 6.0 with 1N aqueous sodium hydroxide solution. The buffer solution was then vacuum filtered through a 0.1 μ m membrane filter (Whatman). Filtered buffer was added to methanol to produce a final methanol content of 20% v/v. Prior to use, the mobile phase was degassed by bubbling helium through for 10 minutes.

iii) Sample preparation

To 0.5 ml of plasma in an Eppendorf tube was added an equal volume of methanol containing 1.7 mg/100 ml sulphadimidine sodium as the internal standard. Addition of methanol resulted in protein precipitation. The tube was vortex mixed (Rotamixer), centrifuged at 13,000 rpm for 10 minutes (MSE Microcentaur), and the clear supernatant removed for HPLC analysis.

An injection volume of 20 μ L was used, and each plasma sample was analysed twice.

iv) Calibration samples

To 0.5 ml of a solution of 3.4 mg/100 ml sulphadimidine sodium in methanol was added 0.5 ml of methanol containing appropriate concentrations of SP and AcSP. 0.5 ml of this mixture was added to 0.5 ml of blank plasma and the clear supernatant prepared as above.

Calibration results were pooled and used to produce calibration graphs of peak area ratio (drug:internal standard) vs. concentration for SP and AcSP which in turn were used to calculate drug concentrations.

v) Data analysis

The areas under the concentration vs. time curve (AUC) and the first moment of concentration vs. time curve (AUMC) were calculated using a pharmacokinetic program (MK Model, Dr.N.Holford, Auckland University Medical School).

The SP elimination half-life was determined from the slope of the elimination phase on a graph of log[plasma concentration] vs time.

9.3. RESULTS

9.3.1. Microsphere characterisation

Physical properties of the microspheres are recorded in table 9.1.

The assayed SP content was considerably higher than expected at 37.2% w/w and represents an incorporation efficiency of 112%. It was also observed in chapter 8 that Sm_2O_3 appeared to increase the drug content of SP-Eudragit RS microspheres.

The in vitro rate of SP release from the microspheres before and after irradiation is shown in figure 9.2. The release rates were identical, and after 12 hours and 24 hours 75% and 93% of the encapsulated drug had been released respectively. The time for 50% of the drug to be released was approximately 5 hours.

SEM micrographs of non-irradiated and irradiated microspheres are shown in figures 9.3 and 9.4 respectively. The microspheres had a generally misshapen appearance (figures 9.3a and 9.4a). High magnification views of the surface appeared to show little difference between the two samples (figures 9.3b and 9.4b).

The radioactivity generated by the 15 minute irradiation was equivalent to 4.4 MBq/g of microspheres at the time of subject dosing (22 hours after irradiation).

Table 9.1. Details of microsphere formulation used for clinical investigation.

Samarium oxide content: 1.12%w/w (=74.7% incorporated).

Sulphapyridine content: 37.2%w/w (=112% incorporated).

Tap density: 0.35 g/ml.

Weight of microspheres, 120-500 μ m: 17.2g (57% by weight).

**Figure 9.2. Release rate of microspheres used for clinical study
pre- and post-irradiation.**

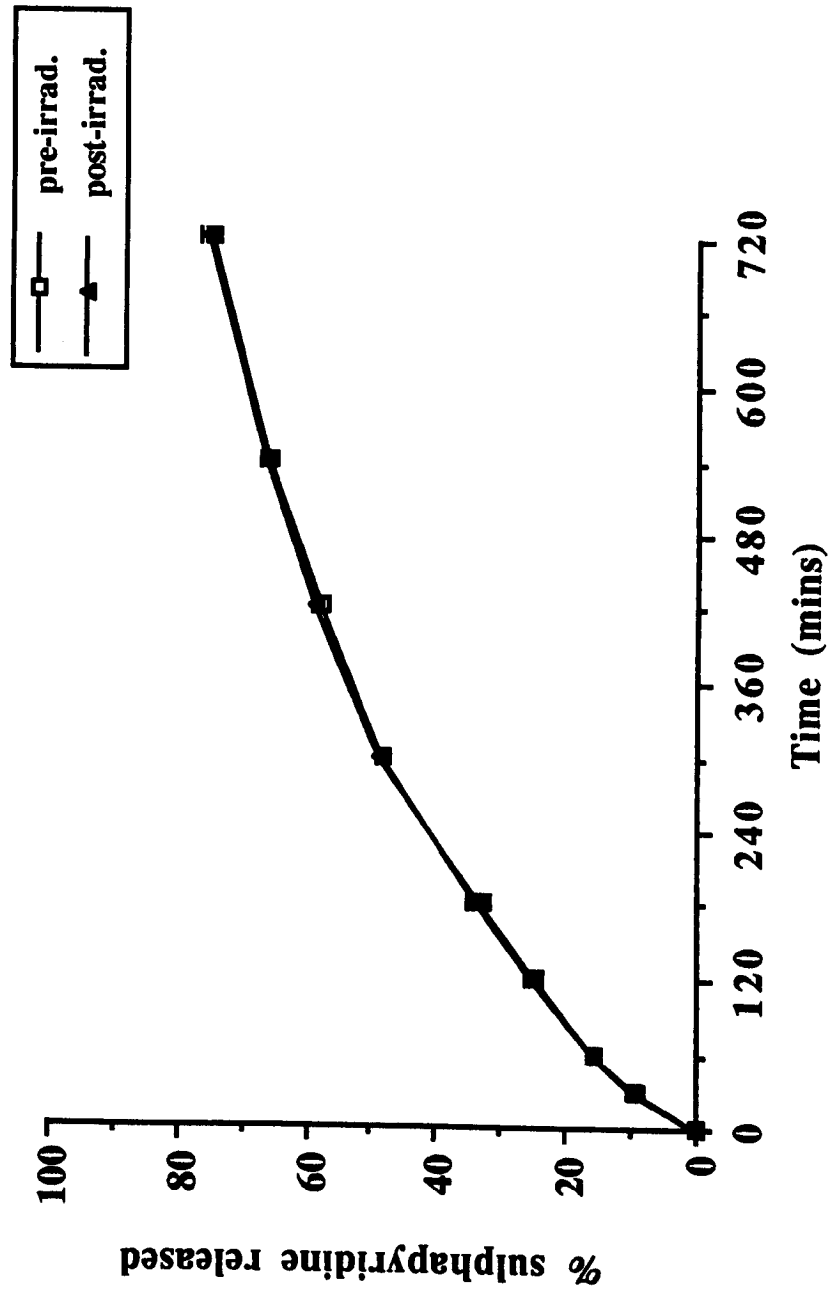
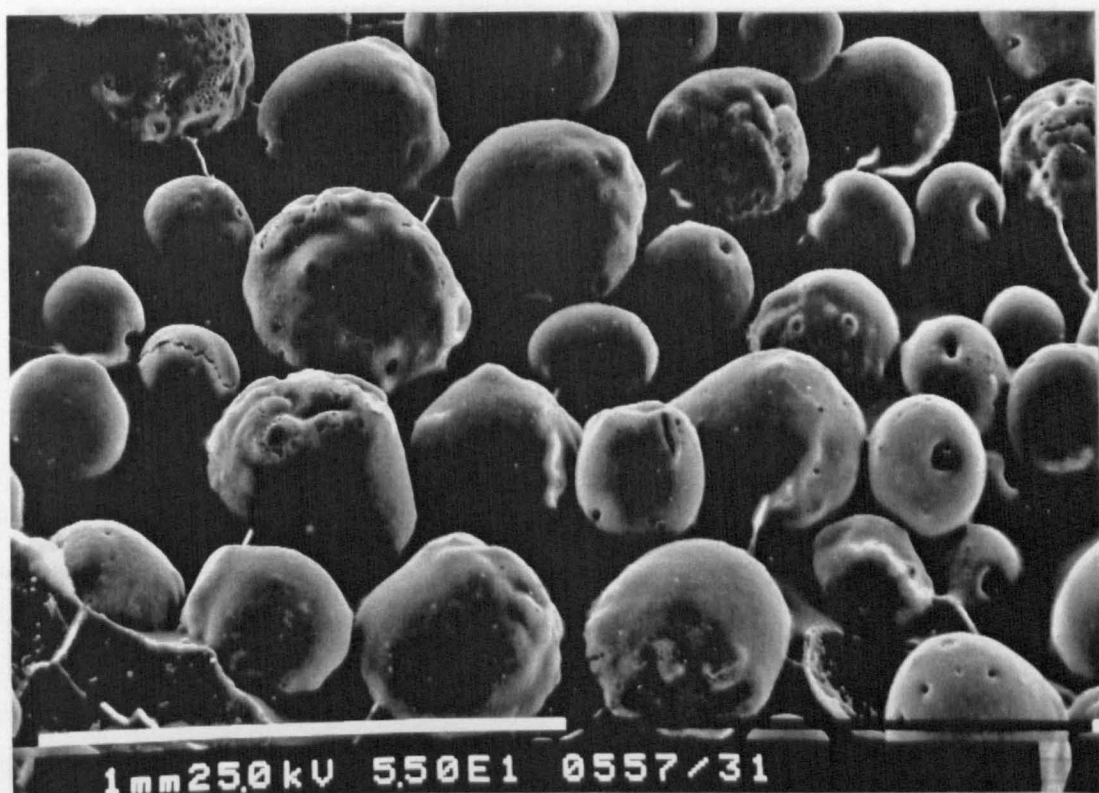


Figure 9.3. Electron micrographs of Eudragit RS:sulphapyridine microspheres used for clinical investigation: non-irradiated.

a) Microsphere population (magnification x55).



b) Microsphere surface (x1000).

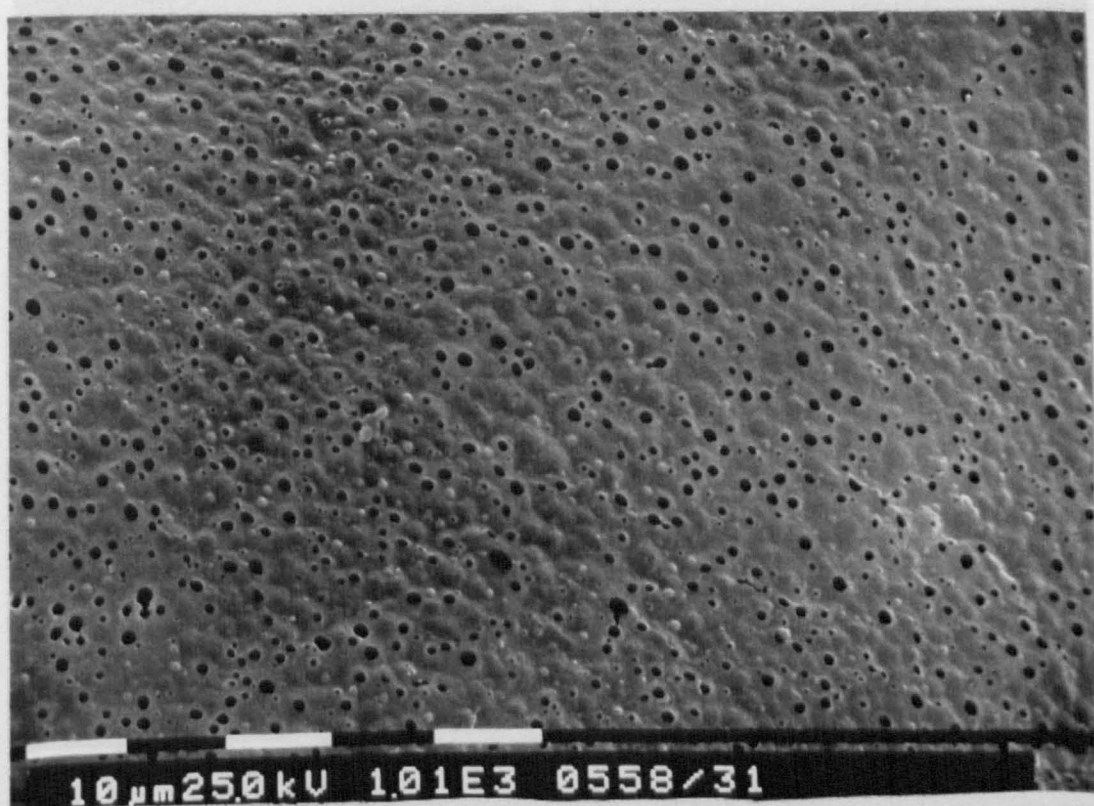
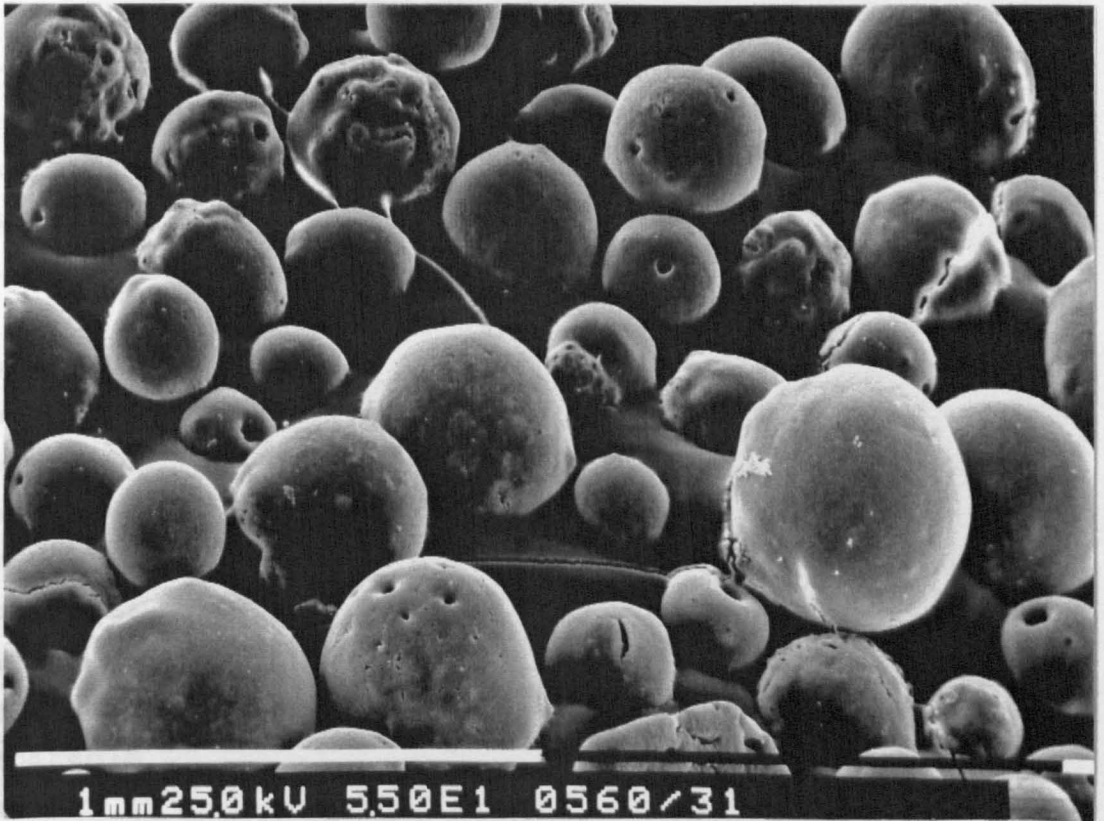
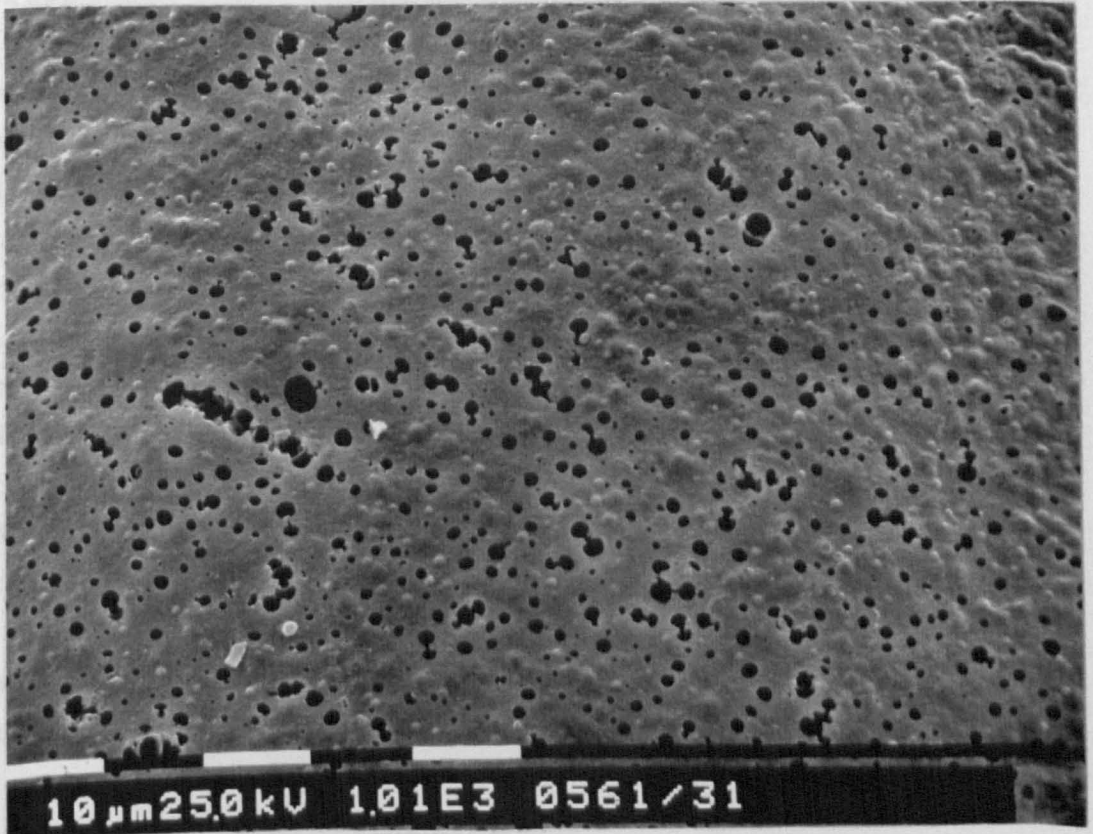


Figure 9.4. Electron micrographs of Eudragit RS:sulphapyridine microspheres used for clinical investigation: irradiated.

a) Microsphere population (magnification x55).



b) Microsphere surface (x1000).



9.3.2. Transit rate

As seen for the scintigraphic studies described in chapter 7, the coated gelatin capsules in general performed as required, releasing their contents into the ICJ or base of ascending colon. However in two subjects (2 and 3), the capsules containing sulphapyridine powder disintegrated prematurely and the contents were released into the lower small intestine.

Table 9.2 presents the mean residence time (MRT) data for the two parts of the study. Data is presented for just five subjects since in the sixth subject, on both occasions, one capsule was resident in the stomach for the entire study day. The MRTs of the 0.2 mm resin and the Eudragit microspheres in the ascending colon were 7.2 ± 1.9 h and 8.4 ± 2.0 h respectively. There was statistically no significant difference between these values and they were comparable to the studies described in chapter 7, where the mean MRT of 0.2 mm particles was 11.0 ± 4.0 h (n=21).

Figure 9.5 shows scintigraphic images of the ^{153}Sm -labelled microspheres for subject 4 at three different time intervals. In figure 9.5a, 2 hours after dosing, the three capsules were all intact in the small intestine and indeed one moved during imaging. In the top left hand corner, the radioactive marker used for alignment is seen. 5 hours after dosing, the microspheres had begun to disperse through the ascending colon (figure 9.5b). After 13 hours, a large area of activity still resided in the base of the ascending colon, whereas the remainder of the microspheres had moved ahead to outline the transverse and descending colon (figure 9.5c). The scintigraphic data indicated that almost 40% of the administered activity resided in the ascending colon at this stage.

The wide spread of the microspheres emphasizes their suitability for delivering agents for topical treatment of

Table 9.2. Ascending colon MRT of radiolabelled ion-exchange resin and Eudragit microspheres.

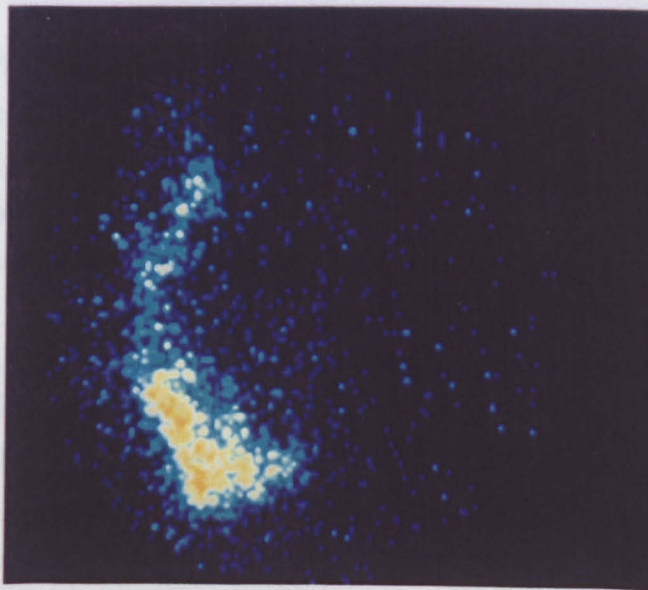
Subject	MRT (hours)	
	Ion-exchange resin	Microspheres
1	5.2	7.3
2	5.4	8.3
3	7.3	11.7
4	8.0	8.3
5	9.9	6.6
Mean	7.2±1.9	8.4±2.0

Figure 9.5. Scintigraphic images of ^{153}Sm -labelled microspheres for subject 4.

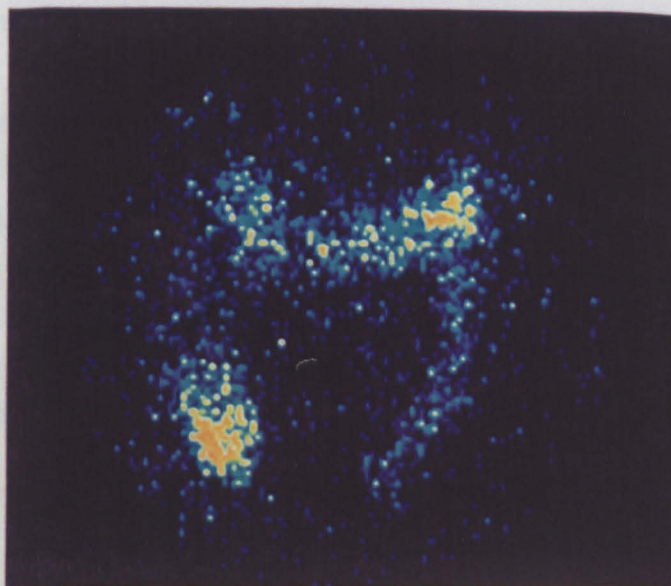
a) 2 hours.



b) 5 hours.



c) 13 hours.



an extensively diseased colon. This spreading might also serve to enhance the absorption of drugs for systemic action, by optimising contact between the carrier and the colon mucosa.

Table 9.3 lists the radioactivity from the microspheres present 24 and 32 hours after administration in the ascending, transverse, descending and whole colon for four subjects (Subject 5 was unable to attend the 24 h and 32 h imaging/blood sampling sessions). In subjects 1 and 3, in excess of 80% of the administered dose of microspheres was still resident in the colon after 24 hours. In subjects 2 and 4, considerably less activity remained.

As noted for the IBS patients in section 7.3.3, there was no apparent correlation between MRT and whole colon transit. In this study, the MRTs for subjects 2 and 4 were no shorter than for subjects 1 and 3 despite the considerable difference in residual activity at 24 and 32 h. Presumably in subjects 2 and 4, loss of the radioactivity, by defaecation, had occurred between the end of imaging on the main study day and the 24 hour image, and as a result the MRT was unaffected. If defaecation had occurred during the main study day, the distal acceleration of the microspheres would have significantly reduced their residence in the ascending colon.

The time of dosing in relation to the time of defaecation could be an important factor in determining colon residence. Indeed, a mass movement associated with approximately 80% of a dose of radiolabelled pellets moving from the ascending into the transverse and descending colon over a 15 minute period has been reported elsewhere (Proano et al., 1991). Therefore, ascending colon residence is not necessarily uniformly long, and in certain situations the opportunity for local drug action or absorption could be limited.

Table 9.3. Radioactivity from microspheres remaining after 24 and 32 hours in the ascending (AC), transverse (TC) and descending (DC) colon.

Subject	% of administered microspheres remaining					
	At 24 h			At 32 h		
	<u>AC</u>	<u>TC</u>	<u>DC</u>	<u>AC</u>	<u>TC</u>	<u>DC</u>
1	22.6	36.4	29.4	16.2	28.2	28.3
2	1.7	5.7	7.6	3.4	0.0	1.1
3	19.5	25.7	35.3	16.1	15.3	0.0
4	8.1	1.6	16.8	7.4	1.6	0.3

9.3.3. Pharmacokinetics

The chosen HPLC conditions allowed SP, AcSP and the internal standard, sulphadimidine sodium, to be resolved and identified in plasma. The total run time for each sample was 15 minutes. Figure 9.6a shows a chromatograph of blank plasma spiked with the three compounds, whereas figure 9.6b shows a chromatograph of a drug-containing sample taken from one of the subjects and containing the internal standard. The elution times were extremely sensitive to buffer methanol content and so slight variations were seen between different batches of buffer.

The minimum measurable concentrations were approximately 0.5 mg/L for SP and 2 mg/L for AcSP. The correlation coefficients for the SP and AcSP calibration graphs were both 0.991.

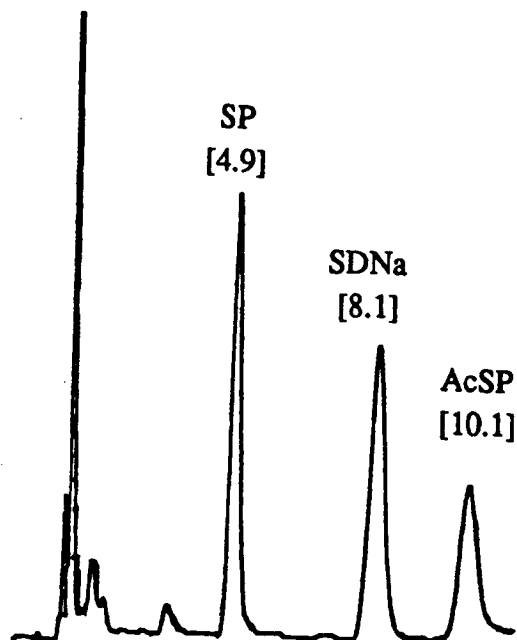
The mean group profiles of SP and AcSP following administration of the drug powder are presented in figure 9.7a. Absorption of SP appeared to be fairly rapid. In all cases, concentrations of SP were higher than AcSP, suggesting that all of the subjects were slow acetylators. In figure 9.7b is a comparison of plasma sulphapyridine levels following administration of the drug powder and the sustained-release microspheres. In most cases, levels of AcSP following microsphere administration were too low to be measured and so are not shown.

Figures 9.8a)-e) present the individual SP plasma data. Subject 5 was unable to attend at 24 and 32 h in the microsphere leg and thus this part of figure 9.8e does not extend beyond 14 hours.

The elimination half-lives of SP were estimated, from the powder leg of the study, to be 8.0, 8.0, 10.4 and 12.4 hours for subjects 2, 3, 4 and 5 respectively.

Figure 9.6. HPLC traces of sulphapyridine (SP), acetyl-sulphapyridine (AcSP), and internal standard, sulphadimidine sodium (SDNa).
([] = elution time in minutes).

a) Blank plasma spiked with the three compounds.



b) Plasma sample from one of subjects spiked with internal standard.

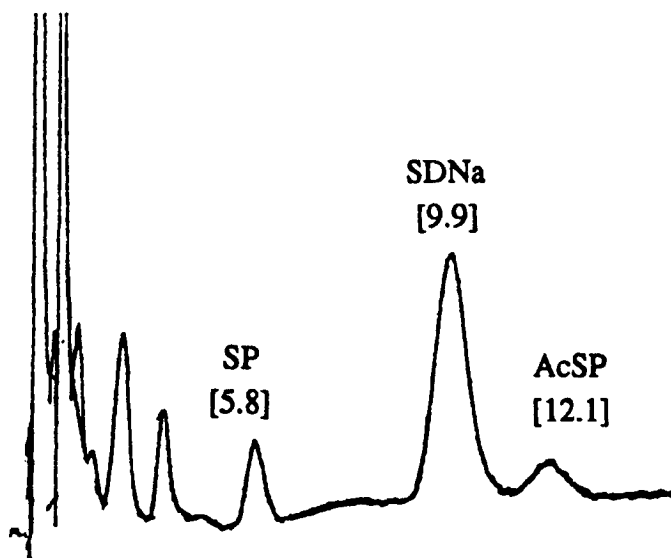
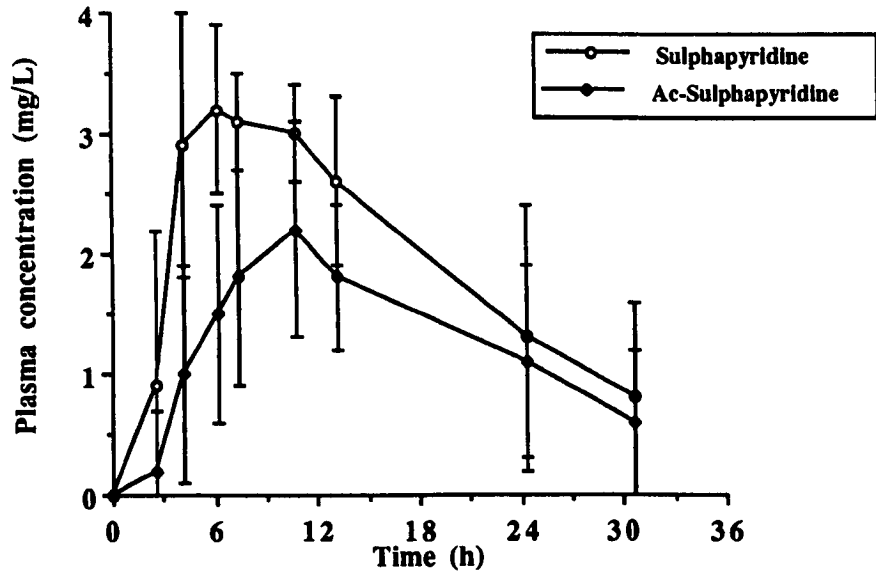


Figure 9.7. Mean plasma data from biopharmaceutical study (5 subjects).

a) Mean sulphapyridine/Ac-sulphapyridine plasma profiles (drug powder).



b) Plasma profiles of sulphapyridine: powder vs. microspheres.

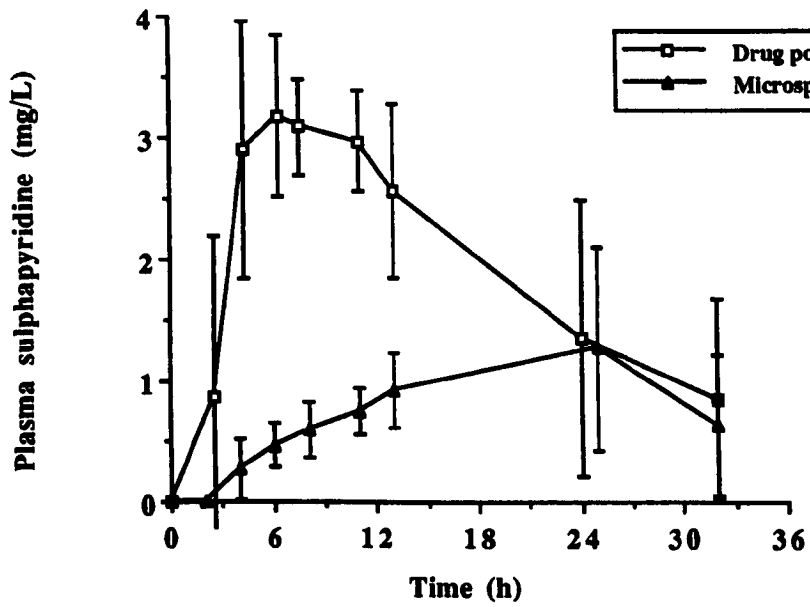
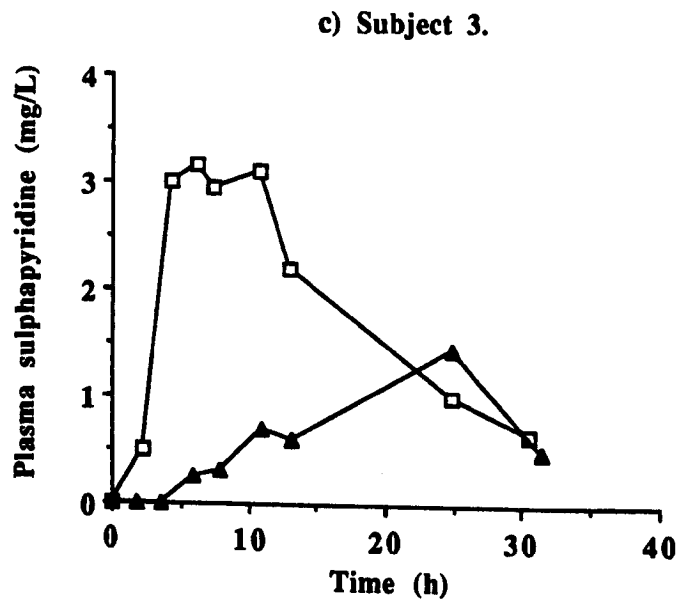
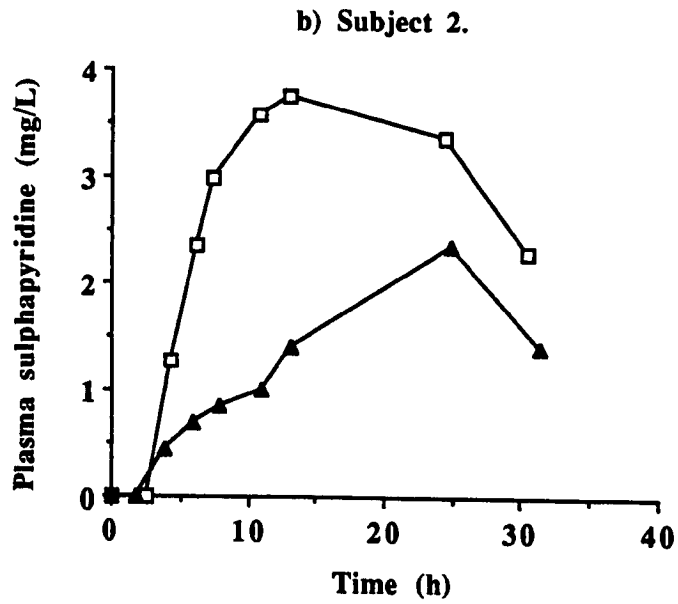
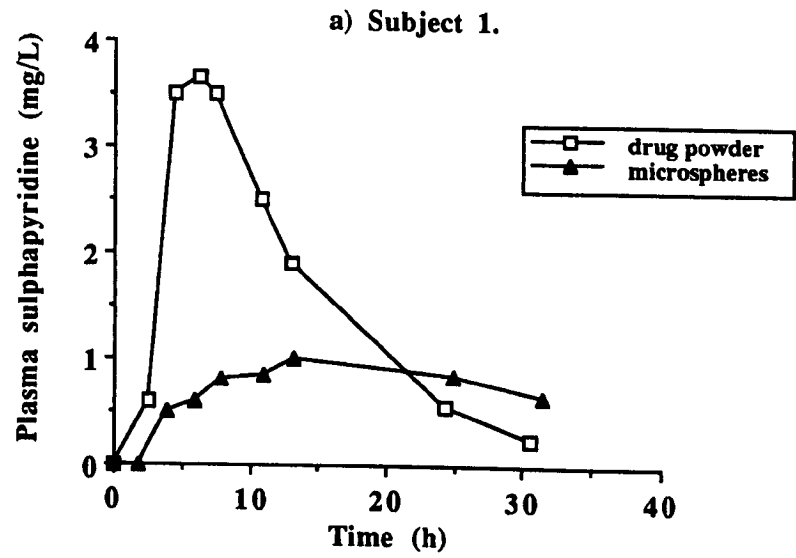
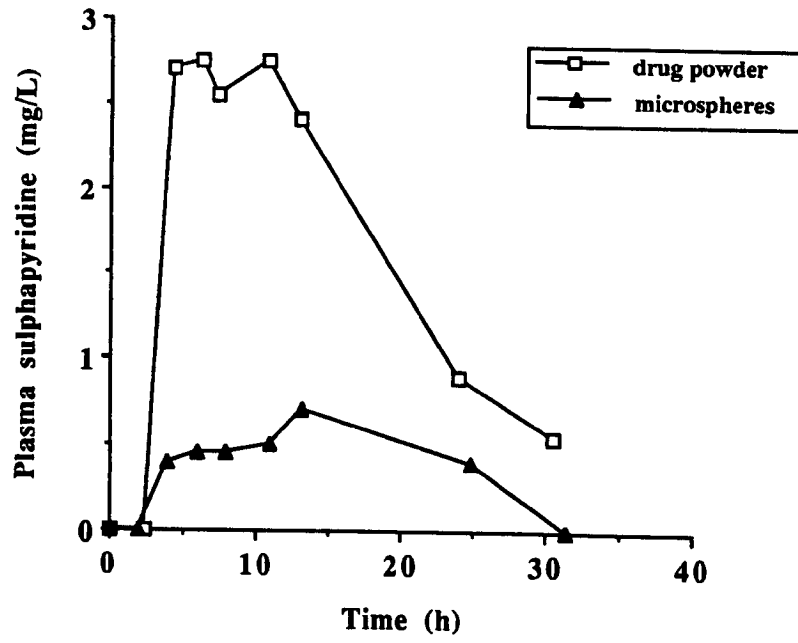


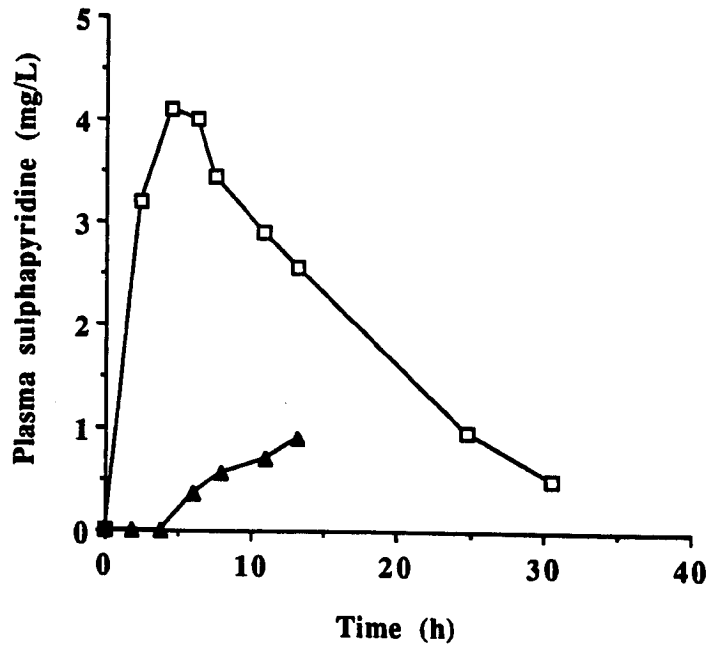
Figure 9.8. Individual sulphapyridine plasma profiles.



d) Subject 4.



e) Subject 5.



The area under the SP plasma concentration vs. time curve (AUC) was calculated for each of the two formulations. By dividing the microsphere AUC by the drug powder AUC, the relative bioavailability of the microsphere formulation was estimated. The mean relative bioavailability of the microspheres was 41.3 ± 12.7 % (table 9.4).

The relative bioavailability was lowest in subject 4. Although this may have been related to the low percentage of the administered microspheres resident in the colon at 24 h (table 9.3), the dose remaining in subject 2 at 24 h was even lower, yet bioavailability was not affected to the same extent.

The relatively long half-life of SP made the in vivo demonstration of microsphere sustained-release properties difficult, although the shape of the microsphere plasma profiles did suggest an extension of release. Looking at figures 9.8a-e, between 13 and 25 hours plasma sulphapyridine either decreased very little or actually increased, implying that drug absorption may have occurred well beyond 13 hours. Since the in vitro release of drug from the microspheres was relatively rapid (50 % released after 5 h and 75 % after 12 h) this suggested that the in vivo release behaviour may be very different.

To assess in a more quantitative manner the degree to which the microspheres demonstrated sustained-release properties, the drug mean residence time was calculated (dMRT). The dMRT is defined as the average time that the number of molecules introduced reside in the body (Rowland and Tozer, 1989). It is calculated by dividing the AUC of the plasma concentration vs. time curve by the area under the first moment of concentration vs. time curve (AUMC) and subtracting the mean absorption time (Rowland and Tozer, 1989). (The first moment of concentration is equal to the product of concentration x time). For the purpose of

Table 9.4. Bioavailability of sulphapyridine:- Eudragit microspheres (m) vs. unencapsulated drug powder (u).

Subject	Relative bioavailability = [AUC(m)/AUC(u)] x 100
1	50.0%
2	50.5%
3	41.3%
4	23.4%

Table 9.5. Mean residence time of sulphapyridine (dMRT) absorbed from powder and microspheres.

Subject	dMRT (h)		Difference (M - P) (h)
	Powder	Microspheres	
1	8.0	14.3	+6.3
2	12.8	17.9	+5.1
3	10.7	18.0	+7.3
4	9.8	10.4	+0.6

demonstrating differences in dosage form performance, the dMRT has been calculated by subtracting from [AUC/AUMC] the time at which drug absorption commenced, represented by the point of capsule disintegration on the scintigraphic images.

The results of this analysis are presented in table 9.5. In three out of four cases, the dMRT was longer for the microsphere formulation. However, this difference was not statistically significant ($p=0.058$), which may reflect the small sample number.

There are a number of possible explanations for the marked reduction in SP bioavailability observed for the microsphere formulation:

1. In vitro/in vivo differences in drug release rate.

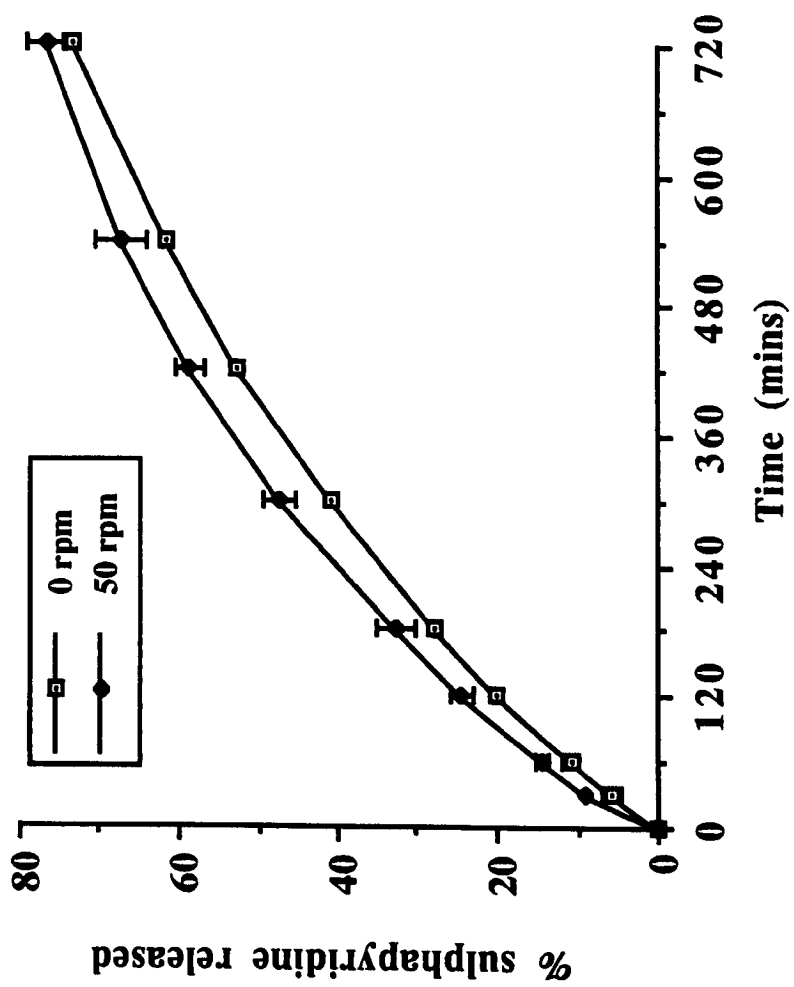
One obvious difference in microsphere in vitro/in vivo performance might result from the degree of agitation the microspheres receive. Whereas the in vitro release rate was established using paddle stirrers at 100 rpm, the degree of agitation in the colon is likely to be considerably less. The effects of the degree of agitation on the rate of SP release were assessed using the USP dissolution apparatus (as described elsewhere) with paddle stirrers set to 50 rpm or 0 rpm (figure 9.9). For comparison, the release rate with agitation at 100 rpm is presented in figure 9.2. The drug release rate appeared to be little affected by the degree of agitation.

Other in vitro/in vivo differences in release conditions which might be of importance are less easy to assess, in particular the viscosity of the colon contents.

2. Regional differences in drug absorption within the colon

In section 1.2.4.3. it was remarked that relatively little is known about the rate of drug absorption in the different

Figure 9.9. Effect of stirring speed on in vitro microsphere drug release rate.



regions of the colon. In theory, the absorptive capacity should decrease the further one travels around the colon, and indeed this has been demonstrated for ciprofloxacin (section 1.2.4.3).

Unfortunately, for the study described here, the long-half life of SP makes assessment of declining drug absorption beyond the ascending colon difficult. Difficulty in assessment is also compounded by the fact that the drug carriers are of a highly dispersed nature and so drug may be simultaneously released throughout a wide area of the colon.

3. Interaction of drug with colonic bacteria

As discussed in chapter 1, colonic bacteria have considerable potential for metabolising a variety of drugs. However, there are no reports of the biotransformation of SP.

It is probable that some of the SP will be sequestered by bacteria. In common with other sulphonamide antibiotics, SP is an analogue of gamma-amino butyric acid (GABA) and inhibits bacterial folic acid production. It decreases folic acid production by competition with endogenous GABA for the bacterial enzyme, dihydropteroate synthetase. In addition, some of the sulphonamide will be incorporated into a folic acid analogue which will disrupt various bacterial functions (Bowman and Rand, 1980).

If inactivation of SP by bacterial action does occur it would have the greatest effect on the bioavailability from the microspheres. With the SP powder, luminal concentrations of drug will initially be very high, and thus overwhelm the bacterial removal processes. However, with the sustained-release microspheres, luminal drug concentrations will be very much lower, saturation of sequestration processes will not occur, and the

bioavailability will be reduced.

9.4. CONCLUSIONS

The work undertaken in this chapter has demonstrated that microspheres radiolabelled with $^{153}\text{Sm}_2\text{O}_3$ by neutron activation techniques can be successfully visualised scintigraphically to provide high quality images, even when highly dispersed.

The MRT of the microspheres in the ascending colon was generally comparable to the studies investigating the transit of model particulates and tablets, described in chapter 7.

There was good evidence to suggest a prolongation of release from the microspheres, both from drug mean residence time calculations and also from the extended appearance of the microsphere plasma-time profiles.

The relative bioavailability of SP absorbed from sustained-release microspheres was reduced by about 50% compared to unencapsulated drug. There are potentially a number of factors which might explain the poor in vivo performance of the microspheres and without a considerable amount of further work it is not possible to isolate any single one as being the most important.

In retrospect, SP was not the ideal candidate drug for this study, for primarily two reasons. Firstly, its plasma half-life is relatively long making assessment of sustained-release more difficult. Secondly, there is the possibility of interaction with colonic bacteria. By choosing a model drug which has less likelihood of interacting with bacteria and which is known to be well absorbed from the colon, for example oxprenolol (Davis et al., 1988) or ibuprofen (Wilson et al., 1989), the evaluation of in vitro/in vivo

differences in release performance and regional variations in drug absorption within the colon would be made easier.

This study has established methods for the in vivo biopharmaceutical evaluation of drug-polymer microspheres in the colon. Further work is needed to assess their relative merits compared to other types of sustained-release dosage form.

CHAPTER 10.
CONCLUDING REMARKS.

One of the areas examined in some detail in this thesis has been the microencapsulation of poorly water-soluble drugs into Eudragit RS using emulsification-solvent evaporation. The effects of parameters such as mixing time and speed on microsphere properties are easily predicted using this process, as demonstrated in Chapter 2. The influence of other factors is less easy to assess and unfortunately is complicated by the dynamic nature of the solvent evaporation process; With a highly volatile solvent such as dichloromethane, probing structural changes taking place during microsphere formation is difficult. However, some of the experiments described in this thesis have provided interesting insights into the mechanism of microsphere formation using emulsification-solvent evaporation.

The work undertaken in Chapter 3 revealed that the concentration of surfactant used for microsphere preparation could influence the subsequent rate of drug release. The mechanism may have been different for the two surfactants investigated, since for SDS the enhancement in drug release was seen at sub-cmc concentrations, whereas at higher concentrations, highly porous and brittle microspheres were produced. On the other hand, for Tween 20, sustained-release microspheres were still produced at greater-than-cmc concentrations. It was considered that the high rate of drug release from microspheres produced using 0.25% w/v SDS was due to a very porous surface and internal structure. It is noteworthy that the internal structure of the SASP microspheres described in Chapter 8 was similar, although the number of surface pores appeared to be lower and the matrix density higher which may have explained the lower rate of drug release. On the other hand, the structure of the 5-ASA microspheres produced without surfactant was similar to the SP microspheres described in Chapter 8. It is perhaps the case that a honeycombed internal structure is associated with high concentrations of surfactant (e.g. 0.25% SDS for 5-ASA microspheres and

0.1% Tween 20 for SASP microspheres) whereas a denser structure is associated with lower concentrations of surfactant (e.g. no surfactant in the case of 5-ASA and 0.05% Tween 20 in the case of SP). With SDS as surfactant, there was also the possibility of an interaction between dodecyl sulphate anions and the cationic trimethyl ammonioethyl functions in Eudragit RS. There is clearly scope for considerably more work in this area, and in particular to investigate the microscopic structure of microspheres across a range of surfactant concentrations, and whether surfactant-enhanced drug release applies to other encapsulating polymers.

Another factor which was shown to influence microsphere structure was the presence of samarium oxide, an apparently inert, insoluble, particulate material. Incorporation of very low concentrations (1% w/w) was able to influence the physical properties of SP-Eudragit RS microspheres, most evident in increased density and a reduced drug release rate. It appeared that one of the effects of samarium oxide was to reduce the porosity of the microsphere surface, perhaps by accumulation at the polymer solution-surfactant solution interface during microsphere formation. It might be possible to determine whether or not this is the case by X-ray microanalysis of microsphere samples to compare surface and bulk concentrations of samarium. The mechanism by which samarium oxide accumulation at the microsphere surface could influence porosity and density is unclear.

Finally, XPS analysis of sulphasalazine-containing microspheres revealed that the surface drug content remained remarkably constant across a wide-range of bulk drug loadings. Further examination of this phenomenon might assist in understanding the microsphere formation process.

The incorporation of samarium oxide followed by neutron irradiation was used successfully to radiolabel

microspheres. From work in the literature investigating this technique for radiolabelling other types of dosage form, it appeared to be desirable to minimise the amount of incorporated target nuclide and the irradiation time. The microsphere investigations in this thesis supported these findings; In the case of sulphasalazine microspheres, high neutron exposure enhanced the rate of drug release, whereas high levels of samarium oxide were shown to suppress the drug release rate. It was not possible to determine the mechanism by which the rate of drug release was enhanced by irradiation. There were certainly physical changes evident from electron micrographs, possibly heat-induced. The polymer molecular weight analysis was inconclusive. More detailed investigations with drug-free microspheres would probably be a more appropriate method of assessing the effects of irradiation on polymer properties.

It was hoped that in vivo investigations of the transit of radiolabelled model dosage forms, described in Chapter 7, would provide more definitive data on the effects of particle size on the rate of transit through the colon. It appeared that in the healthy human colon, there was no difference in the colonic transit rate of materials in the size-range 0.2 mm to 8.4 mm, which conflicted with investigations published in the literature. For example, Proano et al. (1990) reported that the ascending colon transit rate was 9.9 ± 3.8 h for 0.5-1.8 mm pellets, and 11.9 ± 2.0 h for 6 mm pellets. Although these two values were statistically significantly different, the numerical difference was clearly only small. In Chapter 7, particle transit was also investigated in the hypermotile colon, either induced by lactulose or as a consequence of IBS. For lactulose-induced hypermotility, 5 mm tablets passed significantly more rapidly through the ascending colon than 0.2 mm particles. However this effect was not universal, and was only seen in six out of the group of eleven subjects. In the study involving IBS patients, extreme

differences in the transit rate of the particles and tablets were seen. However, due to the small number of subjects investigated and the fact that the disease characteristics differed greatly, it is difficult to draw any definite conclusions. Clearly, as more studies of this nature are undertaken, it will be possible to define more clearly the relationship between particle size and colon residence.

Although it was unclear whether small particles could reside in the ascending colon for longer periods than larger single units, it was considered that there may be benefits in using the former as carriers for sustained-release of drugs into the colon, whether for systemic absorption or local action. Firstly, the dispersed nature of multiparticulates might enhance contact between colonic mucosa and drug carrier. Secondly, using a dispersed system, the probability of longer total residence in the colon is increased, as discussed in Chapter 7. The in vivo pharmacokinetic study indicated a marked difference between the bioavailability of microencapsulated and unencapsulated sulphapyridine. The shortfall in bioavailability with microencapsulated drug could have been due to a number of factors. The most important of these were considered to be the possible sequestration of sulphapyridine by colonic bacteria, or in vitro/in vivo differences in microsphere drug release. Investigations with a different drug, less susceptible to bacterial interaction might allow a better evaluation of the in vivo microsphere performance. It would also be desirable to compare the colonic performance of a sustained-release microparticulate dosage form with a sustained-release single unit, both designed to provide the same in vitro rate of drug release.

The ability of "Polymer A"-coated capsules to deliver materials into the colon for the in vivo investigations was entirely unexpected and deserves further investigation,

particularly in fed human subjects.

To conclude, the work undertaken for this thesis has provided an interesting insight into aspects of the preparation and in vitro and in vivo performance of microparticulate dosage forms intended for colon drug delivery, and has revealed a number of areas worthy of further exploration.

APPENDIX 1.

Recipe for phosphate buffer:

- i) 6.8 g/L potassium dihydrogen orthophosphate (BDH, Poole, UK) dissolved in 800 ml of distilled water.
- ii) Dissolve sodium hydroxide pellets (BDH) in distilled water to produce a 1 N solution.
- iii) Adjust potassium dihydrogen orthophosphate solution to required pH (range 6-8) with 1 N aqueous sodium hydroxide solution.
- iv) Make to 1 L with distilled water.
- v) For microsphere dissolution tests, add 0.02% w/v Tween 20 to buffer solution.

REFERENCES

Abrahamsson, H., Antov, S., and Bosaeus, I.,
Gastrointestinal and colonic segmental transit time
evaluated by a single abdominal X-ray in healthy subjects
and constipated patients, Scand. J. Gastroenterol., 23,
72-80, 1988.

Alpar, H.O., and Walters, V., The prolongation of the in
vitro dissolution of a soluble drug (phenethicillin
potassium) by microencapsulation with ethylcellulose, J.
Pharm. Pharmacol., 33, 419-422, 1981.

Altura, B.M., and Saba, T.M., "Pathophysiology of the
reticuloendothelial system", Raven Press, New York, 1981.

Antonin, K.-H., Bieck, P., Scheurlen, M., Jedrychowski,
M., and Malchow, H., Oxprenolol absorption in man after
single bolus dosing into two segments of the colon
compared with that after oral dosing, Br. J. Clin.
Pharmac., 19, 137S-142S, 1985.

Arshady, R., Microspheres and microcapsules, a survey of
manufacturing techniques. Part I: Suspension cross-
linking, Polym. Eng. Sci. 29, 1746-1758, 1989.

Arshady, R., Microspheres and microcapsules, a survey of
manufacturing techniques. Part II: Coacervation, Polym.
Eng. Sci. 30, 905-914, 1990a.

Arshady, R., Microspheres and microcapsules, a survey of
manufacturing techniques. Part III: Solvent evaporation.
Polym. Eng. Sci. 30, 915-924, 1990b.

Astbury, C., and Dixon, J.S., Rapid method for the
determination of either plasma sulphapyridine or
sulphamethoxazole and their acetyl metabolites using high
performance liquid chromatography, J. Chromatogr., 414,
223-227, 1987.

Avery, G.S., Davies, E.F., and Brogden, R.N., Lactulose: A review of its therapeutic and pharmacological properties with particular reference to ammonia metabolism and its mode of action in portal system encephalopathy, *Drugs*, 4, 7-48, 1972.

Avgerinos, A., and Malamataris, S., Bioavailability of controlled release indomethacin microspheres and pellets, *Int. J. Pharm.*, 63, 77-80, 1990.

Azad Khan, A.K., Howes, D.T., Piris, J., and Truelove, S.C., An experiment to determine the active therapeutic moiety of sulphasalazine, *Lancet*, 1, 892-895, 1977.

Azad Khan, A.K., Guthrie, G., Johnston, H.H., Truelove, S.C., and Williamson, D.H., Tissue and bacterial splitting of sulphasalazine, *Clin. Sci.*, 64, 349-354, 1983.

Babay, D., Hoffman, A., and Benita, S., Design and release kinetic pattern evaluation of controlled release indomethacin microspheres, *Biomaterials*, 9, 482-488, 1988.

Bakan, J.A., Microencapsulation using coacervation/phase separation techniques, in "Controlled Release Technologies: Methods, Theory and Applications", vol.1, Kyodenius, A.F., Ed., CRC Press, Boca Raton, 1980, pp. 83-105.

Bakan, J.A., and Anderson, J.L., in "The Theory and Practice of Industrial Pharmacy", Lachman, L., Leiberman, H.A., and Kanig, J.L., Eds., 2nd edn, Lea & Febiger, Philadelphia, 1976, pp 420-438.

Baker, P., Inflammatory bowel disease, *Pharm. J.*, 241, 180-182, 1988.

Barkai, A., Pathak, Y.V., and Benita, S., Polyacrylate (Eudragit Retard) microspheres for oral controlled release of nifedipine. I. Formulation design and process optimisation, *Drug Dev. Ind. Pharm.*, 16, 2057-2075, 1990.

Barrow, L., Spiller, R.C., and Wilson, C.G., Pathological influences on colonic motility: implications for drug delivery, *Adv. Drug Del. Rev.*, 7, 201-220, 1991.

Beck, L.R., Cowsar, D.R., Lewis, D.H., Cosgrove, R.J., Riddle, C.T., Lowry, S.L., and Epperley, T., A new long-acting injectable microcapsule system for administration of progesterone, *Fertil. Steril.*, 31, 545, 1979.

Beck, L.R., Ramos, R.A., Flowers, C.E., Lopez, G.Z., Lewis, D.H., and Cowsar, D.R., Clinical evaluation of injectable biodegradable contraceptive system, *Am. J. Obstet. Gynecol.*, 140, 799-806, 1981.

Beck, L.R., Flowers, C.E., Pope, V.Z., Wilborn, W.H., and Tice, T.R., Clinical evaluation of an improved injectable biodegradable contraceptive system, *Am. J. Obstet. Gynecol.*, 147, 815-821, 1983.

Beeley, L., and Stewart, P., Drug-induced disorders of the gastrointestinal tract, *Pharm. J.*, 239, 395-397, 1987.

Benita, S., and Donbrow, M., Release kinetics of sparingly soluble drugs from ethylcellulose-walled microcapsules: theophylline microcapsules, *J. Pharm. Pharmacol.*, 34, 77-82, 1982.

Benita, S., Benoit, J.P., Puisieux F., and Thies, C., Characterisation of drug-loaded poly(d,l-lactide) microspheres, *J. Pharm. Sci.*, 73, 1721-1724, 1984.

Benita, S., Hoffman, A., and Donbrow, M.,
Microencapsulation of paracetamol using polyacrylate
resins (Eudragit Retard), kinetics of drug release and
evaluation of kinetic model, J. Pharm. Pharmacol., 37,
391-395, 1985.

Benoit, J.P., Courteille, F., and Thies, C., A
physicochemical study of the morphology of progesterone-
loaded poly(DL-lactide) microspheres, Int. J. Pharm., 29,
95-102, 1986.

Bieck, P.R., Drug absorption from the human colon, Ch.12
in "Drug Delivery to the Gastrointestinal Tract", Hardy,
J.G., Davis, S.S., and Wilson C.G., Eds., Ellis Horwood,
Chichester, 1989.

Bilbrey, J.M., and Versic, R.J., The microencapsulation
of bleaches for use in consumer products, Proceed.
Intern. Symp. Control. Rel. Bioact. Mater., 17, 53-54,
1990.

Binder, H.J., and Sandle, G.I., Electrolyte absorption
and secretion in the mammalian colon, Ch.49 in
"Physiology of the Gastrointestinal Tract", Johnson,
L.R., Ed., 2nd edn., Raven Press, New York, 1987.

Binns, J.S., Anderson, M., Melia, C.D., Davis, S.S.,
Watts, J.F., and Davies, M.C., ESCA surface
characterisation of polymeric matrices, Proceed. Intern.
Symp. Control. Rel. Bioact. Mater., 16, 384-385, 1989.

Bissery, M.-C, Valeroite, F., and Thies, C., In vitro and
in vivo evaluation of CCNU-loaded microspheres prepared
from poly(α -lactide) and poly(β -hydroxybutyrate), Sect.3,
Ch.4, in "Microspheres and Drug Therapy. Pharmaceutical,
Immunological and Medical Aspects", Davis, S.S., Illum.,
L., McVie, J.G., and Tomlinson, E., Eds., Elsevier,

Amsterdam, 1984.

Bodmeier, R., and McGinity, J.W., The preparation and evaluation of drug-containing poly(DL-lactide) microspheres formed by the solvent evaporation method, *Pharm. Res.*, 4, 465-471, 1987a.

Bodmeier, R., and McGinity, J.W., Polylactic acid microspheres containing quinidine base and quinidine sulphate prepared by the solvent evaporation technique. I. Methods and morphology, *J. Microencapsulation*, 4, 279-288, 1987b.

Bodmeier, R., and McGinity, J.W., Polylactic acid microspheres containing quinidine base and quinidine sulphate prepared by the solvent evaporation technique. II. Some process parameters influencing the preparation and properties of microspheres, *J. Microencapsulation*, 4, 279-288, 1987c.

Bodmeier, R., and McGinity, J.W., Solvent selection in the preparation of poly(DL-lactide) microspheres prepared by the solvent evaporation method, *Int. J. Pharm.*, 43, 179-186, 1988.

Bodmeier, R., and Chen, H., Preparation and characterisation of microspheres containing the anti-inflammatory agents, indomethacin, ibuprofen, and ketoprofen, *J. Control. Rel.*, 10, 167-175, 1989a.

Bodmeier, R., and Chen, H., Preparation and evaluation of drug-containing polymeric nanoparticles, *Congr. Int. Technol. Pharm.*, 2, 265-268, 1989b.

Bodmer, D., and Kissel, T., Sustained release of the somatostatin analogue octreotide from microspheres, *Proceed. Intern. Symp. Control. Rel. Bioact. Mater.*, 18,

597-598, 1991.

Bowman, W.C., and Rand, M.J., "Textbook of Pharmacology", 2nd edn., Blackwell, Oxford, 1980.

Briggs, D., and Seah, M.P., Eds., "Practical Surface Analysis (by Auger and X-ray Photoelectron Spectroscopy)", John Wiley, Chichester, 1983.

"British Pharmacopoeia", HMSO, London, 1988, pp.623-624 and p.A141.

Brockmeier, D., Grigoleit, H.-G., and Leonhardt, H., Absorption of glibenclamide from different sites of the gastrointestinal tract, *Eur. J. Clin. Pharmac.*, 29, 193-197, 1985.

Brockmeier, D., Grigoleit, H.-G., and Leonhardt, H., The absorption of piretanide from the gastrointestinal tract is site-dependent, *Eur. J. Clin. Pharmac.*, 30, 79-82, 1986.

Brown, J.P., McGarraugh, G.V., Parkinson, T.M., Wingard, R.E., and Onderdonk, A.B., A polymeric drug for treatment of inflammatory bowel disease, *J. Med. Chem.*, 26, 1300-1307, 1983.

Brondsted, H., and Kopecek, J., Hydrogels for site-specific oral drug delivery, *Proceed. Intern. Symp. Control. Rel. Bioact. Mater.*, 17, 128-129, 1990.

Burris, A.S., Ewing, L.L., and Sherins, R.J., Initial trial of slow-release testosterone microspheres in hypogonadal men, *Fertil. Steril.*, 50, 493-497, 1988.

Campbell, D.E.S., and Berglinde, T., Pharmacology of olsalazine, *Scand. J. Gastroenterol.*, 23 (suppl. 148), 7-

12, 1988.

Campieri, M., Lanfranchi, G.A., Brignola, C., Bazzochi, G., Gionchetti, P., Minguzzi, M.R., Cappello, I.P., Corbelli, C., and Boschi, S., Retrograde spread of 5-aminosalicylic acid enemas in patients with active ulcerative colitis, *Dis. Colon and Rectum*, 29, 108-110, 1986.

Cavalier, M., Benoit, J.-P., and Thies, C., The formation and characterisation of hydrocortisone-loaded poly(lactide) microspheres, *J. Pharm. Pharmacol.*, 38, 249-253, 1986.

Cha, Y., and Pitt, C.G., A one-week subdermal delivery system for L-methadone based on biodegradable microcapsules, *J. Control. Rel.*, 7, 69-78, 1988.

Cha, Y., and Pitt, C.G., The acceleration of degradation-controlled drug delivery from polyester microspheres, *J. Control. Rel.*, 8, 259-265, 1989.

Chan, R.P., Pope, D.J., Gilbert, A.P., Sacra, P.J., Baron, J.H., and Lennard-Jones, J.E., Studies of two novel sulfasalazine analogs, ipsalazide and balsalazide, *Dig. Dis. Sci.*, 28, 609-716, 1983.

Charnley, J., and Pusso, R., The recording and the analysis of gait in relation to the surgery of the hip joint, *Clin. Orthop.*, 58, 153-164, 1968.

Chase, B., Fourier-transform Raman spectroscopy, *Anal. Chem.*, 59, 881A-889A, 1987.

Chattaraj, S.C., Das, S.K., Karthikeyan, M., Ghosal, S.K., and Gupta, B.K., Controlled theophylline release from microcapsules of acrylic and methacrylic acid ester

copolymer, Drug Dev. Ind. Pharm., 17, 551-560, 1991.

Chien, Y.W., Su, K.S.E., and Chang, S.F., "Nasal Systemic Drug Delivery", Marcel Dekker, New York, 1989.

Christensen, J., Motility of the colon, Ch.21, in "Physiology of the Gastrointestinal Tract", Johnson, L.R., Ed., 2nd edn., Raven Press, New York, 1987.

Christie, A.B., X-ray photoelectron spectroscopy, Ch.5 in "Methods of surface analysis", Walls, J.M., Ed., Cambridge University Press, Cambridge, 1989.

Christrup, L.L., Davis, S.S., Frier, M., Melia, C.D., Rasmussen, S.N., Washington, N., Wilding, I.R., and Andersen, C., Deposition of a model substance, ^{99m}Tc E-HIDA, in the oral cavity after administration of lozenges, chewing gum and sublingual tablets, Proceed. Intern. Symp. Control. Rel. Bioact. Mater., 18, 507-508, 1991.

Clark, D.T., ESCA applied to polymers, Adv. Polym. Sci., 24, 123-188, 1977.

Cockbain, E.G., The aggregation of oil particles in emulsions, Trans. Faraday Soc., 48, 185-196, 1952.

Cohen, S., Yoshioka, T., Lucarelli, M., Hwang, L.H., and Langer R., Controlled delivery systems for proteins based on poly(lactic/glycolic acid) microspheres, Pharm. Res., 8, 713-720, 1991.

Colston, A., and Crainich, V.A., Development of taste-masked drugs for aqueous based suspensions, Proceed. Intern. Symp. Control. Rel. Bioact. Mater., 17, 142-143, 1990.

Colthup, N.B., Daly, L.H., and Wiberley, S.E.,
"Introduction to Infrared and Raman spectroscopy",
Academic Press, London, 1975.

Coupe, A.J., Davis, S.S., and Wilding, I.R., The
preparation and characterisation of samarium chelates as
marker compounds for subsequent in vivo dissolution
studies, J. Pharm. Pharmacol., 42 (suppl.), 126P, 1990.

Couvreur, P., Grislain, L., Lenaerts, V., Brasseur, F.,
Guiot, P., and Biernacki, A., Biodegradable polymeric
nanoparticles as drug carriers for antitumor agents, in
"Polymeric Nanoparticles and Microspheres", Guiot, P.,
and Couvreur, P., Eds., CRC Press, Boca Raton, 1986.

"CRC Handbook of Chemistry and Physics", 63rd edn., CRC
Press, Boca Raton, FL, 1987.

Cummings, J.H., Branch, J.W., Jenkins, D.J.A., Southgate,
D.A.T., Houston, H., James, W.P.T., Colonic response to
dietary fibre from carrot, cabbage, apple, bran and guar
gum, Lancet, 1, 5-9, 1978.

Cummins, H.Z., and Pike, E.R., Eds., "Photon Correlation
Spectroscopy and Velocimetry", NATO-ASI series B (no.23),
Plenum, NY, 1977.

Das, K.M., Eastwood, M.A., McManus, J.P.A., and Sircus,
W., The role of the colon in the metabolism of
salicylazo-sulphapyridine. Scand. J. Gastroenterol., 9,
137-141, 1974.

"Data Sheet Compendium, 1989-1990", Datepharm
Publications, London, 1989, p.1498.

Davies, J.D., Touitou, E., and Rubinstein, A., Targeted
enteral delivery system, European Patent 86309305, 1986.

Davies, M.C., Wilding, I.R., Short, R.D., Khan, M.A., Watts, J.F., and Melia, C.D., An analysis of the surface chemical structure of polymethacrylate (Eudragit) film coating polymers by XPS, *Int. J. Pharm.*, 57, 183-187, 1989.

Davies, M.C., Binns, J.S., Melia, C.D., Hendra, P.J., Bourgeois, D., Church, S.P., and Stephenson, P.J., FT-Raman spectroscopy of drugs in polymers, *Int. J. Pharm.*, 66, 223-232, 1990a.

Davies, M.C., Khan, M.A., Short, R.D., Akhtar, S., Pouton, C., and Watts, J.F., XPS and SSIMS analysis of the surface chemical structure of poly(caprolactone) and poly(β -hydroxybutyrate- β -hydroxyvalerate) copolymers, *Biomaterials*, 11, 228-234, 1990b.

Davies, M.C., Lynn, R.A.P., Paul, A., and Heller, J., Surface analysis of poly(orthoesters) by SIMS and XPS, *Proceed. Intern. Symp. Control. Rel. Bioact. Mater.*, 17, 234-235, 1990c.

Davies, M.C., Lynn, R.A.P., Khan, M.A., Paul, A., Domb, A., and Langer, R., Surface analysis of poly(anhydride) homo- and co-polymers using SIMS and XPS, *Proceed. Intern. Symp. Control. Rel. Bioact. Mater.*, 17, 232-233, 1990d.

Davis, S.S., Hardy, J.G., Stockwell, A., Taylor, M.J., Whalley, D.R., and Wilson, C.G., The effect of food on the gastrointestinal transit of pellets and an osmotic device (Osmet), *Int. J. Pharm.*, 21, 331-340, 1984a.

Davis, S.S., Illum, L., McVie, J.G., and Tomlinson, E., Eds., "Microspheres and Drug Therapy. Pharmaceutical, Immunological and Medical Aspects", Elsevier, Amsterdam, 1984b.

Davis, S.S., Hardy, J.G., and Fara, J.W., Transit of pharmaceutical dosage forms through the small intestine, *Gut*, 27, 886-892, 1986.

Davis, S.S., Washington, N., Parr, G.D., Short, A.H., John, V.A., Lloyd, P., and Walker, S.M., Relationship between the appearance of oxprenolol in the systemic circulation and the location of an oxprenolol 16/260 drug delivery system within the gastrointestinal tract as determined by scintigraphy, *Br. J. Clin. Pharmacol.*, 26, 435-443, 1988.

Davis, S.S., and Illum, L., Microspheres as Drug Carriers, in "Drug Carrier Systems", Roerdink, F.H.D., and Kroon, A.M., Eds., Wiley, London, 1989.

Deasy, P.B., "Microencapsulation and related drug processes", Marcel Dekker, New York, 1984.

Deasy, P.B., Microencapsulation of drugs by pan and air suspension techniques, *Crit. Rev. Ther. Drug Carr. Sys.*, 8, 39-89, 1991.

Dew, M.J., Hughes, P.J., Lee, M.G., Evans, B.K., and Rhodes, J., An oral preparation to release drugs in the human colon, *Br. J. Clin. Pharmac.*, 14, 405-408, 1982.

Dew, M.J., Ryder, R.E.J., Evans, N., Evans, B.K., and Rhodes, J., Colonic release of 5-aminosalicylic acid from an oral preparation in active ulcerative colitis, *Br. J. Clin. Pharmac.*, 16, 185-187, 1983.

Dew, M.J., Ebdon, P., Kidwai, N.S., Lee, G., and Evans, B.K., Comparison of the absorption and metabolism of sulphasalazine and acrylic-coated 5-aminosalicylic acid in normal subjects and patients with colitis, *Br. J. Clin. Pharmac.*, 17, 474-476, 1984.

Digenis, G.A., Sandefer, E.P., Parr, A.F., Beihn, R., McClain, C., Scheinthal, B.M., Ghebre-Sellasie, I., Iyer, U., Nesbitt, R.U., and Randinitis, E., Gastrointestinal behavior of orally administered radiolabeled erythromycin pellets in man as determined by gamma scintigraphy, *J. Clin. Pharmacol.*, 30, 621-631, 1990.

Digenis, G.A., and Sandefer, E., Gamma scintigraphy and neutron activation techniques in the in vivo assessment of orally administered dosage forms, *Crit. Rev. Ther. Drug Carr. Sys.*, 7, 309-345, 1991.

Domb, A., Maniar, M., Bogdansky, S., and Chasin, M., Drug delivery to the brain using polymers, *Crit. Rev. Ther. Drug Carr. Sys.*, 8, 1-18, 1991.

Douglas, S.J., Davis, S.S., and Illum, L., Nanoparticles in drug delivery, *Crit. Rev. Ther. Drug Carr. Sys.*, 3, 233-261, 1987.

Ellis, G., Hendra, P.J., Hodges, C.M., Jawhari, T., Jones, C.H., Le Barazer, P., Passingham, C., Royhaud, I.A.M., Sanchez-Blazquez, A., and Warnes, G.M., Routine analytical Fourier transform Raman spectroscopy, *Analyst*, 114, 1061-1066, 1989.

El-Samaligy, M., and Rohdewald, P., Triamcinolone diacetate nanoparticles, a sustained release drug delivery system available for parenteral administration, *Pharm. Acta. Helv.*, 57, 201-204, 1983.

El-Sayed, A.A., Badwai, A.A., and Fouli, A.M., Evaluation of solvent used in the preparation of solid dispersions and microcapsules on the dissolution of drugs, *Pharm. Acta. Helv.*, 57, 61-64, 1982.

Erlich, B.E., and Diamond, J.M., Lithium absorption:

implications for sustained release lithium preparations, *Lancet*, 1, 306, 1983.

Eudragit technical data, supplied by Dumas (UK) Ltd, Tunbridge Wells, Kent, UK.

Evans, D.F., Pye, G., Bramley, R., Clark, A.G., Dyson, T.J., and Hardcastle, J.D., Measurement of gastrointestinal pH profiles in normal ambulant human subjects, *Gut*, 29, 1035-1041, 1988.

Ewing, G.W., "Instrumental Methods of Chemical Analysis", 4th edn., McGraw-Hill, London, 1975.

Farmer, R.G., and Schumacher, O.P., Treatment of ulcerative colitis with hydrocortisone enemas: Relationship of hydrocortisone absorption, adrenal suppression and clinical response, *Dis. Colon Rectum*, 13, 355-361, 1970.

Farr, S.J., Kellaway, I.W., Parry-Jones, D.R., and Woolfrey, S.J., ^{99m}Tc as a marker of liposomal deposition and clearance in the human lung, *Int. J. Pharm.*, 26, 303-316, 1985.

Farthing, M.J.G., Rutland, M.D., and Clark, M.L., Retrograde spread of hydrocortisone-containing foam given intrarectally in ulcerative colitis, *Br. Med. J.*, 2, 822-824, 1979.

Findlay, J.M., Smith, A.N., Mitchell, W.D., Anderson, A.J.B., and Eastwood, M.A., Effects of unprocessed bran on colon function in normal subjects and in diverticular disease, *Lancet*, 1, 146-149, 1974.

Fischer, C., and Klotz, U., Determination of sulfapyridine and its major metabolites in plasma by high

pressure liquid chromatography, *J. Chromatogr.*, 146, 157-162, 1978.

Fitzgerald, P., Hadgraft, J., Kreuter, J., and Wilson C.G., A gamma-scintigraphic evaluation of microparticulate ophthalmic delivery systems: liposomes and nanoparticles, *Int. J. Pharm.*, 40, 81-84, 1987.

Florence, A.T., and Attwood, D., "Physicochemical Principles of Pharmacy", Macmillan, London, 1981.

Fong, J.W., Nazareno, J.P., Pearson, J.E., and Maulding H.V., Evaluation of biodegradable microspheres prepared by a solvent evaporation process using sodium oleate as emulsifier, *J. Control. Rel.*, 3, 119-130, 1986.

Friend, D.R., and Chang, G.W., A colon-specific drug-delivery system based on drug glycosides and the glycosidases of colonic bacteria, *J. Med. Chem.*, 27, 261-266, 1984.

Friend, D.R., and Chang, G.W., Potential prodrugs for colon-specific drug delivery, *J. Med. Chem.*, 28, 51-57, 1985.

Friend, D.R., Colon-specific drug delivery, *Adv. Drug Del. Rev.*, 7, 149-199, 1991.

Fujimoto, S., Miyazaki, M., Endoh, F., Takahashi, O., Okui, K., and Morimoto, Y., Mitomycin C-carrying microspheres as a novel method of drug delivery, *Cancer Drug Delivery*, 2, 173-181, 1985.

Ganong, W.F., "Review of Medical Physiology", 10th edn., Lange, Los Altos, CA, 1981.

Gaska, J.A., and Sarafpour, B., Update on inflammatory

bowel disease, *American Druggist*, 200, 64-74, 1989

Gleiter, C.H., Antonin, K.-H., Bieck, P., Godbillon, J., and Schönleber, W., Colonoscopy in the investigation of drug absorption in healthy volunteers, *Gastrointest. Endosc.*, 31, 71-73, 1985.

Godbillon, J., Evard, D., Vidon, N., Duval, M., Schoeller, J.P., Bernier, J.J., and Hirtz, J., Investigation of drug absorption from the gastrointestinal tract of man. III. Metoprolol in the colon, *Br. J. Clin. Pharmac.*, 19, 113S-118S, 1985.

Goto, S., Kawata, M., Nakamura, M., and Aoyama, T., Effect of magnesium stearate in the preparation of Eudragit-RS microcapsules containing drugs, *Y. Zasshi*, 105, 1087-1095, 1985.

Goto, S., Kawata, M., Nakamura, M., Maekawa, K., and Aoyama, T., Eudragit E, L, and S (acrylic resins) microcapsules as pH sensitive release preparations of ketoprofen, *J. Microencapsulation*, 3, 305-316, 1986a.

Goto, S., Kawata, M., Nakamura, M., Maekawa, K., and Aoyama, T., Eudragit RS and RL (acrylic resins) microcapsules as pH insensitive and sustained release preparations of ketoprofen, *J. Microencapsulation*, 3, 293-304, 1986b.

Green, B.K., and Schleicher, L., US Patents 2,730,456 and 2,730,457, 1956.

Guiot, P., and Couvreur, P., Eds., "Polymeric Nanoparticles and Microspheres", CRC Press, Boca Raton, 1986.

Gupta, P.K., Hung, C.T., and Perrier, D.G., *Albumin*

microspheres. I. Release characteristics of adriamycin, Int. J. Pharm., 33, 137-146, 1986.

Halls, J., Bowel shift during normal defaecation, Proc. Royal Soc. Med, 58, 820-825, 1965.

Hanauer, S.B., Kirsner, J.B., and Barrett, W.E., Treatment of left-sided ulcerative colitis with tixocortol pivalate, Gastroenterol., 90, 1449, 1986.

"Handbook of Pharmaceutical Excipients", Pharmaceutical Press and American Pharmaceutical Association, London, 1986.

Hartas, S.R., Collett, J.H., and Booth, C., The influence of gamma-irradiation on poly(lactide-co-glycolide) microspheres, J. Pharm. Pharmacol., 43 (suppl.), 30P, 1991.

Hardy, J.G., and Perkins, A.C., Validity of the geometric mean correction in the quantification of whole bowel transit time, Nucl. Med. Commun., 6, 217-224, 1985.

Hardy, J.G., Wilson, C.G., and Wood, E., Drug delivery to the proximal colon, J. Pharm. Pharmacol., 37, 874-877, 1985.

Hardy, J.G., Lee, S.W., Clark, A.G., and Reynolds, J.R., Enema volume and spreading, Int. J. Pharm., 31, 151-155, 1986.

Hardy, J.G., Healey, J.N.C., and Reynolds, J.R., Evaluation of an enteric-coated delayed release 5-aminosalicylic acid tablet in patients with inflammatory bowel disease, Aliment. Pharmacol. Therap., 1, 273-280, 1987.

Hardy, J.G., Davis, S.S., Khosla, R., and Robertson, C.S., Gastrointestinal transit of small tablets in patients with ulcerative colitis, *Int. J. Pharm.*, 48, 79-82, 1988.

Hardy, J.G., Lamont, G.L., Evans, D.F., Haga, A.K., and Gamst, O.N., Evaluation of an enteric-coated naproxen pellet formulation, *Aliment. Pharmacol. Ther.*, 5, 69-75, 1991.

Harmia, T., Speiser, P., and Kreuter, J., A solid colloidal drug delivery system for the eye: encapsulation of pilocarpin in nanoparticles, *J. Microencapsulation*, 3, 3-12, 1986.

Harnor, K.J., Perkins, A.C., Wilson, C.G., Sims, E.E., Feely, L.C., and Farr, S.J., Effect of vapour pressure on the deposition pattern from solution phase metered dose inhalers, *J. Pharm. Pharmacol.*, 42 (suppl.), 10P, 1990.

Haubrich, W.S., Anatomy of the colon, Ch.131 in "Bockus Gastroenterology", J.E.Berk (Ed.-in-chief), Saunders, London, 1985.

Hayllar, J., and Bjarnason, I., Sulphasalazine in ulcerative colitis: in memoriam? *Gut*, 32, 462-463, 1991.

Haynes, R.C., and Larner, J., Adrenocorticotrophic hormone; Adrenocortical steroids and their synthetic analogs; inhibitors of adrenocorticosteroid biosynthesis, Ch.70 in "The Pharmacological Basis of Therapeutics", Goodman, L.S., and Gilman, A., Eds., 5th edn., Macmillan, New York, 1975.

Hazrati, A.M., Akrawi, S., Hickey, A.J., Wedlund, P., Macdonald, J., and DeLuca, P.P., Tissue distribution of indium-111 labeled poly(glycolic acid) matrices following

jugular and hepatic portal vein administration, J. Control. Rel., 9, 205-214, 1989.

Hearn, M.J., Ratner, B.D., and Briggs, D., SIMS and XPS studies of polyurethane surfaces. 1. Preliminary studies, Macromol., 21, 2950-2959, 1988.

Hendra, P., and Mould, H., FT-Raman spectroscopy as a routine analytical tool, Int. Lab., 18, 34-45, 1988

Higuchi, W.I., Okada, R., and Lemberger, A.P., Aggregation of oil-in-water emulsions: Effects of dioctyl sodium sulfosuccinate concentration, J. Pharm. Sci., 51, 683-687, 1962.

Hinds, J.P., Stoney, B., and Wald, A., Does gender or the menstrual cycle affect colonic transit? Am. J. Gastroenterol., 84, 123-126, 1989.

Hinton, J., Lennard-Jones, J., and Young, A., A new method of studying gut transit times using radio-opaque markers, Gut, 10, 842-847, 1969.

Ho, K.K.L., Particle size characterisation by laser light scattering, Pharm. J., 245, 51-56, 1989.

Hodges, C.M., and Akhavan, J., The use of Fourier transform Raman spectroscopy in the forensic detection of illicit drugs and explosives, Spectrochim. Acta, 46A, 303-307, 1990.

Holt, R., The bacterial degradation of chloramphenicol, Lancet, 1, 1259-1260, 1967.

Hora, M.S., Rana, R.K., Nunberg, J.H., Tice, T.R., Gilley, R.M., and Hudson, M.E., Release of human serum albumin from poly(lactide-co-glycolide) microspheres,

Pharm. Res., 7, 1190-1195, 1990.

Hossain, M., Abramowitz, W., Watrous, B.J., Szpunar, G.J., and Ayres, J.W., Gastrointestinal transit of nondisintegrating, non-erodible oral dosage forms in pigs, Pharm. Res., 7, 1163-1166, 1990.

Howard, M.A., Gross, A., Grady, M.S., Langer, R.S., Mathiowitz, E., Winn, H.R., and Mayberg., M.R., Intracerebral drug delivery in rats with lesion-induced memory deficits, J. Neurosurg., 71, 105-112, 1989.

Huang, H.-P., and Ghebre-Sellasie, I., Preparation of microspheres of water-soluble pharmaceuticals, J. Microencapsulation, 6, 219-225, 1989.

Ikesue, K., Kopeckova, P., and Kopecek, J., Degradation of proteins by enzymes of the gastrointestinal tract, Proceed. Intern. Symp. Control. Rel. Bioact. Mater., 18, 580-581, 1991.

Illum, L., Davis, S.S., Muller, R.W., Mak, E., and West, P., The organ distribution and circulation time of intravenously injected colloidal carriers sterically stabilised with a block-copolymer - poloxamine 908, Life Sci., 40, 367-374, 1987.

Illum, L., Farraj, N.F., Davis, S.S., Johansen, B.R., and O'Hagan, D.T., Investigations on the nasal absorption of biosynthetic growth hormone in sheep - use of a bioadhesive microsphere delivery system., Int. J. Pharm., 63, 207-211, 1990.

Iwamoto, T., Kawashima, Y., Niwa, T., Takeuchi, H., and Furuyama, S., A new controlled release suspension of spherical matrix of ibuprofen with acrylic polymer, Proceed. Intern. Symp. Control. Rel. Bioact. Mater., 15,

328-329, 1988.

Jalsenak, I., Nicolaidou, C.F., and Nixon, J.R., The in vitro dissolution of phenobarbitone sodium from ethylcellulose microcapsules, *J. Pharm. Pharmacol.*, 28, 912-914, 1976.

Jani, P., Halbert, G.W., Langridge, J., and Florence, A.T., The uptake and translocation of latex nanospheres and microspheres after oral administration to rats, *J. Pharm. Pharmacol.*, 41, 809-812, 1989.

Jarnerot, G., Newer 5-aminosalicylic acid based drugs in chronic inflammatory bowel disease, *Drugs*, 37, 73-86, 1989.

Jay, M., Digenis, G.A., Foster, T.S., and Antonow, D.R., Retrograde spreading of hydrocortisone enema in inflammatory bowel disease, *Dig. Dis. Sci.*, 31, 139-144, 1986.

Jones, C.E., Newton, J.M., and O'Neill, R.C., The physical characterisation of polymeric films for the release of metronidazole, *J. Pharm. Pharmacol.*, 43 (suppl.), 90P, 1991.

Juliano, R.L., Microparticulate drug carriers, in "Directed Drug Delivery", Borchardt, R.T., Repta, A.J., and Stella, N.J., Eds., Humana, Clifton, 1985.

Juni, K., and Nakano, M., Poly(hydroxy acids) in drug delivery, *Crit. Rev. Ther. Drug Carr. Sys.*, 3, 209-232, 1987.

Kaus, L.C., Fell, J.T., Sharma, H., and Taylor, D.C., On the intestinal transit of a single non-disintegrating object, *Int. J. Pharm.*, 14, 143-148, 1984.

Kawata, M., Nakamura, M., Goto, S., and Aoyama, T., Preparation and dissolution pattern of Eudragit RS microcapsules containing ketoprofen, Chem. Pharm. Bull., 34, 2618-2623, 1986.

Kerr, D.J., and Kaye, S.B., Chemoembolism in cancer chemotherapy, Crit. Rev. Ther. Drug Carr. Sys., 8, 19-38, 1991.

Khosla, R., and Davis, S.S., Gastric emptying and small and large bowel transit of non-disintegrating tablets in fasted subjects, Int. J. Pharm., 52, 1-10, 1989.

Kimura, T., Yamaguchi, T., Kurosaki, Y., Nakayama, T., Fujiwara, Y., Unno, K., and Suzuki, T., Design and evaluation of colonic mucosa-specific pro-antedrugs for oral treatment of ulcerative colitis, Proceed. Intern. Symp. Control. Rel. Bioact. Mater., 18, 427-428, 1991.

Kissel, T., Bruckner, W., Brich, Z., Lancranjan, J., Rosenthaler, J., Nimmerfall, F., Prikozovich W., and Vit, P., Microspheres as depot-injections, an industrial perspective, Proceed. Intern. Symp. Control. Rel. Bioact. Mater., 15, 260-261, 1988.

Klotz, U., Clinical pharmacokinetics of sulphasalazine, its metabolites and other prodrugs of 5-aminosalicylic acid, Clin. Pharmacokinetics, 10, 285-302, 1985.

Kojima, T., Nakano, M., Juni, K., Inoue, S., and Yoshida, Y., Preparation and evaluation in vitro of polycarbonate microspheres containing local anaesthetics, Chem. Pharm. Bull., 32, 2795-2802, 1984.

Koosha, F., Muller, R.H., Davis, S.S., and Davies, M.C., The surface chemical structure of poly(β -hydroxybutyrate) microparticles produced by solvent evaporation process,

J. Control. Rel., 9, 149-157, 1989.

Kopeckova, P., Rihova, B., Rathi, R., and Kopecek, J., Bioadhesive polymers for colon specific drug delivery, Proceed. Intern. Symp. Control. Rel. Bioact. Mater., 18, 341-342, 1991.

Krane, K., "Modern Physics", John Wiley, New York, 1983.

Kreuter, J., Possibilities of using nanoparticles as carriers for drugs and vaccines, J. Microencapsulation, 5, 115-128, 1988.

Krevsky, B., Malmud, L.S., D'Ercole, F., Maurer, A.H., and Fisher, R.S., Colonic transit scintigraphy: A physiologic approach to the quantitative measurement of colonic transit in humans, Gastroenterology, 91, 1102-1112, 1986.

Kumana, C.R., Seaton, T., Meghji, M., Castelli, M., Benson, R., and Sivakumaran, T., Beclomethasone dipropionate enemas for treating inflammatory bowel disease without producing Cushing's syndrome or hypothalamic pituitary adrenal suppression, Lancet, 1, 579-583, 1982.

Kwong, A.K., Chou, S., Sun, A.M., Sefton, M.V., and Goosen, M.F.A., In vitro and in vivo release of insulin from poly(lactic acid) microbeads and pellets, J. Control. Rel., 4, 47-62, 1986.

Langer, R., New methods of drug delivery, Science, 249, 1527-1533, 1990.

Lee, V.H.L., and Yamamoto, A., Penetration and enzymatic barriers to peptide and protein absorption, Adv. Drug Del. Rev., 4, 171-207, 1990.

Lehmann, K.O.R., and Dreher, K.D., Methacrylate-galactomannan coating for colon-specific drug delivery, *Proceed. Intern. Symp. Control. Rel. Bioact. Mater.*, 18, 331-332, 1991.

Leong, K.W., Kost, J., Mathiowitz, E., and Langer, R., Polyanhydrides for controlled release of bioactive materials, *Biomaterials*, 364-371, 1986.

Levine, D.S., Raisys, V.A., and Ainaridi, V., Coating of oral beclomethasone dipropionate capsules with cellulose acetate phthalate enhances delivery of topically active antiinflammatory drug to the terminal ileum, *Gastroenterology*, 92, 1037-1044, 1987.

Levy, M.C., Rambourg, P., Levy, J., and Potron G., Microencapsulation IV: cross-linked hemoglobin microcapsules, *J. Pharm. Sci.*, 71, 759-762, 1982.

Li, S.P., Kowarski, C.R., Feld, K.M., and Grim, W.M., Recent advances in microencapsulation technology and equipment, *Drug Dev. Ind. Pharm.*, 14, 353-376, 1988.

Longer, M.A., Woodley, J.F., and Duncan, R., Comparison of the activities of rat small intestine and colon brush border membrane peptidases, *Proceed. Intern. Symp. Control. Rel. Bioact. Mater.*, 16, 225-226, 1989.

Love, W.G., Farr, S.J., Kellaway, I.W., and Williams, B.D., Liposome accumulation within inflamed tissue: Gamma scintigraphic evidence, *Proceed. Intern. Symp. Control. Rel. Bioact. Mater.*, 17, 377-378, 1990.

MacFarlane, G.T., Allison, C., Gibson, S.A.W., and Cummings, J.H., Contribution of the microflora to proteolysis in the human large intestine, *J. Appl. Bact.*, 64, 37-46, 1988.

Madan, P.L., Microencapsulation 1. Phase separation or coacervation, *Drug Dev. Ind. Pharm.*, 4, 95-116, 1978.

Magnusson, J.O., Bergdahl, B., Bogentoft, C., and Jonsson, U.E., Metabolism of digoxin and absorption site, *Br. J. Clin. Pharmacol.*, 14, 284-285, 1982.

Malamataris, S., and Avgerinos, A., Controlled release indomethacin microspheres prepared by using an emulsion solvent-diffusion technique, *Int. J. Pharm.*, 62, 105-111, 1990.

Malvern Mastersizer User Manual, Malvern Instruments, Malvern, UK, 1988.

Mardini, H.A., Lindsay, D.C., Deighton, C.M., and Record, C.O., Effect of polymer coating on faecal recovery of ingested 5-aminosalicylic acid in patients with ulcerative colitis, *Gut*, 29, 974-982, 1988.

Mathiowitz, E., Saltzman, W.M., Domb, A., Dor, P., and Langer, R., Polyanhydride microspheres as drug carriers. II. Microencapsulation by solvent removal, *J. Appl. Polym. Sci.*, 35, 755-774, 1988.

Mathiowitz, E., Kline, D., and Langer, R., Morphology of polyanhydride microsphere delivery systems, *Scanning Microscopy*, 4, 329-340, 1990.

Maulding, H.V., Tice, T.R., Cowsar, D.R., Fong, J.W., Pearson, J.E., and Nazareno, J.P., Biodegradable microcapsules: acceleration of polymeric excipient hydrolytic rate by incorporation of a basic medicament, *J. Control. Rel.*, 3, 103-118, 1986.

McGee, J.P., Davis, S.S., and O'Hagan, D.T., Production of polylactide-co-glycolide (PLGA) microparticles by

phase separation containing a model protein, *J. Pharm. Pharmacol.*, 43 (suppl.), 84P, 1991.

Metcalf, A.M., Phillips, S.F., Zinsmeister, A.R., MacCarty, R.L., Beart, R.W., and Wolff, B.G., Simplified assessment of segmental colonic transit, *Gastroenterology*, 92, 40-47, 1987.

Michel, C., Roques, M., Couvreur, P., Vranckx, H., Balschmidt, P., and Damge, C., Isobutyl cyanoacrylate nanoparticles as a drug carrier for oral administration of insulin, *Proceed. Intern. Symp. Control. Rel. Bioact. Mater.*, 18, 97-98, 1991.

Miller, D.A., and Peppas, N.A., The use of X-ray photoelectron spectroscopy for the analysis of the surface of biomaterials, *J. Macromol. Sci - Rev. Macromol. Chem. Phys.*, C26, 33-66, 1986.

Miyuzaki, S., Hashiguchi, N., Sugiyama, M., Takada, S., and Morimoto, Y., Fibrinogen microspheres as novel drug delivery systems for antitumor drugs, *Chem. Pharm. Bull.*, 34, 1370-1375, 1986.

Morgan, P.J., Harding, S.E., and Petrak, K., Hydrodynamic properties of a polyisoprene/poly(oxyethylene) block copolymer, *Macromol.*, 22, 4461-4464, 1990.

Mumper, R.J., and Jay, M., Biodegradable radiotherapeutic microspheres, *Proceed. Intern. Symp. Control. Rel. Bioact. Mater.*, 18, 664-665, 1991.

Nemoto, R., and Kato, T., Microencapsulation of anticancer drug for intraarterial infusion and its clinical application, sect.3., ch.5., in "Microspheres and Drug Therapy. Pharmaceutical, Immunological and Medical Aspects", Davis, S.S., Illum, L., McVie, J.G.,

and Tomlinson, E., Eds., Elsevier, Amsterdam, 1984.

Nixon, J.R., In vitro and in vivo release of microencapsulated hydrochlorothiazide, J. Pharm. Sci., 70, 376-378, 1981.

Ochs, H., Bodem, G., Schafer, P.K., Kodrat, G., and Dengler, H.J., Absorption of digoxin from the distal parts of the intestine in man, Eur. J. Clin. Pharmacol., 9, 95-97, 1975.

Ogawa, M., Yamamoto, M., Okada, H., Yashiki, T., and Shimamoto, T., A new technique to efficiently entrap leuprolide acetate into microcapsules of polylactic acid or copoly(lactic/glycolic) acid, Chem. Pharm. Bull., 36, 1095-1103, 1988.

O'Hagan, D.T., Jeffries, H., Roberts, M.J.J., McGee, J.P., and Davis, S.S., Controlled release microparticles for vaccine development, Vaccine, 9, 768-771, 1991.

Oppenheim, R.C., Solid colloidal drug delivery systems: nanoparticles, Int. J. Pharm., 8, 217-234, 1981.

Paradissis, G.N., and Parrott, E.L., Gelatin encapsulation of pharmaceuticals, J. Clin. Pharmacol., 8, 54-59, 1968.

Parker, G., Wilson, C.G., and Hardy, J.G., The effect of capsule size and density on transit through the proximal colon, J. Pharm. Pharmacol., 40, 376-377, 1988.

Parr, A., Jay, M., Digenis, G.A., and Beihn, R.M., Radiolabelling of intact tablets by neutron activation for in vivo scintigraphic studies, J. Pharm. Sci., 74, 590-591, 1985.

Parr, A., and Jay, M., Radiolabelling of intact dosage forms by neutron activation: effects on in vitro performance, Pharm. Res., 4, 524-526, 1987.

Parr, A.F., Beihn, R.M., Franz, R.M., Szupnar, G.J., and Jay, M., Correlation of ibuprofen bioavailability with gastrointestinal transit by scintigraphic monitoring of ¹⁷¹Er-labelled sustained-release tablets, Pharm. Res., 4, 486-489, 1987.

Parr, A.F., Digenis, G.A., Sandefer, E.P., Ghebre-Sellasie, I., Iyer, U., Nesbitt, R.U., and Sceinthal, B.M., Manufacture and properties of erythromycin beads containing neutron-activated erbium-171, Pharm. Res., 7, 264-269, 1990.

Paynter, R.W., Introduction to X-ray photoelectron spectroscopy, in "Surface Characterisation of Biomaterials", Ratner, B., Ed., Elsevier, Amsterdam, 1988.

Peppercorn, M.A., Sulfasalazine: pharmacology, clinical use, toxicity and related new drug development, Ann. Intern. Med., 3, 377-386, 1984.

Peppercorn, M.A., and Goldman, P., Drug-bacteria interactions, Rev. Drug Interact., 2, 75-88, 1976.

Pharmaceutical Journal, 247, 138, 1991.

Phillips, S., and Giller, J., The contributions of the colon to electrolyte and water conservation in man, J. Lab. Clin. Med., 81, 733-746, 1973.

Piper, D.W., de Carle, D.J., Doe, W.F., Ngu, M.C., Barbezat, G.O., Priola, R.C., Powell, L.W., Sorrell, T.C., and Roberts, R.K., Gastrointestinal and hepatic

diseases, Ch.XIX in "Avery's Drug Treatment", Speight, T.M., Ed., 3rd edn., ADIS Press, Auckland, 1987.

Pitt, C.G., The controlled parenteral delivery of polypeptides and proteins, *Int. J. Pharm.*, 59, 173-196, 1990.

Pongpaibul, Y., Price, J.C., and Whitworth, C.W., Preparation and evaluation of controlled release indomethacin microspheres, *Drug Dev. Ind. Pharm.*, 10, 1597-1616, 1984.

Pongpaibul, Y., Maruyama, K., and Iwatsuru, M., Formation and in vitro evaluation of theophylline-loaded poly(methylmethacrylate) microspheres, *J. Pharm. Pharmacol*, 40, 530-533, 1988.

Poste, G., Drug targeting in cancer therapy, in "Receptor-Mediated Targeting of Drugs", Gregoriadis, G., Poste, G., Senior, J., and Trouet, A., Eds., pp.427-474, Plenum Press, London, 1985.

Powell, D.W., Barrier function of epithelia, *Am. J. Physiol.*, 241 (Gastrointest. Liver Physiol., 4), G275-G288, 1981.

Price, J.M.C., Davis, S.S., and Wilding, I.R., The effect of fibre on gastrointestinal transit times in vegetarians and omnivores, *Int. J. Pharm.*, 76, 123-131, 1991a.

Price, J.M.C., Davis, S.S., and Wilding, I.R., Variability in the colonic transit of non-disintegrating tablets in healthy volunteers, *J. Pharm. Pharmacol.*, 43 (suppl.), 103P, 1991b.

Proano, M., Camilleri, M., Phillips, S.F., Brown, M.L., and Thomforde, G.M., Transit of solids through the human

colon: regional quantification in the unprepared bowel, Am. J. Physiol., 258 (Gastrointest. Liver Physiol., 21) G856-G862, 1990.

Proano, M., Camilleri, M., Phillips, S.F., Thomforde, G.M., Brown, M.L., and Tucker, R.L., Unprepared human colon does not discriminate between solids and liquids, Am. J. Physiol., 260 (Gastrointest. Liver Physiol., 23) G13-16, 1991.

Raghunathan, Y., Amsel, L., Hinsvark, O., and Bryant, W., Sustained release drug delivery system. I. Coated ion-exchange resin system for phenylpropanolamine and other drugs, J. Pharm. Sci., 70, 379-384 (1981).

Rasmussen, S.N., Bondesen, S., Hvidberg, E.F., Hansen, S.H., Binder, V., Halskov, S., and Flachs, H., 5-aminosalicylic acid in a slow-release preparation: Bioavailability, plasma level and excretion in humans. Gastroenterology, 83, 1062-1070, 1982.

Ratner, B.D., Surface characterisation of biomaterials by electron spectroscopy for chemical analysis, Ann. Biomed. Eng., 11, 313-336, 1983.

Raymond, G., Degennaro, M., and Mikeal, R., Preparation of gelatin:phenytoin sodium microcapsules: An in vitro and in vivo evaluation, Drug Dev. Ind. Pharm., 16, 1025-1052, 1990.

Read, N.W., and Sugden, K., Gastrointestinal dynamics and pharmacology for the optimum design of controlled-release oral dosage forms, Crit. Rev. Ther. Drug Carr. Sys., 4, 221-263, 1987.

Redmon, M.P., Hickey, A.J., and DeLuca, P.P., Prednisolone-21-acetate poly(glycolic acid) microspheres:

influence of matrix characteristics on release, J. Control. Rel., 9, 99-110, 1989.

Reinaccius, C.A., and Risch, S.J., Eds., "Flavor Encapsulation", ACS Symposium Series, vol.370, 1988, American Chemical Society, Washington D.C.

Rhodes, B.A., Zolle, I., Buchanan, J.W., and Wagner, H.N., Radioactive albumin microspheres for study of the pulmonary circulation, Radiology, 92, 1453-1460, 1969.

Rowland, M., and Tozer, T.N., "Clinical Pharmacokinetics", 2nd edn., Lea & Febiger, Philadelphia, 1989.

Rubinstein, A., Microbially controlled drug delivery to the colon, Biopharm. Drug. Disp., 11, 465-475, 1990.

Rubinstein, A., and Radai, R., Pectic salt as a colonic delivery system, Proceed. Intern. Symp. Control. Rel. Bioact. Mater., 18, 221-222, 1991.

Saffran, M., Kumar, G.S., Savariar, C., Burnham, J.C., Williams, F., and Neckers, D.C., A new approach to the oral administration of insulin and other peptide drugs, Science, 233, 1081-1084, 1986.

Salib, N.N., El-Menshawy, M.E., and Ismail, A.A., Preparation and evaluation of the release characteristics of methylcellulose micropellets, Pharm. Ind., 38, 577-580, 1976.

Sandberg-Gertzen, H., Ryde, M., and Jarnerot, G., Long-term treatment with olsalazine for ulcerative colitis: safety and relapse prevention. A follow-up study, Scand. J. Gastroenterol., 23 (suppl.148), 48-50, 1988.

Sanders, L.M., Kent, J.S., McRae, G.I., Vickery, B.H., Tice, T.R., and Lewis, D.H., Controlled release of a luteinising hormone releasing hormone analogue from poly(d,l-lactide-co-glycolide) microspheres, J. Pharm. Sci., 73, 1294-1297, 1984.

Sargent, J.A., Low temperature scanning electron microscopy: advantages and limitations, Scanning Microscopy, 2, 835-849, 1988a.

Sargent, J.A., Cryo-stabilisation of low melting-point materials for scanning electron microscopy, Proc. R. Microsc. Soc., 23, 275-281, 1988b.

Schacht, E., Callant, D., and Verstraete, W., Synthesis and evaluation of polymeric prodrugs of 5-aminosalicylic acid, Proceed. Intern. Symp. Control. Rel. Bioact. Mater., 18, 686-687, 1991.

Schroeder, K.W., Tremaine, W.J., and Ilstrup, D.L., Coated 5-aminosalicylic acid therapy for mildly to moderately active ulcerative colitis, New Engl. J. Med., 317, 1625-1629, 1987.

Shaw, P.N., Sivner, A.L., Aarons, L., and Houston, J.B., A rapid method for the simultaneous determination of the major metabolites of sulphasalazine in plasma, J. Chromatogr., 274, 393-397, 1983.

Shukla, A.T., and Price, J.C., Effect of drug (core) particle size on the dissolution of theophylline from microspheres made from low molecular weight cellulose acetate propionate, Pharm. Res., 6, 418-421, 1989.

Simon, G.L., and Gorbach, S.L., Intestinal flora and gastrointestinal function, Ch.64 in "Physiology of the Gastrointestinal Tract", L.R.Johnson Ed., 2nd edn., Raven

Press, New York, 1987.

Simpkins, J.W., Smulkowski, M., Dixon, R., and Tuttle, R., Evidence for delivery of narcotic antagonists to the colon as their glucuronide conjugates, *J. Pharmacol. Exp. Ther.*, 244, 195-205, 1988.

Sintov, A., Nakar, D., Rokem, J.S., and Rubinstein, A., In vitro studies with modified chondroitin, a potential colonic drug delivery, *Proceed. Intern. Symp. Control. Rel. Bioact. Mater.*, 17, 468-469, 1990.

Smith, A., and Hunneyball, I.M., Evaluation of poly(lactic acid) as a biodegradable drug delivery system for parenteral administration, *Int. J. Pharm.*, 30, 215-220, 1986.

Spenlehauer, G., Vert, M., Benoit, J.-P., Chabot, F., and Veillard, M., Biodegradable cisplatin microspheres prepared by the solvent evaporation process; morphology and release characteristics, *J. Control. Rel.*, 7, 217-229, 1988.

Staib, A.H., Loew, D., Harder, S., Grayl, E.H., and Pfab, R., Measurement of theophylline absorption from different regions of the gastrointestinal tract using a remote controlled drug delivery device, *Eur. J. Clin. Pharmacol.*, 9, 95-97, 1986.

Staib, A.H., Beerman, D., Harder, S., Fuhr, U., and Liermann, D., Absorption differences of ciprofloxacin along the human gastrointestinal tract determined using a remote-control drug delivery device (HF-capsule), *Am. J. Med.*, 87 (suppl.5A), 66S-69S, 1989.

Steed, K.P., Wilson, C.G., and Washington, N., Drug delivery to the large intestine, Ch.9 in "Physiological

Pharmaceutics", Wilson, C.G., and Washington, N., Eds., Ellis Horwood, Chichester, 1989.

Sugibayashi, K., Morimoto, Y., Nadai, T., Kato, Y., Hasegawa, A., and Arita, T., Drug-carrier property of albumin microspheres in chemotherapy. II. Preparation and tissue distribution in mice of microsphere-entrapped 5-fluorouracil, Chem. Pharm. Bull., 27, 204-209, 1979.

Suzuki, K., and Price, J.C., Microencapsulation and dissolution properties of a neuroleptic in a biodegradable polymer, poly(d,l-lactide), J. Pharm. Sci., 74, 21-24, 1985.

Svartz, N., Salazopyrin, a new sulfanilamide preparation, Acta Med. Scand., 110, 577-598, 1942.

Swallow, A.J., "Radiation Chemistry: An Introduction", Longman, London, 1973.

Swarbrick, E.T., Loose, H., and Lennard-Jones, J.E., Enema volume as an important factor in successful topical corticosteroid treatment of colitis, Proc. R. Soc. Med., 67, 753-754, 1974.

Taylor, D.C., Lynch, J., and Leahy, D.E., Models for intestinal permeability to drugs, Ch.11 in "Drug Delivery to the Gastrointestinal Tract", Hardy, J.G., Davis, S.S., and Wilson C.G., Eds., Ellis Horwood, Chichester, 1989.

Toguchi, H., Ogawa, Y., Okada, H., and Yamamoto, M., Once-a-month injectable microcapsules of leuprorelin acetate, Y. Zasshi, 111, 397-409, 1991.

Tomlin, J., and Read, N.W., The relation between bacterial degradation of viscous polysaccharides and stool output in human beings, Br. J. Nutr., 60, 467-475, 1988.

Tomlinson, E., Microsphere delivery systems for drug targeting and controlled release, *Int. J. Pharm. Tech & Prod. Mfr.*, 4, 49-57, 1983.

Tozer, T.N., Colonic drug delivery, *Proceed. Int. Symp. Control. Rel. Bioact. Mater.*, 17, 126-127, 1990.

Tsai, D.C., Howard, S.A., Hogan, T.F., Malanga, C.J., Kandrazi, S.J., and Ma, J.K.H., Preparation and in vitro evaluation of polylactic acid-mitomycin C microcapsules, *J. Microencapsulation*, 3, 181-193, 1986.

Tsuyoshi, T., Suzuki, N., Kawata, M., Uchida, T., and Goto, S., Preparation and pharmacokinetic and pharmacodynamic evaluation of hydroxypropyl cellulose-ethylcellulose microcapsules containing piretanide, *J. Pharmacobio-Dyn.*, 12, 311-323, 1989.

Tudor, A.M., Melia, C.D., Binns, J.S., Hendra, P.J., Church, S., and Davies, M.C., The application of Fourier-transform Raman spectroscopy to the analysis of pharmaceuticals and biomaterials, *J. Pharm. Biomed. Anal.*, 8, 717-720, 1990.

Tudor, A.M., Davies, M.C., Melia, C.D., Lee, D.C., Mitchell, R.C., Hendra, P.J., and Church, S.J., The applications of near infrared Fourier transform Raman spectroscopy to the analysis of polymorphic forms of cimetidine, *Spectrochim. Acta.*, 47A, 1389-1393, 1991a.

Tudor, A.M., Melia, C.D., and Davies, M.C., The application of NIR FT-Raman spectroscopy to the qualitative analysis of chlorpropamide polymorphism, *in-situ*, *J. Pharm. Pharmacol.*, 43 (suppl.), 68P, 1991b.

Tudor, A.M., Melia, C.D., Davies, M.C., Hendra, P.J., Church, S., Domb, A.J., and Langer, R., The application

of Fourier transform Raman spectroscopy to the analysis of poly(anhydride) homo- and copolymers, *Spectrochim. Acta*, 47A, 1335-1343, 1991c.

Uchida, T., and Goto, S., Biopharmaceutical evaluation of sustained-release ethylcellulose microcapsules containing cefadroxil and cephradine using beagle dogs, *Chem. Pharm. Bull.*, 36, 2135-2144, 1988.

Verdun, C., Couvreur, P., Vranckx, H., Lenaerts, V., and Roland, M., Development of a nanoparticle controlled-release formulation for human use, *J. Control. Rel.*, 3, 205-210, 1986.

Wada, R., Hyon, S.-H., Ike, O., Watanabe, S., Shimizu, Y., and Ikada, Y., Preparation of lactic acid oligomer microspheres containing anticancer drugs by o/o type solvent evaporation process, *Polym. Mater. Sci. Eng.* 59, 803-806, 1988.

Wakiyama, N., Juni, K., and Nakano, M., Preparation and evaluation in vitro of polylactic acid microspheres containing local anaesthetics, *Chem. Pharm. Bull.*, 29, 3363-3368, 1981.

Watanabe, Y., Sano, M., Motohashi, K., Yoneda, R., Mitsui, Y., and Botan, Y., Relationship between quality and serum level after the oral administration of commercial erythromycin tablets in man, *Y. Zasshi*, 97, 791-800, 1977.

Weiss, E.L., and Frock, H.N., Rapid analysis of particle size distributions by laser light scattering, *Powd. Tech.*, 14, 287-293, 1976.

Wilding, I.R., Coupe, A.J., and Davis, S.S., The role of gamma-scintigraphy in oral drug delivery, *Adv. Drug Del.*

Rev., 7, 87-117, 1991.

Wilkins, R.M., Ed., "Controlled Delivery of Crop-Protection Agents", Taylor & Francis, London, 1990.

Willard, H.H., Merritt, L.L., Dean, J.A., and Settle, F.A., "Instrumental Methods of Analysis", 7th edn., Wadsworth, Belmont, CA, 1988.

Willoughby, C.P., Cowan, R.E., Gould, S.R., Machell, R.J., and Stewart, J.B., Double-blind comparison of olsalazine and sulphasalazine in active ulcerative colitis, *Scand. J. Gastroenterol.*, 23 (suppl.148), 40-44, 1988.

Wilson, C.G., and Washington, N., Assessment of disintegration and dissolution of dosage forms in vivo using gamma scintigraphy, *Drug Dev. Ind. Pharm.*, 14, 211-281, 1988.

Wilson, C.G., Washington, N., Greaves, J.L., Kamali, F., Rees, J.A., Sempik, A.K., and Lampard, J.F., Bimodal release of ibuprofen in a sustained-release formulation: a scintigraphic and pharmacokinetic open study in healthy volunteers under different conditions of food intake, *Int. J. Pharm.* 50, 155-161, 1989.

Wilson, C.G., Washington, N., Greaves, J.L., Washington, C., Wilding, I.R., Hoadley, T., and Sims, E.E., Predictive modelling of the behaviour of a controlled release buflomedil HCl formulation using scintigraphic and pharmacokinetic data, *Int. J. Pharm.*, 72, 79-86, 1991.

Wise, D.L., Fellmann, T.D., Sanderson, J.E., and Wentworth, R.L., Lactic/glycolic acid polymers, Ch.12, in "Drug Carriers in Biology and Medicine", Gregoriadis, G.,

Ed., Academic Press, 1979.

Woodbury, D.M., and Finch, E., Analgesic-antipyretic, antiinflammatory agents, and drugs employed in the treatment of gout, Ch.17 in "The Pharmacological Basis of Therapeutics", Goodman, L.S., and Gilman, A., Eds., 5th edn., Macmillan, New York, 1975.

Woodley, J.F., Peptidase activity in the GI tract: Distribution between lumenal contents and mucosal tissue, Proceed. Intern. Symp. Control. Rel. Bioact. Mater., 18, 337-338, 1991.

Wong, P.S.L., and Theeuwes, F., Colonic-therapeutic delivery system, US Patent 4,627,851, 1986.

Wong, P.S.L., and Theeuwes, F., Colon delivery system, US Patent 4,693,895, 1987.

Wyman, J.B., Heaton, K.W., Manning, A.P., and Wicks, A.C.B., Variability of colonic function in healthy subjects, Gut, 19, 146-150, 1978.

Yoshioka, T., Hashida, M., Muranishi, S., and Sezaki, H., Specific delivery of mitomycin C to the liver, spleen and lungs: nano- and microspherical carriers of gelatin, Int. J. Pharm., 81, 131-141, 1981.

Zhou, X.H., and Li Wan Po, A., Peptide and protein drugs: II. Non-parenteral routes of drug delivery, Int. J. Pharm., 75, 117-130, 1991.

CORRIGENDA

- p.27, Figure 1.4, "arterial" for "aterial".
- p.29, Line 1, "7-12 μm " for "3-11 μm ".
- p.34, Line 18, "drug" for "drugs" and "is" for "are".
- p.35, Line 28, "In common with the rest.."
- p.49, Line 10, "since it is now.."
- p.89, Line 31, "were" for "was".
- p.95, Line 32, "was" for "were".
- p.119, Line 20, "was" for "were".
- p.145, remove lines 8 and 9.
- p.151, Figure 5.5, "molecule" for "mole".
- p.161, Line 15, In^{3+} .
- p.163, Line 10, "slurry" for "paste".
- p.165, Line 19, "..coating polymer in acetone".
- p.210, Line 32, "with concentration up to 0.67% w/w".
- p.217, Line 14, "bound" for "glued".
- Throughout thesis, "sec" (second) for "s".